DTIC FILE COPY

AD-A229 413

FLOOD INUNDATION MODELLING USING MILHY

Final Technical Report

by

L.Baird and M.G.Anderson

DTIC
S ELECTE
NOV 27 1990
D
D

**Volume 1
User Manual
September 1990**

CONTRACT NUMBER DAJA 45-87-C-0053

Professor M.G.Anderson

VOLUME 1

ACKNOWLEDGEMENTS

A-1

Preface

This report details work undertaken under contract
DAJA-45-C-0053 to September 1990. We report the further development
of the ungauged flood forecasting model MILHY. Specifically, new
routines are introduced to allow the discrete routing of floodplain
and main channel flow and to incorporate the exchange of momentum
between main channel and floodplain. The program (MILHY3) is
applied to a large watershed, the River Fulda, West Germany, where
both MILHY3 developments and MILHY2 developments (DAJA-37-81-C-0221)
are assessed.

In addition, a two-dimensional hydrodynamic model, RMA-2V, has
been applied to a 30km reach of the River Fulda, and 11km reach of
the River Culm, England. Results from the River Fulda application
showed that it is feasible to consider linking RMA-2V with MILHY3 to
generate detailed inundation modelling within a hydrologic catchment
simulator. The River Culm application has explored some of the
limitations and problems of large-scale applications of RMA-2V, and
the importance of topographic resolution is highlighted. Results
from these two applications allow environments to be identified,
where RMA-2V may be successfully applied at the large-scale, and
environments where further developmental work is required.

In Volume 2 of this report, the MILHY3 code is presented with
a user manual and source code details.

Summary Contents

iii.

Detailed Contents

Page

Page

viii.

List of Tables

List of Figures

Page

Chapter 1

Introduction

1.1   Background

This study relates to the further development of an
operational model for ungauged flood forecasting. The model used as
the starting basis for the project was MILHY2; a model delivered to
Waterways Experiment Station in 1986, under contract DAJA-45-C-0029.

The history of MILHY development as an ungauged forecasting
model and research scheme is as follows:

MILHY   :   model for ungauged flow forecasting using Curve Number
            (CN) scheme to generate runoff, 1982

MILHY1 :   adaptation of MILHY under contracts DAJA-37-82-C-0092 and
            DAJA-37-81-C-0221 by Dr M G Anderson to replace CN scheme
            by a physically-based runoff generation method (finite
            difference), 1984

MILHY2 :   development and validation of MILHY1 on small subcatchment
            scale ($\leq 1\text{km}^2$) watersheds by Dr M G Anderson and Dr S
            Howes, under contract DAJA-45-83-C-0029. Code delivered
            to WES in 1986

MILHY3 :   further development of MILHY2 to upgrade the prediction of
            the hydrograph under floodplain inundation conditions.
            Subject of contract here presented by Dr M G Anderson and
            Dr L Baird, 1990

Upon initiation of the current contract MILHY2 represented a
fully working scheme (see Figure 1.1) and was subjected to limited
validation, as shown in Table 1.1 and Figures 1.2 and 1.3. The main
conclusions of contract DAJA-45-83-C-0029 relating to the
development of MILHY2 were that:
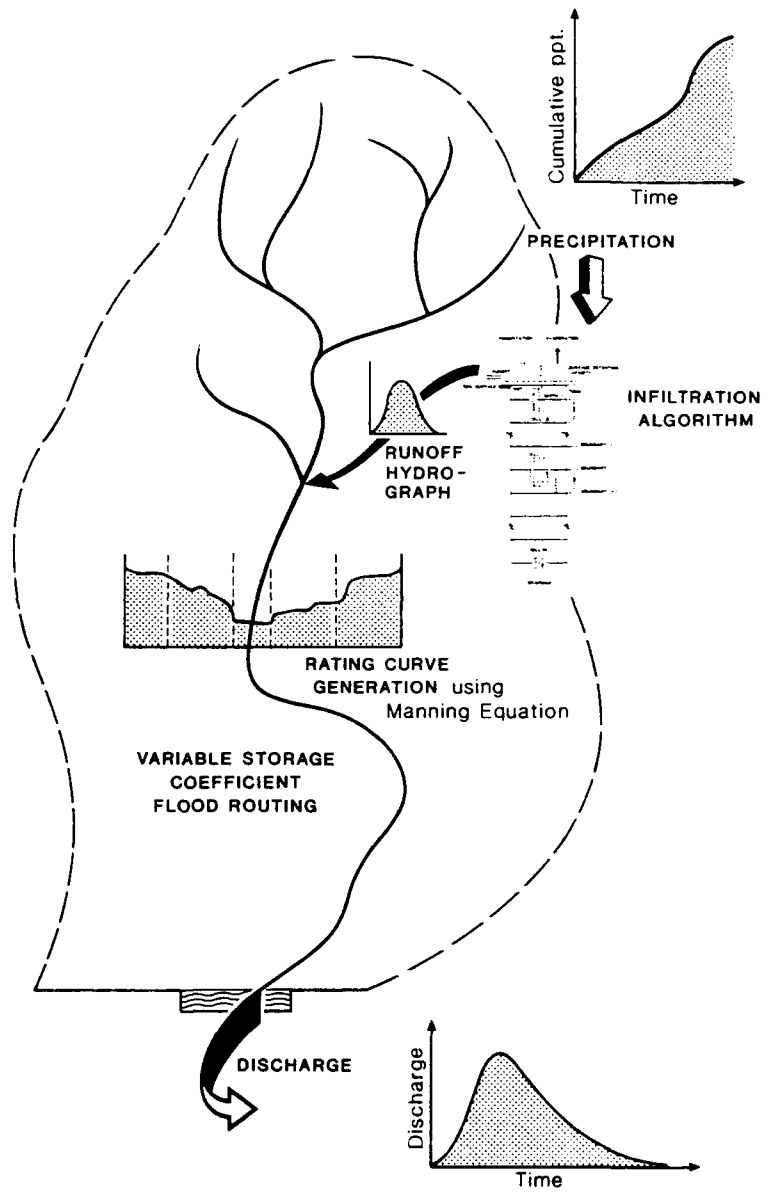
Figure 1.1
Conceptual Structure of MILHY2 Scheme

Table 1.1
Comparison of catchment characteristics which are
required by the unit hydrograph procedure

	Area (km^2)	Difference in elevation (m)	Length of main channel (km)
W-2 North Danville Vermont	0.6	79.3	1.2
W-1 Treynor, Iowa	0.3	27.4	1.1
W-2 Treynor, Iowa	0.3	21.3	0.9
W-4 Treynor, Iowa	0.6	30.5	0.6
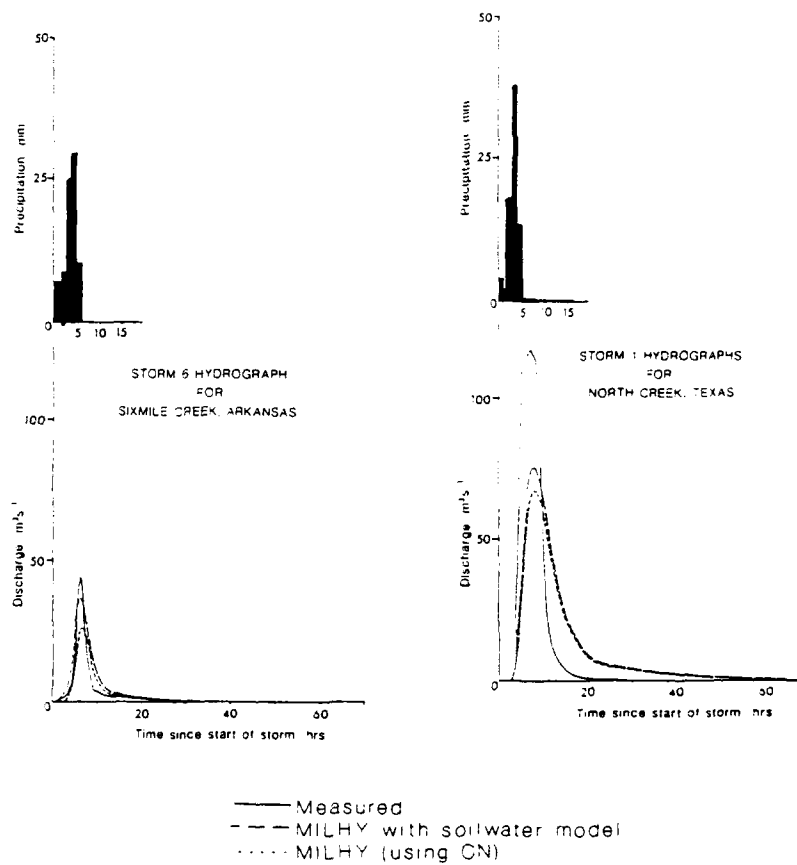
Figure 1.2
Comparison of observed and MILHY, MILHY2 simulations for
a) Sixmile Creek, Arkansas
b) North Creek, Texas
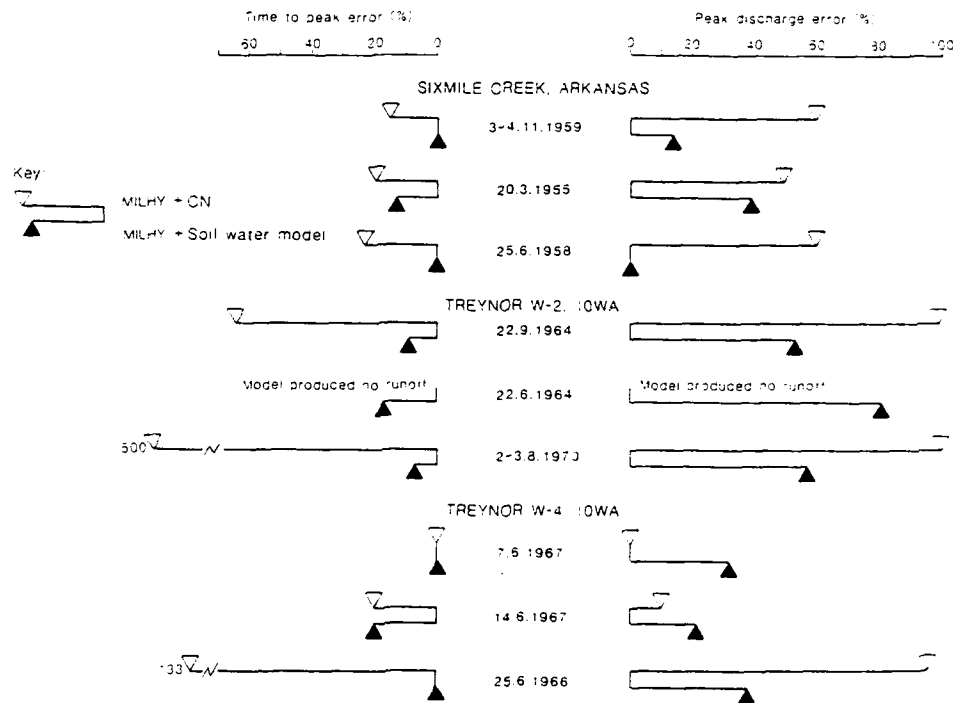
Figure 1.3
Comparison of MILHY and MILHY2 simulations for Sixmile
Creek, Arkansas, Treynor W-2, Iowa, and Treynor W4, Iowa

Chapter 1

  (i) the correlation between predicted and measured peak discharge
using MILHY2 was high (r = 0.91)

 (ii) the time to peak discharge estimation was good using MILHY2
(r = 0.97)

(iii) a comparison of MILHY and MILHY2 for 32 experimental frames
showed strong evidence of the overall improvement achieved by
MILHY2

There was, therefore, a strong basis for pursuing the further
development of MILHY2. In particular, it is important to
investigate the development of MILHY2 for larger subcatchment scales
than previously undertaken, where channel processes become more
significant.

1.2   Objectives and Scope

The overall objective of this contract is to improve the
predictive capabilities of MILHY2 whilst retaining its parsimonious
data requirements, portability and simplicity of application. This
objective has been achieved through the investigation of the
following specific objectives:

1)   to develop the modular structure of MILHY to allow not only
flexibility in catchment representation but also choice in the
process resolution of the solution .

2)   to develop the channel routing components of MILHY2 to improve
prediction of out-of-bank flood events

3)   to investigate and implement several alternative validation
schemes for the revised MILHY scheme, using both field data
and hydrodynamic simulation of the River Fulda catchment in
West Germany

Chapter 1

4)   to explore the suitability of a finite-element hydrodynamic
      model (RMA-2V) for large scale floodplain modelling,

5)   to investigate the linking of MILHY with a hydrodynamic model
      (RMA-2V) to provide enhanced inundation modelling within a
      catchment scheme.

Chapter 2

Research Design

2.1   Introduction

     The overall research design of the MILHY project as developed
by Dr Anderson's group at Bristol University over the last seven
years is shown in Figure 2.1. The initial decision regarding MILHY1
related to utilisation of finite difference methods for runoff
generation. Subsequent research identification suggested the need
to examine modular program structures and out-of-bank channel
modelling, and it is these developments that are major constituents
of MILHY3. However, more general issues are raised here in the
context of the interaction of hydraulic and hydrologic schemes and
their respective suitability for ungauged inundation modelling.

2.2   Modular Program Structures

     Any model design is essentially a two-dimensional matrix of
components. This is illustrated in general terms in Figures 2.2 and
2.3. Decisions have to be made in two principal areas: (1) sub-
model inclusion, and (2) resolution of the selected submodel. It is
the latter decision area that has proved the focus of the current
research. In particular, we have sought to examine the effects of
changes in the channel routing submodel, in the context of examining
and implementing alternative models for out-of-bank flow conditions.
In addition, a somewhat lesser effort has been expended in an
examination of precipitation. Figure 2.3 shows the scope of the
submodel resolution development. An important consideration here
relates to achieving a submodel resolution that is considered,
broadly at least, to be consistent between all submodels. Earlier
research in the MILHY program concentrated on improving the
resolution of the infiltration submodel (see Figure 2.1). An
important consideration in this project has therefore been to assess
the relative performance of the infiltration algorithm in comparison

1983 MILHY	1984 MILHY1	1986 MILHY2	1989 MILHY3	1990 MILHY3	1990 →
Basic model.	Curve number replaced by physically-based infiltration scheme.	Validation at subcatchment scale and code enhancement.	Multiple routing reaches and momentum exchange for improved hydrograph prediction in out-of-bank conditions. Large catchment validation. Initial assessment of RMA-2 for large-scale MILHY3 validation.	Assessment of large-scale inundation modelling using RMA-2. Feasibility study for linking RMA-2 and MILHY3 schemes.	Linking MILHY3 in GIS driven composite expert system with cold regions process models.
		MILHY2 code delivered to WES		MILHY3 code delivered to WES	

Figure 2.1
MILHY Project Research Programme at the University of Bristol

```
        ┌─────────────────┐
        │ Establishment of│
        │ Model Objectives│
        └─────────────────┘
```

Submodel 1 structure 1		Submodel 2 structure 2
Submodel 2 structure 1		Submodel 2 structure 2
Submodel 3 structure 1		Submodel 3 structure 2

Model 1   Model 2   Model 3

Conceptual uncertainty

Numerical /parameterization uncertainty
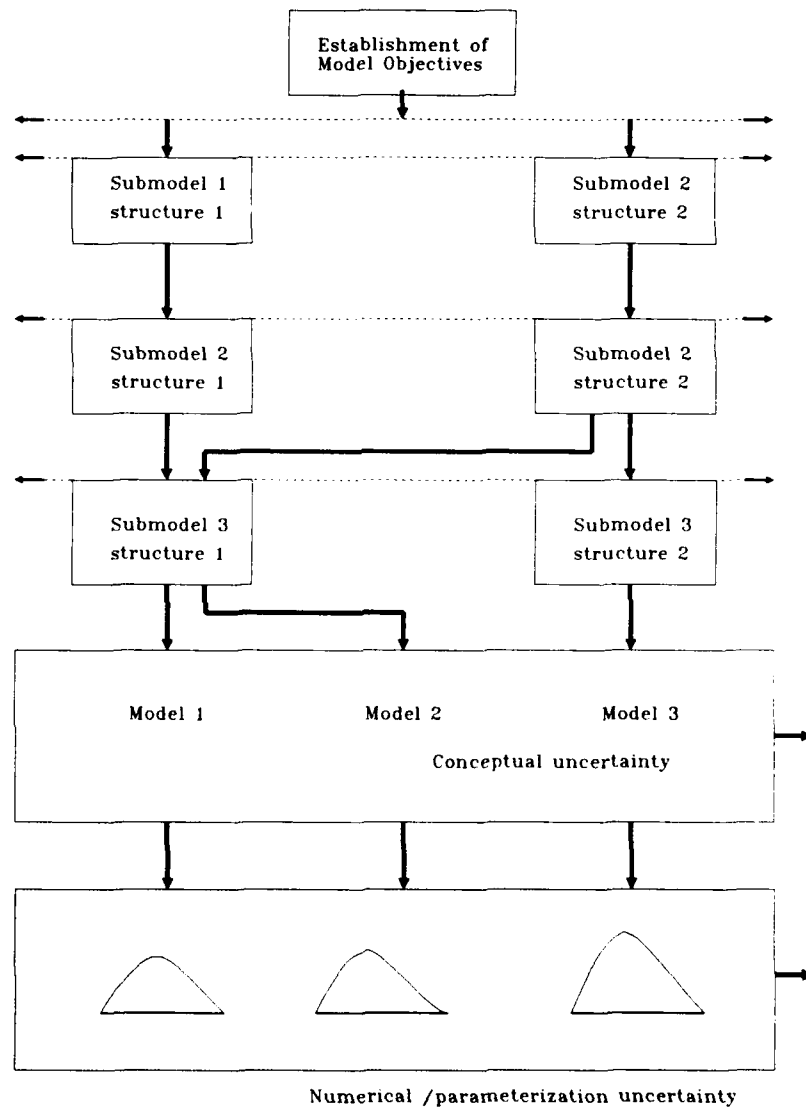
Figure 2.2
Composite Modelling Structure Incorporating Variability in Model Structure
(after Anderson and Sambles, 1988)
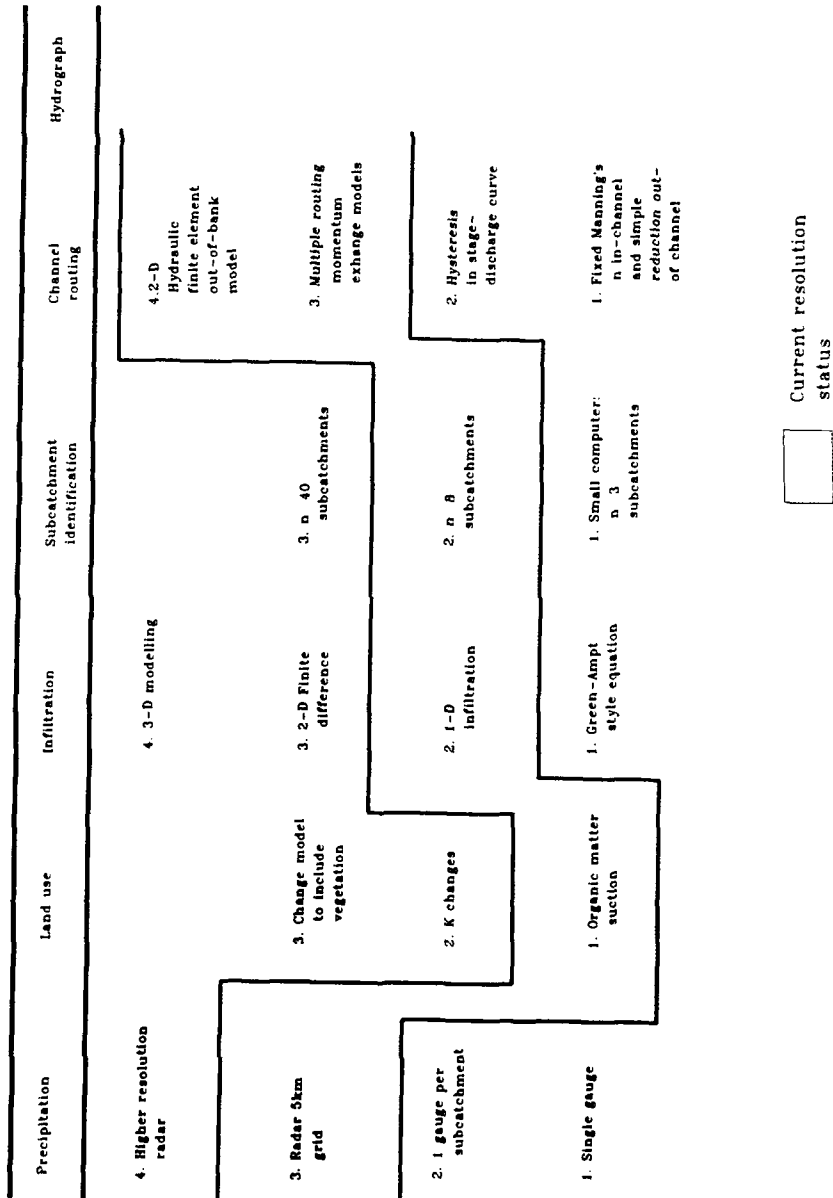
Figure 2.3
Composite Logic Structure for MILHY3

Chapter 2

with improved resolution in the channel routing.

Submodel resolution cannot of course be divorced from the
resolution of user supplied information. Varying, perhaps
unavoidable, resolution in the user supplied information may be
considered, potentially at least, to have significant ramifications
for submodel and overall model performance. Thus user supplied data
resoluion cannot, and should not, be divorced from model
formulation, design and validation.

2.3   Out-of-bank Routing

Out-of-bank flows have highlighted in this research project an
area which allows the investigation of several important issues.
Firstly, as noted above, it allows comparison of modelling
resolution in different process submodels within the MILHY scheme.
Secondly, it extends the range of applications to which MILHY may be
profitably applied and upgrades the out-of-bank channel modelling
beyond any currently available alternative scheme. Finally, it
allows investigation of the narrowing distinction between hydrologic
catchment schemes and hydraulic reach models such as RMA-2V.

Table 2.1 summarizes the current handling of out-of-bank
conditions in a range of hydrologic ungauged catchment models. The
table shows that the resolution of the out-of-bank simulation is
generally low and that channel modelling has been generally ignored
in preference for more sophisticated modelling of the runoff
generation processes.

2.4   Hydrologic and Hydraulic Schemes

It is proposed in this report that the traditional distinction
between hydrologic models and engineering hydraulic schemes is no
longer useful to the modeller, and that all modelling strategies

Chapter 2

must be considered within a suite of schemes. The hydrodynamic
model RMA-2V is evaluated against the interests in modular program
structures and out-of-bank routing noted above. Packages such as
RMA-2V are taken to represent the state-of-the art in river reach
modelling, and yet the utility of the schemes in both a catchment
and ungauged context remains unevaluated. In this report the
potential of RMA-2V is assessed for, firstly, extending
"ground-truth" field data sets against which the MILHY3 scheme may
be evaluated, and, secondly, as a modular component of a future
MILHY scheme. This necessitates application of RMA-2V to reach
lengths significantly longer than previous applications and with
limited topographic data sets.

In the next chapter of this report, the physical behaviour of
out-of-bank flows is assessed; this assessment determines the
structure of the development and validation of the MILHY3 scheme.
In Chapters 4 and 5, components of the MILHY3 model are developed
and assessed. The model is then compiled and validated in Chapters
6, 7 and 8. Chapter 6 describes the establishment of the River
Fulda test catchment, West Germany, whilst Chapter 7 uses the data
set to test the performance of the new modules developed in Chapters
4 and 5. In Chapter 8, RMA-2V is applied to a reach of the River
Fulda, to test its suitability for validating the MILHY3 scheme.
Chapter 9 continues the assessment of the RMA-2V scheme for
large-scale floodplain applications with a test reach of the River
Culm, Devon, UK, In this chapter, the accuracy of the velocity
vector and spatial inundation distributions of the RMA-2V model are
assessed, using a more operational perspective of application.
Chapter 10 concludes this volume, with operational guidelines for
both MILHY3 and RMA-2V models. Future developments of the scheme
are discussed in general.

Table 2.1

Hydrograph Simulators for Ungauged Catchments

Author	Model details	
	Parameter estimation	Routing/ two-stage capability

Calibrated Models

Author	Parameter estimation	Routing/ two-stage capability
NERC (1975)	Empirical regional formula	–
HEC-1 (1981)	Observed or regional catchment coefficients empirical soil parameters	Muskingham or Puls Separate Manning's n
USDAHL Nicks et al. (1980)	Maps and regional groundwater coefficients	Main channel
Stanford Watershed Model Ross (1970)	Optimized parameters for catchment	CSRX, FSRX Parameter for in-bank and out-of-bank routing
4 Parameter Water Yield Model Jarboe and Haan (1974)	Regression analysis	Main channel length, slope

Physical Based Parameters

Author	Parameter estimation	Routing/ two-stage capability
HEC-1 (1981)	Observed or regional parameters	Kinematic wave routing Fixed geometry
Engman and Rogowski (1974)	Observed soil and overland flow parameters	–
HYSIM Manley (1978)	Observed or regional groundwater paremeters	
WATSIM Aston et al. (1980)	Observed and calibrated overland parameters	No channel routing

Table 2.1 (cont.)

TOPMODEL Beven (1977)	Observed or optimized parameters	CHA and CHB channel velocity
SPUR Renard <u>et al.</u> (1984)	All parameters derived from	No channel routing

Chapter 3

Chapter 3
Identification of Key Processes in
Downstream Conveyance in Two-Stage Channels

The need to improve the modelling of two-stage channels in ungauged catchments has been identified in Chapters 1 and 2. The objectives of undertaking an investigation into the modelling of two stage channels are:

    i)   to investigate the importance of the resolution of modules in a composite modelling structure from the perspective of a model user

   ii)   to investigate the relationship between module resolution and the effects of scale, in order to generate guidelines for the user

  iii)   to incorporate hydraulic technique into a hydrologic modelling strategy

   iv)   to potentially improve the predictive accuracy of MILHY2 in out-of-bank conditions

   v)   to initiate the potential for the development of flood-plain inundation modelling in future research projects

The next step in the research strategy is to identify the key processes that control the behaviour of flow in two-stage channels and then consider how these may be incorporated in an ungauged model. In the next section, therefore, a review of the behaviour of flow in two-stage channels is reported and then a

Chapter 3

rationale for selecting certain processes that could profitably
be modelled is developed.

3.1   Difficulties in Modelling Two-Stage Channels

As defined earlier, two-stage channels consist of a main
channel and adjoining floodplain or berm which is subject to
inundation. Water on the floodplains may be either stationary,
when the floodplains act as stores of water, or flowing when the
floodplain acts as a channel conveying water downstream.

3.1.1 The complexity of physical processes

A river is a complex three-dimensional system such that
the inclusion of the floodplain system is not simply a matter of
extending the cross-sectional area of the main channel. As the
floodplains may act as both stores of water or flowing channels,
it is inappropriate to simply extend the rating curve
relationship from in-bank conditions.

Bhowmick and Demissie (1982) have shown the carrying
capacity of a two-stage channel is not directly proportional to
cross-sectional area. Figure 3.1 shows the relationship between
the area ratio (floodplain area/total cross-sectional area) and
the discharge ratio (floodplain discharge/total cross-sectional
area) for a theoretical two-stage channel. The figure also
shows a theoretical line of proportionality which identifies the
relationship we would expect. If, for example, the floodplain
area was half of that of the total area (area ratio = 0.5), then
we might expect the floodplain to contribute half the discharge
(discharge ratio = 0.5). However, the actual relationship
shows that when the area ratio is 0.5, the discharge ratio is
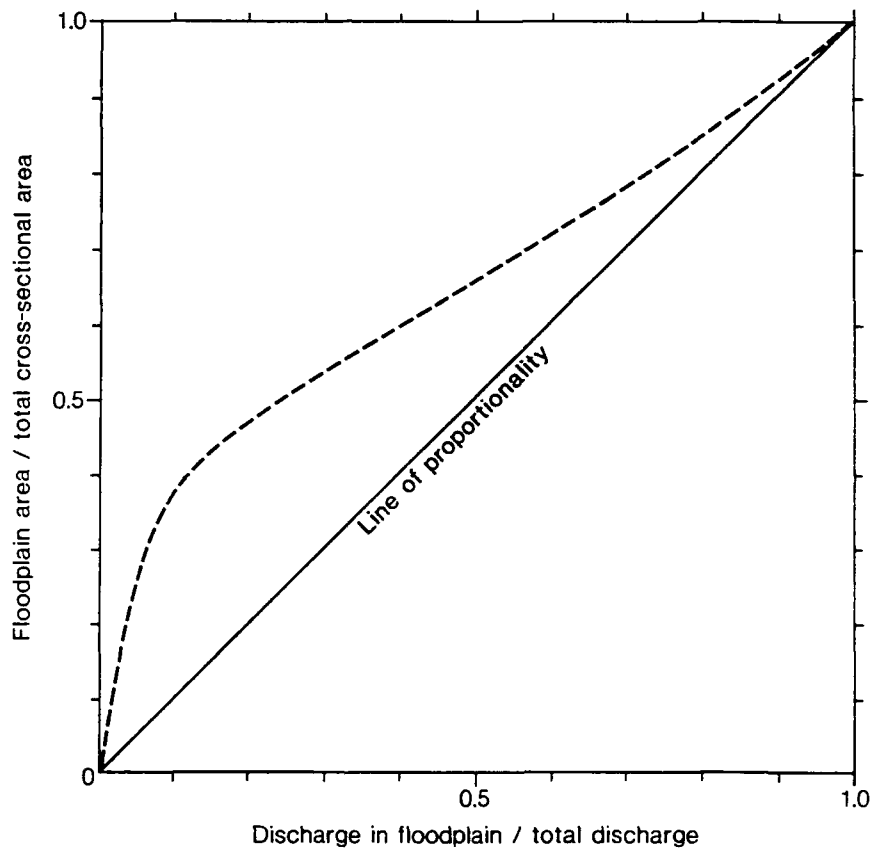
Figure 3.1
Relationship Between Floodplain/Total Area Ratio and Floodplain/Total
Discharge Ratio
(after Bhowmick and Demissie, 1982)

Chapter 3

actually 0.25. When the area ratio is less than 0.5, the
discrepancy between the actual and theoretical is particularly
large, so that as the area ratio increases the two lines
converge. The figure shows that the two-stage channel system
should not, therefore, be treated as a single channel system.

Bhowmick and Demissie (1982) found discontinuities in
the velocity fields of the main channel and shear at the
boundary between the channel and floodplain. Figure 3.2 shows
the stage/velocity relationship in Salt Creek, USA, and
illustrates the discontinuity of velocity in the two-stage
channel. Both the floodplain and main channel show an overall
increase in flow velocities as the depth of flow increases.
This can be attributed to the reduction in the impact of
boundary friction as depth increases. If the two-stage channel
is treated as a single system, shown as the compound channel
line on Figure 3.2, then the velocity decreases as out-of-bank
conditions occur. The separate lines for the floodplain and
main channel velocities show that the behaviour of the compound
flow cannot be simply explained by the additional wetted
perimeter and boundary friction of the floodplain. The velocity
of the main channel flow also drops when out-of-bank conditions
occur. Figure 3.2 shows that the main channel velocity reaches
a local minimum when the floodplain inundation is approximately
35% of the main channel stage. As the floodplain inundation
depth increases, then the velocity of the floodplain flow
increases and the three lines of Figure 3.2 converge to a common
velocity.

Research by Rajaratnum and Ahmadi (1979) confirmed these
velocity patterns and showed discontinuity in the pattern of bad
shear in the main channel and floodplain flow segents in a
series of flume experiments. Together these results suggest

Figure 3.2
Relationship Between Stage and Velocity in a
Two-Stage Channel
(after Bhowmick and Demissie, 1982)

a) floodplain
b) combined floodplain and channel
c) channel
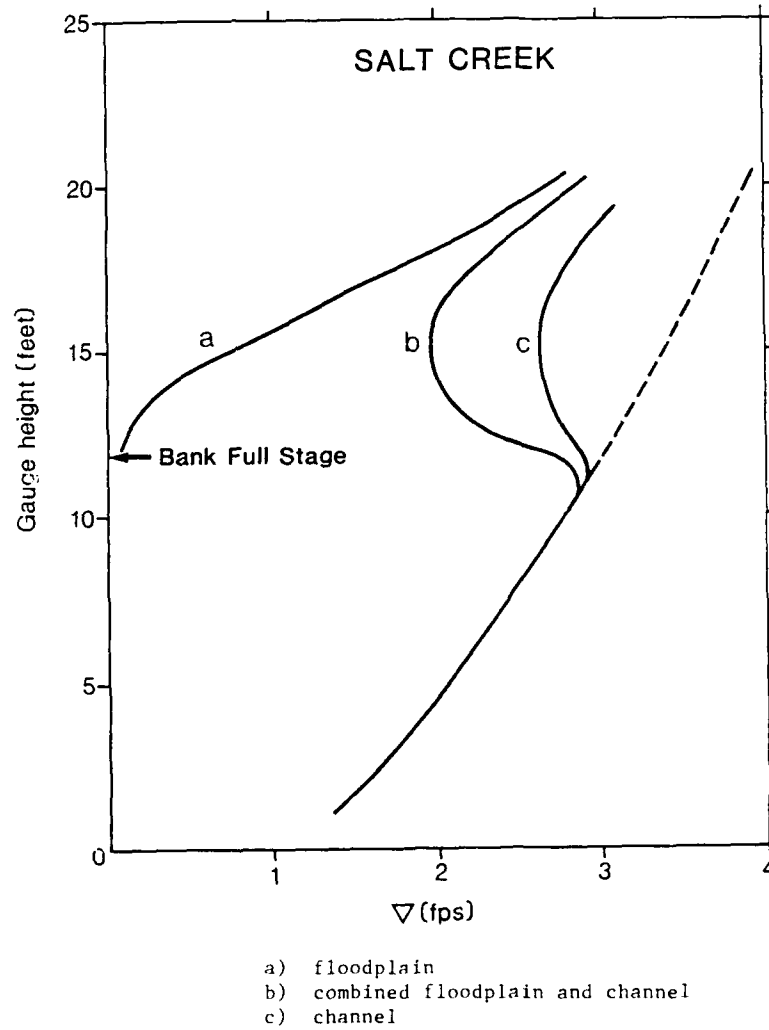
Chapter 3

that there is transverse mass transfer between the fast moving
main channel flow to the slower moving floodplain flows. This
would effectively retard flows in the main channel and
accelerate flows in the floodplain. This momentum transfer
may be envisaged to occur through the action of turbulent shear
stresses, first recognised and photographed by Sellin (1964).

From Bhowmick and Demissie's (1982) research, it is
possible to conclude, therefore, that the floodplain and
main channel flows interact and the nature of this interaction
varies with the depth of floodplain inundation.

So far, however, only the cross-sectional geometry of
the two-stage channel has been considered. The plan geometry,
however, is also important in the prediction of a flood
hydrograph. Along a meandering channel the cross-sectional
geometry of the two-stage channel will vary as the channel
oscillates from one side of the floodplain to the other. This
generates different longitudinal path lengths and downstream
slopes for the floodplain and main channel. The downstream path
length of the main channel is longer than its less sinuous
floodplain and consequently the channel's slope is smaller.
Fread (1976) suggested that such differences exacerbate the
distinct pathways of the floodplain and main channel flows.

However, Toebes and Sooky (1967) showed in a series
of flume experiments, that the momentum transfer between
the floodplain and main channel is exacerbated where flood-
plain flows are not parallel to the main channel. This increase
in the effects of momentum exchange would reduce the effects of
the separate flood paths by accelerating floodplain flows and
retarding main channel flows. As in most ungauged catchments
the channel system meanders, it is important for the accurate
prediction of the discharge hydrograph that the conflicting

Chapter 3

processes identified by Fread (1976) and Toebes and Sooky (1967)
be resolved.

Chang (1983) showed that in a meandering river the energy
expenditure is much greater than in a straight channel. The
increase in energy expenditure can be associated with the
generation of secondary currents usually at meander bends.
Chang also showed that when the depth of flow is high, or when
boundary frictions are small, the energy losses associ..^i with
the secondary current system can be greater than the energy
losses associated with the main longitudinal flow. Chang's work
suggests, therefore, that in the floodplain environment, where
flow depths are relatively small and roughnesses high, even if a
secondary current system were to develop it would be of little
significance.

The literature shows that the processes active in a
two-stage channel occur in the orthogonal and longitudinal
dimension. Orthogonally the flows of the floodplain and main
channel interact through turbulent stresses and these stresses
are exacerbated when the floodplain and channel flows are not
parallel. Longitudinally, floodplain flows tend to be less
sinuous and therefore their downstream path length is shorter.
The effects of this path length difference is increased by the
steeper longitudinal slope of the floodplain flows. In both
dimensions, the impact of boundary shear stresses on the wetted
perimeter must also be considered.

In trying to rationally identify the most important of
these processes which could realistically be modelled, one
alternative would be to undertake a sensitivity analysis of
an existing model which incorporated as many of the processes
active in a two-stage channel as possible. The advantage would
be that the time taken to identify the most important processes

Chapter 3

could be reduced and therefore more time would be available
for the validation of the ungauged model. The disadvantage
would be that the identification would be reliant on the success
of the model used. However, it has been noted already in this
report that the skills available to model the active processes
in a catchment have been sufficiently developed to initiate a
second stage of research, that is the linking of the most
appropriate skills with particular applications. The
originality of this report lies not in the development of
process models from first principles, but the development of
composite modelling structures from the perspective of the model
user.

The potential of using existing models of two-stage
channels for the identification of dominant processes is
therefore accepted. Section 3.1.2 as a consequence investigates
various modelling alternatives available for two-stage channels.

3.1.2 Modelling alternatives for two-stage channels

The handling of the channel and the potential for
two-stage channel modelling in catchment models has already been
summarized in Chapter 2, table 2.1. The review concluded that
the modelling of two-stage channels in these catchment models
was of a resolution no greater than the handling of the channel
in MILHY2. In this section, alternative models specifically for
channel flows are investigated.

Models of two-stage channels have come from the fields
of both hydrology and hydraulics. Hydrologic approaches are
limited to one and (quasi) two dimensional approaches, whilst
hydraulic approaches include one, two and even prototype three
dimensional models.

Chapter 3

One dimensional and quasi two dimensional approaches usually take one of three alternative approaches to the problem of the two-stage channel. These approaches are to:

1)   Treat the channel/floodplain cross-section as a single system and average the boundary roughness and velocity differences between the flow segments, or

2)   Treat the floodplain as an area for storing water only, or

3)   Divide the cross-section into homogeneous segments of flow but do not consider the momentum transfers between these segments.

These one-dimensional approaches may be hydrologic or hydraulic. Hydrologic approaches tend to be incorporated as part of catchment models, whilst hydraulic channel models have been widely developed. Hydraulic techniques approximate the St. Venant equations of flow using either a kinematic or diffusion wave scheme.

Physically based two-dimensional models use the Reynolds equations to model the transfer of momentum between the segments of flow. These usually utilise either finite element or finite difference techniques and compute the fluxes between segments of flow using one of the three following techniques to quantify the fluxes:

1)   Compute the force to provide equilibrium in each segment of flow (apparent boundary shear force).

2)   Compute the effective friction factors for each segment.

Chapter 3

3)   Compute the turbulence between a shear layer and the
     velocity profile (turbulence model).

There are no hydrologic models that incorporate the
processes in the two-stage channel, although some empirical
equations have been developed. Knight and Demetriou (1983)
developed an empirical expression for the relationship between
the shear stresses produced by the momentum exchange and the
cross-sectional geometry, utilizing data from a series of flume
experiments. This relationship has not been incorporated into a
channel routing model.

3.2   Selection of a Two-Stage Conveyance Model

The objective of this section is to select from the model
types identified in section 3.1.3, a model that could be applied
to identify the most significant processes in the prediction
of flow in two-stage channels. From section 3.1, it would seem
that a successful two-stage conveyance model must incorporate:

1)   Plan and cross-sectional geometries.

2)   Momentum transfer between the floodplain and
     main channel flow segments.

3)   Boundary friction differences between the floodplain
     and the main channel.

The most appropriate model for this application, however,

Chapter 3

must exhibit as many as possible of the following criteria:

1)   the model should be physically-based or ideally not
      require calibration

2)   the model should be validated

3)   the model should be easy to understand and apply

4)   the model should not require large amounts of data

5)   the physically-based processes should be clearly
      defined and behave as independently as possible

6)   from the model it must be possible to compute the
      discharge

        State-of-the-art two-stage models incorporate complex
physically-based finite element or finite difference schemes.
The well documented schemes that exist, for example RMA-2V and
EMBER, require extensive system knowledge by the operator, and
demand large amounts of data. In addition, such models have not
been applied to the scale of reach under investigation here
(i.e. greater than 10km in length). The sophistication of
these schemes, therefore, made them unsuitable for this type of
application. A simpler approach was required.

        Analysis of the physically-based one-dimensional schemes
showed that there are no models that incorporate all three of
the essential elements identified from the literature in section
3.1. However, an analytical scheme by Ervine and Ellis (1987)
was identified as incorporating two of the essential physical

Chapter 3

requirements given. Further, it met most of the modelling
requirements.

The Ervine and Ellis scheme incorporates the effects of
plan and cross-sectional geometry and the effects of boundary
friction in a meandering two-stage channel. It does not,
however, attempt to incorporate the effects of momentum exchange
between the segments of flow. However, this is an area which
has been and still is being intensively investigated by, for
example, Knight and Hamed (1984), Myers (1987) and Prinos et
al. (1985). As there are a great number of papers on strategies
for incorporating momentum exchange, it was felt that it would
be reasonable to include the exchange of momentum as an
important process per se, and utilise the Ervine and Ellis
scheme to investigate other active processes.

3.2.1 The Ervine and Ellis model

Ervine and Ellis' model allows a meandering plan geometry
to be modelled by dividing flow into three segments, shown on
Figures 3.3a and b, which can be defined as:

1)   Main channel flow

2)   Floodplain flow contained within the meander belt of
      the main channel

3)   Floodplain flow outside of the meander belt

For each segment, the energy loss is computed and hence
the mean velocity for each segment and the discharge total are
also calculated. Ervine and Ellis (1987) firstly identifieid
the main sources of the energy loss in each flow segment and

Figure 3.3
Definition of Two-Stage Channel Geometry for
Ervine and Ellis Model, 1987

a) plan geometry definition
b) cross-sectional geometry
    definition

Chapter 3

then brought together a series of geometric abd frictional
relationships to describe them.

Main Channel Energy Losses

Ervine and Ellis considered there to be four possible
sources of energy loss in the main channel:

1)   Frictional losses at the boundaries of flow

2)   Transverse currents (secondary currents) at meander bends

3)   Turbulent shear stress (momentum transfer to the
      floodplain)

4)   Pool/riffle sequences causing head losses at low
      flows

They chose to omit the turbulent shear stresses and pool/
riffle losses in their computations. Shear stresses were
omitted because three-dimensional interpretations of established
techniques (e.g. Knight and Demetriou, 1983), are still under
investigation by Willets (see Ervine and Ellis, 1987).
Pool/riffle losses are considered less important in times of
overbank flow, when bed form effects are usually flooded out.

Floodplain Energy Losses

Two sources of loss were identified by Ervine and
Ellis:

1)   Frictional losses at the boundaries.

Chapter 3

2)   Expansion and contraction losses, shown in Figure 3.4,
      where flow orthogonal to the main channel suddenly expands
      as it drops into the channel, and contracts as it
      re-enters the floodplain region.

3.2.2 Quantifying the Energy Losses

Main Channel Energy Losses

1.   Friction

Head losses due to friction are computed over a meander
wavelength $(r\lambda_m)$ as:

$$h_f = \frac{f_c}{4} \cdot \frac{r\lambda_m}{R} \cdot \frac{V_c^2}{2g} \qquad \qquad 3.1$$

where f_c is the Colebrook-White friction factor, given by:

$$\frac{1}{\sqrt{f_c}} = -2\log\left(\frac{K_c}{14.8R} + \frac{2.51}{R_e \cdot (f_c)^{1/2}}\right) \qquad 3.2$$

2.   Transverse Currents

Head losses due to secondary currents at meander bends are
computed using a simplified method developed by Chang (1983).
Chang used a mean transverse current velocity because over a
meander amplitude, the velocity varies from a maximum at the
apex to a theoretical zero at the cross-over thalweg. Chang
ignored the effects of superelevation, where the centrifugal
forces cause the water level on the outside of the bend to be
higher than those of the inside. Yen (1967) showed that in
two-stage flow, superelevation effects are suppressed by the

31
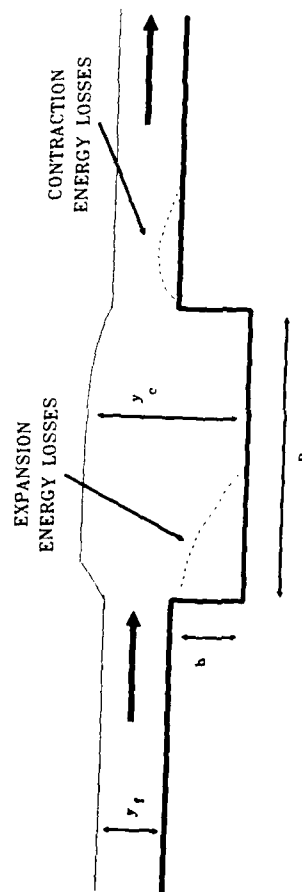
Figure 3.4
Expansion and Contraction Energy Losses
(after Yen and Yen, 1984)

Chapter 3

head of water above the main channel.

Head loss due to transverse currents computed over a
meander wavelength is given by:

$$h_1 = \frac{2.86\,(f_c)^{1/2} + 2.07 f_c}{0.565 + (f_c)^{1/2}} \cdot \left(\frac{R}{R_c}\right)^2 \ \frac{r\lambda_m}{y_c} \cdot \frac{V_c^2}{2g} \qquad 3.3$$

Floodplain within the Meander Belt Width

1. Friction

As in the main channel, the total frictional head loss
along a meander wavelength is described by:

$$h_f \quad \frac{f_{f1.}}{4} \ \frac{1}{y_f} \cdot \frac{V_{f1}^2}{2g} \cdot (W_m \cdot \lambda_m - r\lambda_m \cdot B_c) \qquad 3.4$$

where the last term is the wetted area.

2. Expansion Losses

Assuming: $\quad y_c \simeq y_f + h \qquad\qquad 3.5$

the head loss due to expansion of floodplain flow into the main
channel over a meander wavelength is given by:

$$h_e = r\lambda_m \cdot 1 - \frac{y_f^2}{y_c} \cdot \frac{V_{f1}^2}{2g} \cdot \sin^2\bar{\sigma} \qquad 3.6$$

where $\bar{\sigma}$ is the mean average angle of the floodplain
flow to the main channel over a meander length.

Chapter 3

3. Contraction Losses

The total head loss due to the contraction of flow as
it rejoins the floodplain segment from the main channel
(illustrated in Figure 3.4), is given by:

$$hc = C_L \frac{V_{fl}^2 \cdot \sin^2 \bar{\sigma} \cdot (r\lambda_m)}{2g} \qquad 3.7$$

where C_L is a loss coefficient, generated by Yen and Yen
(1984); and is a function of:

i)   the density, specific weight and kinematic viscosity
     of the flow,

ii) meander wave length and amplitude, the mean angle of
     incidence of floodplain flow in the main channel, the
     valley width, valley slope, floodplain roughness, and
     width and depth of the main channel,
     and

iii) discharge and slope.

Yen and Yen (1984), using data collected from flume experiments
computed the total loss coefficient after flow had been
subjected to expansion and contraction. Then assuming:

$$C = C_E + C_L \qquad 3.8$$

where C = total loss coefficient

C_E = loss coefficient due to expansion

C_L = loss coefficient due to contraction

Chapter 3

and

$$C_E = \left(1 - \frac{y_f}{y_c}\right)^2 \qquad\qquad 3.9$$

the contraction loss coefficient was computed. This is shown
in Table 3.1

Yen and Yen (1984) considered that the coefficients shown in
Table 3.1 should be treated as upper limits because the channel
sidewalls in their flume experiments were vertical rather than a
more realistic trapezoidal shape.

Floodplain Flow outside the Meander Belt

1. ## Friction

In the floodplain segment outside the meander belt, flow
is considered to be uniform, so that the friction slope is given
by:

$$S_o = \frac{f_{f2}}{4} \cdot \frac{1}{y_f} \cdot \frac{V_{f2}^2}{2g} \qquad\qquad 3.10$$

Combining all the head loss equations, Ervine and Ellis (1987)
obtained:

1) for the main channel

$$\frac{f_c}{4} \cdot \frac{r\lambda_m}{R} \cdot \frac{V_c^2}{2g} +$$

$$\frac{2.86(f_c)^{1/2} + 2.07f_c}{0.565 + (f_c)^{1/2}} \cdot \left(\frac{R}{R_c}\right)^2 \cdot \frac{r\lambda_m}{R} \cdot \frac{V_c^2}{2g} = S_o\lambda_m \qquad 3.11$$

Chapter 3

Table 3.1

Contraction Loss Coefficients

(after Yen and Yen, 1984)

y_f/y_c	C_L
0.0	0.5
0.1	0.48
0.2	0.45
0.3	0.41
0.4	0.36
0.5	0.29
0.6	0.21
0.7	0.13
0.8	0.07
0.9	0.01
1.0	0.0

Chapter 3

2) for the <u>floodplain inside the meander belt</u>

$$\frac{f_{f1}}{4} \cdot \frac{1}{y_f} \cdot \frac{V_{f1}^2}{2g} \cdot (W_m Y_m - \lambda_m B_c r) \; +$$

$$r\lambda_m \cdot \frac{V_{f1}}{2g} \cdot \sin^2\bar{\sigma} \cdot \left(\left(1 - \frac{y_f}{y_c}\right)^2 + C_L \right) = S_o \lambda_m \; W_m \qquad 3.12$$

3) for the <u>floodplain outside the meander belt</u>

$$\frac{f_{f2}}{4} \cdot \frac{1}{\bar{y}_f} \cdot \frac{V_{f2}^2}{2g} = S_o \qquad\qquad 3.13$$

4) <u>total discharge</u>

$$Q = V_c(B_c h) + V_{f1} \cdot y_f \cdot W_m + V_{f2} \cdot y_f (W_t - W_m) \qquad 3.14$$

3.3   Sensitivity Analysis of the Ervine and Ellis Scheme

The objective of undertaking a sensitivity analysis of the
Ervine and Ellis model was to identify the physical processes
controlling the velocity and discharge predictions. Once
identified, the most appropriate method of incorporating these
processes into the MILHY2 scheme can be investigated. A
sensitivity analysis of the scheme has not previously been
undertaken and this investigation therefore presents the
opportunity to assess the scheme.

3.3.1 Sensitivity analysis design

Analysis of equations 3.1 to 3.10 and 3.14 identified
five groups of physically based parameters which control

Chapter 3

the processes identified and modelled by Ervine and Ellis.
These five groups are:

1)   slope

2)   plan geometry - channel width, floodplain width,
      meander belt width and radius of curvature

3)   depth of flow - channel and floodplain segments

4)   sinuosity - sinuosity and angle of inclination of
      floodplain flow to the main channel

5)   friction - for consistency with MILHY the sensitivity
      of the model to Manning's n was used, utilizing the
conversion from Colebrook-White f given below:

$$f = \frac{8gn^2}{R^{1/3}}$$

3.15

      Each of these five groups was investigated individually by
varying each one by a systematic, 30% and 5% reduction and 5%
and 30% increase in parameter values.

      As the objective of this analysis was to identify
processes for further investigation, it was decided to apply the
model to a single reach.

      The structure of analysis, varying each of the five
parameter groups four times, generated 30 simulations, each with
the geometry varying in some way. It was felt that to provide
statistically meaningful variations, a much larger number of
simulations would be required, and this would not necessarily

Chapter 3

improve the identification of the most important processes in
the scheme.

The model was applied to a reach for which the parameter
values were generated from a reach on the River Fulda, West
Germany. A reach on the River Fulda was selected as the
catchment was being established for the validation of the
completed MILHY3 model. For the analysis of the Ervine and
Ellis scheme, the exact geometry of the reach is not
significant. In Chapters 4 and 5, a cross-section and reach
from the River Fulda catchment will be similarly utilised. A
description of the River Fulda catchment and the reason behind
its selection is reported in Chapter 6. The initial parameter
values are shown in Table 3.2 where the velocity predictions for
each flow segment and discharge total generated by the Ervine
and Ellis scheme are also given. Observed stage/discharge
relationships from the River Fulda show that the scheme gives
realistic results, the discharge predictions being less than 10%
out.

3.3.2 Results

The results from the sensitivity analysis are tabulated in
Tables 3.3 to 3.7, and show the percentage deviation from the
computed values tabulated in Table 3.2. Below is an analysis of
the velocity predictions by considering each of the sources of
head loss identified by Ervine and Ellis in turn:

(a) Frictional losses are modelled in all three flow segments
and Tables 3.3, 3.4 and 3.5 show that variation in the
frictional parameter values cause the largest variation in the
predicted velocity of the five parameter groups. However, in
the main channel the Darcy-Weisbach friction factor is also
linked to the modelling of the transverse (secondary)
circulation. From the first term in equation 3.3, it can be

Chapter 3

Table 3.2
Parameter Specification for a Hypothetical Reach

	SI units
Bed slope	0.0007
Sinuosity	1.3
Hydraulic radius	2.5
Radius of curvature	125.0
Width of meander belt	175.0
Total floodplain width	300.0
Channel width	30.0
Friction channel (f_c)	0.071
Friction floodplain 1 (f_{f1})	0.356
Friction floodplain 2 (f_{f2})	0.356
Channel depth	3.5
Floodplain depth	0.5
Angle of floodplain flow to channel (radians)	0.785
Contraction loss coefficient	0.47

Results

Main channel, velocity	1.205
Floodplain 1, velocity	0.360
Floodplain 2, velocity	0.278
Discharge	157.2

Chapter 3

seen that as the friction factor decreases, head losses from the
transverse currents decrease, and when the friction factor
increases the head losses are increased. Therefore, the
velocity variations shown in Table 3.3 incorporate both friction
head losses and transverse circulation losses.

(b)   The transverse circulation in the main channel can be
attributed to the friction (as noted above) and the ratio of the
hydraulic radius to the radius of curvature. This ratio is
included in the geometry variation reported in Table 3.3, which
shows that the velocity predictions are not sensitive to
geometric variation in the channel. As noted above, however,
the model is sensitive to the frictional aspects of the
transverse circulation.

(c)   Sinuosity changes generate significant variability in the
channel velocity results (see Table 3.3). From equation 3.11,
it can be seen that the sinuosity term is used to calculate
channel length in both the frictional head losses and transverse
circulation computation. For the main channel, therefore, the
model can be interpreted as being sensitive to channel length.

On the floodplain within the meander width belt (area 1),
Table 3.4 shows the velocity predictions are not sensitive to
sinuosity variations. From equation 3.12 it can be seen that
sinuosity is utilized to compute the flow path length and the
angle of incidence of floodplain flow to main channel flow,
which itself is used in the computation of the expansion and
contraction head losses. From Table 3.4, it would seem
reasonable to conclude that, because of the linear flow path of
the floodplain flow, the velocity predictions are not affected
by the length of the path, and it is not necessary, therefore,
to include the angle of incidence of floodplain flow in the

Chapter 3

Table 3.3

Channel Velocity Results

(% deviation from origin velocity)

% Change in variable	Decrease 30%	Decrease 5%	Increase 5%	Increase 30%
Slope	−19	−2	+3	+13
Friction	+50	+5	−4	−24
Geometry	−5	−0.5	+1	+3
Sinuosity	+20	+3	−11	−12

Chapter 3

Table 3.4
Floodplain 1 Velocity Results
(% deviation from origin results)

% Change in variable	Decrease 30%	Decrease 5%	Increase 5%	Increase 30%
Slope	−19	−2	+2	+13
Friction	+23	+5	−4	−27
Geometry	−4	−0.5	+1	+2
Sinuosity	+1	0.0	0.0	−1
Contraction coefficient	0.0	0.0	0.0	0.0

Chapter 3

Table 3.5

Floodplain 2 Velocity Results

(% deviation from origin results)

% Change variable	Decrease 30%	Decrease 5%	Increase 5%	Increase 30%
Slope	-19	-2	+3	+13
Friction	+25	+5	-5	-28

Chapter 3

modelling of expansion and contraction head losses. Table 3.4
also shows that the exact value of the Yen contraction loss
coefficient need not be of concern to the modeller.

(d)   The effects of slope variations on velocity predictions
were only significant where variations were large (+/- 30%), as
can be seen in Tables 3.3, 3.4 and 3.5. For the purposes of
this sensitivity analysis the frictional slope (S_o) was assumed
to be parallel to the bed slope, S. Hence uniform flow
conditions were assumed. The effects of the different
longitudinal slopes of the main channel and floodplain were not
directly included in the Ervine and Ellis scheme.

(e)   The impact of variation in the depth of flow on the
floodplain velocity results is shown in Table 3.6. Equation
3.11 shows that the main channel depth is incorporated in the
velocity computation as hydraulic radius, and the analysis of
intermediate computations in the analysis shows it is the
frictional head loss computation to which velocity results are
sensitive.

On the floodplain within the meander width belt, equation
3.12 shows it is the ratio of the floodplain to channel depth,
that is utilized to compute the expansion and contraction head
losses. However, the velocity predictions for floodplain area 2
are identical to those in floodplain area 1, and as the head
loss in area 2 is entirely attributable to frictional losses
(see equation 3.13), it would seem that the velocity variations
in area 1 are due to the same frictional effects and not due to
expansion and contraction losses.

Tables 3.6 and 3.7 illustrate the effects of variability
in the five parameter groups on the discharge predictions

Chapter 3

Table 3.6

Flow Depth Effects on Velocity and Discharge

(% deviation from origin results)

Depth		Channel Velocity	Floodplain Velocity		Discharge
y_f	y_c		Area 1	Area 2	
0.33	2.31	−12	−33	−23	−29
0.475	3.325	−2	−20	−20	−19
0.525	3.675	+4	−15	−16	−16
0.665	4.635	+15	−5	−5	−4
0.33	3.5	−	−18	−19	−14
0.475	3.5	−	−2	−2	−2
0.525	3.5	−	+2	+3	+2
0.665	3.5	−	+15	+15	+16

Chapter 3

Table 3.7
Discharge Results
(% deviation from origin results)

% Change in variable	Decrease 30%	Decrease 5%	Increase 5%	Increase 30%
Slope	-19	-2	+3	+13
Channel friction	+35	+4	-3	-17
Floodplain friction	+15	+2	-1	-9
Geometry	-28	-4	+4	+27
Sinuosity	+14	+2	-8	-9

Chapter 3

computed using equation 3.14. Geometry is the only group to
create additional influence on the discharge preictions, over
those already identified in the velocity results reported above.
The geometry variables effectively weight the velocity results
for each flow segments based on their cross-sectional area, to
give the total discharge.

3.3.3 Conclusions

From the analysis of the results above, it is possible to
make a number of conclusions:

1)   The Ervine and Ellis scheme is highly sensitive to
        the Darcy-Weisbach friction factor.

2)   The model is sensitive to the depth of inundation
        (incorporated in the computation of frictional head
        losses) in all flow areas.

3)   The sinuosity of the main channel is important in
        determining the length of the flow path and hence
        time to peak in a hydrograph.

4)   The incorporation of head losses due to expansion and
        contraction of floodplain flow as it crosses the
        the main channel is best achieved through the friction
        head loss computation.

3.4   Implication for the Development of MILHY2

The results of the analysis of the Ervine and Ellis scheme
isolate friction as being the single most important factor in
the prediction of discharge in two-stage channels. Friction is

Chapter 3

identified, therefore, as being the key to improving the channel
routing model in MILHY2. The analysis showed that the handling
of frictional head losses can successfully incorporate both
boundary roughness effects and effects of transverse currents
in the meandering channels. The second area worthy of
investigation is the impact of the relatively longer, sinuous
path length of the main channel over the floodplain path length.

Three key areas that need further investigation have,
therefore, been identified. These are:

i) Improvement of the handling of friction to incorporate
   boundary roughness and transverse circulation within the
main channel.

ii) Incorporation of turbulent shear stresses between
    the main channel and floodplain flow segments.

iii) The adoption of different path lengths for main channel
     and floodplain flow areas thereby incorporating
     sinuosity.

3.4.1 Present frictional capability of MILHY2

Friction is incorporated in the MILHY2 utilizing the
Manning's n coefficient. In selecting the most appropriate
n value, Chow (1959) identified ten factors which should be
considered. These are:

i) surface roughness
ii) vegetation
iii) channel irregularity
iv) channel alignment
v) silting and scouring

Chapter 3

  vi) obstructions
 vii) size and shape of channel
viii) stage and discharge
  ix) seasonal change
   x) suspended material and bed load

The list here shows that the Manning's n coefficient
incorporates the frictional effects identified in the analysis
above as being important in the analysis of two-stage flow.
However, it is impossible to select one Manning's n value that
can represent the frictional conditions at all times during the
passing of the floodwave through a two-stage channel.

At present, the only additional complexity to the
Manning's n handling of friction incorporated in MILHY2, is an
algorithm (equation 3.16) that reduces the coefficient value
with increasing stage:

$$n' = n - 0.0025R \qquad\qquad 3.16$$

If the dominant process active in the channel is boundary
roughness then this algorithm will improve the prediction of the
carrying capacity of the cross-section. In the main channel as
stage increases, the cross-sectional area of flow generally
increases more rapidly than the wetted perimeter, thus reducing
the retarding effects of boundary friction, (SCS, 1954). On the
floodplain too, Manning's n may decrerase as the depth of
inundation increases and the frictional effects of vegetation
become less significant. Table 3.8, taken from Chow (1959),
illustrates this frictional decline with increasing stage for
pasture and meadows.

Chapter 3

Table 3.8

Manning's n values for pasture and meadow floodplains

from Chow (1959)

| Depth of inundation | Manning's n value | |
feet	Pasture	Meadow
<1	0.05	0.10
1-2	0.05	0.08
2-3	0.04	0.07
3-4	0.04	0.06
>4	0.04	0.05

Chapter 3

Petryk and Bosmajian (1975) showed, however, that this is an over-simplification of the frictional effects of vegetation. They accept that when the vegetation is totally submerged the boundary frictional effects will decrease with increasing stage. However, when the inundation depth is below the top of the vegetation, there is a complex relationship between vegetation density and Manning's n. Petryk and Bosmajian (1975) used equation 3.17 to calculate the change in n with depth.

$$n = n_b \sqrt{1 + \frac{C_d \, \Sigma A_i}{2gAL} \left(\frac{1}{n_b}\right)^2 R^{4/3}} \, .$$ 3.17

where n_b = Manning's n value with vegetation effects

C_d = vegetation drag coefficient dependent on vegetation type

L = length of reach

A_i = projected area of ith plant

A = cross-sectional area of flow

Petryk and Bosmajian's (1975) scheme would not be suitable for the ungauged catchment because of the spatially detailed data it would require. However, the scheme does expose the inability of a single Manning's coefficient value to be selected for all stages if the effects of vegetation are considered.

The Manning's n reduction algorithm, equation 3.16, utilized in MILHY2 similarly only considers the effects of boundary friction in developing a relationship between n and stage. In the two-stage channel the boundary friction effects may not be the dominant frictional effect. Pasche and Rouve (1985) suggest that the eddies generated at the main channel/floodplain interface have a much greater frictional effect than boundary friction.

Chapter 3

Investigation of the present frictional capability of MILHY2 has exposed the inadequacy of the routine to incorporate the frictional effects of the dominant processes of two-stage flow. In addition, application of MILHY2 to two-stage flow conditions exposed a situation where the hydraulic radius became so great that the frictional algorithm (equation 3.16) generated negative discharge predictions. An example of this phenomenon is given in Table 3.9. In two-stage flow conditions, therefore, this frictional algorithm has been removed from the computation of the channel capacity.

Having exposed the inability of the present frictional capability of MILHY2 to incorporate the processes identified as being important in two-stage flow, the next stage in the research project is to develop a strategy for the incorporation of two-stage flow processes.

3.4.2 Strategy for the development of HYMO2

The analysis undertaken in this chapter has identified two areas of investigation that could improve the predictive capabilities of MILHY2. These are:

1.   Incorporation of Turbulence

Two significant sources of turbulence have been identified by the analysis in this chapter. These are:

   i) apparent shear stresses between the floodplain and main channel flow segments, and

   ii) transverse circulation stresses generated in meanders of the main channel (also known as secondary currents)

Chapter 3

Table 3.9
Rating Curve Computation for a Wide
Cross-sectional Geometry

Water Surface elevation m	Flow Area m^2	Flow Rate $m3s^{-1}$ $(x10^3)$
1.0	8.0	0
2.2	27.8	0.03
3.3	53.3	0.09
4.4	95.7	0.2
5.4	381.5	0.3
6.5	783.8	1.8
7.6	1200.4	7.3
8.7	1679.6	1009
9.8	1206.3	-1.5
10.9	2841.2	-9.3

Chapter 3

The relative importance of these two sources and the interaction
between them is not clear from the literature, although it does
seem to be dependent on the depth of the flow on the floodplain.
However, the analysis of the Ervine and Ellis (1987) scheme
suggested that the effects of transverse currents at meander
bends could be incorporated in the modelling of boundary
friction, whilst Chang (1983) suggests that the effects of
transverse currents are suppressed in our-of-bank conditions.
This report concentrates, therefore, on the shear stresses
between the main channel and the floodplains.

2.   Incorporation of Multiple Routing Pathways

       Both the analysis of the Ervine and Ellis scheme and work
done by Fread (1976) suggest that the different path lengths of
the main channel and floodplain flows will affect the timing of
the floodwave travelling downstream. At present MILHY2 models a
single pathway for the floodplain and channel flows using a mean
reach length and travel timetable. A priority, therefore, is to
investigate alternative methods of incorporating multiple
routing pathways of flow through the reach.

       Having identified the process areas that can be most
profitably investigated, it is important that a strategy for the
implementation of the investigation is developed. The overall
objectives of this report, outlined in Chapter 1, include the
validation of any new modules.

       The importance of a well structured validation or model
evaluation procedure cannot be under-stated. Miller et al.
(1976) pointed our that model evaluation procedures have usually
been postponed until the stage has been reached when observed
and simulated output can be compared. The danger of leaving
evaluation to this late stage is that a large amount of time and

Chapter 3

resources have been invested in model development and the
friction in any radical change in methodology might be too
great.

Sargent (1982) generated a three-stage model evaluation
programme illustrated in Figure 3.5, incorporating mathematical
validation, model verification and operational validation.
Sargent's scheme shows the importance of model evaluation to all
stages of development; from the conceptual devlopment and
mathematical description of the system to the computer coding
and performance of the completed model.

This report attempts to incorporate Sargent's evaluation
scheme in the development of a composite modelling strategy
utilising MILHY2. The new modules that will be developed in
Chapter 4 and 5 increase the resolution of the channel routing
component, will be evaluated individually before the new
programme, MILHY3, is put together. This individual model
evaluation will include critical assessment of the mathematical
techniques selected and the use of observed and hypothetical
data sets to judge the performance of the module.

MILHY3 will be subject to further evaluation investigat-
ions described and developed in Chapter 6 and analysed in
Chapters 7 and 8.

An approach and an area for this research project have now
been defined. The approach of the project is to develop a model
suitable for flood forecasting in ungauged catchments from the
perspective of the potential user, but utilizing a composite
modelling structure. The research area that has been identified
is the introduction of a two-stage behaviour.

ACTUAL
HYDROLOGICAL
SYSTEM

OPERATIONAL
VALIDATION

MATHEMATICAL
MODEL
VALIDATION

Experi-
mentation

Analysis
and
modelling

COMPUTER
PROGRAM

Programming and

MATHEMATICAL
MODEL

implementation

COMPUTERIZED MODEL VERIFICATION
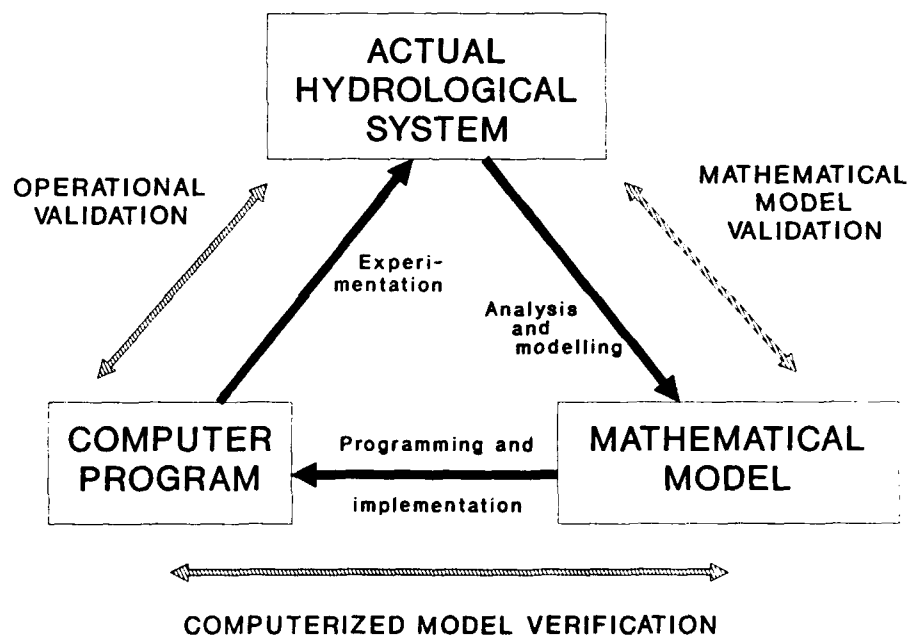
Figure 3.5
Three Stage Model Evaluation Programme
(after Sargent, 1982)

Chapter 3

The development of a composite modelling structure has
highlighted the importance of module resolution in the
establishment of operational guidelines for the potential user
of the MILHY3 scheme. The objective of the rest of this report
is to explore the relationship between module resolution and
model predictive accuracy and performance.

3.5 **Summary**

This chapter has discussed the behaviour of flow in two-stage
channels and alternative methods of identifying the dominant
processes in the system. A model developed by Ervine and Ellis
(1987) was identified as incorporating the cross-sectional and
plane geometry of two-stage channels. This model was then
subjected to a sensitivity analysis to help identify the most
important factors influencing flow prediction in two-stage
channels.

Analysis of the results from the Ervine and Ellis
simulations showed that friction is the most important process
controlling cross-sectional flood prediction. The components of
the friction were then identified as being boundary friction
effects and turbulent eddies. The turbulent eddies are
generated from the interaction of channel and floodplain flows
and at meander bends. The modelling of the turbulent
interaction of channel and flood flows was selected as being the
most profitable as it is an area ignored by other models. An
investigation into the turbulence generated at the
floodplain/channel interface is reported in Chapter 4.

The analysis of the Ervine and Ellis scheme also
identified the importance of the differing path lengths of
channel and floodplain in the prediction of the timing of the
flood hydrograph. The incorporation of such multiple routing
pathways is investigated in Chapter 5.

Chapter 3

The importance of a structured model evaluation strategy
has been stressed and Sargent's (1982) three-stage programme of
development will be followed. This programme includes the
individual evaluation of the turbulent exchange and multiple
routing modules, prior to the evaluation of the new MILHY3
model.

Chapter 4

Chapter 4

Incorporation of Momentum Transfer between

Floodplain and Channel Segments

The transfer of momentum between the main channel and floodplain flow segments was identified in section 3.4 as a process which it was felt would, if incorporated into MILHY2 downstream routing scheme, make a significant improvement to the overall predictive capability of MILHY2. The objective of the work reported in this chapter is, therefore, to investigate, implement and validate a method of incorporating momentum transfer between flow segments whilst retaining MILHY2's parsimonious data requirements. In the first section, therefore, the process of momentum transfer is investigated.

4.1   The Hydraulics of Momentum Transfer

In two-stage channels, the irregular cross-sectional geometry of the deep channel, and its associated shallow floodplains, generate higher velocities in the main channel than those in the floodplain flow segments. This is due to the relatively greater depth of flow and smaller wetted perimeter of the main channel in comparison with the floodplain. Figure 4.1 illustrates the velocity isovels (lines of equal velocity) for a two-stage flume experiment conducted by Knight et al. (1983). The velocity isovels are dimensionless parameters because the observed values are divided by the mean velocity for the cross-section, where $V=Q/A$. Figure 4.1 shows that maximum main channel velocities are at least 25% greater than the average velocity, whilst floodplain velocities are as
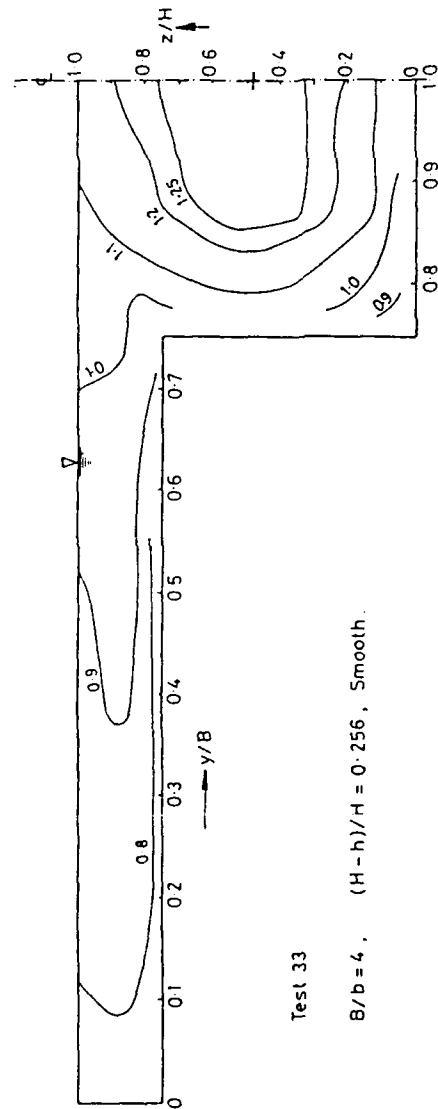
Figure 4.1
Velocity Isovels Generated from a Two-Stage Channel
Experiment Conducted by Knight et al. (1984)

Chapter 4

low as 70% of the average. Figure 4.1 also illustrates the
distribution of the velocity isovels, with maximum channel
velocities occurring in the centre of the channel away
from the influence of the floodplain. In contrast, the maximum
velocities in the floodplain occur close to the main channel,
and velocities decrease with increasing distance from the
channel. The difference in the flow velocities between the main
channel and floodplain cause a transfer of longitudinal momentum
generally from the main channel to the floodplain.

There are four physical mechanisms by which linear
momentum can be transported perpendicular to the direction of
flow. Wright and Carstens (1970) ranked these processes on a
scale of one to four in the order of their effectiveness of
transporting momentum, the first being the most effective.
Their ranking is:

i) transverse circulation stresses (secondary currents)

ii) eddie. generated in the mixing zones of stream tubes
of differing velocities

iii) eddies generated by flow along a boundary

iv) molecular motion

Figures 4.2a and 4.2b illustrate the first three
processes, that is, secondary currents, the eddies generated in
the mixing zones and eddies generated by flow along a boundary.
Figure 4.2a shows that the eddies generated by flow along a
boundary are contained within the main channel and that the
eddies generated by mixing zones are positioned at the main
channel/floodplain interface. Figure 4.2b shows the secondary

a

b

secondary
flows

isovels

bed
shear
stress

maximum stress
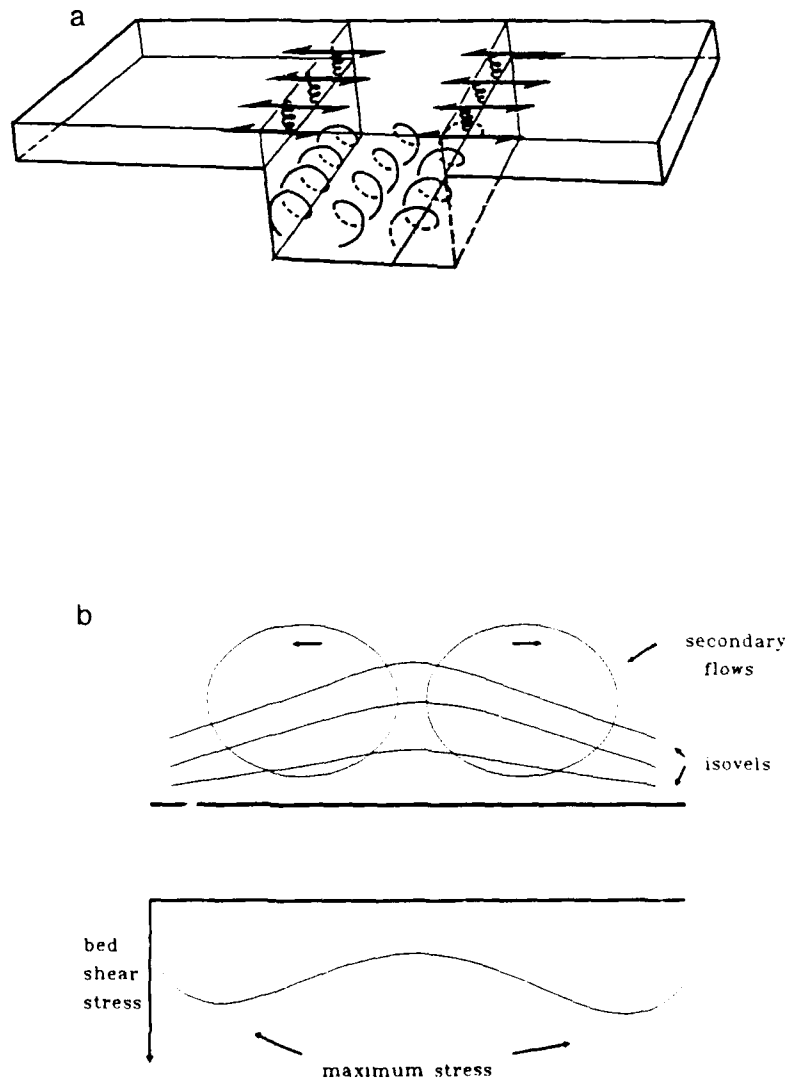
Figure 4.2
Mechanisms by which linea⁻ momentum may be transported
perpendicular to the direction of flow

Chapter 4

currents generated in a meandering main channel. The
centrifugal forces in a meander bend cause the flow to be drawn
to the outer bank of the main channel. This generates a cell
orthogonal to the longitudinal flow; a second cell near the
outer bank may also develop. The direction of the circulation
of these secondary cells varies according to the relative
position of the cells within a meander wavelength. Keller and
Melhorn (1973) show that the cells diverge at the surface in
riffle sections and converge at the surface in pool section. In
addition, Hey and Thorne (1975) have shown that at the apex of
the meander bend the cells may be asymmetric, with the strong
centrifugal forces suppressing the cell nearest the outer bank.

As suggested earlier in section 3.4, it is not known which
of these processes is dominant in two-stage channels. The
analysis of the Ervine and Ellis (1987) scheme identified the
first two of these processes as being important in the two-stage
channel but did not account for the other two processes. In
theory it would seem that the eddies generated by the mixing of
differing velocity tubes must be greater in a two-stage channel
than in a single channel system because the cross-sectional
velocity gradient is greater. It would also seem logical
that the secondary current eddy system would be suppressed by
the head of water in over-bank flow in much the same way as the
effects of superelevation are suppressed (Yen, 1967). The
importance of boundary friction eddies and molecular transport
transfer is also not clear. However, in view of the fact that
Wright and Carstens (1970) ranked these two processes as being
less efficient at the transfer of momentum that the first two
processes, they can for the moment be considered as
insignificant in momentum transfer in two-stage channels.

Chapter 4

It is accepted in this report, therefore, that the
dominant control over the transfer of momentum between the main
channel and the floodplain is the mixing eddies caused by the
velocity gradient. If the validation procedure highlights the
importance of omentum transfer in the improvement of MILHY2's
flood prediction accuracy, then the importance of the other
three processes of momentum transfer would need to be
reconsidered.

A great deal of research on the transfer of momentum in
two-stage channels has been carried out in the last twenty-five
years, starting with Sellin (1964) and Zheleznyakov (1965).
Sellin (1964) was the first to identify turbulence at the
interface between main channel and floodplain by photographing
the vortices generated by turbulence in a flume-based study.
Zheleznyakov found in both flume (1965) and field experiments
(1971) that the momentum transfer mechanism decreased the
overall rate of discharge for floodplain depths just over
bankfull.

Radojkovic (1976) identified the dependence of the shear
stress on the velocity profile in two-stage channels, while
flume studies by Knight (1989) have shown that the momentum
transfer distorts the shear stress profiles on the bed of the
main channel and floodplain. Most noticeable was the increase
in the shear stresses on the floodplains near the junction with
the main channel.

The distribution of the shear stress in two-stage channels
is significant as the pattern provides a means of visualising
and interpreting the behaviour of the momentum exchange process.
Figure 4.3 illustrates a typical shear stress distribution
measured in a flume-based experiment conducted by Knight and Lai
(1985). By analysing this distribution, an interface can be

floodplain   main channel   floodplain

shear layers
velocity
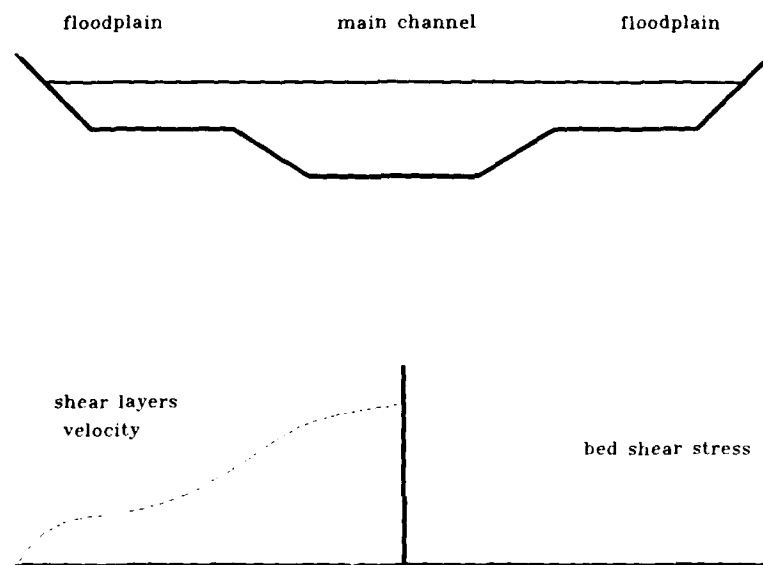
bed shear stress

Figure 4.3
Distribution of Shear Stresses in a Two-Stage Channel
(after Knight and Lai, 1985)

Chapter 4

imagined acting along the velocity gradient between the main
channel and floodplain. The position of this interface is
marked by the concentration of the shear stresses, as shown in
Figure 4.3.

The concept of an interface has been utilised in many
recent investigations in two-stage channels. In the United
Kingdom, the Science and Engineering Research Council is funding
a large flume-based project in four universities, based on the
concept of such an imaginary interface (see Knight et al. 1984).
Further, Holden and James (1989) have attempted to quantify the
rate of momentum transfer utilising the shear stress
distribution on this imaginary interface.

The shear stresses acting on this imaginary interface are
generally known as the 'apparent shear stresses', to distinguish
them from the shear stresses that act on the physical boundary
(bank or berm) between the main channel and the floodplain. In
the next section, the alternative concepts available for
modelling momentum transfer utilising the concept of the
imaginary interface and apparent shear stresses are
investigated.

4.2   Modelling of Momentum Transfer

4.2.1 A theoretical approach

If a geometrically regular two-stage channel experiencing
uniform flow is analysed, then the total retarding shear force
acting on the wetted perimeter is equal to the gravitational
force acting downstream. The gravitation component is given by:

$$F_g = w A_t S_o \qquad\qquad 4.1$$

Chapter 4

where w = weight of water per unit length of channel

A_t = total cross-sectional area

S_o = bed slope

The boundary shear force per unit length is given by:

$$F_b = T_c P_c + T_f P_f \qquad\qquad 4.2$$

where T_c and T_f = average boundary shear stresses for the channel and floodplain respectively

and P_c and P_f = wetted perimeters of the channel and floodplain

Equations 4.1 and 4.2 must balance for the two-stage channel cross-sections but they must also balance for the individual floodplain and channel flow segments. However, if the flow segments are considered individually, then part of the boundary shear force is provided by the apparent shear stress force acting on the boundary between the flow segments. Thus in the case of the main channel the total retarding force per unit length is given by:

$$F_{sc} = T_c P_c + T_{ai} P_{ai} = F_{bc} + 2F_a \qquad\qquad 4.3$$

where T_{ai} = apparent shear stress acting upon the assumed interface i

P_{ai} = length of assumed interface i

F_{bc} = main channel solid boundary shear force

Figure 4.4 illustrates these forces for a theoretical example where the apparent shear stresses are assumed to be acting on a vertical planar boundary where the channel and floodplain meet. Rewriting equations 4.1 and 4.2 for the channel segment only and combining with equation 4.3 gives:
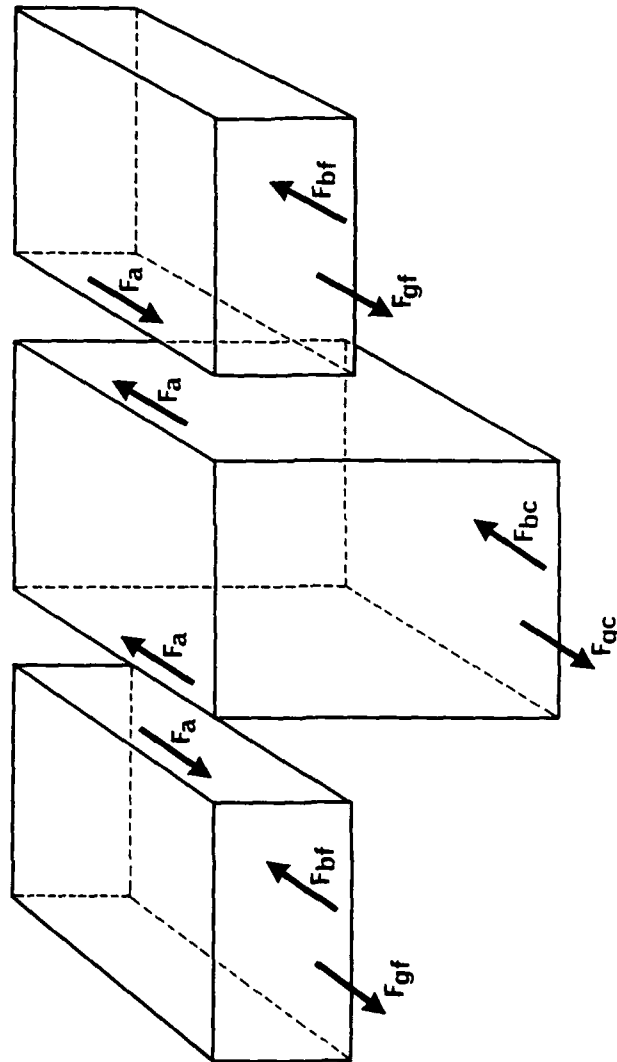
Figure 4.4
Theoretical Shear Stresses Acting on the Boundaries and Assumed
Vertical Interfaces of a Two-Stage Channel

(after Wormleaton et al., 1982)

Chapter 4

$$T_{ai} = \frac{1}{P_{ai}} \ (wA_{ci}S_o - T_c P_c) \hspace{3cm} 4.4$$

In any application A_{ci}, P_c and S_o are known from the geometry of
the cross-section and a length for P_{ai} can be assumed. In the
flume the average boundary shear stresses, T_c, may be measured
and so T_{ai} can be estimated using equation 4.4. The discharge
for each flow segment can be computed from the corrected
retarding forces.

However, in an ungauged catchment, it is unlikely that
boundary shear stress data would be available, or that the
length of the apparent shear stress boundary could be estimated.
It is not suggested, therefore, that this type of analysis be
incorporated into MILHY2 but investigation of the application of
this method in flume experiments does provide a useful insight
into the relationship between the cross-sectional geometry,
apparent shear stress interfaces and accuracy of the discharge
prediction.

4.2.2 Flume experiments investigation of apparent shear stresses

Flume-based research programmes provide, at present, the
only means of collecting data on the distribution boundary shear
stresses which will enable the understanding and later modelling
of the active processes in two-stage channels. Field data of
two-stage flood events can be both very difficult and sometimes
dangerous to collect. The variable nature of flood events means
that flows are never steady enough to allow even reasonable
measurement of the velocity fields, while accurate field
measurements of boundary shear stresses are almost impossible.
Reliance on flume-based investigations has, therefore, led

Chapter 4

to an extensive programme of modelling a variety of geometrical and roughness environments.

In these flume experiments, the principal objective of the investigations is to develop a relationship between the stage and discharge in the main channel and floodplain flow segments. The investigations attempt to achieve this objective by solving equation 4.4 using observed flume data to compute the apparent shear stresses from the solid boundary shear stresses. The boundary shear stresses are computed using the Prandtl-Von Karmen velocity law, utilizing observed velocity data, or using Patel's (1965) relationship between head difference and boundary shear stresses. As noted earlier, however, and seen in equation 4.4, the value of the computed apparent shear stresses is dependent on the length of the assumed interface over which the apparent shear theoretically acts. Figure 4.4 illustrates an assumed interface in a vertical plane, a method which has been utilized by Chow (1959) and Wright and Carstens (1970). Figure 4.5 shows the vertical plane and diagonal interfaces used by Wormleaton et al. (1980), and Yen and Overton (1973), and the horizontal interfaces utilized by Deuller et al. (1967).

Wormleaton et al. (1982) carried out a comparative investigation of the apparent shear stresses computed over the three types of planar interface; vertical, diagonal and horizontal. Their results were reported as an apparent shear stress ratio, that is the ratio of the apparent shear stress to the average shear stress including the assumed interface. As the apparent shear stress tends to zero, the ratio will tend to zero, implying no shear on the interface, The results of Wormleaton et al. (1982) are shown in Figures 4.6a, 4.6b and 4.6c for the vertical, diagonal and horizontal interfaces respectively, where the apparent shear stress ratio and an

Figure 4.5
Vertical, Diagonal and Horizontal Assumed Interfaces
Between Floodplain and Main Channel Flows
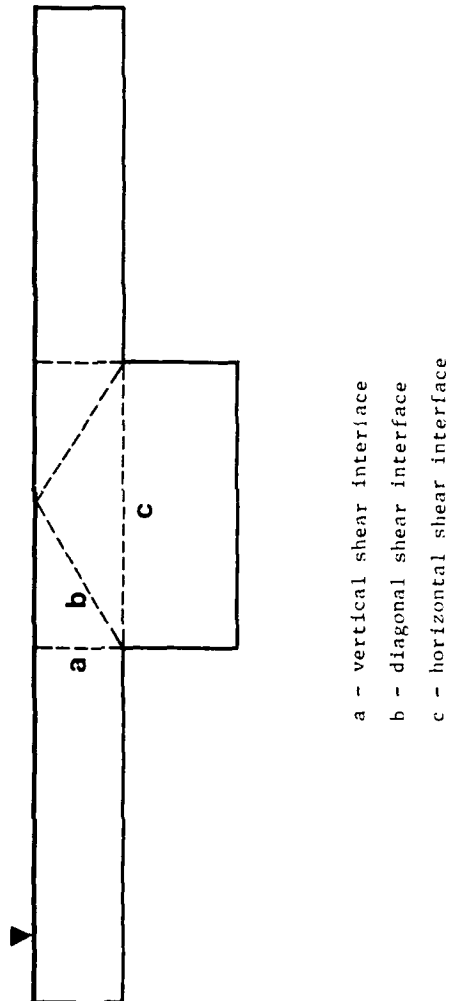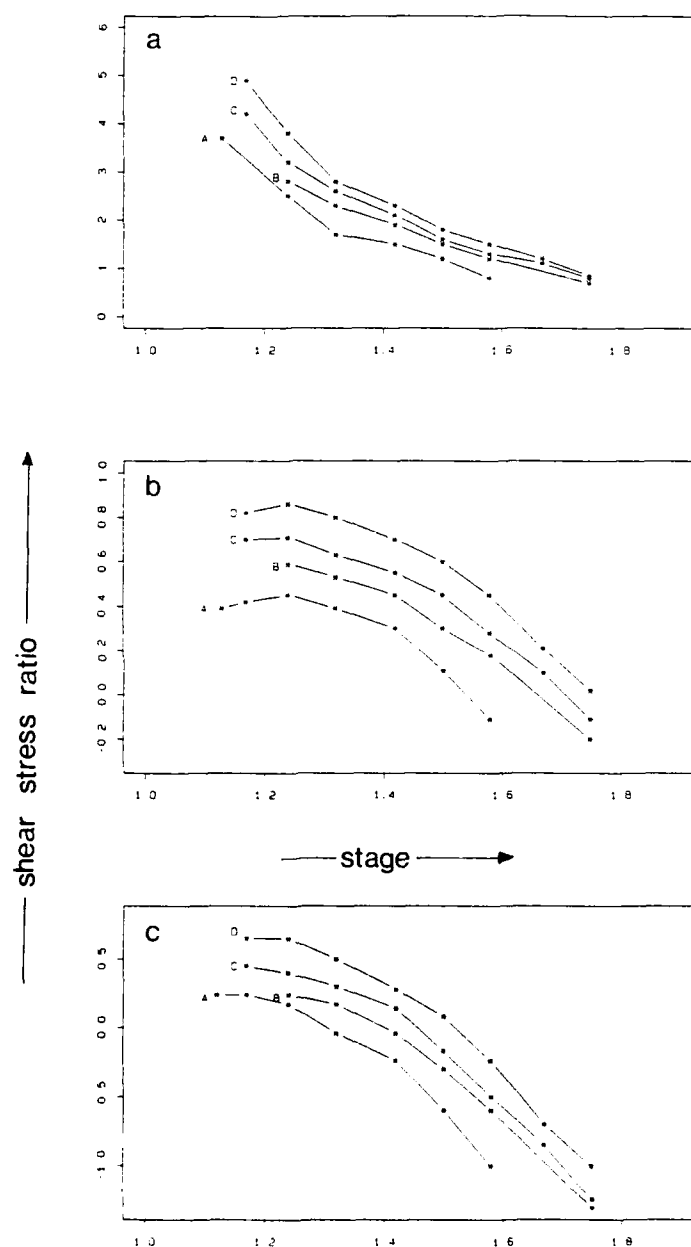
Figure 4.6
Stage/Apparent Shear Stress Ratio Relationships for Vertical, Diagonal
and Horizontal Assumed Interfaces
(after Wormleaton et al., 1982)

Chapter 4

inundation ratio are compared. The inundation ratio is defined as the depth of flow on the floodplain divided by the depth of the main channel. The series A, B, C and D illustrate the effects of increasing the floodplain Manning's n roughness coefficient from 0.011 for series A through 0.014 (B), 0.017 (C), to 0.021 for series D.

Analysis of Figures 4.6a, 4.6b and 4.6c shows that the apparent shear stress declines with increasing depth of flow on the floodplain in all three planar interfaces. The order of magnitude difference between the apparent shear stresses computed for the vertical interfaces and those computed on the diagonal and horizontal interfaces should be noted. This shows that the vertical interface is much nearer to the turbulent eddies photographed by Sellin (1964). Analysis of the boundary stress distributions showed that the negative apparent shear stress ratios computed for the diagonal and horizontal interfaces at higher floodplain inundation depths indicate a transfer of momentum from the zone of flow above the main channel to the within-bank main channel zone.

Wormleaton et al. (1982) apparently aware of the criticism that all their shear stress values were computed using a single cross-sectional width, developed a relationship by regression analysis between geometric and velocity parameters for the apparent shear stresses. This could then be compared with data collected by other authors, often for very different applications, and so utilize data from a wide variety of cross-sectional geometries. Wormleaton et al. (1982) give a final regression equation for the stresses on a vertical interface as:

Chapter 4

$$T_{av} = 13.84 (\Delta V)^{0.882} \cdot \frac{y_t}{d_c}^{-3.123} \cdot \frac{B_f}{B_c}^{-0.727} \qquad 4.5$$

where ΔV is the velocity difference between the floodplain
and main channel flow segments, computed from the Manning
equation. Utilizing the data from 34 experimental frames, the
coefficient of determination was 0.983. Data collected by Myers
(1978), Crory and Elksawy (1980) and Ghosh and Jena (1971) were
found to conform closely with the relationship given in equation
4.5.

Yen and Overton (1973) tackled the problem from an alternative
perspective by using the measured boundary shear stress profiles
to position an interface along which no shear would take place.
The cross-section could then be divided up using these no-shear
boundaries and the discharge computed easily, as it would be
directly related to the segment's cross-sectional area. Yen and
Overton (1973) attempted to relate the angle of a zero shear
interface, pivoting around the main channel/floodplain intercept
(see Figure 4.7) to observed discharge values. If this angle
could then be related to cross-sectional geometric parameters,
this method could be applied simply to a wide variety of
problems.

Yen and Overton's (1973) results showed that the angle of
inclination of the zero shear stress plane varied with both the
ratio of floodplain to main channel width, and the ratio of
floodplain inundation to main channel depth. With a range of
width ratios between 2.2 and 5.4, the angle of inclination
varied by as much as 20°, with the angle increasing as the width
ratio decreased. The angle of inclination varied with a depth
ratio range of 0.2 to 1.8 by 60°, the angle increasing linearly
(between 15° and 50°) until a depth ratio of about 1.0, after
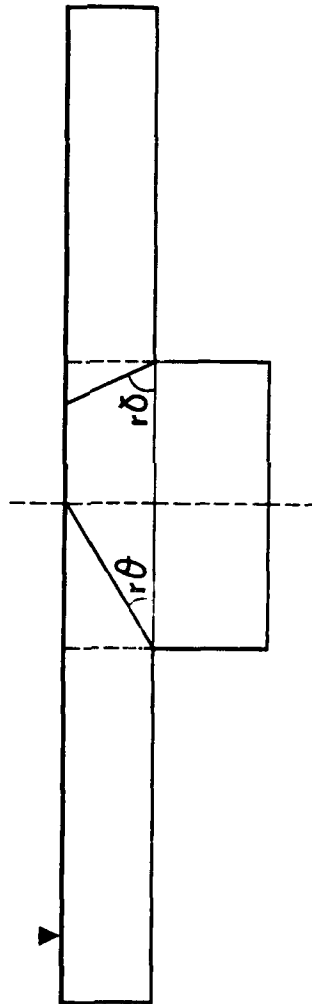
Figure 4.7
Angle of Assumed Interface Inclination
(after Yen and Overton, 1973)

Chapter 4

which the relationship became exponential. The angle of
inclination of zero shear stress for a particular cross-section
does not vary, therefore, when the depth ratio is above 2.

The results of Wormleaton et al. (1982) reported in
Figure 4.6 agree with those of Yen and Overton (1973) and show
that when the ratio of the floodplain inundation to main channel
depth is approximately 2 or above, the two-stage channel may be
considered as a single system. Below this ratio, the distrib-
ution of the turbulent shear stresses has been shown to be
complex, where no one single position of the apparent shear
stress interface or stress ratio can be adequately applied to
describe the boundary shear stresses over a variety of
cross-sectional geometries.

4.2.3 Implications of flume-based experiments for the prediction of the discharge capacity of two-stage channels

It was noted earlier in Section 4.1, that the main
reason that the relationship between cross-sectional area and
discharge does not hold for two-stage channels is the transfer
of momentum between the main channel and the floodplain. The
flume-based experiments reported in Section 4.2.2 attempt to
quantify these momentum transfers by balancing the gravitational
and retarding forces by the introduction of an apparent shear
stress over a dividing interface between segments of flow.
However, in order to compute the discharge capacity, there
is a need to develop a relationship between easily measured
geometric parameters and the stage/discharge rating curve.
There are several alternatives that could be used in this
respect:-

Chapter 4

1)   Empirical relationships, developed for flume experiments,
     designed to predict the percentages of flow in each cross-
     sectional segment. These are developed from regression
     analysis of the computed apparent shear stresses on
     assumed interfaces. Examples include the relationships
     developed by Wormleaton et al. (1982) and by Knight and
     Demetriou (1983).

2)   Division of the cross-section using the zero-shear
     interfaces, suggested by Yen and Overton (1973).

3)   Division of the cross-section using shear interfaces
     and making some assumption about the amount of momentum
     transfer across these interfaces

     Each of these alternatives are now considered. The
first proposition to use empirically developed relationships
seems attractive, in that it would be simple to apply. However,
the relationships have been developed using data collected in
flume experiments which have limited cross-sectional geometries.
Table 4.1 shows the geometric parameters of the major flume
investigations that have published this type of data.
Comparison of the floodplain to main channel widths shows a
maximum ratio of 3 where, in many catchments, flood inundation
maps illustrate a width ratio of up to 50. Similarly, the
maximum Manning's n roughness coefficient applied to the
floodplain is 0.022, whilst Chow (1959) suggests a typical
grazed pasture to have a Manning's value of 0.03. To
generate empirical relationships applicable to the sorts
of two-stage channels, typical in Europe, therefore, there
is a need for further flume experiments with much wider
and rougher floodplains. Until this is achieved, it would

Table 4.1

Cross-sectional geometric and roughness parameters for flume-based investigations
into the transfer of momentum between the main channel and floodplain

Author	Channel width m	Floodplain width m	Channel depth m	Floodplain inundation range m	Manning's 'n' channel	floodplain
Wormleaton et al. (1982)	0.29	0.46	0.12	0.02-0.09	0.011	0.011-0.021
Myers (1984)	0.16	0.18,0.30	0.08	0.01-0.07	perspex	
Crory & Elksawy (1980)	0.10,0.15	0.36	0.10			
Ghosh & Jena (1971)	0.20	0.15	0.10			
Knight & Demetriou (1983)	0.15	0.00-0.30	0.08	0.01-0.03	perspex	
Rajaratnam & Ahmadi (1981)	0.51	0.71	0.10	0.01-0.06	0.013	0.013
Prinos et al. (1985)	0.51	0.38	0.10	0.05-0.12	0.011	0.011-0.022
Noutsopoulos & Hadjipanos (1983)	0.51	0.26-0.43	0.08	0.09-0.15	0.011	0.011-0.021
Smith (1978)	0.27	0.47	0.08	0.05-0.08	0.013	0.013
Asano et al. (1985)	0.9-2.4	3.0	0.03-0.12	0.01-0.21	0.009-0.01	0.013

Chapter 4

be inadvisable to extrapolate the existing relationships to
geometries and roughnesses outside those reported in Table 4.1

The second alternative given is to divide the cross-
section using zero-shear interfaces, as suggested by Yen
and Overton (1973). As there is no momentum transfer across the
zero-shear interfaces, the Manning equation will hold for each
cross-sectional flow segment. Although Yen and Overton computed
the angle of incidence of the interfaces for width ratios up to
5, the sensitivity of this angle to floodplain roughness means
the results cannot be reliably applied. It is also rather more
difficult to compute the area of flow in a cross-section
using Yen and Overton's method than a vertical, diagonal or
horizontal interface method.

However, zero-shear interface has been applied widely
for a number of years. One of the most frequently used
techniques was developed by Lotter (1933) and computes the
capacity of a cross-section by dividing the section using
vertical interfaces. These interfaces are designated as being
zero shear faces and, therefore, the length of the interface is
not included in the computation of the channel capacity. As Yen
and Overton (1973) have shown, however, such interfaces are not
vertical, but vary from the inclined towards the horizontal as
the depth of flow increases. Zero-shear interfaces can be
applied, therefore, for vertical, diagonal and horizontal
inclinations by ignoring the assumed interface in the wetted
perimeter computation and taking into consideration the solid
boundaries only.

The third suggested means of computing the discharge
capacity of the cross-section involves dividing the cross-
section using the shear interfaces, making an assumption

Chapter 4

about the amount of momentum transfer across these interfaces.
In a similar way to the zero-shear interfaces, shear interfaces
have been applied in a great number of environments, using
vertical, diagonal and horizontal inclinations. The assumption
here is that the apparent shear stress is equal to the average
shear stress (apparent shear stress ratio = 1, see Figure 4.6),
so that the interface can be included as part of the wetted
perimeter in the discharge capacity computation.

Wormleaton et al. (1982) computed the discharge for the
zero-shear and shear interfaces for all three inclinations over
a variety of floodplain roughnesses up to n = 0.021. As
expected, their results showed that for all interface
inclinations the computed discharge values converged to, or were
smaller than, the observed values, when the floodplain/channel
depth ratio increased to 2. However, the accuracy of the
discharge prediction using these six techniques was considered
only with variation in the depth ratio and floodplain roughness;
the width ratios were not considered.

The implication of the flume-based experiments to the
computation of discharge in two-stage channels, is that no
single technique of incorporating turbulent exchange between the
main channel and floodplain is appropriate for all geometric and
roughness environments. The flume experiments need to be
extended before a set of operational rules on the suitability of
zero-shear or shear interfaces and their angle of inclination
can be developed.

Chapter 4

4.3   Incorporation of Momentum Transfer into MILHY2

Analysis of the flume-based experiments, in section 4.2,
has shown that there is no single method of incorporating
momentum transfer between flow segments that is appropriate for
cross-sectional geometries and roughnesses. For this reason,
and because of the lack of comparative work on wide and rough
floodplains, it seems appropriate to incorporate a number of
different methods into MILHY2 and test the accuracy of the
discharge predictions against observed field data.

4.3.1 Selection of methods for incorporation into MILHY2

Four methods of dividing the cross-section to incorporate
momentum transfer were selected from the alternatives identified
above. These four were selected primarily because of the ease
with which they could be incorporated into the MILHY2 code and
because they are the four techniques utilised by Knight and
Hamed (1984). By using the same techniques as Knight and Hamed,
a comparison between field data collected for this project and
flume experiments would be possible. It is accepted, therefore,
that the four techniques selected offer no theoretical
advantages over the other methods of dividing the cross-section
identified earlier. The four techniques selected are:

1)   Vertical subdivision, with zero shear interfaces

2)   Vertical subdivision, with an apparent shear stress
      ratio = 1

3)   Diagonal subdivision, with zero shear interfaces

4)   Diagonal subdivision, with an apparent shear stress
      ratio = 1

Chapter 4

At present, method 2, that is vertical subdivision with an
apparent shear stress ratio equal to 1, is incorporated into
MILHY2. By application of these four techniques it should be
possible to test the sensitivity of the generated rating-curve
to the interface inclination and apparent shear stress ratio.
This sensitivity could then be compared to the impact on the
rating curve of the variation in the cross-sectional geometry
and roughness parameters. If the analysis showed that the
rating-curve is sensitive to the computational method then
further methods including horizontally inclined interfaces and
Yen and Overton's (1973) angle of inclination could be
incorporated and tested.

4.3.2 Incorporation of the four methods into MILHY2

The four methods, identified above, of incorporating
momentum transfer between the main channel and floodplain, are
the same four methods utilized by Knight and Hamed (1984).
Knight and Hamed tested the accuracy of the four identified
techniques in predicting discharge by comparing the predicted
results with those collected from flume experiments conducted by
Knight and Demetriou (1983), reported in Table 4.1. For
consistency, and to ensure that the correct cross-sectional
definitions were being applied to MILHY2 for each of the four
methods, the equations of definition reported in Knight and
Hamed's (1984) paper were incorporated into MILHY2. These
equations are given in Table 4.2, whilst Figure 4.8 defines the
cross-sectional geometry variables used. The equations in
Table 4.2 show that the wetted perimeter of the interface is
included in the main channel computation in methods 2 and 4,
where the apparent shear stress ratio is 1, and the interface

Table 4.2

Alternative geometric definitions to incorporate segment interaction

(after Knight and Hamed, 1984)

| Method | Flood Plain | | Main Channel | |
	Area	Wetted Perimeter	Area	Wetted Perimeter
1	$(H-h)(B-b)$	$B-b + H-h$	$2bH$	$2b + 2h$
2	$(H-h)(B-b)$	$B-b + 2(H-h)$	$2bH$	$2b + 2H$
3	$(H-h)(B-b/2)$	$B-b + H-h$	$b(H+h)$	$2b + 2h$
4	$(H-h)(B-b/2)$	$B-b + H-h$	$b(H+h)$	$2b + 2h + 2((H-h)^2+b^2)^1/2$
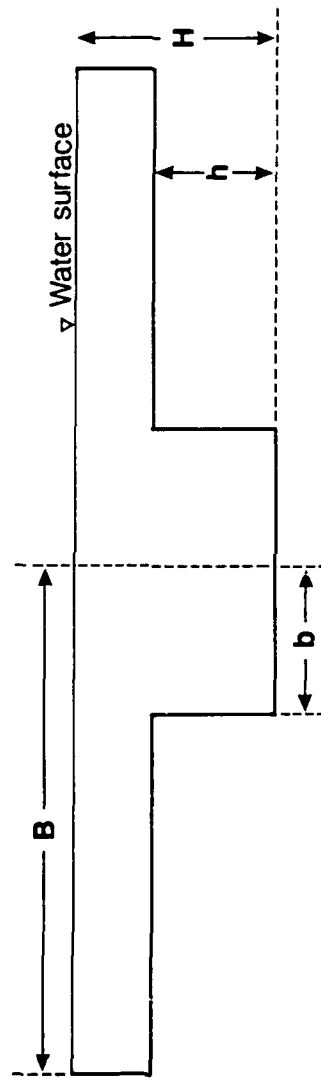
Figure 4.8
Definition of Cross-Sectional Geometric Parameters
Utilised by Knight and Hamed (1984)

Chapter 4

is excluded in methods 1 and 3 where zero shear is assumed.
These four methods were incorporated into the rating curve
generation routine (subroutine CMPRC) of MILHY2 for stage
elevations above bankfull.

4.4   Sensitivity of the Rating Curve to Interface
       Inclination

       There are a number of objectives in undertaking a
sensitivity analysis of the rating curve to the interface
computation method. These are:

1)   to establish whether any one method improves the
       accuracy of the predicted rating curve in comparison
       with observed field rating curves for a field
       cross-section;

2)   to establish whether there is a significant
       difference in the predicted rating curve generated
       by each of the four methods for wide floodplains
       with greater boundary roughnesses than those
       reported in Table 4.1;

3)   to compare the difference in the computed rating
       curve attributable to the interface inclination
       method, with the difference due to variability in
       the cross-sectional geometry and roughness
       parameters.

       To answer these three questions, it was necessary to
apply the four interface inclination methods to both field
cross-sections, to achieve objective one, and hypothetical
reaches to achieve objectives two and three. Whilst the
field cross-sections are similar to the theoretical cross-

Chapter 4

sections in that they have broadly rectangular main channels and
flat wide floodplains (see Figure 4.9) application of field
cross-sections provided the only comparison to an observed
rating curve possible. Objectives two and three can be achieved
by comparison of the predicted rating-curves generated by the
four computation methods utilizing to hypothetical cross-
sections.

4.4.1 Application of the four interface inclination
methods

The cross-section at Bad Hersfeld on the River Fulda, West
Germany, was selected in order to compare the accuracy of the
four computation methods against a field rating curve. The
rating curve at Bad Hersfeld was extended to out-of-bank
conditions using data from gauged extreme events for floodplain
inundation depths of up to 3.2 metres. This depth corresponds
approximately to the 1 in 100 year event. At Bad Hersfeld, the
floodplains are symmetrical about the main channel with a
floodplain to main channel width ratio (B/b) of 10. The
bankfull depth (h) is 4.1 metres, whilst the floodplains on
either side of the main channel are pasture. The four interface
inclination methods were applied for three sets of geometric and
roughness environments and the discharge at stage increments of
0.5 metres computed. The rating curve was also computed for the
first two cases with the cross-section being treated as a single
system, that is with no interfaces to divide the cross-section
into segments. The rating curves produced from these
applications are given in Tables 4.3, 4.4 and 4.5.

A theoretical cross-section was established to achieve
objectives two and three noted above, with a rectangular main
channel and a floodplain rise from the channel to the valley

Figure 4.9
Channel Cross-Section at Mecklar, 10km Downstream of
Bad Hersfeld on the River Fulda, West Germany.

Chapter 4

side of 0.1 metres. The floodplain to main channel width
ratios considered were 10 and 20. As noted earlier, flume
experiments by numerous authors have investigated smaller width
ratios. Wormleaton et al. (1982) reported that discharge
predictions from all the interface inclination methods, that is
vertical, diagonal and horizontal, converged to a common
solution as the floodplain inundation depth to main channel
depth ratio (H/h) approached 2. To check this, discharge
predictions calculated for depth ratios of up to 2.2 were
computed at 0.5 metre stage increments. As well as the four
interface inclination methods, the rating curves were computed
treating the cross-section as a single flow segment. Where
friction or slope parameters varied between the main channel and
floodplain segments, a mean average was applied to the single
segment case. This was true for both the hypothetical and Bad
Hersfeld cross-sections. The hypothetical cross-section results
are given in Tables 4.6, 4.7, 4.8, 4.9 and 4.10.

4.4.2 Results of the sensitivity analysis

The results of the sensitivity analysis of the computed
rating curve to the interface inclination and variation in
geometric parameters, are tabulated in Tables 4.3, 4.4, 4.5,
4.6, 4.7, 4.8, 4.9 and 4.10. Tables 4.3, 4.4 and 4.5 show the
results computed for the Bad Hersfeld cross-section and also
record the percentage error of each of the interface inclination
methods against an observed rating curve. Tables 4.6, 4.7, 4.8,
4.9 and 4.10 show the results for a hypothetical cross-section,
and the percentage error in these tables indicates the deviation
from the MILHY2 solution as no observed rating curve was
available.

Chapter 4

Table 4.3 contains the observed discharge values and the
computed values from MILHY2 and interface methods 1 to 4. Table
4.3 confirms that MILHY2 incorporates inclination method 2 and
in further tables, therefore, both are not shown. Manning's n
values of 0.035 for the main channel and floodplain were
selected for the first simulation reported in Table 4.3. This
value corresponds to the tabulated values suggested in Chow
(1959). The channel and floodplain slopes were set at 0.0006,
computed from the field rating curves from Bad Hersfeld and
Rotenburg, the next gauging station downstream.

Results from the Bad Hersfeld Station

Table 4.3 shows the discharge predictions from the four
interface methods computed using the parameter values reported
above. The mean average error of the discharge predictions over
the observed figures was computed for each method over a range
of inundation depths.

Table 4.3 shows that all methods - all inundation depths
overpredicted the carrying capacity of the cross-section. The
average error shows that method 2, (vertical interfaces with an
apparent shear stress ratio = 1), the method utilized by MILHY2,
gave the worst prediction. The best overall prediction was
given by the single segment method. This, however, was not so
surprising as both the boundary roughness and slope variables
were constant across the section.

Table 4.3 also shows that there was no consistent
difference in the predictive performance between the methods
incorporating the shear face, that is methods 2 and 4, and the
zero shear, methods 1 and 3. It is also important to note that
the percentage error increases with depth in all methods except
method 3.

Table 4.3

Comparison of the predictive accuracy of interface inclination methods

1-4 for Bad Hersfeld, River Fulda

Height above bankfull m	Observed m^3s^{-1}	MILHY2 Q m^3s^{-1}	MILHY2 Error %	Method 1 Q m^3s^{-1}	Method 1 Error %	Method 2 Q m^3s^{-1}	Method 2 Error %	Method 3 Q m^3s^{-1}	Method 3 Error %	Method 4 Q m^3s^{-1}	Method 4 Error %	Single Segment Q m^3s^{-1}	Single Segment Error %
0.29	86	134	+55	118	+37	134	+55	163	+89	124	+44	67	-22
0.78	134	232	+73	212	+58	232	+73	240	+79	197	+47	152	+14
1.27	205	411	+101	286	+88	411	+101	400	+95	352	+72	336	+64
1.76	321	650	+103	619	+93	650	+102	617	+92	563	+76	572	+78
2.25	490	950	+94	913	+86	949	+94	891	+82	833	+70	866	+77
2.74	675	1311	+94	1268	+88	1310	+94	1224	+81	1160	+72	1219	+81
3.22	830	1734	+109	1684	+103	1732	+109	1617	+95	1547	+86	1631	+97
Mean error			+90		+79		+90		+88		+67		+55

$B/b = 10$ $n_{fp} = 0.035$

$h = 4.1m$ $S_{ch} = 0.0006$

$n_{ch} = 0.035$ $S_{fp} = 0.0006$

Chapter 4

Comparison of Tables 4.3 and 4.4 shows how increasing the
floodplain boundary roughness can more than halve the error of
the predictions for all four methods. The difference in mean
average errors between computation methods is, however, the same
as those in Table 4.3. This suggests that the carrying capacity
computation is more sensitive to the boundary roughness value
than the form of the main channel/floodplain interface.

Table 4.4 also shows that the percentage   r does not
increase with increasing floodplain inundation depth, as
suggested in Table 4.3. In Table 4.4 the percentage error
values indicate that all four computation methods are converging
to the observed discharge as the inundation depth increases and
approaches the main channel depth. This suggests that a
floodplain roughness value of 0.07 corresponds more closely to
the field conditions than the initial value used of 0.035. The
logic behind this argument lies in the acceptance that as the
floodplain inundation depth increases to the main channel depth,
the two-stage channel behaves as a single system and therefore
all the computation methods should converge on a common
solution. If the solutions do not converge this suggests that
the initial boundary conditions are not realistic.

Table 4.3 shows the effects of incorporating meandering
in the channel by reducing the slope value used to 0.0001 from
0.0006. This value is calculated from the ratio of the main
channel routing length to the valley length between Bad Hersfeld
and Rotenburg on the River Fulda. Comparison of Tables 4.3 and
4.5 shows that reducing the slope of the main channel improves
the predictions of the carrying capacity in all computation
methods.

The results from the Bad Hersfeld (see Tables 4.3 and 4.4)

Table 4.4

Comparison of the predictive accuracy of interface inclination methods 1-4 for Bad Hersfeld, River Fulda, with variation in the floodplain roughness

Height above bankfull (m)	Observed m^3s^{-1}	Method 1 Q m^3s^{-1}	Error %	Method 2 Q m^3s^{-1}	Error %	Method 3 Q m^3s^{-1}	Error %	Method 4 Q m^3s^{-1}	Error %	Single Segment Q m^3s^{-1}	Error %
0.29	86	113	+31	129	+50	155	+80	116	+35	47	-46
0.78	134	176	+32	197	+47	202	+51	158	+18	101	-24
1.27	205	281	+37	306	+49	291	+42	243	+18	224	+9
1.76	321	416	+30	447	+39	408	+27	355	+11	381	+19
2.25	490	583	+19	620	+27	555	+13	497	+1	577	+18
2.74	675	782	+16	825	+22	732	+8	668	-1	812	+20
3.22	830	1013	+22	1062	+28	939	+13	869	+5	1087	+31
Mean error			+27		+37		+34		+12		+4

$B/b = 10$ $n_{ch} = 0.035$ $n_s = 0.0525$ $S_{fp} = 0.0006$

h 4.1m $n_{fp} = 0.07$ $S_{ch} = 0.0006$

Table 4.5

Comparison of the predictive accuracy of interface inclination methods

1-4 for Bad Hersfeld, River Fulda, with variation in the downstream main channel slope

Height above bankfull	Observed	Method 1		Method 2		Method 3		Method 4		Single Segment	
m	$m^3 s^{-1}$	Q $m^3 s^{-1}$	Error %	Q $m^3 s^{-1}$	Error %	Q $m^3 s^{-1}$	Error %	Q $m^3 s^{-1}$	Error %	Q $m^3 s^{-1}$	Error %
0.29	86	53	-38	60	-30	76	-12	39	-56	51	-41
0.78	134	129	-4	137	+2	143	+7	61	-55	116	-13
1.27	205	282	+38	292	+42	293	+43	126	-39	257	+25
1.76	321	493	+54	505	+57	498	+55	273	-15	437	+27
2.25	490	763	+56	777	+59	761	+55	477	-3	661	+35
2.74	675	1092	+62	1108	+64	1082	+60	737	+9	931	+38
3.22	830	1481	+78	1500	+81	1462	+76	1056	+27	1246	+50
Mean error			+35		+39		+41		-18		+17

$B/b = 10$ $n_{fp} = 0.035$

$h = 4.1m$ $S_{ch} = 0.0001$

$n_{ch} = 0.035$ $S_{fp} = 0.0006$

Chapter 4

simulations suggest that the computation utilised in MILHY2 give
the poorest prediction of the carrying capacity of the
cross-section. Tables 4.4 and 4.5 show that the prediction can
be much improved by the more accurate selection of parameter
values than by altering the computation technique.

Results from a Hypothetical Cross-section

Tables 4.6, 4.7, 4.8, 4.9 and 4.10 give the predictions of
the carrying capacity for a hypothetical cross-section,
comparing computation methods 1 to 4 and the discharge
prediction computed by treating the section as a single flow
segment. The percentage error values reported are computed from
the MILHY2 predictions, which utilise method 2 (vertical
interface, apparent shear stress ratio = 1). The percentage
error values allow comparison of the relative sensitivity of the
discharge predictions to variation in the computation method and
parameters. The absolute accuracy of the techniques cannot be
computed as this is a hypothetical application.

Analysis of Tables 4.6, 4.7, 4.8, 4.9 and 4.10 shows
that method 1 (vertical interface, zero shear) produces very
close approximations to the predictions produced from the
MILHY2 computation for all the boundary roughness and geometry
environments. In all cases, methods 3 and 4 (diagonal
interface, zero shear and shear ratio =1, respectively), rank
second and third consistently in their closeness to the MILHY2
predictions. Methods 1, 3 and 4 under-predict the carrying
capacity in comparison to the MILHY2 predictions in all five
experimental frames.

Comparison of Table 4.6, where the floodplain/channel
width ratio is 10, with Table 4.10, width ratio = 20,

Table 4.6

Comparison of the predictive accuracy of interface inclination methods 1-4

for a hypothetical reach

Height above bankfull m	MILHY2 $m^3 s^{-1}$	Method 1 Q $m^3 s^{-1}$	Method 1 Error %	Method 3 Q $m^3 s^{-1}$	Method 3 Error %	Method 4 Q $m^3 s^{-1}$	Method 4 Error %	Single Segment Q $m^3 s^{-1}$	Single Segment Error %
0.56	61	58	-5	42	-31	34	-44	33	-45
1.01	153	150	-2	127	-17	118	-23	131	-14
1.56	295	291	-1	261	-12	250	-15	275	-7
1.90	477	472	-1	433	-9	421	-12	460	-4
2.35	695	689	-1	641	-8	636	-10	679	-2
2.80	946	939	-1	880	-7	863	-9	931	-2
			-2		-14		-19		-12

$B/b = 10$ $n_{fp} = 0.035$

$h = 2.4m$ $S = 0.0005$

$n_{ch} = 0.035$

Table 4.7

Comparison of the predictive accuracy of interface inclination methods 1-4

for a hypothetical reach, with variation in the floodplain roughness

Height above bankfull	MILHY2	Method 1		Method 3		Method 4		Single Segment	
		Q	Error	Q	Error	Q	Error	Q	Error
m	$m^3 s^{-1}$	$m^3 s^{-1}$	%	$m^3 s^{-1}$	%	$m^3 s^{-1}$	%	$m^3 s^{-1}$	%
0.56	53	51.	-4	34	-36	26	-51	68	+28
1.01	107	103	-2	110	-26	70	-35	275	+157
1.56	185	181	-2	241	-20	137	-26	580	+214
1.90	284	279	-2	410	-16	225	-21	969	+241
2.35	401	396	-1	614	-14	330	-18	1432	+257
2.80	536	529	-1	850	-13	451	-16	1963	+266
Mean error			-2		-21		-28		+194

B/b = 10 n_{fp} = 0.07

h = 2.4m n_s = 0.0525

n_{ch} = 0.035   S = 0.0005

Table 4.8

Comparison of the predictive accuracy of interface inclination methods 1-4
for a hypothetical reach, with variation in the downstream main channel slope

Height above bankfull	MILHY2	Method 1		Method 3		Method 4		Single Segment	
	$m^3 s^{-1}$	Q $m^3 s^{-1}$	Error %	Q $m^3 s^{-1}$	Error %	Q $m^3 s^{-1}$	Error %	Q $m^3 s^{-1}$	Error %
0.56	35	34	-4	28	-21	24	-32	25	-30
1.01	121	119	-2	110	-9	106	-12	101	-17
1.56	254	252	-1	241	-5	236	-7	213	-16
1.90	427	425	-1	410	-4	404	-5	356	-17
2.35	635	633	0	614	-3	608	-4	526	-17
2.80	876	873	0	850	-3	843	-4	721	-18
Mean error			-1		-8		-11		-19

$B/b = 10$ $S_{ch} = 0.0001$
$h = 2.4m$ $S_{fp} = 0.0005$
$n_{ch} = 0.035$ $S_c = 0.0003$
$n_{fp} = 0.035$

Table 4.9

Comparison of the predictive accuracy of interface inclination methods 1-4 for a
hypothetical reach with variation in the downstream main channel and floodplain slope

Height above bankfull	MILHY2	Method 1		Method 3		Method 4		Single Segment	
m	$m^3 s^{-1}$	Q $m^3 s^{-1}$	Error %	Q $m^3 s^{-1}$	Error %	Q $m^3 s^{-1}$	Error %	Q $m^3 s^{-1}$	Error %
0.56	192	184	-4	132	-31	107	-44	103	-46
1.01	485	475	-2	403	-17	374	-23	413	-15
1.56	933	920	-1	824	-12	790	-15	870	-7
1.90	1508	1493	-1	1370	-9	1330	-12	1453	-4
2.35	2197	2179	-1	2026	-8	1980	-10	2148	-2
2.80	2990	2968	-1	2783	-7	2731	-9	2945	-2
Mean error			-2		-14		-19		-13

$B/b = 10$ $n_{fp} = 0.035$
$h = 2.4m$ $S = 0.0005$
$n_{ch} = 0.035$

Table 4.10

Comparison of the predictive accuracy of interface inclination methods 1-4

for a hypothetical reach with variation in the floodplain/main channel width ratio

Height above bankfull m	MILHY2 $m^3 s^{-1}$	Method 1		Method 3		Method 4		Single Segment	
		Q $m^3 s^{-1}$	Error %	Q $m^3 s^{-1}$	Error %	Q $m^3 s^{-1}$	Error %	Q $m^3 s^{-1}$	Error %
0.56	77	74	-4	58	-25	50	-35	48	-38
1.01	254	251	-1	228	-10	219	-14	231	-9
1.56	531	527	-1	497	-6	486	-9	511	-4
1.90	891	886	-1	847	-5	834	-6	873	-2
2.35	1324	1318	0	1270	-4	1256	-5	1308	-1
2.80	1825	1818	0	1759	-4	1743	-5	1811	-1
Mean error			-1		-9		-12		-4

$B/b = 20$ $n_{fp} = 0.035$

$h = 2.4m$ $S = 0.0005$

$n_{ch} = 0.035$

Chapter 4

shows that this increase has made little impact on the
comparative accuracy of the computation methods. There has been
no radical change in the difference in the mean average errors
between the four computation methods.

Comparison of the Hypothetical and Bad Hersfeld
Applications

Analysis of the two sets of results has shown that the
method incorporated into MILHY2, that is method 2, generates the
gratest carrying capacity of the cross-section in both the Bad
Hersfeld and hypothetical sections. The Bad Hersfeld section
results suggest that method 2 generates the poorest prediction
of the four methods, which all over-predict the carrying
capacity. This suggests that all four methods do not introduce
enough friction over the assumed interfaces between the
floodplain and main channel to mimic the retarding effects of
momentum exchange. Method 4 assumes a diagonal interface and an
apparent shear stress ratio equal to one, and introduces the
greatest additional boundary friction of the methods, hence
producing the lowest prediction of carrying capacity (see Tables
4.3 to 4.10). This suggests that in the field apparent shear
stress ratios on diagonal interfaces may be greater than 1,
rather than less than 1, as Wormleaton et al. (1982) found (see
Figure 4.6b). Alternatively, these results suggest that the
true position of the interface is between the vertical and the
diagonal, as the apparent shear stress ratios on the vertical
interface are very much greater than 1 (see Figure 4.6a).
Apparent shear stress ratios of greater than 1 could be
incorporated into the MILHY2 scheme by increasing the length of
the wetted perimeter of the apparent interface in the main
channel computation until the stress ratio was reduced to one.

Chapter 4

4.4.3 Conclusions

From the analysis of the results above, it is possible to make several conclusions:

1)   The three methods utilized to incorporate turbulent exchange between the main channel and floodplain, predict more accurately the carrying capacity of a cross-section than the technique used in MILHY2.

2)   All four methods (section 4.3.1) over-predicted the carrying capacity because they failed to introduce enough additional boundary friction to mimic the effects of turbulent exchange. Method 4 introduced the most additional friction and gave the best predictions.

3)   Increasing the boundary roughness, Manning's n, for the floodplain was more effective at reducing the over-prediction of the carrying capacity of the section than increasing the wetted perimeter of the interface, or assuming an apparent shear stress ratio of one.

4.5   Implications of the Incorporation of Momentum Exchange

The results of the introduction of the incorporation of momentum exchange into MILHY2 show that the predictive accuracy of the model could be improved. The results also suggested that method 4 (diagonal interface, apparent shear ratio = 1) gave the best prediction. This is in contrast to the results of Knight and Hamed (1984), who found that method 3 (diagonal interface, zero shear) gave the best prediction. One explanation for this is that the field data used in this application were for more turbulent conditions than the flume experiments conducted

Chapter 4

by Knight and Hamed (1984). This turbulence may have been
generated from the rougher boundary friction conditions in the
field. Another explanation for the different results from this
chapter and Knight and Hamed, is that this analysis looked at
the effects of the four methods on the rating curve, that is at
a point of the reach. Knight and Hamed investigated the
accuracy of the four methods at the end of a reach after the
water has been routed. Knight and Hamed, therefore, compared
the accuracy of the methods with a three-dimensional flume
result, whilst this analysis only considered the predictive
accuracy with reference to two dimensions. It is important,
therefore, that the significance of the incorporation of the
four methods along a reach should be considered as part of the
MILHY3 evaluation programme.

The results of the evaluation of the routine also showed
that increasing the Manning's n coefficient was just as
successful at reducing the over-prediction of the channel
capacity as the introduction of momentum exchange. This
suggests that boundary friction effects are more significant on
the prediction of the rating curve than the introduction of
momentum exchange. However, the incorporation of momentum
exchange may still be considered to be significant as it allows
the more accurate selection of the Manning's n coefficient based
on the effects of boundary friction. If evaluation of the
MILHY3 model further highlights the importance of boundary
friction, then it may be appropriate to consider replacement of
the Manning's n coefficient with a more sophisticated measure of
boundary friction.

The success of the incorporation of momentum exchange
supports the approach taken of evaluating hydraulic concepts and
techniques for incorporation into hydrologic models. The

Chapter 4

concepts of the interface and apparent shear stresses have been shown to be portable.

The evaluation of the momentum exchange routine explored in this chapter is seen to be part of the first two stages of Sargent's (1982) model evaluation programme. The investigation of hydraulic concepts and techniques is considered to be part of the mathematical evaluation, whilst the evaluation of the four methods is part of the computerised model verification. The success of the introduction of momentum exchange in improving the predictive accuracy of MILHY2 means that it is considered suitable for inclusion in the further evaluation of the module as a catchment model. The four methods are therefore evaluated further in the analysis of the MILHY3 catchment model and are reported in Chapter 7.

4.6   Summary

This chapter investigates the transfer of momentum between the main channel and the floodplain. It has explored various methods of incorporating the transfer of momentum into the MILHY3 composite scheme, applied and evaluated four techniques. The results and conclusions of this chapter can be summarized into several points. These are:-

1)   It is accepted in this chapter that the dominant process controlling the transfer of momentum is the velocity gradient across the floodplain/main channel cross-section. This transfer can be visualised using an imaginary interface and the apparent shear stresses acting on this interface. These concepts have been developed by hydraulic engineers.

Chapter 4

2)   The concepts of an interface and apparent shear stresses
have not previously been applied to hydrological modelling.
Attempts at empirical formulations using results from flume
experiments are inappropriate for hydrological applications, as
the flume reaches utilised cross-sectional geometries that were
too narrow and floodplain roughnesses too smooth.

3)   Two interface inclinations and two apparent shear stress
ratios were selected for evaluation. These four techniques were
successfully incorporated into the MILHY3 scheme. Evaluation of
the four techniques on a hypothetical and field rating curve
showed that method four produced the greatest effect by
introducing the greatest amount of momentum exchange. In
addition, the rating curve produced by method 4 was the closest
to the observed field cross-section.

4)   The results of this evaluation were compared with the
results of Knight and Hamed (1984), who applied the same four
techniques. The results of the Knight and Hamed (1984)
experiments had shown that method 3 produced the rating curve
closest to the observed curve measured in the flume. It is
suggested that the success of method 3, which incorporated less
momentum exchange than method 4, was due to the narrow and
smooth floodplain used in the flume experiments and the possible
effects of the third downstream dimension.

5)   The results showed that the effects of increasing the
Manning's n coefficient were greater than the introduction of
the momentum exchange routine. It is suggested, therefore, that
boundary roughness may be more significant on the prediction of
channel flow than momentum exchange.

6)   It is considered essential that the momentum exchange
routine is evaluated as part of a catchment model if the

Chapter 4

importance of the effects of the longitudinal dimension are to
be considered, and if the relative importance of the effects of
boundary friction are to be established.

Chapter 5

Chapter 5
Incorporation of Multiple Routing Reaches

Analysis of the behaviour of flow in two-stage channels undertaken in Chapter 3, identified three key processes that need further investigation. These were the handling of boundary friction and transverse circulations, the incorporation of turbulent shear stresses between the main channel and the floodplain, and the incorporation of the different path lengths for the main channel and floodplain. The incorporation of turbulent shear stresses has been investigated and reported in Chapter 4. This chapter, therefore, concentrates on the handling of the different path lengths of the main channel and floodplain flow segments. The relative importance of the effects of boundary friction are discussed in both Chapter 4 and this chapter; the effects of transverse circulations are not investigated.

The sensitivity analysis of the Ervine and Ellis (1987) scheme reported in Chapter 3, found that the sinuosity of the main channel was important in determining the length of the downstream or longitudinal flow path. In two-stage channels, the downstream reach length in the relatively sinuous main channel may be up to 30% longer than the straighter floodplain flows. The concept of multiple routing paths has been identified as a useful tool in visualising these different pathways.

In this chapter, the downstream behaviour of two-stage flow is investigated and alternative methods of incorporating the concept of multiple routing pathways considered. A method

Chapter 5

incorporating multiple routing reaches will then be selected
and an initial sensitivity analysis undertaken in order to
validate the new module.

5.1   The Behaviour of Downstream Two-Stage Channel Flow

Water on the floodplain may return to the channel either
by overland flow or by throughflow. Water that is ponded by
the topographic pattern of the floodplain must return via
throughflow but flowing water may return directly to the
channel, or may route down slope for some distance before
rejoining the channel. In bankfull conditions floodplain flows
may cross and recross the sinuous main channel beneath them,
with only relatively small amounts of momentum exchange taking
place. It is these high flow conditions when the main channel
is full that this chapter is primarily concerned with. The
effects of throughflow of ponded water and the direct return of
floodplain flow to the main channel are not considered. The
effects of the more direct return of floodplain flow in
comparison with the larger flood events will have a nominal
effect on the nature of the predicted hydrograph. The
importance of throughflow of floodplain water on the hydrograph
is not known but it is considered that the effects would only
be significant in the predictions of a continuous simulator.
This is because it is likely that the seepage from the
floodplain would only have an impact on the hydrograph long
after the main floodwave had passed.

In two-stage channels there is a tendency for floodplain
flow to "short-circuit" the generally more sinuous route of the
main channel, taking a more direct route downstream (Fread,
1976). One possible explanation for the phenomenon of less
sinuous floodplain flows is that the infrequency of out-of-bank

Chapter 5

events do not provide the opportunity for the development of a
secondary flow system on the floodplain. A secondary flow
system is thought to be a necessary precursor for the
development of a meander system (Richards, 1982). Einstein and
Shen (1964) suggested that the secondary flow system is itself
initiated by shear, possibly along a rough bank.

The reason for the generally less sinuous pathway of the
floodplain flow in comparison with the main channel flow is no
nearer explanation than is agreement on the initiation of
meanders. Whatever the explanation, the shorter path length of
the floodplain is exacerbated by the steeper gradient of the
floodplain in comparison with the main channel. This increases
velocities on the floodplains and potentially generates faster
travel times for floodwaves passing downstream on the
floodplain than in the main channel.

The accelerating effects of the path length and slope on
floodplain flows are diminished, however, by the effects of
boundary friction. If floodplain flow depths are small, then
the hydraulic radius will also be small and hence velocities
will be reduced. Floodplain boundary roughnesses also tend to
be higher than those in the main channel because of vegetation
and obstructions such as hedges.

As noted earlier in Chapter 3, the retarding effects of
boundary roughness tend to decline as the hydraulic radius or
stage increase. This is particularly true for the broadly
rectangular main channels such as those found in the River
Fulda catchment. On the floodplains, however, the situation is
complicated by vegetation and man-made structures. Petryk and
Bosmajian (1975) showed that the boundary friction of
vegetation is related to the drag and cross-sectional area of
particular plant species. This drag may be increased when

Chapter 5

the floodplain inundation depth increases because debris may
become trapped in hedges and fences causing an increase in
boundary roughness. Klassen and Zwaard (1974) showed that the
spacing of hedges and trees is critical in determining the
debris build up and hence in computing the friction of floodplains.

The correct selection of the Manning's n coefficient for
the floodplain flow segments for MILHY2, must consider not only
the general land use but also the spacing and height of any
hedges or fences and how the pattern varies with the inundation
stage.

Overall, velocities on the floodplain tend to be lower
than those in the main channel. This is because of the
relatively greater frictions on the floodplain, whilst the
travel time of the floodwave tends to be faster on the
floodplain because of the shorter reach length. The faster
floodwave travel times on the floodplain generate complexity in
the prediction of two-stage flows. It has been assumed in the
previous chapters that the primary direction of momentum
transfer has been from the main channel to the floodplain.
This effectively caused the floodplain flows to act as a drag
on the main channel flows whilst the floodplain flows are
accelerated by the main channel flows. In a sinuous reach,
however, where the floodwave in the floodplain may be
travelling downstream at a much greater rate than the floodwave
in the channel, the transfer of momentum may be from the
floodplain to the channel.

The concept of multiple routing reaches incorporates the
effects of large flood events in two-stage channels, where the
floodplain flows have a separate and direct route downstream
crossing and recrossing the bankfull main channel. The

Chapter 5

importance of the routing path in two-stage channels is
summarised by Fread (1976), who noted:

"The characteristics of the floodwave are influenced
predominantly by the one-dimensional motion of the
floodwave along the longitudinal axes of the river
and the floodplain."

In the next section alternative methods of incorporating
multiple routing reaches into the composite structure of MILHY2
are considered.

5.2   Modelling Alternatives

The objectives of incorporating the concept of multiple
routing reaches into MILHY2 are:-

1)   to improve the representation of the downstream routing
of flow in two-stage channels by incorporating the effects of
the sinuosity of the main channel and the short-circuiting of
floodplain flows;

2)   to improve the selection of the appropriate Manning's n
coefficient for two-stage flows. By removing considerations of
the sinuosity of floodplain flows, the selection of the correct
n value should be simplified as it would then only incorporate
the effects of boundary friction.

The aim of this chapter is therefore to develop a one-
dimensional or quasi-two-dimensional technique that can be
incorporated into MILHY2. Such a technique should therefore
have:

Chapter 5

-   little additional data requirements
-   low computer demands
-   be capable of validation

These restrictions leave several alternative approaches available. These are:-

1) To develop a stage/reach length relationship. This approach was suggested by Perkins (1970), when he incorporated a routine to increase reach length linearly from the main channel thalweg distance at bankfull to the shortest reach length dictated by the floodplain slope, at the maximum stage.

2) To develop an empirical adjustment to the roughness coefficients of the floodplain and main channel. This approach was suggested by Tingsanchali and Ackermann (1976), where the Manning's n value was weighted by the ratio of reach lengths between the actual floodplain distance and the schematized straight floodplain and main channel, such that:

$$n^* = n_f \frac{L_f^{3/2}}{L_{mc}} \qquad 5.1$$

where n^* - adjusted Manning's n

n_f - Manning's n floodplain

L_f - reach length of floodplain

L_{mc} - reach length of the main channel

3) Replace the Variable Storage Coefficient Routing routine in MILHY2, with a St. Venant technique utilizing a weighted four-point implicit difference solution

Chapter 5

modified by Fread (1976) to incorporate the differing
path lengths of floodplain and main channel flows.

4)   Separate floodplain and main channel flows and route,
        using the existing routines in MILHY2, assuming no
        exchange of flow along the reach.

The simplest solution to apply is approach four, where
the inflow hydrograph is apportioned to the cross-sectional
segments using the rating curves developed for the upstream
cross-section. Each segment of the cross-section is then
routed individually downstream using travel time tables
developed for each cross-sectional segment. Conceptually this
solution may seem rather simplistic and it does have several
disadvantages. These are:-

  i) flow has to be apportioned to floodplain or channel
      at the top of the reach, and these proportions are
      fixed throughout the reach. This assumes that the cross-
      sectional geometry is fairly constant downstream;

 ii) there is no exchange of momentum between the main
      channel and floodplain along the reach;

iii) floodplain flows on either bank cannot cross the main
      channel flows.

However, the other three possible alternatives also
exhibit some of these and other disadvantages. None of the
other three methods incorporate the momentum exchange between
the main channel and the floodplain in either direction.
Perkin's (1970) method assumes that there is a gradual transfer
in the routing reach length from the main channel to the flood-
plain. This conceptually seems attractive because when flood-
plain flows are relatively small, the frictional effects of the

Chapter 5

sinuous main channel may be great; and as floodplain flow
depths increase, the effects of the main channel are flooded
out.

The approach suggested by Tinsanchali and Ackermann
(1976), of modifying the Manning's n coefficient to incorporate
the effects of the differing routing length, would not improve
the ease of selection of the coefficient (objective 2
identified above). It would also not improve the physical
representation of the pathways as it is essentially a
calibration procedure.

Fread's (1976) method incorporated into the FLDWAV
package (Fread, 1985) separates floodplain and main channel
flo' , a similar way to the simple procedure proposed by
MTLHY2. The advantage of Fread's model, however, is that the
mass balance between the floodplain and main channel flows are
computed in each cell.

Despite the disadvantages of approach 4, it is an
approach which seems to be a logical first step in tackling the
problem of floodplain flows "short-circuiting" the main
channel. Exchange of momentum between the main channel and
floodplain has been incorporated at the valley-sections (see
Chapter 4), and it is felt important at this stage to compare
the sensitivity of the outflow hydrograph to the effects of
variability in the momentum exchange routines, or the multiple
routine of floodplain and channel flows. If, as Fread (1976)
suggests, the downstream short-circuiting effects were
identified as being significant, then it would be appropriate
to investigate Perkin's approach as a simple alternative, or to
attempt a more radical replacement of the routing subroutine
with Fread's (1976) St. Venant solution.

Chapter 5

5.3   Application of Multiple Routing Reaches

Testing the impact of multiple routing on the accuracy of
the predicted outflow hydrograph is an essential part of the
model evaluation procedure identified by Sargent (1982). The
relative importance of the technique compared to other
modifications, and the sensitivity of the whole scheme to
parameter variability, is investigated in Chapter 7. In this
section, therefore, MILHY2 is applied using only the
routing routines with an observed or generated hydrograph being
input at the upstream end of the reach. The results of the
analysis are notated such that the label MILHY2 refers to the
model without the incorporation of the separate or multiple
routing reaches. The notation multiple routing or m. routing
implies the MILHY2 model with the multiple routing routine.

Multiple routing reaches were applied to a theoretical
reach with rectangular cross-sectional geometry assumed to be
constant downstream and an observed reach from the River Fulda,
between Bad Hersfeld and Rotenburg. A variety of inflow
hydrographs were applied to the theoretical reach, in order to
investigate the impact of the depth of inundation on the travel
time of the floodplain and the effects on the outflow
hydrograph. The River Fulda, however, provided field data
against which various roughness and routing lengths could be
tested but with a limited number of observed flood events. A
1 in 10 year event was available and enough flood frequency
data were available to generate a 1 in 100 year event, assuming
a similar hydrograph shape to the 1 in 10 year event.

Chapter 5

5.3.1 Application to the Bad Hersfeld - Rotenburg reach

The results from the application of multiple routing
reaches to the Bad Hersfeld to Rotenburg reach are found in
Tables 5.1 and 5.2, and Figures 5.3, 5.4 and 5.5. As reported
earlier in Section 4.4.1, the cross-sectional geometry at Bad
Hersfeld is broadly rectangular with the floodplains being
symmetrical about the main channel. The reach from Bad
Hersfeld to Rotenburg is approximately 24km in length with a
sinuous main channel; this can be seen in Figure 5.1. At
Rotenburg, the bankfull depth is 4.8m as compared to 4.1m at
Bad Hersfeld, with a bankfull discharge of $180m^3s^{-1}$. The
valley section is asymmetrical at Rotenburg, with the left hand
floodplain being approximately 300m wide whilst the right hand
floodplain rises steeply. The bankfull width at Rotenburg is
approximately 50m as compared with 30m at Bad Hersfeld.

When multiple routing is invoked, the observed hydrograph
at Bad Hersfeld is apportioned to floodplain and main channel
segments according to the rating curve developed from the Bad
Hersfeld cross-section. The travel timetable is then developed
for each cross-sectional segment using the smaller of either
the upstream or downstream rating curve. The maximum
floodplain values reported in Tables 5.1 and 5.2 are computed
at the downstream station, that is Rotenburg.

The 1 in 10 year observed inflow at Bad Hersfeld and
observed outflow at Rotenburg is shown in Figure 5.2. This
figure shows that the travel time of the 1 in 10 year event
between the two stations is approximately nine hours. The
inflow hydrograph at Bad Hersfeld has been scaled up, in line
with the flood frequency data available to provide the 1 in 100
year event, and consequently the 1 in 100 year event has the
same form as the 1 in 10 year event. At Bad Hersfeld the 1 in
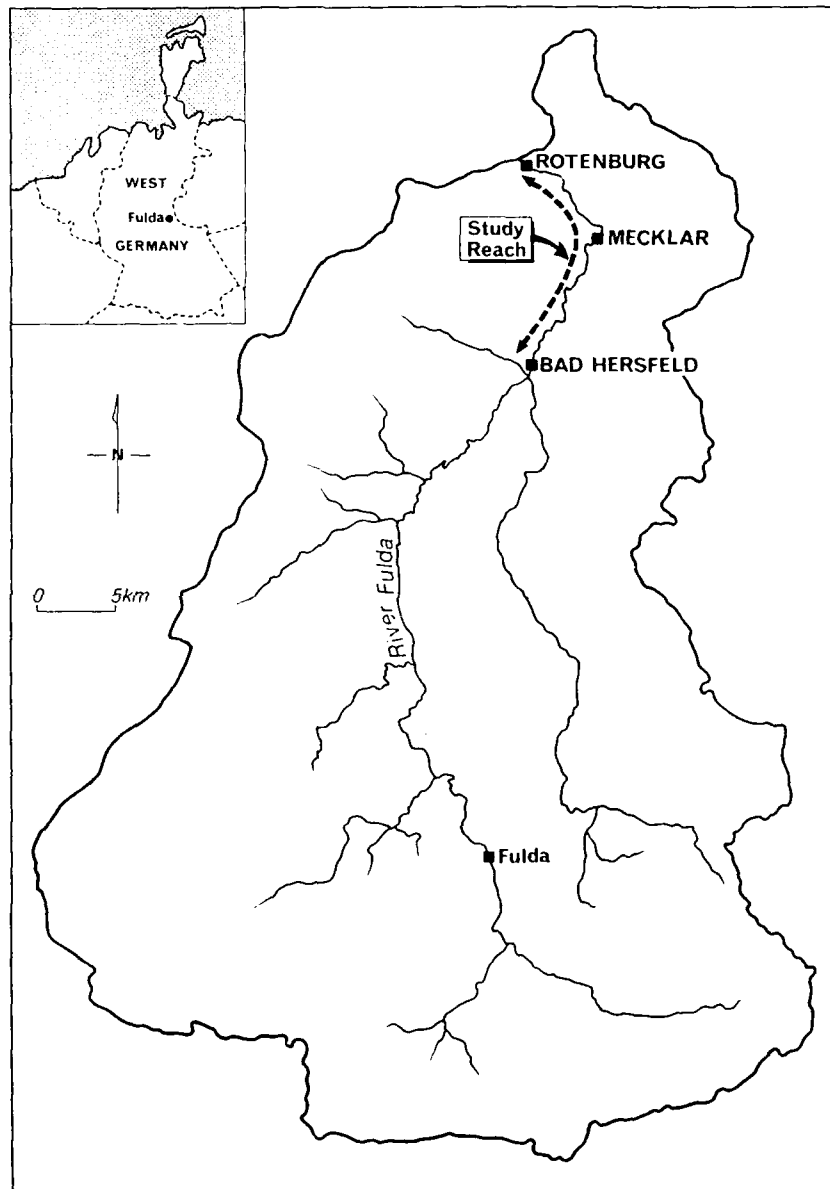
Figure 5.1
Location of the Bad Hersfeld-Rotenburg Reach
of the River Fulda, West Germany

117
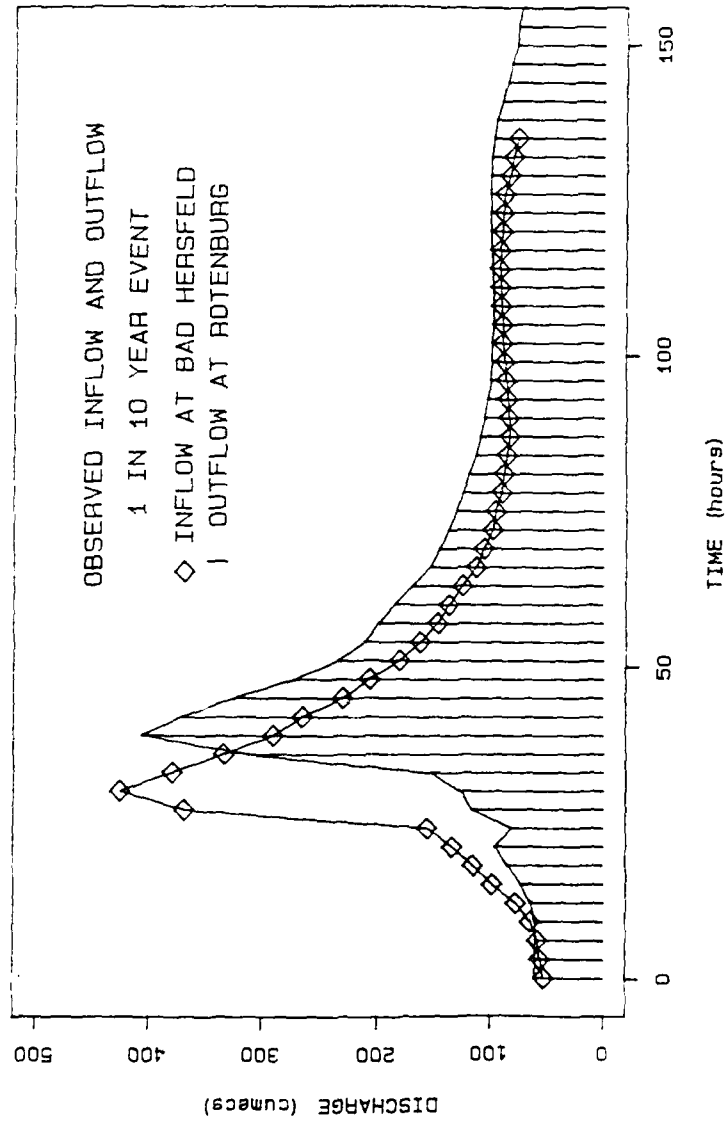
Figure 5.2
Observed Inflow and Outflow Hydrographs at Bad Hersfeld and
Rotenburg for the 1 in 10 Year Event

Chapter 5

100 year event corresponds to an increase in the floodplain
inundation depth of approximately 1m over the 1 in 10 year
event. At Bad Hersfeld the 1 in 100 year event corresponds to
an increase in the floodplain inundation depth of approximately
1m over the 1 in 10 year event.

Figure 5.3 compares the observed outflow hydrograph at
Rotenburg with the outflow hydrograph simulated by MILHY2 and
the multiple routing technique. The greatest difference in the
three hydrographs occurs in the overbank section of the
hydrographs; the bankfull discharge is marked on the figure.
The corresponding time to peak, peak discharge and maximum
inundation depths of these three hydrographs are recorded in
Table 5.1. Both Figure 5.3 and Table 5.1 show that the single
routing technique used in MILHY2 effectively smooths the inflow
hydrograph to too great an extent. This reduces the peak
discharge and inundation depth. The multiple routing technique
reduces the attenuation of the floodwave and thereby halves the
HYMO2 errors in both the peak discharge and the inundation
depth. Table 5.1 also shows that the multiple routing
technique produced a time to peak of 40 hours, two hours later
than the observed peak. However, as the observed inflow and
outflow hydrographs were digitised at three hour intervals,
errors of less than three can be ignored.

As noted earlier in this section, the main objective of
incorporating multiple routing reaches was to simulate the
effects of the short-circuiting of floodplain flow, reducing
the floodplain reach length. In the next simulation reported
in Table 5.1, therefore, the reach length of the floodplain
segments was reduced by 5%. This produced only very small
variations in the outflow hydrograph in comparison with the
multiple routing hydrograph shown in Figure 5.3.

BAD HERSFELD TO ROTENBURG: 1 in 10 year event
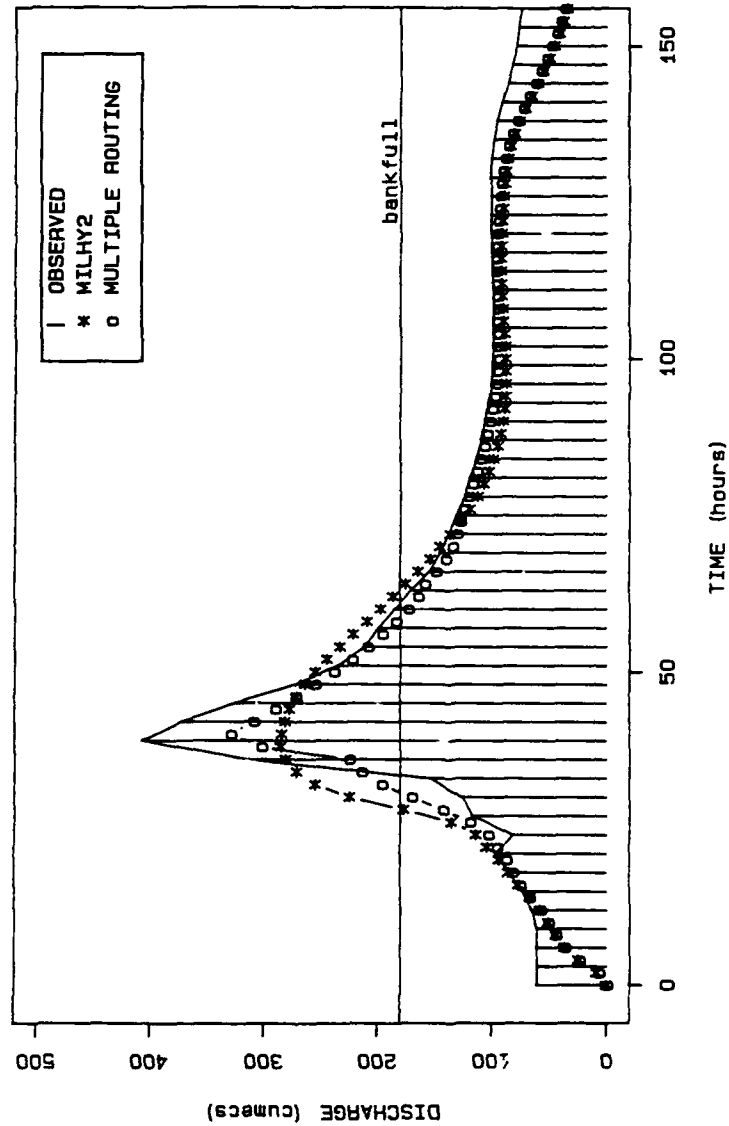
Figure 5.3
Comparison of MILHY2 and Multiple Routing Reach
Simulated and Observed Hydrographs for the 1 in 10
Year Event at Rotenburg

Chapter 5

Table 5.1
Characteristics of Observed and Simulated Hydrographs
at Rotenburg, for the 1 in 10 Year Event

	Time to peak	Peak discharge	Maximum floodplain inundation
	hours	$m^3 s^{-1}$	m
Observed	38	407	0.33
MILHY2	38	285	0.09
Multiple routing	40	330	0.17
Multiple routing floodplain length ↓5%	40	333	0.18
Multiple routing floodplain length ↓30%	40	352	0.21
Multiple routing floodplain n ↓30%	38	355	0.22

Chapter 5

Analysis of the flood inundation maps available for the
River Fulda indicated, however, that the floodplain reach
length may be up to 30% shorter than the main channel. The
hydrograph produced by reducing the floodplain reach length by
30% is shown on Figure 5.4. Comparison of Figures 5.3 and 5.4
shows that reducing the floodplain length by 30% makes a
significant improvement in the accuracy of the prediction.

Figure 5.4 shows, though, that a similar effect can be
achieved by reducing the Manning's n roughness coefficient by
30%. Chow (1959) showed that the effects of sinuosity of a
channel can alter the n coefficient by up to 30%. As noted
earlier, however, one of the objectives of this investigation
is to incorporate processes operating in two-stage channels and
reduce reliance of empirical coefficients.

Table 5.2 and Figure 5.5 show the simulation results for
the 1 in 100 year event on the River Fulda reach. In contrast
to the 1 in 10 year event, the MILHY2 prediction gives higher
peak discharge results than the multiple routing reach. The
percentage error between the MILHY2 and multiple routing
technique is, though, much smaller in the 1 in 100 year storm
being approximately 4%; whilst the 1 in 10 year event
difference was 11%. This suggests that as the floodplain
inundation depth increases, the cross-section behaves as a
single system causing the solutions to converge.
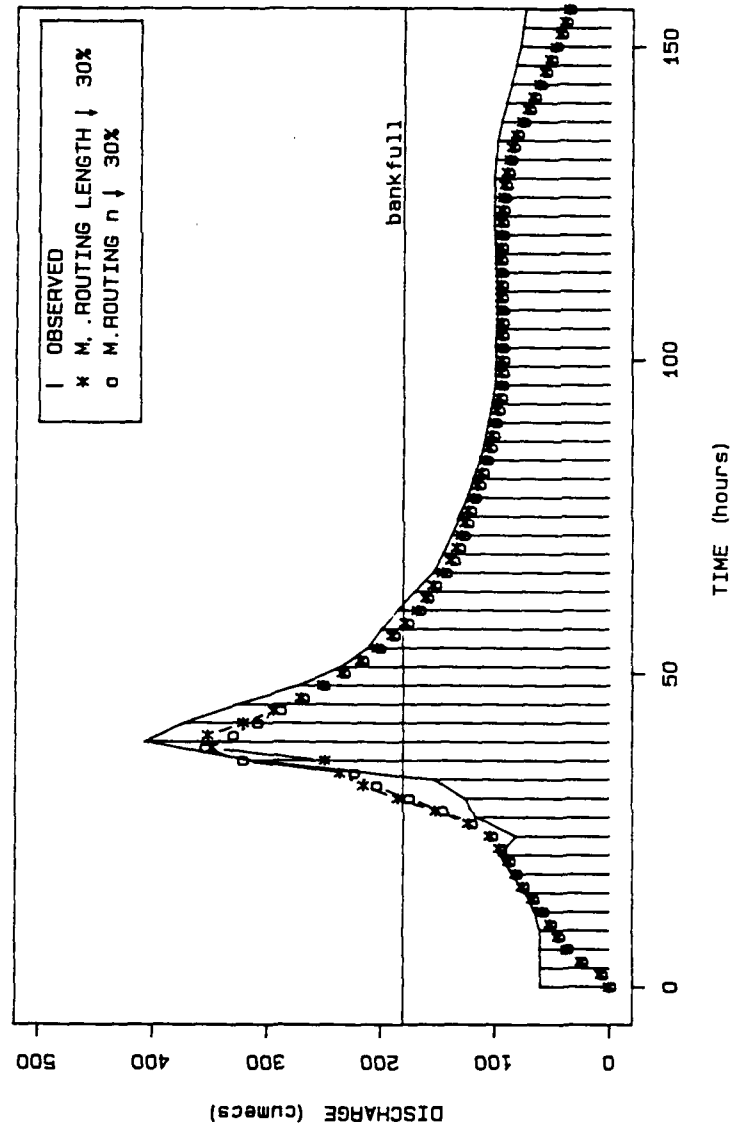
Figure 5.4
Comparison of Observed and Multiple Routing Reach
Simulated Hydrographs with Variations in Reach Length
and Boundary Roughness for the 1 in 10 Year Event

Chapter 5

Table 5.2

Characteristics of the Observed and Simulated Hydrographs

at Rotenburg, for the 1 in 100 Year Event

	Time to peak	Peak discharge	Maximum floodplain inundation
	hours	$M^3 s^{-1}$	m
Observed	38	744	0.90
MILHY2	38	665	0.78
Multiple routing	40	634	0.73
Multiple routing floodplain length ↓30%	36	684	0.81
Multiple routing floodplain n ↓30%	36	668	0.78
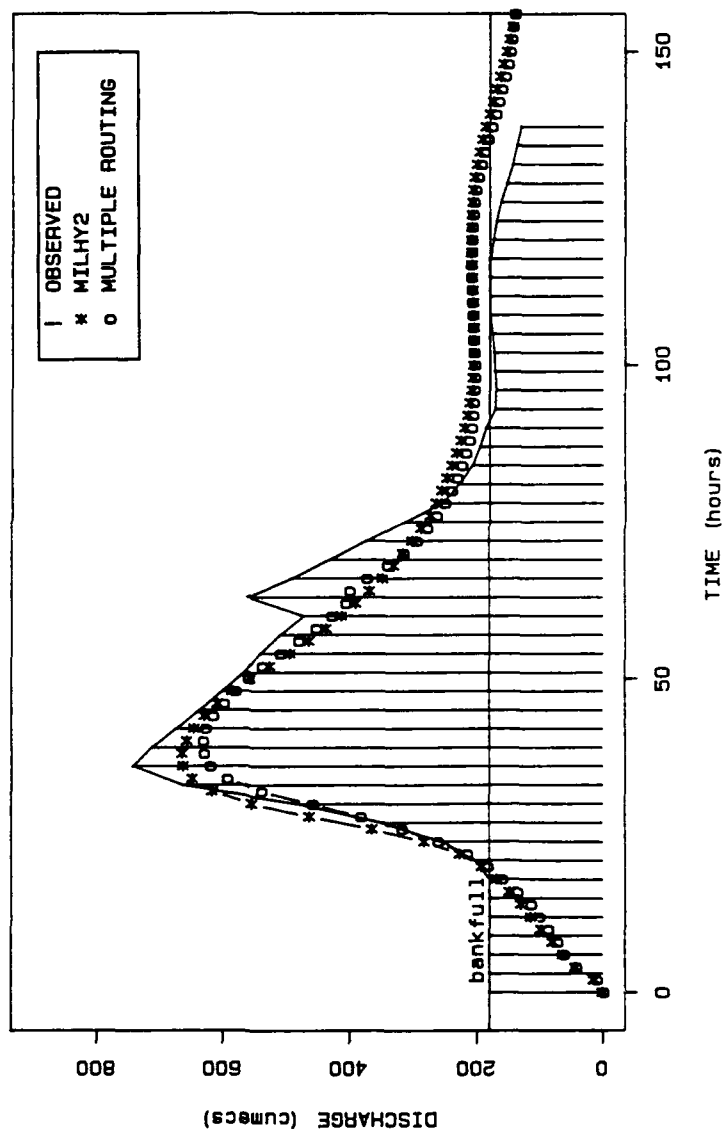
Figure 5.5
Comparison of MILHY2 and Multiple Routing Reach
Simulated and Observed Hydrographs for the 1 in 100
Year Event at Rotenburg

Chapter 5

5.3.2 <u>Application to a hypothetical reach</u>

The aim of investigating the impact of multiple routing
on a hypothetical reach was to examine the relative impact of
the floodplain inundation depth on the outflow hydrograph. A
hypothetical reach was set up with symmetrical rectangular
cross-sections at upstream and downstream stations with
floodplain/main channel width ratios of 10. The main channel
was a constant depth of 2.4m, so that the main channel capacity
remained constant downstream. This meant that the proportion
of flow on the floodplain was correct throughout the reach and,
therefore, the analysis could concentrate solely on the effects
of the floodplain inundation depth.

Table 5.3 and Figures 5,6 and 5.7 summarize the results
from this investihation into the impact of floodplain
inundation depth on the outflow hydrograph. In all these
simulations, the floodplain and channel reach length were held
constant at 20km. The seven inflow hydrographs were generated
by scaling the 1 in 10 year observed hydrograph from Bad
Hersfeld (see Figure 5.2).

Analysis of Table 5.3 shows that the predictions from the
two techniques converge as the floodplain/main channel depth
ratio increases to 0.8. When the depth ratio is less tha 0.4
the MILHY2 model gave greater peak discharge predictions. As
depth ratios increased up to 0.5, the multiple routing routine
generated greater peak discharge predictions. The maximum
error between the two techniques occurs when the depth ratio is
approximately 0.3.

When floodplain inundation depths are small, that is with
a depth ratio of 0.4, the MILHY2 generated larger peak
discharges because the separate floodplain flows of the
multiple routing routine are retarded by the effects of

Chapter 5

Table 5.3
Hydrograph Characteristics
Hypothetical Reach Application

Storm	Multiple		Time to peak hours	Peak discharge m^3s^{-1}	Maximum floodplain inundation m
1	1	MILHY2	36	309.8	1.16
		M. Routing	36	317.4	1.18
2	0.1	MILHY2	36	34.8	—
		M. Routing	36	32.8	—
3	0.2	MILHY2	42	57.2	0.09
		M. Routing	36	55.0	0.07
4	0.5	MILHY2	40	139.5	0.61
		M. Routing	38	126.9	0.56
5	1.5	MILHY2	36	536.0	1.68
		M. Routing	36	540.8	1.74
6	2	MILHY2	34	682.0	1.98
		M. Routing	34	685.0	1.99
7	3	MILHY2	34	1061.0	2.65
		M. Routing	34	1062.0	2.65
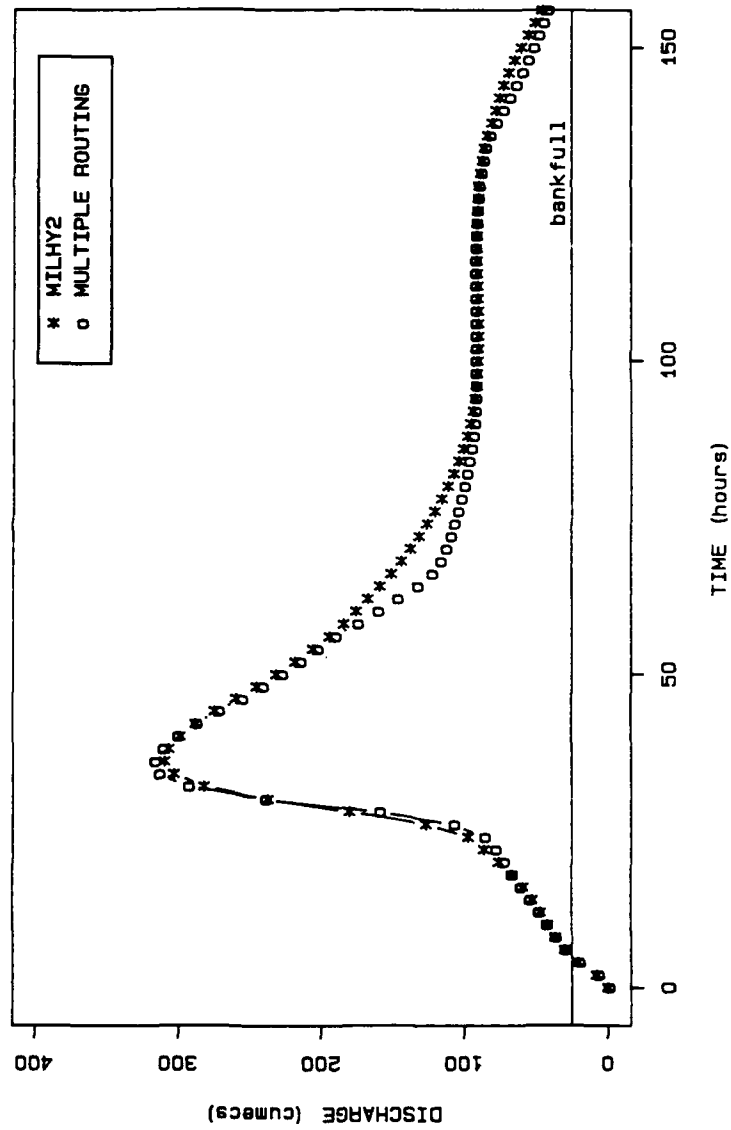
Figure 5.6
Comparison of MILHY2 and Multiple Routing Simulations
of Storm 1 in a Hypothetical Reach
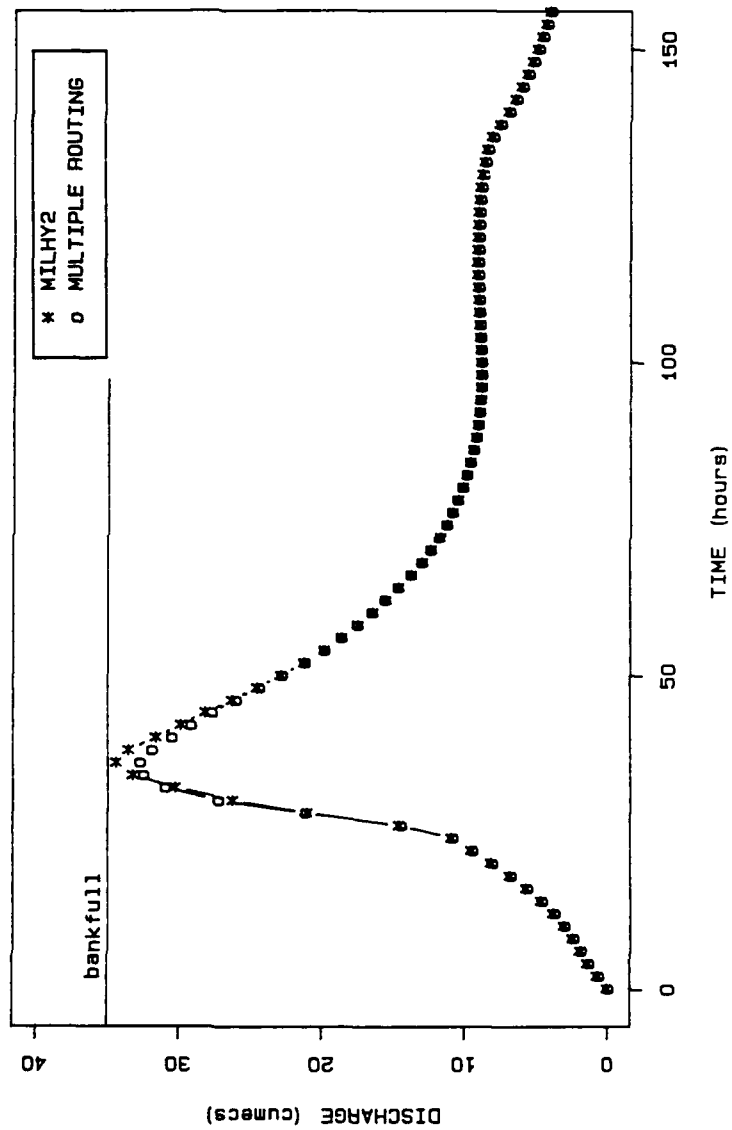
Figure 5.7
Comparison of MILHY2 and Multiple Routing Simulations
of Storm 2 in a Hypothetical Reach

Chapter 5

boundary friction. However, as Table 5.3 shows, the percentage
error between the two methods is small when the depth ratio is
very small and increases as the depth ratio increases up to
0.4. When the depth ratio is very small, that is less than
0.1, the majority of the flow is carried in the main channel
and in the multiple routing routine the wetted perimeter of the
main channel is small. The flow in the floodplain segments in
the multiple routing routine in very low flow conditions will
have very large travel times but they only contribute a small
percentage of the total discharge predictions. In MILHY2
simulations with very small floodplain inundation depths, the
wetted perimeter calculations include the floodplain boundaries
as well and, therefore, flows are retarded by the effects of
boundary friction.

As the depth ratio increases beyond 0.1 but remains
smaller than 0.4, the percentage of discharge on the floodplain
is large enough to be a significant part of the hydrograph.
However, the inundation depths on the floodplain are not great
enough to overcome the effects of boundary friction and,
therefore, the MILHY2 simulation generates much larger peak
discharge predictions.

When inundation depths are larger, that is greater than
0.4, the multiple routing routine generates peak discharge
pedictions greater than the MILHY2 prediction. This is because
the inundation depth of the floodplain is large enough to
overcome the effects of boundary friction and the travel time
of the floodplain flows at this stage is small. The predicted
outflow hydrograph of the multiple routing routine is then less
attenuated and so a larger peak discharge is produced.
However, the error between the two methods is small, and is not
greater than 2%.

Table 5.3 also compares the effects of reducing the

Chapter 5

length of the floodplain routing length on the p... discharge
prediction. The table shows that when the depth ratio exceeds
0.1, the reduced multiple routing length generates larger peak
discharge predictions than the MILHY2 simulation. Table 5.3
shows, therefore, that the effect of reducing the length of the
floodplain routing reach is to decrease the inundation depth
from 0.3 to 0.1. At this depth, the multiple routing routine
lowers the attenuation of the floodwave below that of the
MILHY2 simulation.

5.3.3 Conclusions

1. The maximum impact of the multiple routing technique
   occurs when the floodplain inundation depths are small.

2. At these small inundation depths (depth ratios = 0.3),
   when the utilization of multiple routing significantly
   improves the prediction of the peak discharge, errors are
   halved.

3. Reducing the floodplain routing length by 30% reduced the
   travel time of the peak discharge and decreased the
   attenuation of the floodwave.

4. Reducing the floodplain Manning's n coefficient by 30%
   reduces the attenuation of the floodwave to a similar
   degree as 30% reduction in the routing length of the
   floodplain flow segment.

5.4 Implications for the Improvement of MILHY2

The concept of multiple routing routines has been
approached hydrologically and hydraulically. Tingsanchali and
Ackerman (1976) use a hydrologic empirical adjustment of the

Chapter 5

Manning's n coefficient (equation 5.1), which is incorporated
into a hydrologic linear adjustment of the routing length with
increasing stage, this is incorporated into a hydraulic routing
model. Perkins (1970) utilizes a similarly hydrologic linear
adjustment of the routing length with increasing stage; this
is incorporated into a hydraulic routing model. Fread's (1976)
approach is the only hydraulic based routine; this routine is
incorporated into a full hydraulic reach model. The approach
utilized in this chapter is the simple separation of floodplain
and channel flows and discrete routing of them downstream.
This approach has not been used in either hydrologic or
hydraulic routines. Conceptually, this approach has advantages
over empirical adjustments and still provides the potential for
the incorporation of a more sophisticated adjustment of stream
flow length with a stage such as the scheme proposed by Perkins
(1970). Importantly, this is also the first application of the
concept of multiple routing with an hydrologic or storage flood
routing routine.

The results of the analysis of the multiple routing
routine suggest that the predictive accuracy of MILHY3 could be
improved by the introduction of the module. This is
particularly true for flow conditions where floodplain
inundation depths are great enough for the floodplain water to
be flowing rather than stored and where floodplain flows
contribute a significant proportion of the total discharge from
the reach. The introduction of the multiple routing concept,
therefore, has been shown to be important even when the
hydrological flood routing techniques are used.

The results also showed that decreasing the floodplain
routing length by 30% reduced the attenuation of the floodwave
and that a similar effect could be achieved by reducing the
floodplain Manning's n coefficient by 30%. This shows that
Chow's (1959) suggestion that the sinuosity of the channel

Chapter 5

accounts for 30% of the Manning's n coefficient value, is
correct. It also highlights the importance of boundary
friction. Comparison of Figures 5.3 and 5.4 shows, however,
that the introduction of the multiple routing routine and
adjustment in the Manning's n coefficient have a similar effect
on the shape of the predicted hydrograph. It is concluded,
therefore, that the multiple pathways of floodplain and main
channel flows and boundary friction effects are of equal
importance.

The positive results of this chapter support the further
evaluation of the multiple routing routine. This analysis has
shown that a simple technique can improve the predictive
performance of the model and incorporate the basic behaviour of
the two-stage channel. Further evaluation of the multiple
routing routine as part of a catchment model is considered in
Chapters 7 and 8.

5.5 **Summary**

This chapter has investigated methods of incorporating
the multiple pathways taken by floodplain and main channel
flows. A simple routine has been selected which apportions
flow to floodplain and channel segments and routes them
downstream using separately derived travel timetables. This
approach allows the adjustment of the lengths of the reaches,
thus incorporating the effects of the sinuosity of the main
channel on the travel time of the hydrograph.

Application of the routine to a hypothetical and a field
reach show that the routine improves the prediction of the
hydrograph, by the more accurate simulation of the attenuation
of the hydrograph. The results of this application show that

Chapter 5

the introduction of the multiple routing routi.. has just as
great an effect on the hydrogtaph as variation in the Manning's
n coefficient. The multiple routing routine, therefore, is
included in the final evaluation and validation of MILHY3.

Chapter 6

Chapter 6

Validation of MILHY3

I - A Strategy for Model Validation and Evaluation

The third objective of this report, outlined in
Chapter 1, is to validate the new model, MILHY3, which
incorporates the new turbulent exchange and multiple
routing modules. The validation of MILHY3 needs to answer
the following questions:

1)   Do the mathematical algorithms introduced represent
     the processes we are trying to model?

2)   Are the mathematical algorithms robust?

3)   Is the accuracy of the predicted outflow hydrograph
     a significant improvement over earlier versions of
     MILHY?

4)   Is the resolution of each new module appropriate for
     ungauged applications?

5)   Can a set of operational rules be developed for
     MILHY3?

The strategy for the validation programme can be
divided into three parts. Part I, reported in this
chapter, provides an introduction to the basis of model
validation and evaluation. It will also include the
identification and establishment of a data set for the
validation procedure. In Part II of the programme,
reported in Chapter 7, a hydrological validation will be

Chapter 6

undertaken, investigating the sensitivity of the composite
modelling structure. In Part III, a hydraulic analysis is
undertaken to investigate the utility of using hydraulic
models to provide "ground-truth" records against which
MILHY3 may be evaluated. This analysis is reported in
Chapter 8.

As noted earlier in Chapter 4 the validation of
MILHY3 will follow the model evaluation programme developed
by Sargent (1982). Sargent's programme provides one of the
few structured approaches available for model evaluation
and consists of three parts; mathematical validation,
computerised model verification and operational validation.

Mathematical Validation

The first of these stages is the mathematical
validation of the model. Howes and Anderson (1988) noted
that the objective of this section of the model evaluation
programme is to:

> "establish that the assumptions made about the real
> system by the model are reasonable and that the model
> adequately reflects the essential features and
> behaviour of the real system which are relevant to
> their application in mind."

However there is no deterministic method of testing
the assumptions and representativeness of a model; instead
the procedure must be rather subjective. In any modelling
exercise it is important that the modeller has a clear
understanding of the processes active in the physical
system to be modelled so that the implications of the
assumptions necessary to model the system are fully
appreciated. In this report, the importance of
appreciating the potential applications and uses of the

Chapter 6

model in the selection of a modelling strategy, has also
been stressed. This 'user's perspective' of the modelling
strategy determines to a greater degree the selection of
the modelling techniques than the ability and availability
of techniques or solutions to modelling problems.

Computerised Model Verification

This second stage of model evaluation attempts to
check the transfer of the mathematical techniques, that
approximate the physical environment, into a computer
code. The verification procedure needs to ensure,
therefore, that several aspects of the program are checked.

1)   that the program is internally valid, (Hermann,
1967). This ensures that if all the program input data and
controls are kept constant then the output from the model
remains constant;

2)   that there is conservation of mass. That is that the
volume of flow entering the simulation is matched by the
output from the simulation;

3)   that the model behaves under a range of input
conditions and the limits of the physical conditions that
a model can handle are specified.

One of the most effective tools available for
computerised model verification is a sensitivity analysis.
A sensitivity analysis measures the change in one variable
when one or more parameters are varied. Other available
techniques utilise hand calculations to check the validity
of simple routines.

Chapter 6

Operational Validation

The third stage of the model evaluation programme
involves measuring the accuracy of the model to predict
the behaviour of the natural environment, and developing a
set of rules or guidelines for the operation of the model.

Alternative strategies of undertaking an operational
validation programme include the use of goodness-of-fit
and error estimates, both utilised by Howes (1986). These
have been used primarily with data sets of field data,
however the availability of field data is not always
guaranteed. The availability of field data is a
particular problem for extreme events which by their very
nature occur infrequently and are difficult to measure.

It is proposed in this report that the model in
question can be tested against other modelling strategies
utilising the goodness-of-fit and error estimates. The
technique is potentially useful in assessing the accuracy
of models in extreme conditions when field data is
unavailable or the record is not long enough. Assessing
one model's performance against another could potentially
replace some hardware flume scale models.

6.1 Present Model Evaluation Status

The importance of a systematic model evaluation
programme was appreciated at the initiation of this
report. The programme therefore began with the selection
of the most appropriate modelling solutions to the
incorporation of the effects of momentum exchange and
multiple routing in two-stage channels in ungauged
catchments. The evaluation procedure continued with an
initial analysis of the module's performance. All three

Chapter 6

stages of Sargent's evaluation programme have therefore
already been initiated.

The validation programme has so far utilised a data
set from the River Fulda, West Germany and hypothetical
data sets based on rectangular channel geometries. It is
accepted therefore that the results of these simulations
are by no means exhaustive. However, given the limited
availability of data sets for extreme events and the time
available for this project, it is not the aim of this
report to undertake an extensive validation procedure.
This does not under-emphasize the importance of the
validation procedure, rather it was felt that a more
pressing objective would be to investigate alternative
techniques of validation. The validation procedure will
therefore concentrate on a limited number of simulations
and maximize the interpretations possible from these
simulations.

The results of the validation procedure so far, therefore,
have been summarised below.

6.1.1 Mathematical validation

The selection of the momentum exchange and multiple
routing techniques involved an investigation of the
alternative techniques available. The philosophy
forwarded in this report is that there is a need for
models to be developed from the perspective of the
potential user rather than from the state-of-the-art
conceptual or technical progresses in hydrology. This
report therefore proposes that the most important part of
Howes and Anderson's (1988) statement on mathematical
evaluation, noted above, is that "the model adequately
reflects the essential features and behaviour of the real
system which are relevant to their application in mind".

Chapter 6

In the selection of the most appropriate techniques for the
modelling of the momentum exchange and multiple routing,
the primary determining factor was the limitations
posed by the ungauged catchment perspective. These
limitations were:

1)   the data requirements of the new algorithms should
      be small; in particular, field work should not be
      required;

2)   any additional demands made of the user in the
      establishment of the data sets should not require
      detailed hydrological knowledge of the physical
      processes or computer expertise.

3)   The computer demands, in terms of CPU and operating
      space, of the new routines should allow the
      application of the model to the IBM-PC level.

Both the momentum exchange and multiple routing
routines developed in Chapters 4 and 5 meet these
limitations. It is accepted, however, that the solutions
proposed are not the only feasible alternatives to meet
these limitations. However, the techniques selected from
the shortlist of techniques identified in Chapters 4 and 5
were, it was felt, the simplest techniques to implement
that still incorporated the essential features of the
behaviour of the system in question. If the increased
resolution of the modelling of two-stage channels should
prove significant in improving the predictive accuracy
of the catchment model, then some of the other technical
solutions should be reconsidered.

The mathematical validation of the momentum exchange

Chapter 6

and multiple routing modules (sections 4.3 and 5.2) show,
therefore, that the modules 'adequately represent' the real
system and that the assumptions made are reasonable for a
first assessment of the relative importance of two-stage
modelling.

6.1.2 Computerised model verification

The simulations reported in Chapters 4 and 5 of the
performance of the momentum exchange and multiple routing
modules, serve to illustrate that the modules are
internally valid (Hermann, 1967) and the algorithms are
mathematically robust. The new model version, MILHY3,
given the same model control parameters and data set, will
simulate an identical set of results to the earlier MILHY2.
This confirms that the coding of the new routines has not
altered the continuity of the program.

The results reported in Chapters 4 and 5 also appear
to be logical. When more turbulent shear stresses are
introduced into the momentum exchange routines, for
example, the predicted capacity of the cross-section is
reduced. Similarly, when the length of the floodplain
routing length is reduced, the travel time of the
floodplain is reduced.

The behaviour of the modules under 1 in 10 year and
1 in 100 year events has been tested. The behaviour of
much smaller events in hypothetical reaches has also been
tested. Tables 4.3, 4.4 amd 4.5 explore the application of
the four momentum exchange routines to the Bad Hersfeld
station on the River Fulda. Tables 4.6, 4.7, 4.8, 4.9 and
4.10 explore the impact of the same four techniques on a
hypothetical reach. These tables show that the routines
are stable for a variety of geometrical conditions and

Chapter 6

boundary roughness values. Table 4.3 also confirms the
correct coding of the routines by comparing MILHY2
solutions with momentum exchange method 2. Both of these
techniques utilize the same interface inclination method
and have an apparent shear stress ratio of 1. Table 4.3
confirms, therefore, that identical computation methods
produce identical results.

Tables 5.1 and 5.2 report the results of the
application of the multiple routing routine to the Bad
Hersfeld-Rotenburg reach on the River Fulda. Table 5.3
reports the results of the application of the routine to a
hypothetical reach. These tables show that the multiple
routing routine is stable for a variety of storm events
and that there is continuity in the conservation of mass
in the routine.

Application of the momentum exchange and multiple
routing routines confirms, therefore, that the codings
remain stable under a range of conditions and that the
routines seem to operate logically.

6.1.3 Operational validation

The initial simulations reported in Chapters 4 and 5
suggest that both the momentum exchange and multiple
routine modules make a significant improvement in the
predictive accuracy of the hydrograph. The improvement in
the predictive accuracy generated by the two models
supports the advancement of the two modules into the next
stage of the validation procedure.

This initial analysis, therefore, has confirmed
the mathematical validity of the two modules and verified
their computer coding. The analysis has also suggested
that the predictive performance of the modules is an

Chapter 6

improvement over the previous techniques. However, there
are still several important questions in the evaluation of
the new model that must be answered. These outstanding
questions are:

1)   Is the outflow hydrograoh more sensitive to
      variability in the physically-based parameters, or
      to the process submodels utilised?

2)   What is the relative impact of the submodels
      introduced in MILHY3 in comparison with the
      infiltration algorithm introduced in MILHY2?

3)   What is the impact on the outflow hydrograph of the
      conflicting effects of the new submodels?

4)   What are the effects of the scale of the catchment
      on the three questions posed above?

These questions show the need to investigate both the
*verification of the computer modelling and the validation
of the operational performance of MILHY3.*

6.2   **Design of a Model Evaluation Strategy**

The analysis of the initial evaluation of the new
modules has shown the need for further computerized model
verification and operational validation.

The computerized model verification procedure must
investigate the relative impact of the new modules when
they are part of a catchment simulation model. It must
also investigate the interaction between the new modules.
Perhaps most importantly, the verification procedure needs
to investigate the effects of variability in the model

Chapter 6

structure. The composite structure of MILHY3 offers
differing module resolution solutions for both the
simulation of the runoff excess (Curve Number and
Infiltration Algorithm) and the simulation of channel
routing. The composite structure therefore generates the
need for a sensitivity analysis that will investigate not
only the sensitivity of the outflow hydrograph to
variability in the parameters but also the sensitivity of
the predicted outflow to variation in the structure of the
model.

A well structured sensitivity analysis could provide
answers to all the questions posed above. An operational
validation is still required, however, to establish the
accuracy of the new routines.

The undertaking of a sensitivity analysis and an
operational validation requires the availability of a data
set. As noted earlier, however, the provision of data sets
for extreme events is not necessarily easy. A sensitivity
analysis can utilise relatively small amounts of field
data and still achieve an acceptable level of accuracy.
The number of data sets required for an operational
validation, however, is much greater. One of the
objectives of this report is therefore to investigate the
utility of using other models to validate the operational
performance of a new model.

The evaluation of the MILHY3 model will therefore be
split into two parts; the sensitivity analysis and the
operational analysis. Both of these analyses will utilise
the same data sets collected from the River Fulda. The
problem of data availability is a common one in model
evaluation and it is felt that an investigation into
alternative techniques and the maximizing of the utility
of the data available would be profitable. The implement-

Chapter 6

ation and results of the sensitivity analysis is reported
in Chapter 7 and the operational validations are reported
in Chapter 8. In the the rest of this chapter, the Fulda
data set is established.

6.3   Selection of a Field Catchment

There are three sources that generate prerequisites
on the selection of a suitable data set for the validation
and evaluation of MILHY3. These three sources are:

1)   the outstanding questions to be answered in the
       evaluation and validation of MILHY3. These
       outstanding questions are listed in section 6.1;

2)   the capabilities of MILHY2, in particular the
       boundary conditions for which the model has been
       validated, see section 2.2;

3)   data characteristics or additional information
       that make the model evaluation simpler or more
       efficient.

These three sources place differing prerequisites on
the selection of a suitable field catchment. The first and
the second of the groups of prerequisites, noted above,
must be met; the third group is not essential.

6.3.1 Prerequisitres of a study catchment

1.   Outstanding questions

a)   The catchment should be large so that it can be
divided into a number of smaller subcatchments. Each of
these subcatchments should have a gauging station for which

Chapter 6

the cross-sectional geometry is known and for which rating
curves and hydrographs are available. A multi-subcatchment
environment will allow the establishment of a suite of
catchment scales. These requirements will allow the
investigation of the effects of the inclusion of the
infiltration algorithm in a multi-subcatchment environment
and allow the relative impact of the new modules to be
assessed.

b)   The catchment must be subject to floodplain inundat-
ion so that the new modules may be utilized.

2.   MILHY2 limitations

All of these limitations are generated from the
operational conditions set out by Williams and Hann (1973)
and Howes (1986). These limitations represent the environ-
mental conditions for which the process modules have been
incorporated and for which the model has been validated.

a)   The catchment must be in a temperate region with a
      minimum of forested area.

b)   The catchment must not exceed a maximum area of
      $2500km^2$.

c)   There should be a minimum of man-made interferences
      in the catchment, such as urban areas or land
      drainage schemes.

d)   A minimum data set should consist of:
      - topographic maps
      - soils classificatory maps
      - upstream and downstream valley cross-sections,
        rating curves and hydrographs

Chapter 6

- precipitation data corresponding with the observed
  hydrograph events.

3.   Evaluation convenience

a)   Selection of a relatively simple and regular cross-
sectional geometry would allow the importance of the two
new modules to be assessed in the most unambiguous of
environments. A simple cross-sectional geometry would
make comparison of the four multiple routing routines
easier. Regularity of the cross-sectional geometry of the
floodplain environment between gauging stations would
provide the environment for which the multiple routing
routine would make the greatest improvement in the
predictive accuracy of the model.

b)   Additional data such as a flood frequency analysis
and a greater resolution in the rainfall, soils, or
topography parameters, would allow more accurate comparison
between observed and simulated results.

6.3.2 The River Fulda Catchment

      These prerequisites limited prospective study
catchments to the rural regions of Western Europe and areas
of the U.S.A. From a short list of regions meeting the
prerequisites, the River Fulda catchment in West Germany,
(see Figure 6.1) was selected, primarily because of the
efficiency and rapid response to requests for data from
the relevant water authorities and meteorological offices.
As well as the prerequisite data, the local authorities*
in the River Fulda catchment were able to provide:

    i) an outline of the extent of floodplain inundation
       for a storm event in 1946, corresponding to the 1 in
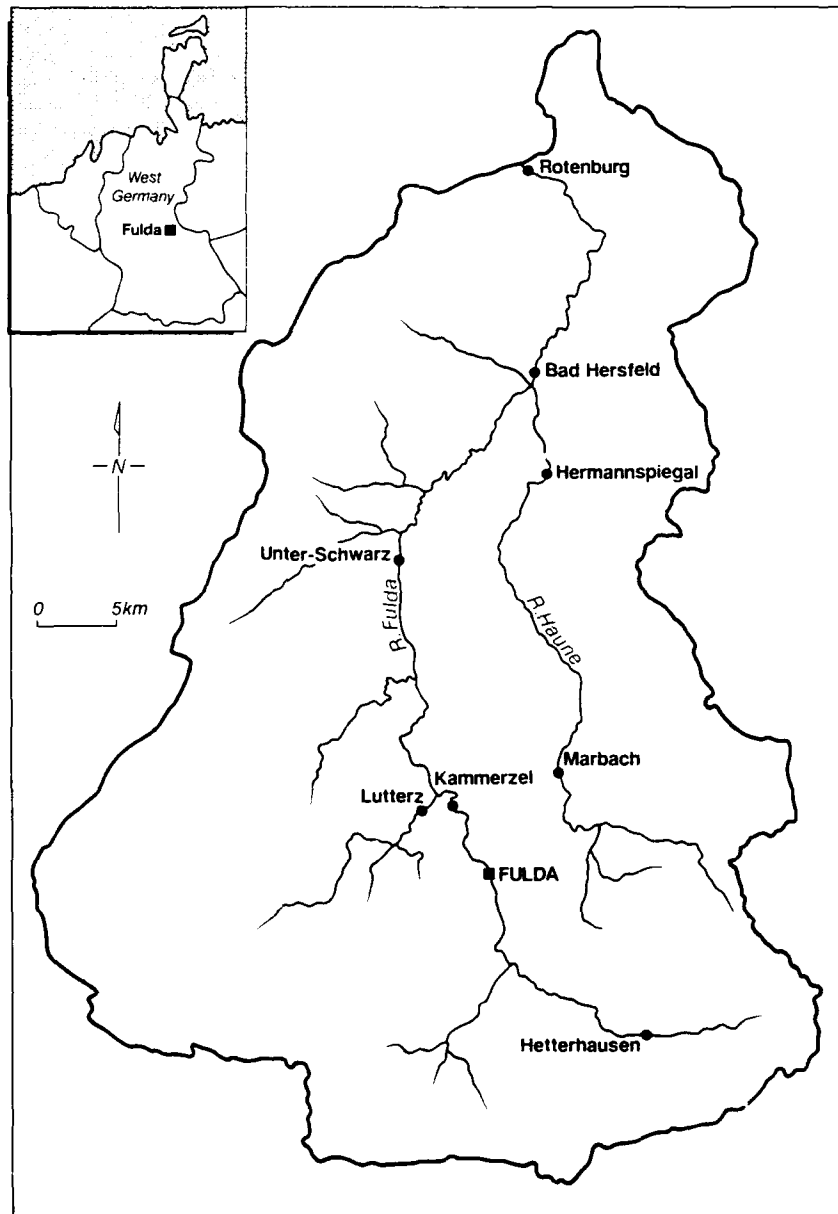
Figure 6.1
River Fulda Catchment and Gauging Stations

Chapter 6

200 year event.

ii) daily precipitation values for approximately 45 rain
gauge stations (see Figure 6.2)

iii) continuous rainfall data for two stations, Bad
Hersfeld and Kunzell-Dietershausen

lv) for one storm, the water-equivalent of snow, daily
minimum and maximum, temperature, relative
humidities and cloud cover

v) long-profiles of two of the reaches, between Bad
Hersfeld and Rotenburg, on the River Fulda, and
between Marbach and Hermannspiegal, on the River
Haune (a tributary of the River Fulda).

The provision of further meteorological data provides
the potential for the use of the River Fulda catchment in
the simulation of snow melt events. Although snow melt
events are not considered in this report, the potential for
the simulation of such events is available within the MILHY
project (Pangburn, 1987). This, therefore, provided
further impetus for the selection of the River Fulda
catchment.
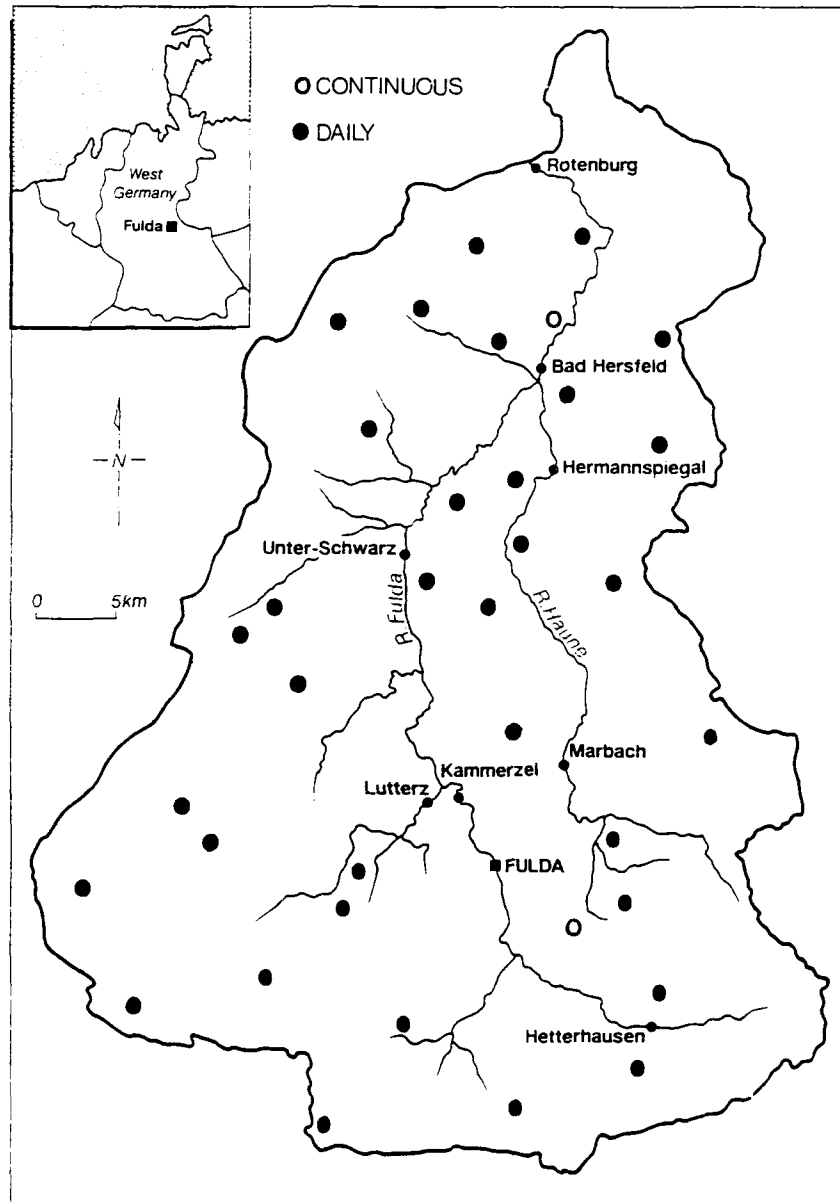
Figure 6.2
Raingauge Network for the River Fulda Catchment

Chapter 6

6.4   Establishment of the River Fulda Catchment

The River Fulda catchment to Rotenburg consists of a drainage area of approximately 2523km^2, drained by the River Fulda and its tributaries. The main tributary is on the River Haune, which joins the Fulda at Bad Hersfeld; in addition, the River Luder joins the Fulda at Lutterz. There are eight river gauging stations in the catchment, marked on Figure 6.1, for which six storm events have been collected. The positions of the gauging stations have enabled the division of the catchment into nine subcatchments, depicted in Figure 6.3.

During the visits to the catchment, drawings were made and photographs taken that enabled the technical channel cross-sections to be extended across the floodplains. Estimates were also made during these visits of the Manning's n roughness values of the channels and floodplains throughout the catchment. Figures 6.4, 6.5 and 6.6 are photographs taken at Hetterhausen, Unter-Schwarz, and Rotenburg, and show the topography and land-uses typical throughout the catchment. In the photographs it can be seen that:

i)   in the upper reaches the channel is tree-lined

ii) the floodplains are extensive and relatively flat

iii) the floodplains throughout the catchment are
     vegetated by short grass

iv) there are few obstructions on the floodplains,
     there are few fences, and the small villages tend
     to have been built clear of the areas subject to
     flooding
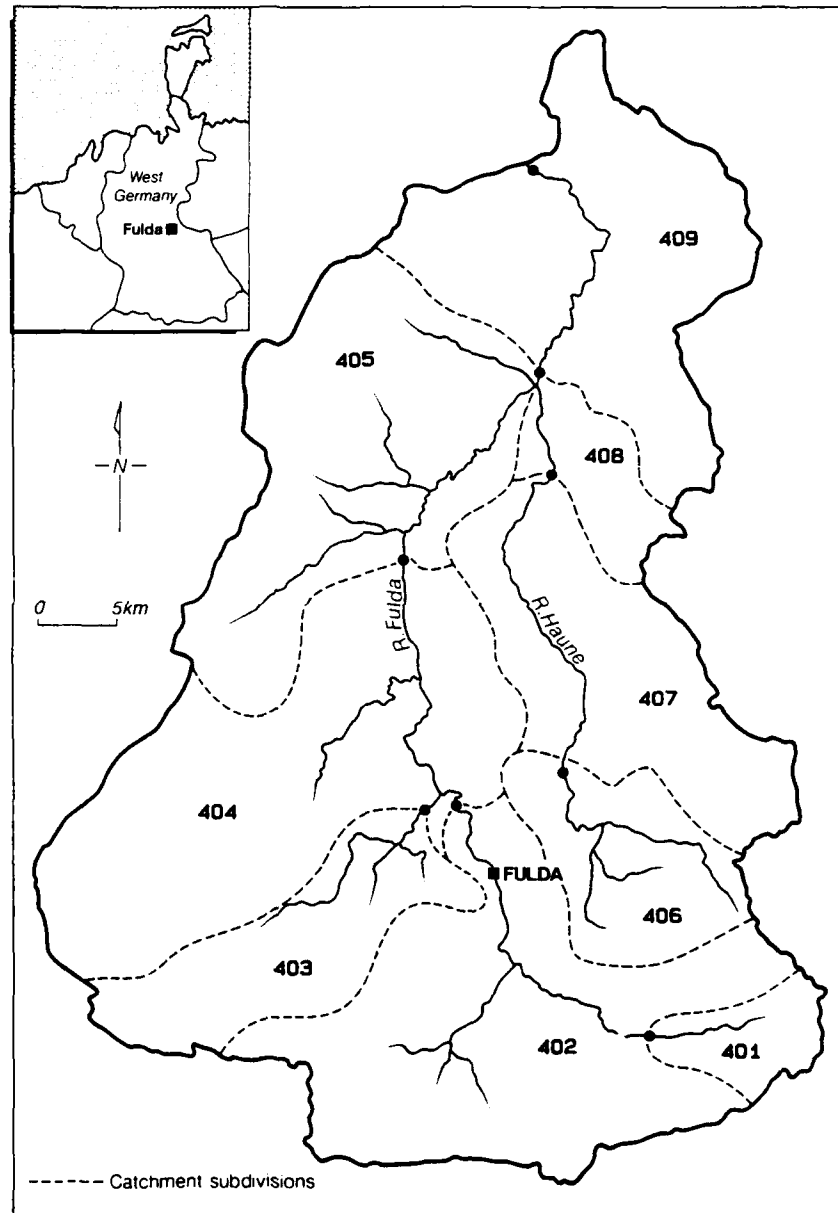
Figure 6.3
Catchment Subdivision of the River Fulda Catchment

Figure 6.4
Cross-Section at Hetterhausen, River Fulda

Figure 6.5
Cross-Section at Unter-Schwarz, River Fulda

Chapter 6
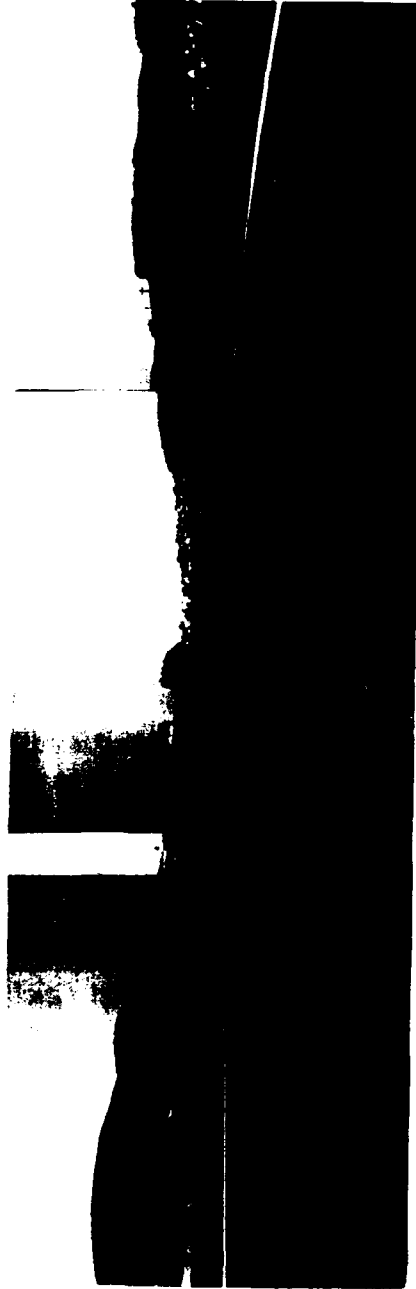
Figure 6.6
Cross-Section at Rotenburg, River Fulda

Chapter 6

v) the channel is broadly rectangular in cross-
section

vi) the channel is sinuous

Tables 6.1 and 6.2 collate some of the topographic
dimensions of the subcatchments and the channel geometries
at the gauging stations.

Six storm events were identified as being discrete
events, that is where the hydrographs rose and fell back to
baseflow conditions within a single seven day record. For
each of these events, the daily rainfall totals for the
three preceding weeks were collected in order to compute
antecedent conditions.

In order to compute the rainfall in each of the nine
subcatchments, the Theisson polygon technique was used to
weight the daily rainfall total from each of the 45 rain
gauges shown in Figure 6.2. Polygons of the area
associated with a particular raingauge were drawn as if the
catchment had no relief.

Table 6.3 shows the percentage occurrence of each of
the major soil groups in each of the nine subcatchments.
A certain amount of interpolation and generalisation
occurred during the computation of this table, as the
pixel definition of the soils classificatory maps was
1 pixel = 100 metres. The use of a graphics tablet
attached to an IBM-AT, however, considerably speeded the
computation of both the raingauge polygons and soil group
areas.

Chapter 6

Table 6.1

Parameter Values for Subcatchments in

the River Fulda Catchment

Subcatchment	Area	Max. elev	Min. elev	Main channel length
	km^2	m	m	km
401	56	838	365	14
402	506	550	232	36
403	182	700	232	25
404	469	775	216	27
405	394	416	193	33
406	148	700	265	24
407	274	610	209	34
408	90	518	193	9
409	403	391	179	24
Total	2523	838	179	227

Chapter 6

Table 6.2

Parameter Values for Gauging Stations

in the Fulda Catchment

Station	Bankful depth m	Bankfull width m	Bankfull capacity $m^3 s^{-1}$
Hetterhausen	2.3	17.0	26
Kammerzell	2.0	20.1	33
Lutterz	3.2	18.0	18
Unter-Schwarz	3.0	18.0	50
Marbach	2.3	8.0	10
Hermannspiegel	2.5	16.5	22
Bad Hersfeld	4.1	30.3	76
Rotenburg	4.8	50.0	179

Chapter 6

Table 6.3

Soil Group Classification for the Sub-Catchments in

the River Fulda Catchment

Subcatchment	USCS Soil Classification System				
	percentage occurrence				
	SC/SM	ML	CH	CL	G
401	54.6	11.6	11.3	10.5	12.1
402	45.6	10.3	5.2	27.7	11.4
403	25.0	2.9	4.0	59.9	7.9
404	36.6	2.7	15.2	33.0	12.0
405	65.8	4.1	4.7	8.2	17.3
406	50.1	13.4	9.8	21.4	5.4
407	46.4	8.4	25.2	15.5	4.6
408	41.0	0.0	15.2	34.7	9.2
409	86.5	0.0	4.8	0.0	8.6

SC Clayey sands or clayey gravelly sands

SM Silty sand or silty gravelly sand

ML Silts, sandy silts, gravelly silts

CH Fat clays

CL Lean clays, sandy clays, or gravelly clays

G   Gravels

Chapter 6

6.4.1 Establishment of the data sets

Two data sets are required by MILHY3: 'data1'
contains the program commands, hydrological commands and
associated data, whilst 'data2' contains only data for the
infiltration algorithm. The rules for setting up these
data sets and examples of them are given in Volume 2.

Data1

Figure 6.3 illustrates the division of the River
Fulda catchment into nine catchments. In each of these
subcatchments, a runoff hydrograph must be developed, for
all except the headwater subcatchments, and this must be
added to the flow routed through the subcatchment. In
each routing reach, two cross-sections are developed, one
at either end of the reach. In subcatchment 404, where
the River Luder joins the River Fulda at its inflow, the
Kammerzell cross-section is used.

The Curve Number routine for the generation of the
runoff hydrograph using the SCS method were identified from
tables in the Student Handbook on streamflow forecasting by
James and Stinson (1981).

Data2

Each soils group in each subcatchment was represented
by a single column, giving a total of 42 columns, see
Table 6.3. The runoff generated by these columns was
weighted by the percentage area of each subcatchment that
a soil group occupied. For the six storm events identified
during the establishment of the River Fulda catchment,
a common theme was a period preceding each event of small
low intensity showers. This enabled the fairly safe
assumption that the soils were saturated three days prior

Chapter 6

to the beginning of each of the six identified events.
The infiltration generation routines were then used to
simulate the three days prior to the storm, in order to
generate the antecedent conditions.

Each of the 42 soil columns was split into 3 layers,
typical of well-developed soils, and a total of 10 cells
were specified in each column. The soils hydrological
parameters were calculated using the empirical charts and
regression equations developed by Brakensiek and Rawls
(1983), and reported in Anderson and Howes (1986).

A test simulation using an observed 1 in 10 year
event to check the establishment of both the data sets,
showed that the infiltration algorithm was failing to
generate sufficient runoff in comparison with the observed
hydrographs from the gauging stations. Figure 6.7
illustrates the generated hydrograph at the Hetterhausen
station and shows that the simulated discharge is signific-
antly smaller than the observed discharge. Investigation
of the rainfall distribution procedure showed that the
observed runoff volume was feasible for the rainfall
distribution and therefore the error was associated with
the soils data.

As noted earlier, the soils at the start of the
simulation is assumed to be saturated and then the
simulation is allowed to run for three days prior t the
commencement of the storm event to allow antecedent
conditions to be generated. Analysis of the results from
the infiltration algorithm suggested that the hydraulic
conductivity of the soils were too high. This was because
during the storm event, despite being the 1 in 10 year
event, the rainfall failed to saturate the soil and the
rainfall was lost as drainage from the bottom of the
soil columns. This suggests that either the hydraulic
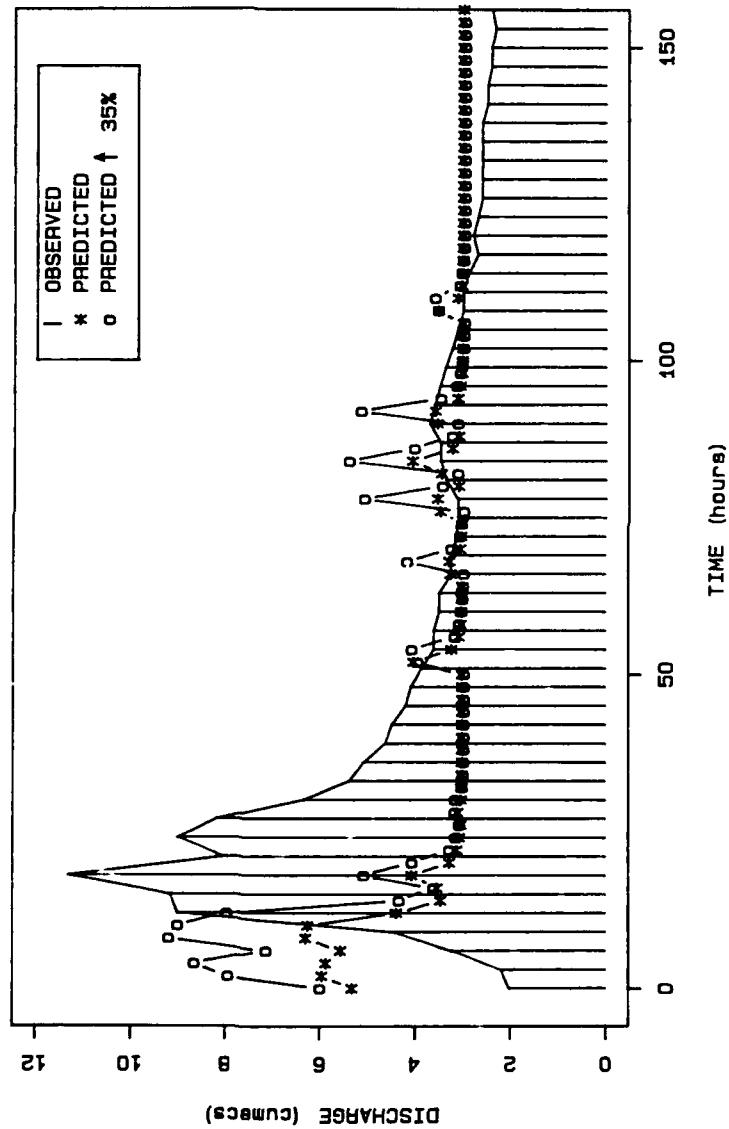
Figure 6.7
Comparison of Observed and Simulated Hydrographs with
Varying Percentage Clay Cobtributions, for the 1 in
10 Year Event at Hetterhausen

Chapter 6

conductivities were too high, or that the dominant process
in the catchment was throughflow rather than overland
flow. The review of the simulation of infiltration in
MILHY3, reported in section 2.2.3, shows that the model is
capable of simulating the movement of water soil in the
vertical dimension only. It was important, therefore, to
establish whether such an error in the generation of the
runoff hydrograph could feasibly be attributed to the
selection of too high a hydraulic conductivity. If a
throughflow dominated catchment was shown to be the only
possible explanation, then it is important to identify the
limitation of the MILHY3 scheme and to possibly identify
operational guidelines to allow the more approximate
application of MILHY3 in such circumstances.

There are two possible sources of error that could
generate too low a hydraulic conductivity. Either the
incorrect hydraulic conductivity from the Brakensiek and
Rawls (1983) charts was selected for each or some of the
soil groups, or the soil groups in the high hydraulic
conductivity groups were too highly represented.

A second simulation used the lowest hydraulic
conductivity feasible for each soil group using the
Brakensiek and Rawls (1983) charts. This simulation still
failed to generate sufficient runoff and therefore this
source of error was excluded.

6.4.2. Soils classificatory errors

There are several feasible sources of error in the
generation of the proportion of a subcatchment that a
soils group occupies. These include:

1)   **Resolution.** This includes the resolution of the soil

Chapter 6

surveyor's report, and the interpretive work carried out
in the establishment of the data set. The resolution of
the original survey will depend upon the purpose to which
the map is aimed. Beckett and Webster (1971) point out
that there is little practical purpose in having a
resolution size less than the minimum land-use management
area, usually a field.

2)   Purity. This is the percentage of each group that is
occupuied by that group. Beckett and Webster (1971)
identify the level of purity of many of the soil survey
organisations aim to achieve. This includes the USDA
purity level of 80-90%, and the US Bureau of Reclamation
purity level of 75%.

Analysis of the results from the infiltration
algorithm simulations showed that it was only the clay
groups (CH and CL in Table 6.3) that had a low enough
saturated hydraulic conductivity to generate overland flow,
given the intensity of the 1 in 10 year event. It is
possible, therefore, that the purity of the high conduct-
ivity groups was particularly low, or that the resolution
of these groups ignored lower conductivity areas. Could
the percentage occurrence of the clay groups be legitim-
ately increased in line with the purity level suggested by
Beckett and Webster (1971)? If this proved successful,
then the purity level could potentially provide an
important operational guideline.

Closer analysis of the soils classificatory maps
showed that the distribution of the clay groups were
heavily biased to the floodplain area where runoff could
be expected to join the channel flow, due to high water
tables and the effect of topography. Under-estimating
these groups, therefore, would have a large effect on the
predicted hydrograph. These results suggest that in event

Chapter 6

simulations such as MILHY3 that do not simulate the
throughflow contribution to the hydrograph, it is important
to accurately estimate the percentage contribution of the
soil groups with low hydraulic conductivities. This is
particularly true for low intensity rainfall events, where
the resolution of high conductivity groups may be reduced.

Trials showed that a 35% increase in the occurrence
of the clay groups was required before the required volume
of runoff was generated, see Figure 6.7 As the 35%
increase is somewhat larger than the purity levels noted by
Beckett and Webster (1971), who gave a maximum error of
around 20-25%, this suggested that the minirum misclassif-
ication error was approximately 10-15%. Estimation of the
classificatory map and the distribution of the clay groups
suggests such an error is feasible.

In the simulations reported in the rest of this
report, therefore, the soils classificatory groups have
been adjusted in line with the error sources identified
above. It is accepted that this is a partial calibration
of the model, which could not occur in a truly ungauged
application. However, given the concentration of this
report on the channel routing components of MILHY and on
the development of a composite modelling structure, and
given the problems of collecting another data set to
validate the assumptions relating to the sources of the
classificatory errors, it seems appropriate to accept this
limitation of the data set and pursue the rest of the
evaluation analysis.

P

Chapter 7

Chapter 7

Validation of MILHY3

II - Hydrological Sensitivity Analysis of MILHY3

The sensitivity analysis of MILHY3 aims to complete the computerised verification section of Sargent's (1982) model evaluation programme. Howes and Anderson (1988) identified three areas that a well structured sensitivity analysis should investigate. These three areas are:

1) The analysis should demonstrate that the model behaves realistically when the model inputs and parameter values are varied

2) The analysis should show that the model is sufficiently sensitive to represent the actual variation in the system

3) The analysis should identify the model parameters or inputs to which the model is most sensitive

The design of the sensitivity analysis will incorporate these three areas into the specific objectives of the analysis of MILHY3.

7.1 **Design of the Sensitivity Analysis**

The main objectives of the sensitivity analysis are to investigate:

1) the sensitivity of the hydrograph to variation in MILHY3's parameters;

Chapter 7

2)   the sensitivity of the hydrograph to the submodels
      used in its derivation;

3)   the interaction of the effects of the momentum
      exchange and multiple-routing submodels;

4)   the relative impact of the inclusion of infiltration
      algorithm if sub-catchments are utilized;   and

5)   the effects of scale.

First it is necessary to identify the parameters and
submodels that make up MILHY3's composite structure.
Table 7.1 lists all the variables in three groups;
spatial variables, temporal variables and physically-based
parameters. The spatial and temporal variables describe
the resolution of information in each submodel or process
area, whilst the physically-based parameters describe the
initial conditions and geometry of the catchment.

Figure 7.1 shows the composite structure of MILHY3
and the process modules available. The figure shows that
there are five stages in the development of the outflow
hydrograph. These five stages are: the spatial
variability of the precipitation, the runoff generation
technique, generation of the rating curve, designation of
the routing pathways, and finally the routing of the
hydrograph. The figure also shows that at the first four
stages of the hydrograph development the user is now given
a choice in the resolution of module required. The
original modules prior to the developmental work in this
report are shown on the left-hand side of the diagram,
whilst the new, higher resolution modules are on the
right-hand side of the diagram. The user may now choose
modules at either resolution levels at each of the
hydrograph development stages. One of the aims of this

Chapter 7

Table 7.1

Variables Utilised in MILHY 3

Spatial Variability

Number of subcatchments

Number of raingauges

Number of soil columns

Number of soil cells

Thickness of soil cells

Number of valley sections in reach

Number of segments in cross-section

Rating curve increment

Temporal Variability

Rainfall time increment

Infiltration simulation iteration period

Routing time interval

Physically-based parameters

Initial soil moisture content

Saturated soil moisture content

Suction moisture curve

Saturated hydraulic conductivity

Surface detention capacity

Maximum evaporation

Watershed area

Watershed elevation

Main channel length

Cross-sectional geometry

Slope, channel and floodplain

Routing length

Manning's 'n', channel and floodplain

Reservoir outflow storage

Soil, crop, conservation and gradient factors

Precipitation, storm duration and intensity

167

MILHY3
COMPOSITE MODEL STRUCTURE
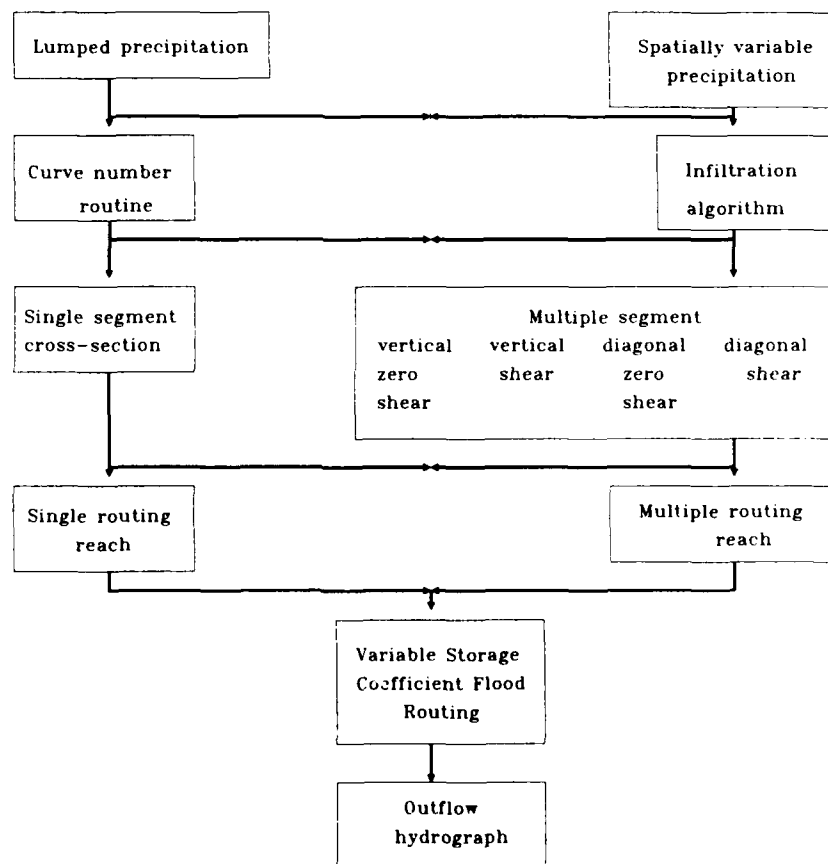
Figure 7.1
MILHY3
Composite Model Structure

Chapter 7

report is to develop a series of guidelines to help the
user select the most appropriate module resolution level
for a particular application.

To avoid repetition of the analysis of sensitivity of
any of the parameters identified in Table 7.1, a review
was made of all previous evaluation programmes undertaken
on all versions of MILHY and MILHY2. A summary of this
review is reported in Table 7.2, which shows that previous
evaluation programmes have concentrated on the parameters
and controls of runoff excess generation. Most
importantly, the evaluation of the incorporation of the
infiltration algorithm has taken place only in single
catchments. This is significant in the evaluation of the
success of the composite structure of MILHY3 and in
particular the problem of module resolution. An important
part of this analysis will be to investigate the
performance of the high resolution infiltration algorithm
in multiple subcatchments.

Comparison of Figure 7.1 showing the variable
structure of MILHY3 comprising of 12 process modules, and
Table 7.1 detailing 34 parameter and control variables for
these modules, shows that there are a total of 46
parameters in the MILHY3 model. Taking into consideration
the parameters that have already been investigated and
that are summarised in Table 7.2, there are still 32
parameters to investigate.

If these 32 parameters were to be varied in a
statistically meaningful way, that is considering twenty
storm events, twenty cross-sectional geometries, twenty
routing reach lengths, twenty boundary roughness ratios,
and utilising all the possible module combinations, then
several thousand simulations would be required. This
would take 5 years of central processing time on the SUN

Chapter 7

Table 7.2
Existing Sensitivity Analyses of MILHY2

Author	Parameter or Variable
Williams (1975)	Routing length
	Routing time interval
Anderson (1982)	Detention capacity
Anderson and Howes (1984)	Suction moisture curve
	Saturated moisture content
	Saturated hydraulic conductivity
	Initial moisture content
Anderson and Howes (1986)	Watershed area
	Watershed elevation
	Main channel length
	Storm intensity
	Cell size
	Infiltration simulation increment

Initial results

Chapter 4	Number of segments in cross-section
	Rating curve stage increment
	Cross-sectional geometry
	Manning's n coefficient
	Slope

Chapter 7

workstation. It is important, therefore, to select
carefully a series of simulations that will enable the
sensitivity of MILHY3 to be ascertained within a fair
degree of certainty.

Interest has been directed in this project to the
modelling of the frictional effects of over-bank flow or
flow in two-stage channels. The sensitivity analysis will
reflect this concentration and therefore focus primarily
in this area. The analysis will investigate the structure
of MILHY3 in terms of its module components and explore
variability of the physically-based parameters in the
downstream conveyance submodels. These parameters will
include the slope of the channel and floodplain, the
routing length, and Manning's 'n' values for the channel
and floodplain.

Having identified a manageable group of variables for
investigation, the next stage is to develop a strategy for
investigating the sensitivity of these variables.

7.1.1 Alternative methods of undertaking a sensitivity
       analysis

McCuen (1973a and b) defines sensitivity as:

"the rate of change in one factor with respect to
change in another factor"

McCuen points out that it is the failure of
researchers to appreciate the generality of this
definition that has limited the application of the
sensitivity analysis tool to the final verification of
models. Several authors have identified the utility of
the sensitivity analysis in all stages of the development
of a model (McCuen, 1973a and b, 1976; Miller et al. 1976;

Chapter 7

Hornberger and Spear, 1981). This is why an initial
analysis was incorporated in the identification of the
most important processes in two-stage channels (Chapter
3), and in the development on the submodels to model these
processes (Chapters 4 and 5).

Jones (1982) identified two approaches to undertaking
a sensitivity analysis: one involves a deterministic
methodology, the other a stochastic methodology. A
deterministic methodology involves making small changes in
the input parameters and investigating changes these
changes effect on the models output. A stochastic
approach involves selecting the input parameter values
from a probability distribution according to, either the
accuracy of the input values or the error bands to which
the model internally operates. Because the probability
distributions can contain all the physically realistic
data input values, a stochastic analysis can usually
encompass a wider range of input data values than a
deterministic analysis. In a deterministic analysis the
operator must usually either select input values
systematically, or use intuitive knowledge of the
behaviour of input parameters.

Work by Anderson and Howes (1984 and 1986) has
concentrated on a stochastic analysis of the soil input
parameters of the infiltration algorithm. The
difficulties of measuring these parameters in the field
mean that a relatively large error distribution can be
associated with the observed field values. A stochastic
analysis was an ideal method of incorporating these error
distributions in an analysis of the effects of parameter
variability on the model output.

In the sensitivity analysis reported here, the
objective is to investigate the behaviour of the model

Chapter 7

output with respect to both the model structure and
variability in certain parameters. As the model structure
cannot be described by a probability distribution, this
necessitates a deterministic analysis.

There are two methods of computing the sensitivity of
a model to a parameter, known as the sensitivity function,
in a deterministic approach. These are:

1) Differentiation: the model described as a function is
parametrically differentiated with respect to each
parameter. The mathematics of this approach have yet to
be made portable enough to enable this approach to be
widely used.

2) Factor Perturbation: each parameter is incremented and
the changes in the output quantified. This method was
used by Smith (1976) and as noted earlier has extensive
computing time requirements.

Given the mathematical difficulties in utilising the
differential solution for the derivation of the
sensitivity function, the factor perturbation technique
was selected. The prospect of initialising a large number
of simulations necessary for the factor perturbation
approach, however, provided the impetus for an
investigation into other feasible alternatives. One
interesting alternative would be the utilisation of
optimization techniques, previously generally only
utilised for the calibration of hydrologic models.

Although optimization techniques are well-
established, it seems that they have not been used as an
alternative to the sometimes tedious development of factor
perturbation matrices. It was hoped that, if successful,
the intermediate values of the optimization scheme would

Chapter 7

provide a good indication of the sensitivity of the
outflow hydrograph, as the scheme searched to find the
'best-fit' between an observed and a computed hydrograph.
This would remove the necessity to initialize a great
number of data sets and manually search through the
results sets. A post-processor could search through the
iterations of the optimization scheme and find the
parameter values that caused the greatest or smallest
impact on the computed outflow hydrograph. Although there
would not be any direct control over the pa.ameter values
selected by the optimization scheme, in a factor
perturbation anaylsis the selection of values is usually
subjective and therefore could just as easily overlook
significant points. However, it must be noted that this
investigation into the utility of optimization is rather
exploratory. The feasibility of using optimization
schemes as an alternative to tradiitional factor
perturbation techniques will depend upon:

1)   interpretative techniques required to interrogate the
     results of the simulations

2)   the initialization time period set-up of the scheme

3)   computer demands
      i) CPU
      ii) disk storage

As the potential benefits of the optimization
approach seemed large, it was decided to divide the
sensitivity analysis into two parts, the factor
perturbation approach and the optimization approach.

Figure 7.1 illustrates the composite structure of
MILHY3 and shows there are 12 modules which generate a

Chapter 7

possible 40 module combinations. As this is a finite
number and of manageable proportions it seemed appropriate
to utilize the established factor perturbation technique
to investigate the importance of variability in the
structure of MILHY3. The investigation of this source of
variability is significant if the implications of module
resolution are to be discussed, and it was important to
guarantee results from the analysis.

By contrast, the variability of the physically-based
parameters identified earlier in this section provided for
a possible infinite number of combinations and
permutations. The scope for the potential results from an
optimization approach are much larger therefore.

The sensitivity analysis will firstly investigate the
importance of variability in the structure of MILHY3 using
traditional factor perturbation techniques and secondly
investigate the potential utility of optimization
techniques using the variability in parameters.

The River Fulda catchment has been introduced in
Chapter 6 and six storms have been established. However,
only two of these events are out-of-bank events. This
once again highlights the problems of obtaining consistent
data sets for extreme events and stresses the importance
of alternative methods of synthetically extending these
records using other models (see Chapter 8).

In this analysis, therefore, two storms are utilised.
Storm 1 is the 1 in 10 year event used in the initial
analyses in Chapters 4 and 5 (the outflow at Rotenburg of
this event is shown in Figure 5.3). The second storm has
a return period of 1 in 1.5 years and is known as Storm 3
to distinguish it from the synthetic 1 in 100 year event
used in Chapters 4 and 5. For both storms, observed

Chapter 7

hydrographs are available for all of the intermediate
stations identified in Figure 6.1, except one. The
exception is the observed hydrograph for the 1 in 1.5 year
event at Rotenburg. For this reason, the simulations of
both events are halted at Bad Hersfeld, upstream of
Rotenburg. This still gives a catchment of 2100 km^2, with
eight subcatchments.

7.2 Traditional Factor Perturbation

The objective of this analysis is to investigate the
sensitivity of the outflow hydrograph to variability in
the structure of MILHY3. The variable or composite
structure of MILHY3 is summarised in Figure 7.1.

The first stage of the development of the outflow
hydrograph is the specification of the precipitation input
into the catchment. MILHY3 offers two modules with
varying spatial resolution for the specification of the
precipitation pattern. The lower resolution module, used
in previous versions of MILHY, lumps the precipitation
into subcatchments, so the distribution for each
subcatchment is specified by a single hyetograph. If
there is only one raingauge in the catchment then the user
may choose to use the same hyetograph for all the
subcatchments.

The alternative higher resolution module, introduced
in the development of MILHY3, incorporates the spatial and
temporal effects of frontal rainstorms tracking across the
catchment. In the next section, the importance of
variability in the precipitation distribution in the
MILHY3 scheme is assessed.

Chapter 7

7.2.1 Spatially variable precipitation

The importance of the effects of variability in the spatial and temporal distribution of precipitation has been accepted by many authors, for example; Huff (1967), Dawdy and Bergmann (1969) and Beven and Hornberger (1981). Authors have investigated the effects of the resolution of raingauge networks, (Wilson et al., 1978), the effects of the resolution of the catchment, (Huff, 1968), and the effects of catchment shape, (Tabios et al., 1986). All authors have agreed, however, that it is difficult to quantify the significance of spatial and temporal variability on the prediction of flood hydrographs, given the complexity of storm events and the variability of catchment geometrical characteristics.

Modelling approaches to incorporate this variability range from manual distributions using Theisson polygons (Nguyen and Berndtsson, 1986), stochastic distributions (Tabios et al., 1986), to geomorphic distributions (Corradini and Singh, 1985). Engdahl and Collins (1985) conclude, however, that such models preclude realistic predictions of hydrographs from ungauged catchments where calibration data is not available, or for catchments where extrapolation of gauge data would be unacceptable. In such circumstances, Engdahl and Collins recommend the use of weather radar systems, such systems are explored by Cluckie et al., (1982).

Given the importance of spatial variability in the precipitation distribution on the predictive performance of hydrological models, it was essential to assess the effects of such variability on the performance of MILHY3. The relative importance of such variability in comparison with other sources of variability in differing process modules, must also be assessed. Following Engdahl and

Chapter 7

Collins (1985) recommendations, therefore, a grid network
was established to distribute rainfall throughout the
subcatchments during the generation of the runoff
hydrograph in the MILHY3 model. The resolution of the
grid utilised was 5km, this being the resolution of
weather radar data available for the UK, (see Collinge and
Kirkby, 1987).

As the purpose of the investigation was to rank the
importance of the effects of variability in rainfall
distribution in comparison with other processes, the
experimental frames utilised were restricted to a single
subcatchment. It is accepted, therefore, that such an
investigation does not allow an exploration of the
absolute importance of such variability, nor does the
investigation allow conclusions to be drawn on the
techniques available for incorporation. However, the
literature suggests that there are many models readily
available for the distribution of rainfall that could be
included in MILHY3's composite structure, if this initial
analysis showed the distribution to be significant in the
MILHY3 scheme.

The subcatchment utilised in this investigation is
catchment 406, which has an area of 145 km^2. The
subcatchment is on Figure 7.2 with the 5 km^2 grid network
superimposed. This subcatchment was further divided into
seven smaller catchments, ranging in area from 14 km^2 to
31 km^2, shown in Figure 7.2. An experimental design of 6
frames was established and executed. The analysis
included two storms; a 13 mm storm in a 24 hour interval,
typical of a frontal storm system, and a 25 mm storm
in 6 hour interval, typical of a convective cell system.
Two storm velocities were utilised to compute the temporal
distributions. These were; 5kmhr^{-1} and 10kmhr^{-1}, typical
respectively of frontal and convective cell systems.

SUBCATCHMENT BOUNDARIES
AND MAJOR RIVERS
(5km GRID)
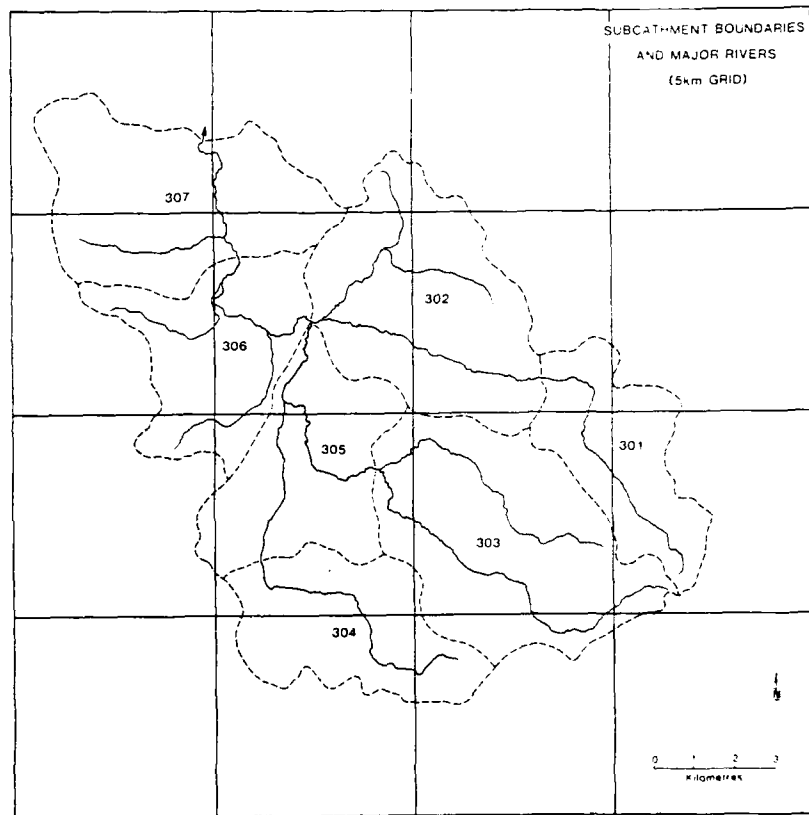
Figure 7.2
Marbach Subcatchment 406
Division into Further Subcatchment and 5km² Grid

Chapter 7

Four directions of storm movement were also considered, north, south, east and west. Rainfall distributions were computed assuming that rainfall was homogeneously distributed throughout a 5 km^2 grid square. Rainfall falling in grid squares in several catchments was distributed between the catchments depending on the percentage area on each catchment in the square.

Table 7.3 contains the simulated peak discharge results for the 13 mm in 24 hours storm event for the seven smaller subcatchments and for subcatchment 406. Table 7.4 contains similar results from the 25 mm in 6 hour event. Table 7.3 shows that the runoff hydrograph generated for subcatchment 406 and the seven smaller subcatchments varies very little for the eight experimental frames simulating the 13 mm in 24 hour storm event. By contrast, in Table 7.4 certain differences in the prediction of the peak discharge of the 25 mm in 6 hour event are apparent. The largest difference is to be found in the $10kmhr^{-1}$ northerly moving storm compared with the $5kmhr^{-1}$ southerly moving storm. In this case the peak discharges are respectively 123 m^3s^{-1} and 114.2 m^3s^{-1}. These results suggest that a catchment area of 145 km^2 may be regarded as the minimum for which 5 km^2 grid square precipitation data is required for low intensity storms. For higher intensity storms at 145 km^2 then differences of perhaps not greater than 5% in the predicted peak discharge parameter are attributable to variability in the precipitation distribution.

This analysis has shown, therefore, that the runoff hydrograph is sensitive to variability in the precipitation distribution when subcatchment areas are greater than 145 km^2 for all storm events and for smaller areas for intense storm events. However, the simulations from the validation of the multiple routing routine,

Chapter 7

Table 7.3

Peak discharge prediction of

13 mm in 24 hour storm event

| Catchment | Peak discharge ($m^3 s^{-1}$) | | | | | | | |
| | 5kmhr^{-1} | | | | 10kmh^{-1} | | | |
	n	s	e	w	n	s	e	w
301	1.11	1.13	1.13	1.12	1.14	1.25	1.13	1.13
302	1.96	1.92	1.92	1.94	1.95	1.94	1.93	1.95
303	2.29	2.33	2.31	2.28	2.31	2.32	2.30	2.31
304	1.33	1.34	1.33	1.33	1.35	1.35	1.34	1.33
305	1.37	1.36	1.38	1.38	1.37	1.37	1.38	1.38
306	1.20	1.22	1.21	1.22	1.21	1.21	1.21	1.31
307	1.90	1.90	1.90	1.89	1.89	1.90	1.91	1.90
406	10.99	10.90	10.93	10.79	11.04	10.97	10.99	11.14

Chapter 7

Table 7.4
Peak discharge prediction of
25 mm in 6 hour storm event

| Catchment | Peak discharge (m^3s^{-1}) | | | | | | | |
| | 5kmhr^{-1} | | | | 10kmh^{-1} | | | |
	n	s	e	w	n	s	e	w
301	14.85	14.51	14.22	14.66	14.81	24.61	14.71	14.71
302	22.72	22.66	22.30	22.36	22.72	22.76	22.81	20.94
303	29.56	29.63	29.41	29.62	29.64	29.72	29.77	29.73
304	15.86	15.79	16.08	16.00	15.99	16.11	16.08	16.15
305	14.97	14.97	15,30	15.36	15.18	15.24	15.36	15.18
306	11.42	11.42	11.35	11.37	11.58	11.55	11.58	11.52
307	19.49	19.50	19.57	19.58	20.02	20.05	20.07	20.26
406	120.8	114.2	114.4	117.3	123.0	118.8	120.9	120.0

Chapter 7

reported in Tables 5.1 and 5.2, suggest variability in the predicted hydrograph of around 30%. Given the concentration of this report on the two-stage channel aspects of ungauged flood forecasting and the availability of models for the distribution of rainfall data, the utility of the 5 km^2 grid distribution is not explored further in this report. In the remaining simulations of this report, the lower resolution rainfall module is utilised.

7.2.2 Baseflow conditions

The precipitation data are used by the Curve Number routine in MILHY and the infiltration algorithm in MILHY2, to generate the Hortonian runoff excess. To this baseflow must be added. For the purpose of this investigation the baseflow levels have been taken from the observed hydrographs. As the thrust of this analysis is the importance of module resolution in the MILHY3 scheme the use of observed baseflow conditions is felt to be acceptable.

It is acknowledged that this would not necessarily be possible in an ungauged catchment and there is a need for the development of a module generating baseflow conditions for inclusion in the MILHY3 scheme. Such a module could utilise either catchment characteristics or channel geometry characteristics that are already available in the MILHY3 scheme.

The notation used in this analysis refers to module combinations that have been available in previous versions of the MILHY program. The term MILHY therefore refers to a module combination that utilises the curve number generation of the runoff excess, whilst MILHY2 uses the infiltration algorithm generation. Both MILHY and MILHY2

Chapter 7

however, do not utilise the modules developed in this
report, although they do incorporate the second method of
incorporating momentum exchange, namely the use of
vertical interfaces with an apparent shear stress ratio
=1. The term MILHY3 is used to represent a module
combination that utilises the highest resolution in all
stages of the development of the outflow hydrograph.
MILHY3 therefore uses the infiltration algorithm and
momentum exchange and often the multiple routing routine.
The exact combination of modules used in the MILHY3
simulations is specified in each case using the IT and MR
notation. IT varies from 1 to 4 to indicate the method of
incorporating the momentum transfer, whilst MR indicates
that the multiple routing routine is either invoked (MR=1)
or not invoked (MR=0). This notation was utilised in
Chapter 5.

To summarise:

MILHY - Curve Number routine, IT=2, MR=0
MILHY2 - Infiltration Algorithm, IT=2, MR=0
MILHY3 - Infiltration Algorithm, IT=1/2/3/4, MR=0/1

IT=1 Vertical interface, apparent shear stress ratio=0
IT=2 Vertical interface, apparent shear stress ratio=1
IT=3 Diagonal interface, apparent shear stress ratio=0
IT=4 Diagonal interface, apparent shear stress ratio=1

MR=0 Single routing reaches
MR=1 Multiple routing reaches

7.2.3 Storm 1: 1 in 10 year event

Figure 7.3 illustrates the precipitation pattern at
Fulda and the observed hydrograph at Bad Hersfeld for the
1 in 10 year event. The temporal distribution of

184
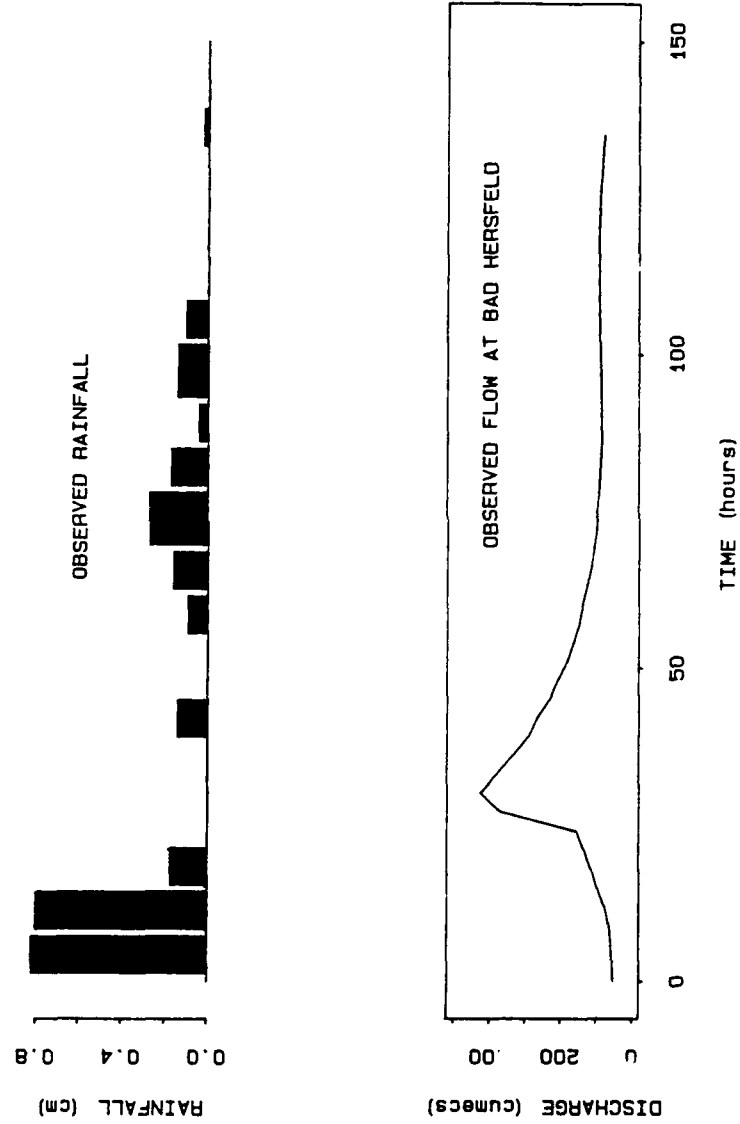
Figure 7.3
Observed Hyetograph for the River Fulda Catchment
and Observed Hydrograph at Bad Hersfeld for the
1 in 10 Year Event

Chapter 7

precipitation for all the subcatchments is based on this
hyetograph. The magnitude of the rainfall in each
subcatchment is determined from the daily precipitation
records of the stations shown in Figure 6.2. The
rainfall is assumed to be lumped and the spatial
distribution of the rainfall over the catchment for the
duration of the storm is not considered. The
specification of the rainfall therefore assumes the lower
resolution offered in the composite structure of MILHY3
shown in Figure 7.1.

The minimum cumulative rainfall total for this storm
event occurs in subcatchment 408 where 45mm fell; the
maximum total occurs in subcatchment 403 where 75mm fell.
The daily precipitation values indicate, therefore, a
strong spatial element in the distribution pattern of this
storm.

The observed hydrograph shown in Figure 7.3
illustrates that the discharge peak occurred approximately
24 hours after the rainfall peak. The time to peak of the
observed hydrograph is 30 hours from the start of the
storm event and the peak discharge is 426 m^3s^{-1}.

The simulated outflow hydrographs at Bad ersfeld
using Curve Number and Infiltration algorithms for all the
momentum exchange and multiple routing combinations are
shown in Tables 7.5 and 7.6 respectively. These tables
summarize the characteristics of the predicted hy .o-
graphs, noting the peak discharge, time to peak and
equivalent runoff depths.

Figure 7.4 illustrates the impact of the computation
method on the predicted hydrograph at Bad Hersfeld. MILHY
utilizes the Curve Number routine, whilst MILHY2 uses the
Infiltration algorithm. Both MILHY and MILHY2 use

Chapter 7

Table 7.5

Storm 1 : 1 in 10 year event

Predicted Outflow at Bad Hersfeld Utilising the

Curve Number Routine

Computation method		Peak discharge $m^3 s^{-1}$	Time to peak hours	Runoff depth m
IT=1	MR=0	265	17.5	0.03
IT=2	MR=0	272	17.5	0.03
IT=3	MR=0	265	17.5	0.03
IT=4	MR=0	249	17.5	0.03
IT=1	MR=1	312	16.5	0.03
IT=2	MR=1	328	16.5	0.03
IT=3	MR=1	323	16.5	0.03
IT=4	MR=1	281	17.0	0.03

IT = momentum exchange routine

IT=1 vertical interface, zero shear

IT=2 vertical interface, apparent shear stress ratio = 1

IT=3 diagonal interface, zero shear

IT=4 diagonal interface, apparent shear stress ratio = 1

MR = multiple routing routine

MR=0 routine not invoked

MR=1 routine invoked

Chapter 7

Table 7.6

Storm 1 : 1 in 10 year event

Predicted Outflow at Bad Hersfeld Utilising the
Infiltration Algorithm

Computation method		Peak discharge $m^3 s^{-1}$	Time to peak hours	Runoff depth m
IT=1	MR=0	312	18.5	0.03
IT=2	MR=0	321	18.0	0.03
IT=3	MR=0	310	18.0	0.03
IT=4	MR=0	290	18.0	0.03
IT=1	MR=1	364	16.5	0.04
IT=2	MR=1	383	16.5	0.04
IT=3	MR=1	372	16.5	0.04
IT=4	MR=1	332	17.5	0.04

IT = momentum exchange routine

IT=1 vertical interface, zero shear

IT=2 vertical interface, apparent shear stress ratio = 1

IT=3 diagonal interface, zero shear

IT=4 diagonal interface, apparent shear stress ratio = 1

MR = multiple routing routine

MR=0 routine not invoked

MR=1 routine invoked

Chapter 7

momentum exchange method 2, that is a vertical interface
with an apparent shear stress ratio =1, and do not
incorporate multiple routing. MILHY3 uses the
infiltration algorithm and in this case momentum exchange
method 3 (diagonal interface, zero shear), and the
multiple routing routine is invoked.

The initial trial simulations and consequent changes
in the specification of the soils classificatory data
during the establishment of the Fulda data set, reported
in Chapter 6, ensure that the runoff depths reported are
comparable with the observed data for all the
subcatchments. The Curve Number routine, for example,
predicted a runoff depth of 0.02m for subcatchment 407,
whilst the Infiltration algorithm generated 0.03m of
runoff. The observed runoff at Hermannspiegal at the
downstream extremity of the catchment showed the measured
runoff to be 0.028m.

The predicted peak discharge is used as a measure of
the accuracy of the prediction in this analysis because of
the simple shape of the hydrograph and because of the
importance of the peak discharge in determining the depth
and extent of the floodplain inundation. The initial
analysis of the behaviour of two-stage channels reported
in Chapters 3, 4 and 5 shows that the depth of inundation
is significant in determining whether the floodplain acts
as a store of water when stages are low, a separate
channel, or if the two-stages act as a single flow unit
when inundation depths are large.

Comparison of the Curve Number and Infiltration
algorithm predictions of peak discharge at Bad Hersfeld
and Hermannspiegal (Figures 7.4 and 7.5) shows that at
both stations the infiltration algorithm produces higher
peak discharges. This behaviour has been noted previously

189
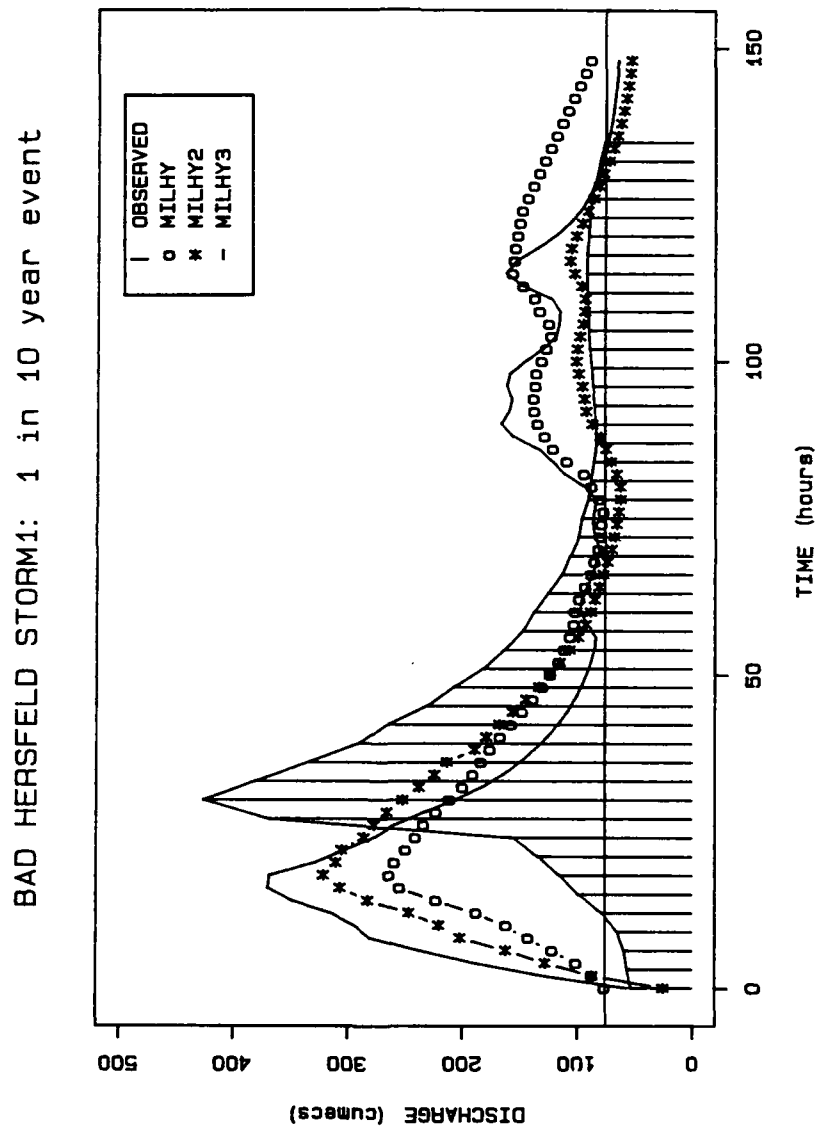
Figure 7.4
Comparison of Observed and Simulated Hydrographs from
MILHY, MILHY2 and MILHY3 Models at Bad Hersfeld for
the 1 in 10 Year Event
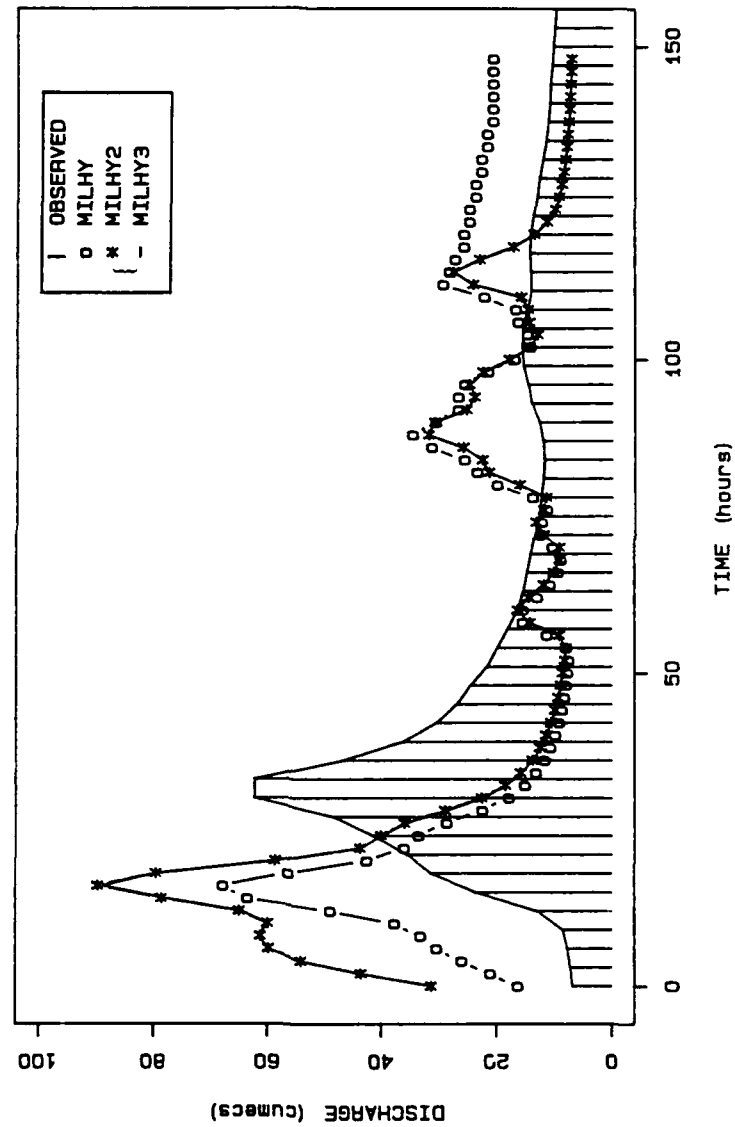
Figure 7.5
Comparison of Observed and Simulated Hydrographs from
MILHY, MILHY2 and MILHY3 Models at Hermannspiegal for
the 1 in 10 Year Event

Chapter 7

by Anderson (1982) and Anderson and Howes (1984), in
single subcatchments, where this behaviour occurred during
high and low intensity storms. In this analysis it is
worth noting that this behaviour is still visible after
the hydrographs have been routed and hence attenuated
through up to four subcatchments. This re-emphasises
earlier work by Anderson and Howes (1984, 1986) that
illustrated the importance of the shape of the runoff
hydrograph in determining the outflow hydrograph.

Analysis of Tables 7.5 to 7.6 shows that the peak
discharge is the parameter most sensitive to the
downstream computation method. The impact of the momentum
exchange and multiple routing routines seems to be related
to the depth of flow on the floodplain. The outflow
hydrograph at Hermannspiegal, shown in Figure 7.5, is
routed from Marbach, located upstream on the River Haune.
The distribution of the inflow hydrograph at Marbach as
part of the multiple routing routine means that only three
coordinates at the peak of the hydrograph are assigned to
the floodplains. The impact of the momentum exchange and
multiple routing routines on the predicted outflow
hydrograph at Hermannspiegal is therefore minimal.

At Bad Hersfeld, however, the impact of the new
modules is more pronounced. Tables 7.5 and 7.6 show that
the momentum exchange methods that assume zero shear
stress, (methods 1 and 3) produce very similar results,
whilst the apparent shear stress ratio=1 (methods 2 and 4)
produce smaller peak discharge predictions. These results
show that the modules are behaving realistically, as the
methods that introduce the greatest degree of turbulence,
(2 and 4), produce the greatest changes in the predicted
outflow hydrograph.

Chapter 7

Table 7.7

Storm 1 : 1 in 10 year event

Predicted Outflow at Hermannspiegal Utilising the

Curve Number Routine

Computation method		Peak discharge $m^3 s^{-1}$	Time to peak hours	Runoff depth m
IT=1	MR=0	70	15.5	0.02
IT=2	MR=0	70	15.0	0.02
IT=3	MR=0	70	15.0	0.02
IT=4	MR=0	69	15.0	0.02
IT=1	MR=1	70	15.0	0.02
IT=2	MR=1	71	15.0	0.02
IT=3	MR=1	69	15.0	0.02
IT=4	MR=1	68	15.0	0.02

IT = momentum exchange routine

IT=1 vertical interface, zero shear

IT=2 vertical interface, apparent shear stress ratio = 1

IT=3 diagonal interface, zero shear

IT=4 diagonal interface, apparent shear stress ratio = 1

MR = multiple routing routine

MR=0 routine not invoked

MR=1 routine invoked

Chapter 7

Table 7.8
Storm 1 : 1 in 10 year event

Predicted Outflow at Hermannspiegal Utilising the Infiltration Algorithm

Computation method		Peak discharge $m^3 s^{-1}$	Time to peak hours	Runoff depth m
IT=1	MR=0	89	16.0	0.03
IT=2	MR=0	90	16.0	0.03
IT=3	MR=0	90	16.0	0.03
IT=4	MR=0	89	16.0	0.03
IT=1	MR=1	90	16.0	0.03
IT=2	MR=1	90	16.0	0.03
IT=3	MR=1	89	16.0	0.03
IT=4	MR=1	87	16.0	0.03

IT = momentum exchange routine

IT=1 vertical interface, zero shear

IT=2 vertical interface, apparent shear stress ratio = 1

IT=3 diagonal interface, zero shear

IT=4 diagonal interface, apparent shear stress ratio = 1

MR = multiple routing routine

MR=0 routine not invoked

MR=1 routine invoked

Chapter 7

Comparison of the results from Bad Hersfeld and
Hermannspiegal show that relative difference between the
momentum exchange methods remains relatively constant
whatever the magnitude of the absolute discharge. From
these results and the early results reported in Chapter 4
it is possible to conclude that the discrepancy generated
between the various momentum exchange techniques is a
function of the depth ratio between the floodplain depth
and the main channel depth and not the absolute floodplain
inundation depth.

Tables 7.4, 7.5, 7.6, 7.7 amd 7.8 show that all the
modules incorrectly predict the time to peak of the
hydrograph, all simulating the peak too early. As the
error is similar in both the Curve Number and Infiltration
algorithm approaches, this suggests that the source of the
error is the precipitation data.

The hyetograph shown in Figure 7.3 was developed from
data of the rainfall totals at three time intervals during
the day. These data were then distributed throughout the
eight hour intervals assuming a minimum intensity of
1mm/hour. The accuracy of the rainfall data can therefore
only be guaranteed at the eight hour intervals. The
estimates of the time to peak, therefore, should only be
judged to the nearest eight hours.

Despite the accuracy bounds posed by the
precipitation data, the predicted time to peak are
undoubtedly too small for all the module combinations.
One feasible interpretation of these results is that the
resolution of the subcatchments is too large. The runoff
excess is convolved with the unit hydrograph to generate
the outflow from a catchment; however, this is only added
to channel outflow from the upstream catchment at the
downstream extremity of the subcatchment in question.

Chapter 7

This means that the time taken for the runoff to reach the channel is not directly considered.

In the case of the River Fulda catchment and this particular storm event, the analysis in Chapter 6 showed that only the clay soil groups generated runoff and these groups were situated close to the channels. The runoff hydrograph would very rapidly have an effect on the channel flows. However, the subcatchments used in the River Fulda are relatively large; Table 6.1 shows that the largest is 506 km^2 and the smallest is 56 km^2. The time taken for rainfall falling on the upstream extremity of a subcatchment to be converted into runoff and then routed to the downstream extremity of the catchment could in reality be measurable. The solution to this problem would be to reduce the size of the subcatchments considerably. However, this is not possible in the Fulda catchment as the data set is not detailed enough in this regard.

The importance of the size of the subcatchment in the accuracy of the predicted runoff hydrograph has not been fully investigated by the previous MILHY evaluation programmes. All the test catchments used in the evaluation of the infiltration algorithm were relatively small. The largest subcatchment utilised was the North Creek catchment, Texas, which has an area of 61.6 km^2; and many of the subcatchments were less than 1 km^2 in size (Howes, 1986).

This analysis suggests that the subcatchment size utilised in the River Fulda simulation was too large to accurately simulate the time to peak of the runoff hydrograph. The relationship between the accuracy of this characteristic and subcatchment size is not clear and is worthy of further investigation.

Chapter 7

The impact of the momentum exchange and multiple
routing routines is investigated in section 7.2.5 where
the results of the two storms are compared.

7.2.4   Storm 3:   1 in 1.5 year event

Figure 7.6 shows the hyetograph for subcatchment 402
and the observed outflow hydrograph at Bad Hersfeld for
the 1 in 1.5 year event. The hyetographs for each of the
subcatchments were derived for this storm from the hourly
rainfall data available for a raingauge situated in Bad
Hersfeld. The spatial variability of the rainfall was
generated from the daily precipitation records available
for the 45 rain gauges identified in Figure 6.2. The
minimum subcatchment rainfall total occurred in
subcatchment 403 where a total of 58mm of rainfall fell,
whilst the maximum rainfall of 71mm fell in subcatchment
406.

In comparison with the 1 in 10 year event, the
rainfall total of the 1 in 1.5 year event is very similar.
The difference between the two events is that in the 1 in
10 year event most of the precipitation fell in one
discrete event, whilst the 1 in 1.5 year event is
characterised by a double peak in the rainfall and
consequent discharge hydrographs.

In both peaks of the 1 in 1.5 year event, the
observed hydrograph shown in Figure 7.6 shows that the
discharge peak occurs approximately 30 hours after the
peak of the rainfall event. This is a similar response
time to the 1 in 10 year event.

A summary of the hydrograph characteristics of the
simulations using the Curve Number and Infiltration

197
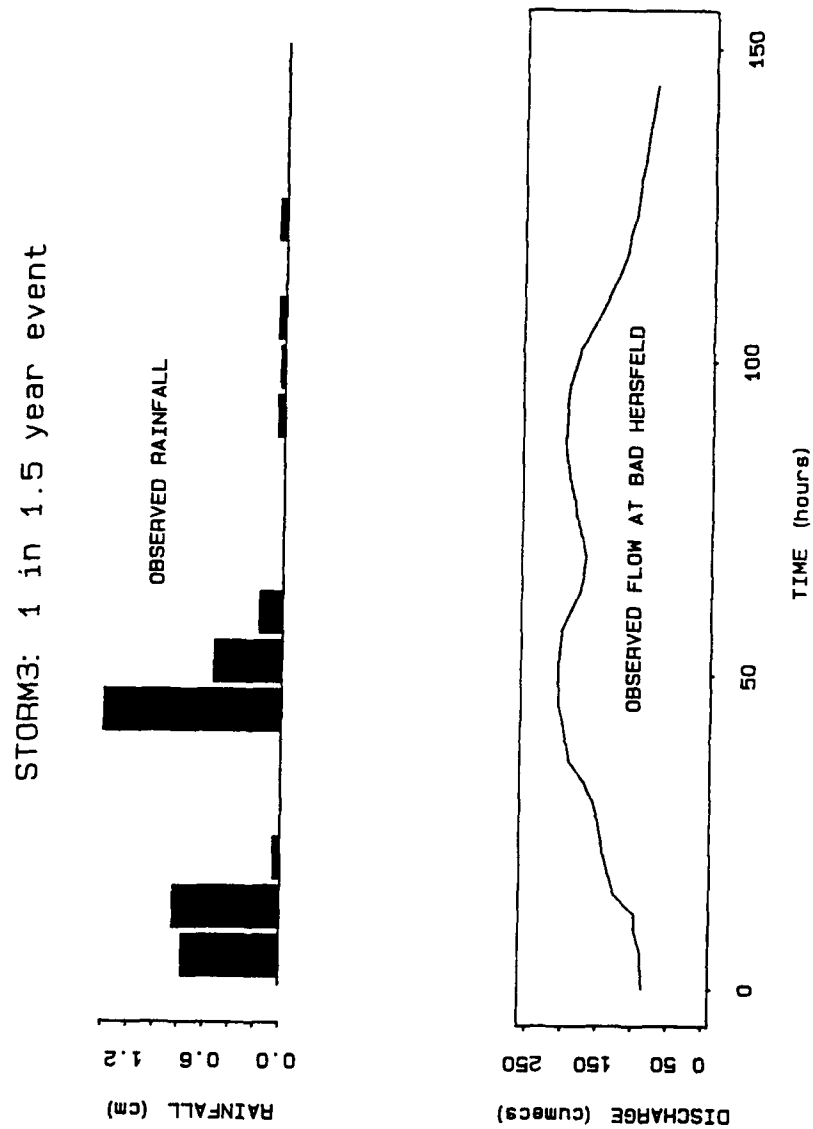
Figure 7.6
Observed Hyetograph for the River Fulda Catchment
and Observed Hydrograph at Bad Hersfeld for the
1 in 1.5 Year Event

Chapter 7

algorithm routines are recorded in Tables 7.9 and 7.10 for
the Bad Hersfeld station and Tables 7.11 and 7.12 for
Hermannspiegal station. Figures 7.7 and 7.8 show the
MILHY, MILHY2 and MILHY3 simulated hydrographs for Bad
Hersfeld and Hermannspiegal respectively.

Comparing the Curve Number and Infiltration algorithm
simulations at both the Bad Hersfeld and Hermannspiegal
stations shows that the error in the prediction between
the two techniques is much smaller for the first discharge
peak of the hydrograph than for the second. The maximum
error between the techniques for the first peak at Bad
Hersfeld is approximately 4%, whilst the maximum error in
the second peak is 35%. Figure 7.7 illustrates this error
and shows that it is the Curve Number module (MILHY) that
generates the error by over-predicting the size of the
second peak of the hydrograph. This behaviour is
confirmed in the Hermannspiegal simulations where the
Curve Number second peak prediction is even more
pronounced, having only been smoothed by one routing
routine.

These simulations expose the superior predictive
capability of the infiltration algorithm over the Curve
Number. The improved performance of the infiltration
algorithm in this storm is due to the capability of the
routine to model the infiltration of the rainfall between
the two peaks when the rainfall intensity was too low for
runoff to occur. Modelling of the infiltration process
generated conditions below saturation, so that when the
next rainfall peak began the first part of the rainfall
was utilised to bring the soil back to saturation before
runoff occurred again. The Curve Number routine does not
model the process of infiltration and assumes a constant

Chapter 7

Table 7.9

Storm 3 : 1 in 1.5 year event

Predicted Outflow at Bad Hersfeld Utilising the
Curve Number Routine

Computation method		Peak discharge $m^3 s^{-1}$		Time to peak hours		Runoff depth m
		1	2	1	2	
IT=1	MR=0	238	355	19.5	55.5	0.04
IT=2	MR=0	242	359	19.5	55.0	0.04
IT=3	MR=0	235	361	19.5	55.0	0.04
IT=4	MR=0	224	353	19.5	55.0	0.04
IT=1	MR=1	262	364	19.0	54.5	0.04
IT=2	MR=1	273	383	19.0	54.0	0.04
IT=3	MR=1	273	377	19.0	54.5	0.04
IT=4	MR=1	224	352	19.5	55.5	0.04

IT =   momentum exchange routine

IT=1   vertical interface, zero shear

IT=2   vertical interface, apparent shear stress ratio = 1

IT=3   diagonal interface, zero shear

IT=4   diagonal interface, apparent shear stress ratio = 1

MR =   multiple routing routine

MR=0   routine not invoked

MR=1   routine invoked

Chapter 7

Table 7.10

Storm 3 : 1 in 1.5 year event

Predicted Outflow at Bad Hersfeld Utilising the
Infiltration Algorithm

Computation method		Peak discharge m^3s^{-1}		Time to peak hours		Runoff depth m
		1	2	1	2	
IT=1	MR=0	236	238	16.0	55.0	0.04
IT=2	MR=0	241	232	16.0	54.5	0.04
IT=3	MR=0	238	235	16.0	54.5	0.04
IT=4	MR=0	229	235	16.0	54.5	0.04
IT=1	MR=1	240	255	16.0	54.0	0.04
IT=2	MR=1	249	269	16.0	54.0	0.04
IT=3	MR=1	253	266	16.0	54.5	0.04
IT=4	MR=1	226	234	16.0	54.0	0.04

IT = momentum exchange routine

IT=1 vertical interface, zero shear

IT=2 vertical interface, apparent shear stress ratio = 1

IT=3 diagonal interface, zero shear

IT=4 diagonal interface, apparent shear stress ratio = 1

MR = multiple routing routine

MR=0 routine not invoked

MR=1 routine invoked

Chapter 7

Table 7.11
Storm 3 : 1 in 1.5 year event

Predicted Outflow at Hermannspiegal Utilising the
Curve Number Routine

Computation method		Peak discharge $m^3 s^{-1}$		Time to peak hours		Runoff depth m
		1	2	1	2	
IT=1	MR=0	81	138	18.0	52.0	0.05
IT=2	MR=0	81	139	18.0	52.0	0.05
IT=3	MR=0	81	138	18.0	52.0	0.05
IT=4	MR=0	81	135	18.0	52.5	0.05
IT=1	MR=1	81	138	18.0	52.0	0.05
IT=2	MR=1	81	140	18.0	52.0	0.05
IT=3	MR=1	81	132	18.0	52.0	0.05
IT=4	MR=1	81	134	18.0	52.0	0.05

IT = momentum exchange routine

IT=1 vertical interface, zero shear

IT=2 vertical interface, apparent shear stress ratio = 1

IT=3 diagonal interface, zero shear

IT=4 diagonal interface, apparent shear stress ratio = 1

MR = multiple routing routine

MR=0 routine not invoked

MR=1 routine invoked

Chapter 7

Table 7.12
Storm 3 : 1 in 1.5 year event

Predicted Outflow at Hermannspiegal Utilising the
Infiltration Algorithm

Computation method		Peak discharge $m^3 s^{-1}$		Time to peak hours		Runoff depth m
		1	2	1	2	
IT=1	MR=0	67	88	13.0	52.0	0.05
IT=2	MR=0	67	88	13.0	52.0	0.05
IT=3	MR=0	67	89	13.0	51.0	0.05
IT=4	MR=0	66	88	13.0	52.0	0.05
IT=1	MR=1	66	88	13.0	52.0	0.05
IT=2	MR=1	66	89	13.0	52.0	0.05
IT=3	MR=1	67	87	13.0	52.0	0.05
IT=4	MR=1	66	84	13.0	52.0	0.05

IT = momentum exchange routine

IT=1 vertical interface, zero shear

IT=2 vertical interface, apparent shear stress ratio = 1

IT=3 diagonal interface, zero shear

IT=4 diagonal interface, apparent shear stress ratio = 1

MR = multiple routing routine

MR=0 routine not invoked

MR=1 routine invoked
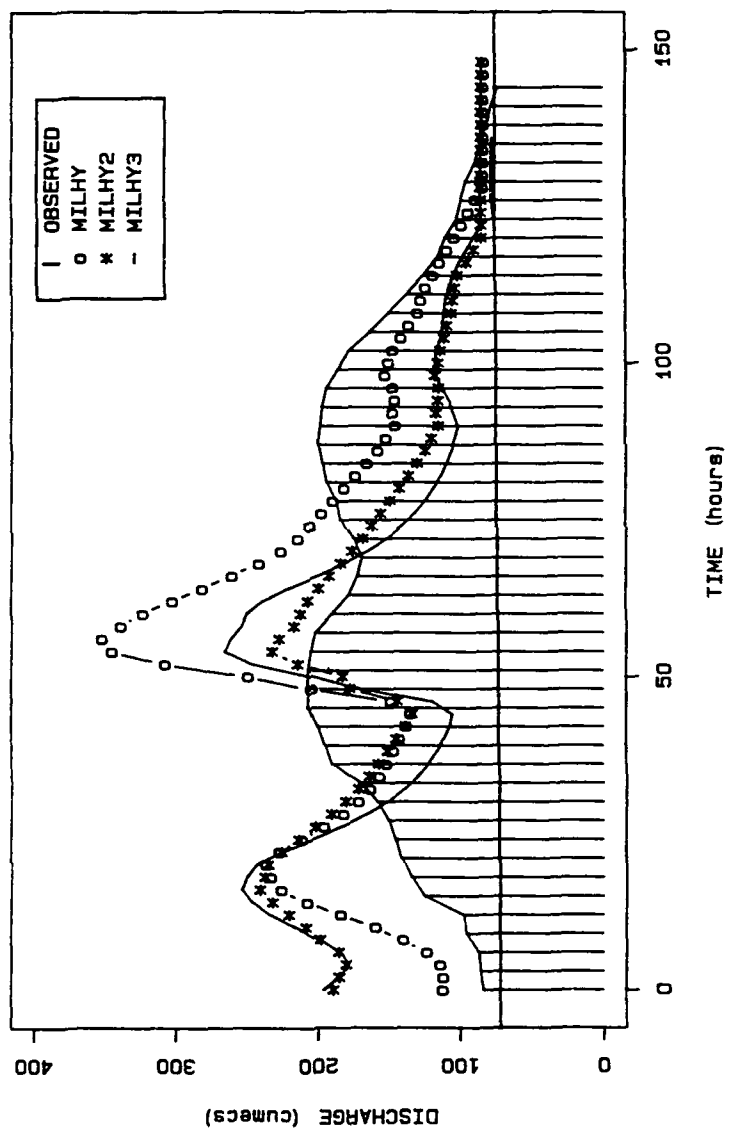
Figure 7.7
Comparison of Observed and Simulated Hydrographs from
MILHY, MILHY2 and MILHY3 Models at Bad Hersfeld for
the 1 in 1.5 Year Event
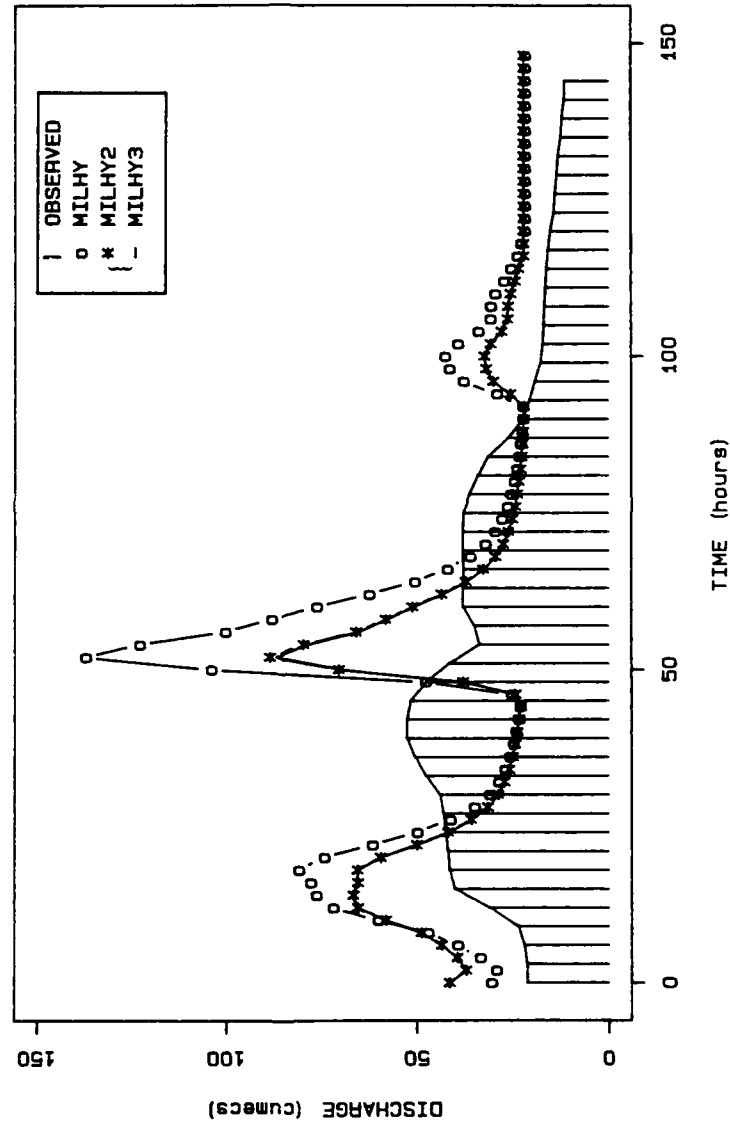
Figure 7.8
Comparison of Observed and Simulated Hydrographs from
MILHY, MILHY2 and MILHY3 Models at Hermannspiegal for
the 1 in 1.5 Year Event

Chapter 7

amount of the rainfall is stored throughout the storm.
Consequently the Curve Number routine generated too much
runoff in the second peak.

Figures 7.7 and 7.8 confirm the conclusions drawn
from the 1 in 10 year event, that the subcatchment areas
are too large for the accurate prediction of the time to
peak discharge of the hydrograph. The figures show that
the observed time to peak of the first peak is
approximately 50 hours from the start time of the
simulation. The simulated time to peak for the Curve
Number and Infiltration algorithm predict the time to peak
being approximately 16 and 19 hours respectively.
Compared to the error between the observed and predicted
time to peak, the discrepancy between the two techniques
is insignificant.

The effects of the momentum exchange and the multiple
routing routines is explored in the next section, where
the results from the two storms are compared.

7.2.5 Comparison of the two storm events

Comparison of the simulation results from the 1 in 10
year and 1 in 1.5 year events provides a means of
investigating the impact of the inundation stage on the
relative importance of the momentum exchange and multiple
routing routines.

The Tables 7.5, 7.6, 7.7, 7.8, 7.9, 7.10, 7.11 and
7.12 show that the impact of the multiple routing routine
on the prediction of the peak discharge is greater than
the impact of the momentum exchange techniques. This is
particularly true at the Bad Hersfeld station, where a
much greater proportion of the flow is routed on the

Chapter 7

floodplain. At Hermannspiegal only a small proportion of
the flow is carried on the floodplain.

The pattern of predictions made by the four momentum
exchange routines confirms the analysis made in Chapter 4,
which showed the method employed in MILHY2, that is IT=2,
gives the highest estimate of the channel capacity.
Method 4, with a diagonal interface and an apparent shear
stress ratio = 1, introduces the most turbulence into the
cross-section and as a result predicts the lowest channel
capacity of the four methods.

In this analysis the impact of the differences in the
cross-sectional conveyance capacity are converted to
discrepancies in the peak discharge predictions. Method
4, which produces the lowest channel capacity estimate,
therefore assigns the greatest proportion of the flow into
the floodplain segments. At these relatively low
inundation depths on the floodplain, the effects of
boundary friction are large and hence the attenuation of
the floodwave is increased and the peak discharge estimate
reduced.

Figures 7.9 and 7.10 illustrate the impact of the
momentum exchange and multiple routing routines on the
predicted outflow at the Bad Hersfeld station for both of
the storms. By comparing these figures with Figures 7.4
and 7.7, the effects of the two routines applied
separately and together can be assessed. The momentum
exchange method utilised throughout this analysis is
method 3, which uses a diagonal interface and zero shear.
This method was selected because it was the technique
recommended by Knight and Hamed (1984), and because it
incorporates a different interface inclination and
apparent shear stress ratio to the method incorporated in
the MILHY2 model.
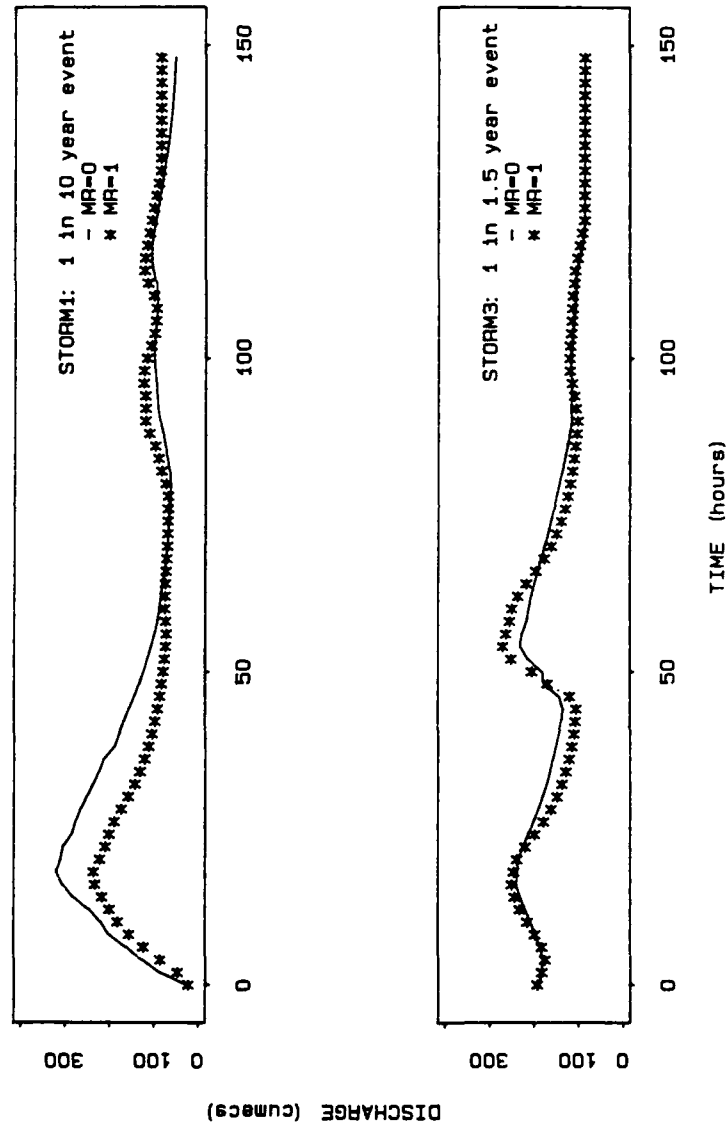
Figure 7.9
Comparison of the Impact of the Introduction of
Multiple Routing for the 1 in 10 and 1 in 1.5 Year Events
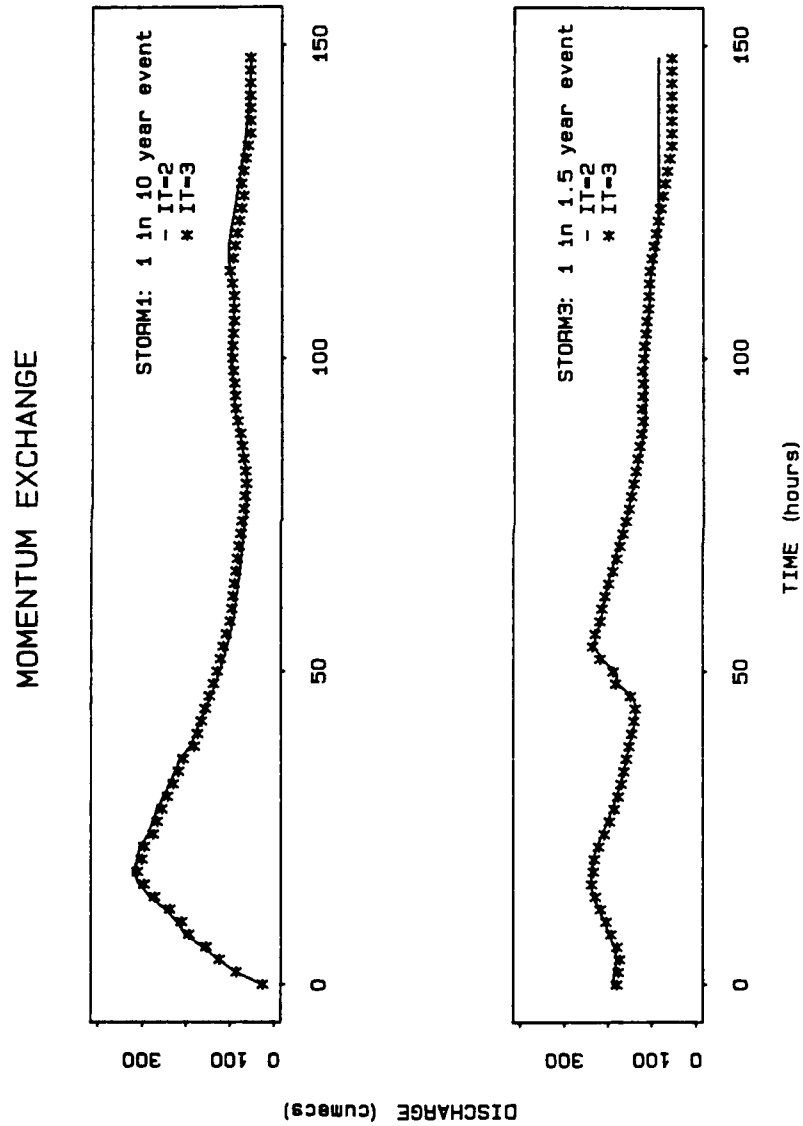
Figure 7.10
Comparison of the Impact of the Introduction of
Momentum Exchange for the 1 in 10 and 1 in 1.5 Year Events

Chapter 7

Figure 7.10 shows that the momentum exchange method 3 has no noticeable impact on the predicted hydrographs of either storm event when applied without the multiple routing routine. Figure 7.9 shows, however, that the multiple routing routine does have a significant effect on the hydrographs and that the routine's impact varies between the two storm events. In Storm 1 the main peak of the hydrograph is reduced whilst the minor peaks on the recession limb are accentuated. In Storm 3, by contrast, the recession from the first peak is steepened and the second peak is significantly accentuated.

In Storm 1 it is important to appreciate that the floodplain flow only occurs from the station at Unter-Schwartz to Bad Hersfeld on the River Fulda, a channel length of 33 km. The inflow hydrographs at Unter-Schwarz for the simulation utilizing the multiple routing routine are identical to that without the routine, and the inflow from the River Haune is channel flow only and therefore can be ignored from the analysis. Comparison, therefore, concentrates on the travel times for the Unter-Schwarz to Bad Hersfeld reach for the two simulations.

At the main peak of the hydrograph of around $350m^3s^{-1}$, in the application without the multiple routing, the time taken for the peak to travel the length of the reach is 13 hours. In the multiple routing simulation, 45% of this peak is apportioned to the floodplain where the travel time is 19 hours. The remaining 55% is assigned to the main channel where the travel time is only 5 hours. This difference in travel times means that the peak of the hydrograph is flattened out in the multiple routing simulations, as there are effectively two peaks coinciding from the floodplain and main channel.

Chapter 7

In the minor peaks, the effect of the division of the floodplain and channel flows is rather different. Looking at two points on the inflow hydrograph, the travel time without multiple routing is 11.4 hours, whereas with multiple routing the floodplain travel time is 55 hours, and the main channel travel time is 6 hours. However, as only 4% of the flow is assigned to the floodplain, when the multiple routing routine is invoked the flow arrives earlier and the peaks are less attenuated.

The results from the simulation of Storm 1 suggest that the effects of the multiple routing routine are determined by the percentage of flow that is assigned to the floodplain and channel segments.

Storm 3 confirms this conclusion, because when 15% of the flow is assigned to the floodplain, the multiple routing routine prediction is more attenuated than the single routine prediction, due to the longer travel time of the floodplain flow segment. Where the floodplain flows account for 10% or less of the total discharge the multiple routing prediction is less attenuated than the single routing technique, due to the travel time of the channel flow segment.

The predicted hydrographs at Bad Hersfeld for the application of both the momentum exchange and multiple routing routines (MILHY3) are shown in Figures 7.4 and 7.7, for Storms 1 and 3 respectively. Comparison with Figures 7.9 and 7.10 shows that the hydrograph for Storm 1 is significantly different from those produced by the application of the two routines separately. The joint application of the routines in Storm 3 hydrograph matches the predicted hydrograph from using the multiple routing routine alone. It would seem that the effects of applying both routines varies according to the storm.

Chapter 7

In Storm 1, the MILHY3 prediction seems particularly strange as, when compared to the MILHY2 solution, the MILHY3 model predicts the main peak as being earlier and the attenuation is less. This contrasts with the results shown in Figure 7.9, where the multiple routing routine increases the attenuation of the peak. Analysis of the rating curves and travel times generated by MILHY3 and those from the simulation shown in Figure 7.9 showed that it was the travel times that control the attenuation of the hydrograph. When the routines are applied together, the travel times are reduced and more of the flow is assigned to the floodplain. The momentum exchange routine generates small changes in the rating curve and in the travel time. However, these changes have no impact when the momentum exchange routine is applied without the multiple routing routine, see Figure 7.10. When applied with the multiple routing routine, these small changes become significant. For example, at the fifth hour of the simulation, for IT=2 and MR=1, 18% ($39m^3s^{-1}$) of the total discharge is assigned to the left floodplain. This water has a travel time of 70 hours. In contrast, when IT=3, MR=1 (MILHY3), 26% ($58m^3s^{-1}$) of the discharge is assigned to the left floodplain and the travel time is 60 hours.

In Storm 3, however, there are no noticeable differences in the hydrographs produced by the single application of the multiple routing routine and the joint application of the multiple routing routine and momentum exchange routines. Although there are differences in the travel times between these two techniques, these differences do not become significant as a much greater proportion of the hydrograph is out-of-bank.

Chapter 7

7.2.6 <u>Conclusions</u>

The analysis of the factor perturbation investigation reported above has identified several important points for the application of MILHY3. These points are:

1) Catchment areas of 145 km^2 may be regarded as the minimum for which 5 km^2 grid square precipitation data has an impact on the outflow hydrograph for low intensity storms. For higher intensity storms, then the application of 5 km^2 resolution data generates a maximum variability in the outflow hydrograph of no greater than 5%.

2) The analysis has shown that there is a need to investigate the relationship between the subcatchment area utilised and the accuracy of the time to peak predictions. The area of subcatchments used in this analysis have proved to be too large.

3) The analysis has shown that the infiltration algorithm predicts the complex two-peaked hydrograph of Storm 3 to a much greater degree of accuracy than the Curve Number routine.

4) With a simpler hydrograph shape, such as Storm 1, the analysis has shown that the improvement in the accuracy of the hydrograph generated by the utilisation of the infiltration algorithm over the Curve Number routine is much smaller (5-10%). Given the extra time taken to establish the data set and the CPU demands of the infiltration algorithm, the user may consider the infiltration algorithm is not necessary for such an application.

5) The impact of the multiple routing routine on the predicted hydrograph is generally much greater than the

Chapter 7

impact of the momentum exchange routines when they are
applied separately. The impact of each of these routines
is dependent on the proportions of the total flow
contained in the floodplain and main channel segments.

6)   The impact of the momentum exchange and multiple
routing routines when applied together is different from
their impact when applied separately.

7)   When the multiple routing routine is applied
separately, the attenuation of the floodwave is increased
if the floodplain flows account for 15% or more of the
total flow. When floodplain flows account for 10% or less
of the total flow, the attenuation of the floodwave is
reduced. This is due to the larger travel times of the
floodplain and smaller travel times of the channel in
comparison with the single channel method of computation.

8)   When applied separately, the momentum exchange
routine makes no significant impact on the predicted
hydrograph, despite the small changes the four routines
make on the calculated conveyance capacity of the channel
and the travel time table.

9)   When the momentum exchange routine and multiple
routing routine are applied together, the small changes
generated by the momentum exchange become significant if
15% or more of the flow is assigned to the floodplain.

10) For cases where the floodplain flow accounts for 15%
or more of the total discharge, then the joint application
of the momentum exchange and multiple routing routine
improves the accuracy of the predicted hydrograph.

Chapter 7

7.3 The Optimization Approach

There are two objectives for undertaking a
sensitivity analysis utilising optimization techniques.
These are:

1) to investigate the sensitivity of the various module
    combinations of MILHY3 to variability in the
    parameters, by analysing the intermediate iterati-
    solutions as the optimization scheme converges to a
    minimum, and

2) to explore the utility of optimization techniques as
    part of a structured sensitivity analysis
    specifically for areas where field data is limited.

As noted earlier, the technique of optimising the fit
of parameters in hydrologic models using a sensitivity
analysis for the purposes of calibration, is well
established. Applications have included Armstrong et al.
(1980) and Ibbit and O'Donnell (1971). McCuen (1973a)
identifies a range of techniques mostly based on the work
of Cauchy (1847), who developed the method of converging
the solution utilizing the rate of descent or gradient of
an objective function of the models output in response to
parameter input variability.

A range of optimization techniques for minimising and
maximising a function is available in the NAG (Numerical
Algorithms Group) library. Libraries such as these are
widely available on high and low level main frame and mini
computers. Depending on the level of sophistication
required, and the availability of the derivatives of the
function, an appropriate routine can be selected. A
simple routine was selected for this exploratory
investigation (e04jaf) which allows the user to select the

Chapter 7

upper and lower boundaries of each variable and does not
require derivatives. The routine works by developing a
surface of values for a function (F) that describes the
difference between a computed value and an observed value.
The routine then searches for a minimum in this surface by
selecting parameter values within specified boundaries.

A prerequisite, therefore, of this approach is that a
function can be computed that adequately describes, in
this case, the difference betwe.n an observed and computed
hydrograph. The 'least squares' approach was identified
as being a function already computed by MlLHY3, in
subroutine 'ERROR', and provided a simple test of the fit
of the observed hydrograph. Figure 7.11 describes how the
MILHY3 model, the function and the optimization routine,
eO4jaf, fit together schematically. In terms of the
computer coding, MILHY3 is treated as a function called by
eO4jaf, which is itself called by a short front program
which sets up the boundary conditions. Once the routine
is running, it is difficult to interrupt as all the
commands are issued by the library routine, eO4jaf.

As this investigation was exploratory in nature and
because of the concentration of the analysis on the
downstream conveyance subroutine, the infiltration
algorithm and Curve Number routines were not included in
the optimization scheme. The demands of the processor due
to the iterative nature of the optimization scheme, and
the storage of the results files were foreseen as
potential problem areas.

Setting up the optimization scheme, shown in Figure
7.11, proved a reasonably straight forward task,
complicated only by the intermittent nature of the 'read'
statement in MILHY3. The 'read' statements were rewritten
so that all the commands and data were read in the front

OPTIMIZATION SCHEME
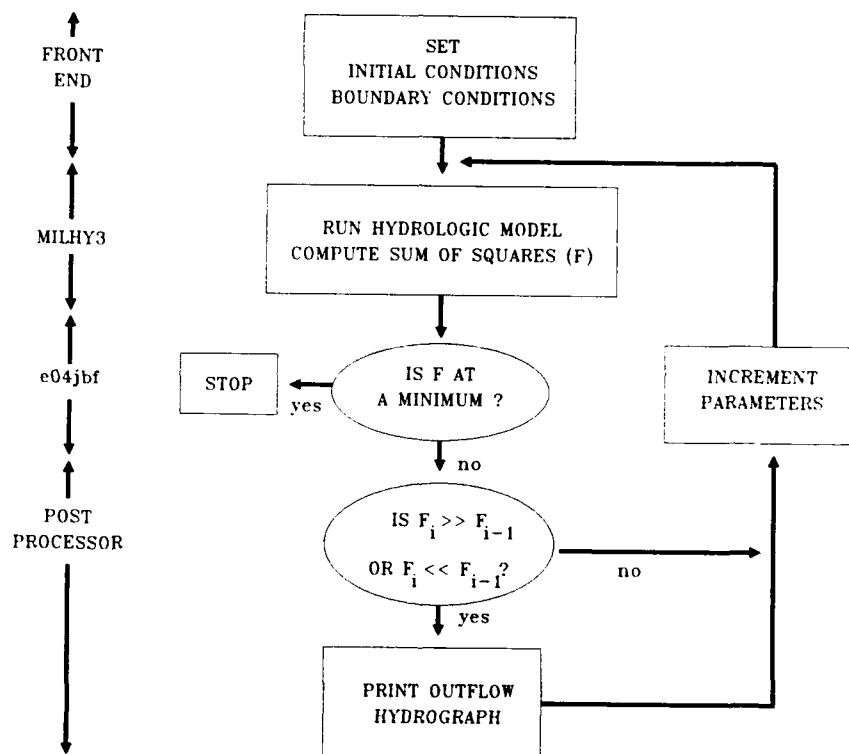
Figure 7.11
Optimization Scheme

Chapter 7

and routine. All 'write' statements were edited out, bar the warnings and failure statements, and the printing of the outflow hydrograph. The ability of MILHY3 to tolerate any set-up structure in the 'datal' data set was retained, to allow the use of the multiple routing routine which is invoked using additional commands in the data set.

MILHY3 then had to be fronted so that it appeared as a function to the optimization routine. This necessitated the addition of several COMMON BLOCKS to ensure all the data was correctly passed from the initialization (front-end) routine. Lastly, all the parameters had to be defined as being double-precision to enable them to be correctly incremented by e04jaf.

To test that the optimization was working properly and reaching a minimum, for one particular application, three simulations were undertaken. In each of these simulations the initial parameter values were changed to check that the scheme was stopping at an absolute minimum. Each of the three simulations started from either the upper or lower boundary limits or mid-point between these limits, The function values at which these three simulations stopped at, however, were not the same.

Analysis of the iterative solutions of the three simulations showed that each of the simulations became lodged in local minima close to the initial conditions. The local minima and the hydrograph predictions resulting from the three simulations, were widely different. A closer examination of the parameter values as each of the simulations converged on its local minimum showed that the parameter values were only changing from iteration to iteration by approximately 1×10^{-4}. The resolution of such parameter changes is too small to generate any change in the predicted hydrograph and hence there was no change in

Chapter 7

the objective function and the solution converged. Three
problems asociated with the resolution of the parameter
variability were therefore identified. These are:

1)   that the simulation failed to converge on an
      absolute minimum

2)   the parameter variability increments cannot be
      resolved with the accuracy of the data available,in
      ungauged catchment applications

3)   the parameter variability increment caused no
      interpretable changes in the predicted hydrograph.

The solution to these problems was to replace the
optimization scheme, e04jaf, with a scheme that allows the
user to select the size of the increment steps. Such a
scheme, e04jbf, also allows the maximum number of
iterations to be specified and allows an estimate of the
likely value of the objective function at its minimum to
be specified. These additional features should reduce the
number of iterations required and therefore reduce the
time taken by the simulation. However, as the routine
e04jbf is more complex it would take the novice user
longer to establish. Further, the CPU demands of the
scheme are greater.

Having established the logic of the optimization
scheme for the e04jaf, the alterations for the e04jbf
scheme were minimal as the overall scheme, shown in Figure
7.11, remained unchanged. Trial simulations of e04jbf
showed that an absolute minimum was reached from the
simulations initiated at the upper and lower boundary
conditions. These results proved promising enough to
encourage application to the River Fulda data set.

Chapter 7

7.3.1 Application of optimization to the River Fulda

As this investigation is rather exploratory in
nature, a single reach and storm were selected to
investigate the utility of optimization techniques. As
noted earlier, the optimization scheme is being tested on
only the downstream conveyance components of MILHY3; that
is the rating curve, travel time and routing modules. An
observed hydrograph is input at the top of the reach and
the observed outflow at the downstream end of the reach is
compared with the simulated hydrograph. The additional
runoff generated between the upstream and downstream
gauging stations is not simulated.

The reach selected is between the stations Bad
Hersfeld and Rotenburg on the River Fulda, and the storm
event is the 1 in 10 year event shown in Figure 5.3.

Two methods of computing the objective function (F),
were selected to investigate whether the value of the
function (F) had any influence on the parameter values
selected. The function (F) describes the difference
between the observed and predicted outflow hydrographs.
These two techniques are:

1) ordinary sum of squares

$$OF2 = \sum_{1}^{n} (qm_i - qm_c)2 \qquad\qquad 7.1$$

Chapter 7

2) absolute error divided by variance

$$OF7 = \frac{\sum\limits_{i}^{n} (qm_i - qm_c)^2}{\sum\limits_{i}^{n} (qm_i - \bar{q}m)^2}$$

7.2

where qm - observed peak discharge

      qc - computed peak discharge

      $\bar{q}m$ - mean peak discharge

Both of these methods of analysis are incorporated in the
subroutine 'ERROR', which is described in Volume II and
remains unchanged in MILHY3.

    Five variables were identified for this
investigation; these are:

1) Floodplain Manning's n

2) Main channel Manning's n

3) Floodplain slope

4) Main channel slope

5) Floodplain routing reach length

    These five parameters were selected as they represent
the most important physical parameters identified by the
analysis of the Ervine and Ellis (1987) scheme in
controlling the discharge and velocity predictions in two-
stage channels, (see Chapter 3).

Chapter 7

The upper and lower boundary limits for the five
parameters identified are given in Table 7.13, which also
includes the initial values for the values at the start of
each simulation and specifies the increment intervals.
The maximum number of iterations was specified as 500,
although the trial simulations showed that a minimum at
the parameter resolution feasible for field investigations
was reached after 400 iterations. The specifications for
the acceptance of the absolute minimum in the optimization
scheme were rather more stringent than necessary for the
purposes of a sensitivity analysis. All of these values
were selected based on experience in application of the
MILHY3 scheme during the development of the program and
the evaluation programme. It is accepted that an
investigation of these limits is necessary before the
sensitivity of MILHY3 can be determined with any degree of
confidence. However, the subjective selection of the
boundary conditions is sufficient for this exploratory
investigation.

As the computer demands of this approach were
foreseen as being a major limitation of the scheme, a
record was kept of the CPU demands and the size of the
output files. Output at each iteration was limited to the
parameter values and the function (F) value, the post-
processor added the computed hydrograph approximately
every tenth iteration. The CPU demands for 500 iterations
for the single reach varied from 400 to 800 seconds,
depending on the module combination utilised. Trial
simulations for the 2500 km^2 Fulda catchment, utilising
the Curve Number routine for the generation of the runoff
hydrograph took 6000 seconds of CPU. As every iteration
using the Infiltration Algorithm was taking approximately
9 hours (324000 seconds) an optimization trial using the
infiltration algorithm was not attempted.

Chapter 7

Table 7.13

Initial Conditions, Boundary Conditions and Variable

Increments for the Optimization Scheme

	Initial Conditions	Boundary Limits		Variable Increments
		Upper	Lower	
Floodplain Manning's n	0.05	0.16	0.025	0.01
Channel Manning's n	0.035	0.1	0.025	0.01
Floodplain Slope	0.0006	0.001	0.0001	0.0001
Channel Slope	0.0006	0.001	0.0001	0.0001
Floodplain routing reach length(m)	21951	23750	16860	1525

Chapter 7

The size of the output files proved to be more of a limitation. Sizes varied from 12 kbytes to 2.9 megabytes, the latter being too large to edit. Clearly the post-processor needs to be more selective in the iteration results it saves. Because of the size of the results files, the results presented here are only a small selection of the most interesting data produced by the analysis.

The representation of the results has been structured in order to answer three questions. These are:

1) to which of the five parameters is the hydrograph most sensitive?

2) does the method of computation affect this sensitivity?

3) do the parameters interact to increase or decrease the sensitivity of the hydrograph?

In much of the analysis presented, the relative error and absolute errors are used to compare the differences between the computational methods. The relative error is dimensionless and is defined as:

$$RE = \frac{x_c - x_i}{x_i} \qquad\qquad 7.3$$

where x_c - computed value of x

x_i - value of x under initial conditions

Chapter 7

7.3.2 Sensitivity to parameter variability

Tables 7.14, 7.15, 7.16, 7.17 and 7.18 show the
absolute error (AE) and relative error's (RE) for the peak
discharge, time to peak and sum of squares (OF2) for five
of the possible module combinations. The errors are
computed for one increment step above and below the
initial conditions. These tables contain data from the
the first iterations of the optimization simulations,
shown schematically in Figure 7.12.

Analysis of these tables shows the asymmetrical
sensitivity of the three indicators, peak discharge, time
to peak and sum of squares, around the initial conditions.
For example, Table 7.14 shows that the sensitivity of the
peak discharge to variation in the floodplain Manning's n
value, is markedly different for values greater than the
initial conditions than for values less than the initial
conditions. This asymmetrical effect is particularly
noticeable for the variation in Manning's n, both in the
floodplain and channel (see Tables 7.14 and 7.15),
suggesting that the sensitivity of the hydrograph to
variation in 'n' is not linear.

Tables 7.14 to 7.18 show the sensitivity of the
hydrograph to a one increment step in the mid-point
between the upper and lower boundary limits for all five
variables. Table 7.19 shows an example of the relative
errors generated from a one increment step in each of the
parameters at the boundary limits, and compares these with
the mid-limit values. This particular example compares
the relative errors in the peak discharge for one module
combination and is typical of the tables derived for other
combination methods.
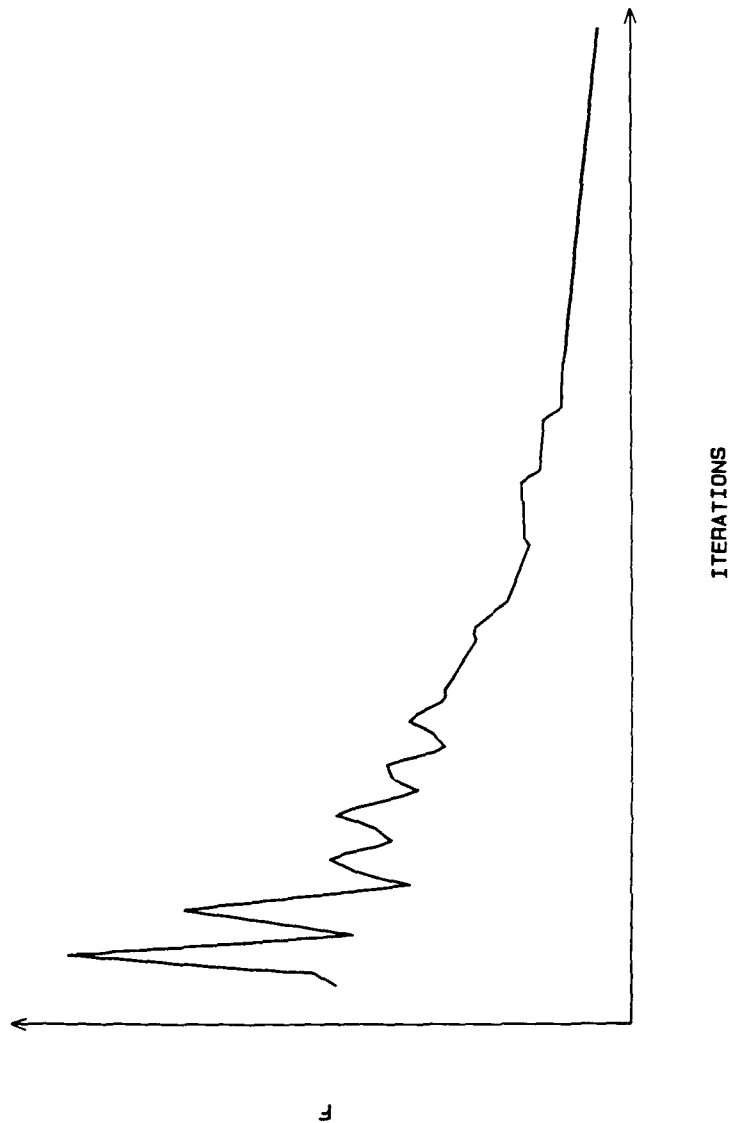
Figure 7.12
Conceptual Convergence of Function F to a Minimum During
Application of the Optimization Scheme

Chapter 7

Table 7.14
Errors from one increment step variation in
floodplain Manning's n

Increment	Computation method	Peak discharge		Time to peak		Sum of squares	
		$\underset{m^3 s^{-1}}{AE}$	RE	AE hours	RE	AE OF2	RE
	IT=2 MR=0	−125	0.01	0	0.00	62941	0.00
	IT=3 MR=0	−115	0.13	0	0.08	62951	0.31
+1	IT=1 MR=1	−107	0.01	+9	0.00	124796	0.12
	IT=2 MR=1	−127	0.10	+9	0.07	105431	0.12
	IT=3 MR=1	−88	0.03	0	0.00	86893	0.08
	IT=2 MR=0	−121		0		63177	
	IT=3 MR=0	−72		−3		91568	
0	IT=1 MR=1	−110		+9		111038	
	IT=2 MR=1	−95		+6		94106	
	IT=3 MR=1	−79		−3		94782	
	IT=2 MR=0	−123	0.01	0	0.00	68801	0.09
	IT=3 MR=0	−71	0.00	−3	0.00	92675	0.01
−1	IT=1 MR=1	−71	0.13	+6	0.06	92118	0.17
	IT=2 MR=1	−102	0.02	+3	0.07	70169	0.25
	IT=3 MR=1	−70	0.03	−3	0.00	106950	0.13

IT =   momentum exchange routine
IT=1 vertical interface, zero shear
IT=2 vertical interface, apparent shear stress ratio = 1
IT=3 diagonal interface, zero shear
IT=4 diagonal interface, apparent shear stress ratio = 1

MR =   multiple routing routine
MR=0 routine not invoked
MR=1 routine invoked

Chapter 7

Table 7.15
Errors from one increment step variation in
channel Manning's n

Increment	Computation method	Peak discharge		Time to peak		Sum of squares	
		AE $m^3 s^{-1}$	RE	AE hours	RE	AE OF2	RE
+1	IT=2 MR=0	-138	0.06	0	0.00	68270	0.08
	IT=3 MR=0	-91	0.06	-3	0.00	74276	0.19
	IT=1 MR=1	-143	0.11	+9	0.00	85134	0.23
	IT=2 MR=1	-103	0.03	+9	0.07	107817	0.15
	IT=3 MR=1	-82	0.01	-3	0.00	91518	0.03
0	IT=2 MR=0	-121		0		63177	
	IT=3 MR=0	-72		-3		91568	
	IT=1 MR=1	-110		+9		111038	
	IT=2 MR=1	-95		+6		94106	
	IT=3 MR=1	-79		-3		94782	
-1	IT=2 MR=0	-105	0.06	0	0.00	68694	0.09
	IT=3 MR=0	-96	0.07	-3	0.00	73639	0.19
	IT=1 MR=1	-96	0.05	+3	0.13	70847	0.36
	IT=2 MR=1	-58	0.12	+3	0.07	68635	0.27
	IT=3 MR=1	-73	0.02	-3	0.00	107051	0.13

IT = momentum exchange routine
IT=1 vertical interface, zero shear
IT=2 vertical interface, apparent shear stress ratio = 1
IT=3 diagonal interface, zero shear
IT=4 diagonal interface, apparent shear stress ratio = 1

MR = multiple routing routine
MR=0 routine not invoked
MR=1 routine invoked

Chapter 7

Table 7.16
Errors from one increment step variation in
floodplain slope

Increment	Computation method	Peak discharge		Time to peak		Sum of squares	
		AE $m^3 s^{-1}$	RE	AE hours	RE	AE OF2	RE
+1	IT=2 MR=0	-120	0.00	0	0.00	63421	0.00
	IT=3 MR=0	-72	0.00	-3	0.00	92115	0.00
	IT=1 MR=1	-105	0.02	+9	0.00	109250	0.02
	IT=2 MR=1	-89	0.02	+6	0.00	92953	0.01
	IT=3 MR=1	-75	0.01	-3	0.00	98774	0.04
0	IT=2 MR=0	-121		0		63177	
	IT=3 MR=0	-72		-3		91568	
	IT=1 MR=1	-110		+9		111038	
	IT=2 MR=1	-95		+6		94106	
	IT=3 MR=1	-79		-3		94782	
-1	IT=2 MR=0	-123	0.01	0	0.00	62997	0.00
	IT=3 MR=0	-112	0.12	0	0.08	63756	0.30
	IT=1 MR=1	-99	0.04	+9	0.00	124144	0.12
	IT=2 MR=1	-110	0.05	+3	0.07	104471	0.11
	IT=3 MR=1	-83	0.01	-3	0.00	90447	0.05

IT = momentum exchange routine
IT=1 vertical interface, zero shear
IT=2 vertical interface, apparent shear stress ratio = 1
IT=3 diagonal interface, zero shear
IT=4 diagonal interface, apparent shear stress ratio = 1

MR = multiple routing routine
MR=0 routine not invoked
MR=1 routine invoked

Chapter 7

Table 7.17
Errors from one increment step variation in
channel slope

Increment	Computation method	Peak discharge		Time to peak		Sum of squares	
		ΔE $m^3 s^{-1}$	RE	AE hours	RE	AE OF2	RE
	IT=2 MR=0	-117	0.01	0	0.00	63290	0.00
	IT=3 MR=0	-107	0.10	0	0.08	66138	0.28
+1	IT=1 MR=1	-112	0.01	+9	0.00	107855	0.03
	IT=2 MR=1	-100	0.02	+6	0.00	90519	0.04
	IT=3 MR=1	-78	0.00	-3	0.00	96431	0.02
	IT=2 MR=0	-121		0		63177	
	IT=3 MR=0	-72		-3		91568	
0	IT=1 MR=1	-110		+9		111038	
	IT=2 MR=1	-95		+6		94106	
	IT=3 MR=1	-79		-3		94782	
	IT=2 MR=0	-126	0.02	0	0.00	63223	0.00
	IT=3 MR=0	-78	0.02	-3	0.00	84485	0.08
-1	IT=1 MR=1	-103	0.02	+9	0.00	110171	0.01
	IT=2 MR=1	-121	0.08	+9	0.07	108635	0.15
	IT=3 MR=1	~80	0.00	-3	0.00	93286	0.02

IT =   momentum exchange routine
IT=1   vertical interface, zero shear
IT=2   vertical interface, apparent shear stress ratio = 1
IT=3   diagonal interface, zero shear
IT=4   diagonal interface, apparent shear stress ratio = 1

MR =   multiple routing routine
MR=0   routine not invoked
MR=1   routine invoked

Chapter 7

Table 7.18
Errors from one increment step variation in
floodplain routing reach length

Increment	Computation method	Peak discharge		Time to peak		Sum of squares	
		ΔE $m^3 s^{-1}$	RE	AE hours	RE	AE OF2	RE
	IT=1 MR=1	−114	0.01	+9	0.00	114505	0.03
+1	IT=2 MR=1	−100	0.02	+6	0.00	96189	0.02
	IT=3 MR=1	−82	0.01	−3	0.00	91338	0.04
	IT=1 MR=1	−110		+9		111038	
0	IT=2 MR=1	−95		+6		94106	
	IT=3 MR=1	−79		−3		94782	
	IT=1 MR=1	−106	0.01	+9	0.00	106985	0.04
+1	IT=2 MR=1	−111	0.05	+9	0.07	91810	0.02
	IT=3 MR=1	−769	0.01	−3	0.00	98741	0.04

IT = momentum exchange routine
IT=1 vertical interface, zero shear
IT=2 vertical interface, apparent shear stress ratio = 1
IT=3 diagonal interface, zero shear
IT=4 diagonal interface, apparent shear stress ratio = 1

MR = multiple routing routine
MR=0 routine not invoked
MR=1 routine invoked

Chapter 7

Table 7.19
Relative error in peak discharge from one increment
variation at the boundaries and mid-way

Variable	Relative Errors		
	Upper Boundary	Mid-way	Lower Boundary
Floodplain Manning's n	0.053	0.10	0.01
Channel Manning's n	0.003	0.025	0
Floodplain Slope	0.083	0.019	0.058
Channel Slope	0.083	0.014	0.03
Routing reach length	0.029	0.014	0.011

Chapter 7

Table 7.19 shows that at both the upper and lower
boundaries the outflow hydrograph is most sensitive to
slope. In the mid-ranges, the hydrograph is most
sensitive to Manning's n. For MILHY3 applications with
significant inundation, it is important to define the
Manning's n values as accurately as possible, especially
on the floodplain. Table 7.19 also shows that the outflow
hydrograph is not sensitive to relatively small changes in
the floodplain routing length, except when the slopes are
steep, that is approximately 1×10^{-3} or greater.

7.3.3 Sensitivity variations associated with the computational method

The computational method of the optimization scheme
incorporates two sources of variation:

1) the structure of MILHY3, specifically in this case
    which of the momentum exchange routines has been
    used and whether the multiple routing routine has
    been invoked;

2) the factor (F) used to quantify the difference
    between the observed and computed hydrographs

Section 7.2 investigated the sensitivity of the
outflow hydrograph to variations in MILHY3's structure for
two storms in the River Fulda catchment. Here the
relative impact of variability in the model structure in
comparison with the effects of variability in the physical
parameters can be assessed. In addition the impact of the
module combination on the sensitivity of the hydrograph to
parameter variability is investigated. Tables 7.14 to
7.18 compare the relative errors for three measures of
hydrograph fit, for a range of model structures.

Chapter 7

Section 7.3.2 identified Manning's n as being the variable to which the predicted hydrograph is most sensitive. Tables 7.14 and 7.15 show, however, that the relative errors between momentum exchange and multiple routing routine combinations are as great, if not greater in some circumstances, than errors generated from Manning's n variability. This suggests, therefore, that the momentum exchange and multiple routing routines are significant processes in comparison with the effects of boundary friction.

If the sensitivity of the model to variation in the five physically-based parameters were not affected by the model structure, then it could be expected that the relative errors for all the module combinations would be the same. The fact that there are variations suggests that certain module combinations increase the sensitivity of the model to parameter change. This problem is particularly noticeable in the sensitivity to variation in floodplain Manning's n and in the channel Manning's n with the introduction of the multiple routing routine.

The variation in the relative error between the momentum exchange techniques can be attributed to the difference in the predicted conveyance capacity of the two-stage channel computed by the four alternative techniques. The four techniques utilise the Manning equation to compute the conveyance capacity and the discrepancy between the techniques is attributable to the different methods the four techniques utilise to compute the hydraulic radius of the two-stage channel.

For example, momentum exchange method 3 (diagonal interface with a zero shear interface) reduces the peak discharge prediction when the Manning's n coefficient is increased by one increment step in Table 7.14. The

Chapter 7

discharge prediction is reduced to a greater extent than
momentum exchange method 2. This is because more of the
flow is assigned to the floodplain segment in method 3
than in method 2, as the predicted conveyance capacity of
the channel is smaller in method 3 than in method 2. This
makes method 3 more sensitive to increases in the
Manning's n coefficient. An increase in the Manning's n
coefficient does not have the opposite effect, however,
and increase the peak discharge prediction of method 3 to
any large degree. As the analysis in Chapter 4 has shown,
an increase in the volume of water on the floodplain can
increase the attenuation of the floodwave, as there is an
effective double peak from the channel and the floodplain
flow segments.

The results from Chapter 4 show that momentum
exchange method 4 (diagonal interface with an assumed
apparent shear ratio = 1) has the lowest conveyance
capacity and therefore method 4 has the greatest
proportion of water on the floodplain. In contrast,
momentum exchange method 2 (vertical interface with an
apparent shear stress ratio = 1) has the highest
conveyance capacity and, therefore, the lowest proportion
of flow on the floodplain. Method 1 (vertical interface
with zero shear) and method 3 (diagonal interface with
zero shear) produce conveyance estimates between the two
extremes. It is logical, therefore, to expect the
increase in Manning's n coefficient in the floodplain to
affect method 3 and 4 most, whilst the increase in channel
Manning's n to affect methods 1 and 2 most.

However, this situation is complicated by the
addition of the multiple routing routine which, depending
on the depth of flow on the floodplain, can increase or
decrease the attenuation of the floodwave. So whilst
method 2 is most sensitive to the increase in the

Chapter 7

Manning's n in the channel, with most of the water being
assigned to the channel, the multiple routing techniques
route this water more rapidly down the reach than the
single routing technique. The peak discharge of the
multiple routing technique is therefore less reduced than
the single routing method, for momentum method 2.

The results confirm that the effects of the momentum
exchange and multiple routing routine on the hydrograph
are often opposing. In terms of the sensitivity of the
modules to variation in the five physically-based
parameters, these results show that variation in the
Manning's n coefficient is most sensitive to change in the
modules. The effects of Manning's n sensitivity of the
momentum exchange routines, whether it is in the channel
or on the floodplain, is reduced by the addition of the
multiple routing routine.

The second question raised in this section is: does the
function (F) utilized to describe the fit of the
predicted, affect the utility of using optimization
techniques as part of a sensitivity analysis? Analysis of
the results showed that the exact function value did not
influence the routine's selection of parameter values;
only the relative function value between simulations was
used. The solutions from both functions converged on
minima for which the five parameter values were very
close. It is accepted, however, that this may not be the
case if a radically different function were applied.

7.3.4 Conclusions

The optimization results have shown that the
relationship between the sensitivity to the five
physically-based techniques and the modules selected is an
extremely complex one, dependent on the depth and

Chapter 7

proportion of the flow that is contained in the channel
and floodplain segments. The results from the one storm
and reach do, however, suggest several conclusions:

1)   An optimization scheme may well provide a viable
     alternative to traditional factor perturbation
     sensitivity analysis, provided that:-

     i)   the interpretative approaches required to
         analyse the results are further developed
     ii) the CPU demands can be met
     iii) a satisfactory function can be found to
         describe the fit of the hydrograph

2)   The sensitivity of MILHY3 in two-stage applications
     is dominated by:

     i)   slope when slopes are $> 1 \times 10^{-2}$
     ii) floodplain Manning's when slopes are $> 1 \times 10^{-4}$

3)   The short-circuiting of floodplain flows is only
     significant if the floodplain slopes are $< 1 \times 10^{-3}$
     and the floodplain routing length is at least 10%
     shorter than the main channel routing length.

4)   The momentum exchange and multiple routing routines
     generate similar relative errors in the predicted
     hydrograph as variation in the Manning's
     coefficient.

5)   The sensitivity of the hydrograph to variation in
     the Manning's n coefficient is reduced if the
     momentum exchange and multiple routing routines are
     utilised.

Chapter 7

7.4 <u>Summary</u>

This chapter has explored the sensitivity of MILHY3
to variability in certain physical parameters and to
variability in the process modules used to construct the
MILHY3 scheme. In particular, the interaction between the
momentum exchange and multiple routing routines has been
explored, and the relative impact of these modules in
comparison to the introduction of the infiltration
algorithm has been assessed. The effects of scale and
resolution of the precipitation distribution and catchment
subdivision has also been investigated.

The sensitivity of MILHY3 has been investigated using
two techniques; a traditional factor perturbation
analysis, reported in section 7.2, investigated the
effects of variability in the physical parameters, and a
new approach utilizing optimization techniques, reported
in section 7.3, investigates the composite structure
variability. The conclusion of these investigations are
found in subsections 7.2.6 and 7.2.4. The main
conclusions from these two analysis are:

1) For slopes less than $1x10^{-2}$ and greater than $1x10^{-4}$,
the outflow hydrograph is most sensitive to variability in
the Manning's n coefficient. However, this sensitivity is
reduced by the joint application of the momentum exchange
and multiple routing routines. In addition, the joint
application of these two routines simplifies the selection
of the Manning's coefficient by removing the effects of
turbulent exchange and sinuosity, thus the coefficient now
only represents the effects of boundary friction.

2) Variation in the predicted hydrograph generated from
variation in the momentum exchange and multiple routing
routines has been shown to be of a similar magnitude to

Chapter 7

the variation generated by variability in the Manning's n
coefficient. This suggests that the inclusion of the
effects of momentum exchange and multiple routing pathways
is as significant as the effects of boundary friction.

3)   The momentum exchange routines do not have a
significant effect on the outflow hydrograph when applied
without the multiple routing routine. The influence of
the joint application of the multiple routing and momentum
exchange routines is on the attenuation of the outflow
hydrograph. The exact nature of the influence of the
routines on the attenuation of the floodwave is determined
by the proportion of the discharge carried on the flood-
plain and in the main channel flow segments.

4)   Comparison of the relative importance of the
infiltration algorithm, momentum exchange, and multiple
routing routines in the River Fulda catchment, utilizing
large subcatchments, has shown that the infiltration
algorithm generates the largest improvement in the
prediction of the outflow hydrograph. However, for simple
storm events the user may consider that the improved
performance generated by the inclusion of the infiltration
algorithm does not justify the additional computational
demands.

5)   The application of the optimization technique has
been shown to be a viable alternative to traditional
factor perturbation sensitivity analysis. There is a
need, however, for the interpretative techniques required
to interrogate the results, to be further developed.

Chapter 8
Validation of MILHY3
III - Hydraulic Validation of MILHY3

The objective of this chapter is to investigate the utility
of applying state-of-the-art models in order to validate
developments made in simpler models such as MILHY3. The need for
such an investigation arises from the difficulties of establishing a
field data set large enough to allow a meaningful evaluation of
MILHY3's performance, and for a set of operational guidelines for
MILHY3 to be developed.

The main limitation of the evaluation of MILHY3 using the
River Fulda data set is the limited number of observed out-of-bank
events. This is a common problem as extreme events are not only
difficult to measure but also occur infrequently. The collection of
further data sets from other catchments that meet the other
requirements of the model evaluation programme would not necessarily
negate this problem of a limited number of events.

The objective of this chapter is therefore to utilise a
state-of-the-art model to extend the number of out-of-bank events
for the River Fulda catchment. Ideally, such a scheme would operate
by taking certain "design" rainfall events and developing the
outflow hydrographs at each of the eight gauging stations. These
hydrographs could then be treated as the "observed" or ground-truth
against which the performance of MILHY3 could be judged.

The only feasible alternative to using a state-of-the-art
model to extend the record of extreme events would be to utilise the
flood frequency data. Pilgrim and Doran (1987) noted that:

"The extent to which a flood frequency analysis can be
extrapolated before an alternative rainfall-based method
becomes preferable depends, among other factors, on the
relative accuracy of the latter method."

Chapter 8

The "other factors" include the characteristics of the available
sample of recorded flows for the development of the flood frequency
analysis. In catchments with limited data, regression of flood
parameters may be used, or parameters transferred from other
catchments, or regional rules developed. In reality, in order to
generate a complete hydrograph from the flood frequency analysis,
rather than just the usual peak discharge, the frequency data are
used to calibrate a hydrograph produced by either a unit hydrograph
procedure or a runoff routing method.

As noted earlier, the collection of data for extreme events is
difficult for nearly all catchments, and therefore the derivation of
empirical coefficients for a flood frequency analysis would not
easily be achieved. The determination of the shape of the
hydrograph in flood frequency analysis is also unsatisfactory for
the purpose of evaluating the performance of MILHY3. In MILHY3 a
unit hydrograph procedure is already utilised for the development of
the runoff hydrograph, which is then routed downstream using the
modules developed in this report. To extend the record of storm
events utilising a similar technique to that used in MILHY3 would
not provide any indication of the predictive accuracy of MILHY3. In
order to extend the record of extreme events, the level of
confidence in the predictive accuracy of the techniques used needs
to be high.

The alternative available for the derivation of the hydrograph
shape in flood frequency analysis is to utilise runoff routing.
Runoff routing gives a more realistic account of the stores in the
catchment than the unit hydrograph approach. However, both the unit
hydrograph and the runoff routine technique generate the runoff
hydrograph for a subcatchment. No account is made of the routing of
these flows downstream. Application of a runoff routing routine
would therefore only allow validation of the runoff generation
modules in MILHY3.

Chapter 8

Analysis of the flood frequency analysis approach has shown
that in order to extend the record of storm events and to generate a
complete hydrograph, there is no alternative but to employ another
model. Traditionally, flood frequency analysis has employed
relatively simple hydrologic techniques, namely the unit hydrograph
or runoff routing. The level of resolution in the process areas of
these models is similar to or lower than the modules that make up
MILHY3. To extend the record of extreme events using the
traditional flood frequency analysis and then evaluate MILHY3 using
this record, would thus be comparing like with like. Although this
may be a useful exercise, and would help determine the efficiency of
the MILHY3 model, it is not the objective of this evaluation
programme. A different modelling approach to MILHY3 is required for
the evaluation programme, a model to which the level of confidence
in the predictive accuracy of the hydrograph is high.

A series of prerequisites for a model that would meet the
demands and limitations specified for the extension of the record of
extreme events, can now be drawn up. Such a list would consist of:-

1)   the model's strategy in conceptualizing the physical processes
      needs to be different to MILHY3's conceptual strategy

2)   the model needs to be evaluated against field data and have an
      acceptable predictive accuracy

3)   the data set demands of the model, including any calibration
      requirement, must be met by the data set for the River Fulda
      catchment

4)   the model should be well-documented and readily available

The conceptual strategy of MILHY3 is basically semi-lumped.
Variations within the catchment are considered on the subcatchment
level. An alternative strategy would therefore be distributed to

Chapter 8

some degree; this would include catchment models such as the SHE
and VSAS2. However, review of these distributed physically-based
models shows that such models have a doubtful level of predictive
accuracy and require large data sets. In addition, such models tend
not to incorporate the cross-sectional and plan geometrical effects
of two-stage flows. Using a distributed catchment model, therefore,
to extend the record of extreme events would seem to be
inappropriate.

An alternative to using catchment models would be to consider
using models that simulate certain processes in the catchment. For
example, the development of the runoff hydrograph in MILHY3, and the
associated problems in specification of the subcatchment size, could
be investigated using a data set developed from a model
incorporating the routing of the overland excess and throughflow.
More relevant to the main thrust of this report would be the
evaluation of the two-stage flow capability using a data set
developed from a model specifically for channel and floodplain
flows.

With the advent of computer technology, models of river
channels have been developed rapidly and are widely used, (Cunge, et
al., 1980). All of these models can be classified as being
hydraulic in approach, in contrast to the simpler hydrologic
approaches of models such as MILHY3. A hydraulic approach to
modelling involves solving the equations of the conservation of
momentum in addition to the conservation of mass. In a hydrologic
approach only the conservation of mass is solved and a simple
storage equation replaces the conservation of momentum.

In the next section hydraulic approaches to two-stage flows
are investigated, with the aim of identifying a model that could be
used to extend the record of extreme events in order to complete the
operational validation of MILHY3.

Chapter 8

8.1   Identification of a Hydraulic Model of Two-stage Flow

8.1.1 Hydraulic modelling alternatives

Hydraulic approaches to the modelling of channel flows have
traditionally been divided into classes depending on the number of
spatial dimensions the model incorporates. In one-dimensional
models the flow is averaged across a section perpendicular to the
main direction of flow, and the St. Venant equations of open channel
flow are used. One-dimensional models are widely used, especially
in long reaches. However, they do not incorporate the exchanges
that take place in a two-stage channel. Two-dimensional models
divide the floodplain into a number of cells. The exchange of flow
between adjacent cells is computed using the difference in the water
elevation between the two cells and the condition of the common
boundary. Three-dimensional approaches, where the velocity depth
profiles and the river bed boundary are allowed to vary, are not
usually utilised in geomorphological investigations in temperate
regions, as the time-scales of bed elevation changes in such
climatic regions are large. The complexity of three-dimensional
modelling approaches means that the number of applications has been
limited, and often to single channel systems, see for example
Tominga et al. (1989), despite the potential of such schemes.

The prerequisites in the selection of an appropriate model,
for the extension of the number of extreme events, require that the
model has been evaluated; this excludes three-dimensional models
which are in the early stages of development and may currently only
be considered to be research tools. Evaluated models that are well
documented adopt one or two-dimensional approaches. The resolution
of one-dimensional models is usually greater than that of MILHY3 in
the handling of the routing component of the downstream conveyance.
However, the handling of the complex geometry of a two-stage channel
system is usually of a lower resolution than the new modules of
MILHY3. This leaves a two-dimensional approach as being the most

Chapter 8

appropriate for the objectives of this chapter.

8.1.2 <u>Two-dimensional models of two-stage flow</u>

In contrast to one-dimensional models where the St. Venant
solution to the equations of flow are widely accepted, there is no
generally accepted single solution to the equations of flow in
two-dimensions. Solutions vary widely in complexity, from simple
steady state solutions to complex forms that include the energy
dissipation and plan geometry variations with stage.

Samuels (1985) classifies these models into two groups, based
on the type of solution to the equations of flow. These are:

i)   cell type – flow is computed from cell to cell on the
     floodplain according to certain laws

ii) differential type equations – flow is described by a set
     of coupled partial differential equations derived from
     physical parameters

Cell type models are based on grids determined from the
topography of the river reach, usually following the outline of the
main channel and extremity of the floodplain, for example
Lesleighteer (1983). Lesleighter's model, shown conceptually in
Figure 8.1, neglects the effect of inertia and the convection terms
in the solution of the conservation of momentum, and uses a Manning
type relationship to compute the flow between adjacent cells. These
models work well when the stresses between the computational cells
are greater than the boundary stresses on the bed on the floodplain
and main channel; such conditions could occur where slopes or flow
velocities are small. Generally, flow is controlled in cell type
models by equations such as:

$$Q_{ij} = K_1(h_i - h_j)^{0.5} \qquad\qquad 8.1$$
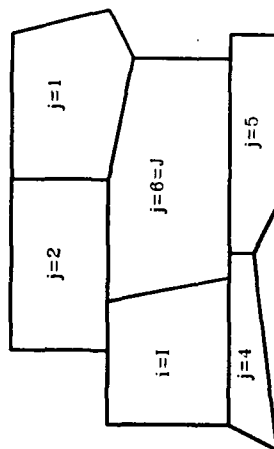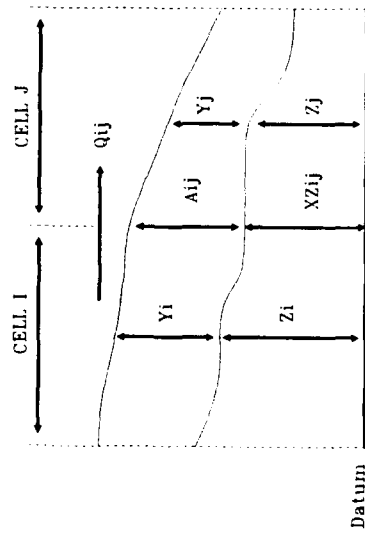
Figure 8.1
A Two-Dimensional Cell Type Model
(after Lesleighter, 1983)

Chapter 8

where   i and j   consecutive cells

K_1 conveyance function at link 1 between cells i and j

H   water surface elevation

Q_{ij} discharge flux between cells i and j

The limitation of cell type models is that the conveyance function K is dependent on the local direction of flow, so that K_1 may change if the floodplain inundation changes dramatically. Cell type models, therefore, work best in fairly stable inundation conditions.

Differential type solutions to two-dimensional modelling utilize one of three methods. These are:

  i)   the method of characteristics

 ii)   finite difference methods

iii)   finite element methods

In the method of characteristics, the partial differential equations are transformed into ordinary differential equations. An example was developed by Schmitz et al. (1983), who utilised a rectangular grid capable of greater resolution in required areas. Schmitz et al. (1983) acknowledge, however, that computer requirements of their scheme are large, and that an approximation of the streamlines required prior to computation may be a limitation.

Finite difference schemes utilise regular grid systems to solve the equations of flow, although the most complex schemes now allow for the curving or stretching of cell boundaries to improve the physical representation of the channel and floodplain, see for example Banks and Falconer (1989). Vreugdenhil and Wijbenga (1982) compared the results of a finite difference scheme using a 30m grid resolution, with the results from a flume-based experiment. The predictive

Chapter 8

accuracy of the finite difference model compared favourably with the
results from the flume experiments. Milityeev and Shkolnikov (1981)
and Zielke and Urban (1981) agree, however, that the main problem
with finite difference schemes is the resolution of the cell size in
order to represent the complex plan geometry of the channel and
floodplain. Reducing the size of the computational cell so that the
channel and floodplain flow segments are resolved separately,
increases the overall number of cells required to describe the reach
and thereby increases the computation time.

Finite element models utilize a flexible computational grid
that more accurately portrays the geometry of the two-stage channel.
A variety of element shapes have been used to build up the
computational grid, including triangles, rectangles and
quadrilaterals, examples of which include Su et al. (1980), and
Zielke and Urban (1981). The finite element method uses the
computational grid elements to approximate the solution of equations
of flow using some type of continuous function. The computational
difficulties of finite element models are generally greater than
their finite difference counterparts because of approximation
techniques required to solve the continuous function.

All three methods of differential type two-dimensional
analysis involve complex mathematical analysis. The relative
advantages offered by each technique depend upon the degree of
complexity in the geometry of the application. In the case of
two-stage models a method that offers a flexible grid element system
would be most advantageous. This excludes the method of
characteristics and the finite-difference approach and leaves the
finite element approach.

Comparison of the cell type model and finite element model,
which both offer a flexible grid network, shows that the
finite-element systems have been more widely developed and evaluated
than their cell type counterparts. In the next section, two-

Chapter 8

dimensional finite element models suitable for two-stage flow and for the extension of the record of extreme events are, therefore, investigated.

8.1.3 Two-dimensional finite-element models

Two-dimensional finite-element models have been developed over the past fifteen years, primarily for the simulation of flows in estuaries, or for complex flow environments around bridges or weirs. Examples of models developed for these environments include Tseng (1975) and King and Norton (1978), who simulate flows around a bridge, and Herrling (1978) and Holtz and Nitsche (1980), who simulate estuarine flow conditions.

More recently these models have been adapted for flow in two-stage channels. Zielke and Urban (1981) adapted the Holtz and Nitsche (1980) estuary model for flow in the floodplain system, and Su et al. (1980) developed a model simulating the flows at the confluence of two channels.

In all of these applications finite-element models have been utilised as alternatives to the establishment of flume-based experiments, and the scale of interest has been small. An exception to this has been a study of McAnnally et al. (1984a, 1984b), who undertook a large scale (tens of miles) simulation of an estuary and utilised a hybrid approach using both finite-element and flume-based simulations.

The limitation of finite-element models in the context of this investigation is, therefore, that all previous river reach applications have been on a small scale, whilst the river reach lengths in the River Fulda catchment range from 9 to 36 km. It is not clear whether finite element models would provide the level of predictive accuracy required at this scale to provide the ground-truth hydrographs for the evaluation of MILHY3. Specifically, it is

Chapter 8

not known if the size of the element in the computational grid may
be increased sufficiently to maintain a manageable computational
problem, or if the stability of the solution would be maintained.
If the water elevation drop were too great from one element to the
next, the simulation may, for example, become unstable. In
addition, would the resolution of data available for a typical reach
in the River Fulda catchment be great enough?

An investigation into the utility of finite-element methods as
part of the MILHY3 evaluation programme has therefore raised further
general conceptual questions. These are:

1)   can a finite-element model suitable for two-stage flow,
      that has been evaluated and documented on small scale
      applications, be identified?

2)   could this model be applied to larger reach lengths without
      increasing the number of computational cells beyond a
      manageable level and without requiring additional data?

3)   what would the predictive accuracy of such a large-scale
      application of a finite-element model be?

If a finite-element scheme could be successfully applied to
extend the record of an extreme event and meet all the criteria
above, could this not be incorporated as a high resolution module in
the MILHY3 scheme? Although this was not the objective of this
investigation, the issue of the development of a composite modelling
strategy and the inclusion of hydraulic techniques in hydrologic
modelling, have been identified as some of the most pertinent issues
in flood forecasting. The feasibility of including a finite-element
module in MILHY3 should therefore be considered.

The first task, however, is to identify a finite-element model
that incorporates two-stage flows, has been evaluated, and is

Chapter 8

well-documented. The number of finite-element models that meet all
these criteria is small, as many models are still in the
developmental stage. Two schemes have been evaluated here: RMA-2V
developed for the US Corp of Engineers (King and Norton, 1978), and
FLOUT developed at Hydraulics Research, Wallingford, (Samuels, 1983
a and b). Both of these packages are commercially available and
neither seems to offer any conceptual advantage over the other.

The RMA-2V package was selected as the backup and support was
offered by the US Corps of Engineers. All simulations of the RMA-2V
model were undertaken at the Hydrologic Engineering Centre, Davis,
California, on a Harris 100 super microcomputer with the help and
cooperation of Dr D.M. Gee. It should be noted that the simulations
undertaken using RMA-V2 in this chapter are the first applications
of any hydrodynamic finite-element model at a large scale in a
floodplain environment. These simulations are also the first
applications of RMA-2V using only the limited data available in
ungauged catchments. In addition, RMA-2V has not been previously
used to develop ground-truth hydrographs for the evaluation of other
models. In the next section, the RMA-2V model is briefly described.

8.2 RMA-2V A Two-Dimensional Finite-Element Model

RMA-2V is a finite element model for the solution of the
two-dimensional depth averaged shallow water flow equation. It can
simulate both steady and unsteady flow conditions by using the
Reynolds form of the Navier-Stokes equations of flow. Velocity is
used as the flow variable and it is computed at every node in each
element of the finite-element network. Three energy transfer
computations are included in the Reynolds solution. These are:

1)   the effects of boundary friction
2)   the effects of surface wind friction
3)   the effects of momentum exchange

Chapter 8

The finite-element network enables boundary roughness and topographic variations to be realistically simulated. The computational cell network is usually constructed based on series of lines running the length of the reach parallel to the contours. The resolution of the cells is determined by the operator, so that a greater number of cells can be utilized to give more detail in areas required.

The RMA-2V package, written in FORTRAN 77, was originally developed by Norton and King (Norton et al. 1973), under contract to the US Corps of Engineers. The model has since undergone many further developments and the version now being operated is version 4.1. This version allows the incorporation of one- and two-dimensional cells, thereby reducing the computational demands of the model. RMA-2V is also incorporated into the TABS-2 package (Thomas and McAnnally, 1984), which also offers a sediment budget routine and a water quality package.

RMA-2V consists of network generation and checking module (RMA1), the hydrodynamic package (RMA2), a contour plotting package (CONTUR), and a velocity vector package (VECTOR). A geometry file is generated by the RMA1 module, which once verified by the operator passes into the hydrodynamic package. The CONTUR and VECTOR packages allow the interpretation of solution files from the RMA1 and RMA2 modules. The CONTUR package draws the network and the topographic features incorporated in the cell network allowing the operator to check the representation of the topography in the reach. The VECTOR package allows the operator to plot the velocity vectors over the whole reach at any computational time increment.

8.2.1 Establishing the mesh: RMA1

The geometrical network is specified by the operator and consists of a series of quadrilateral and triangular ccells that represent the river reach. Each of the cells and corner nodes of

Chapter 8

the cells must be numbered and a connection table developed that
describes the number of the nodes in each cell, starting at any node
but always in an anti-clockwise direction. In addition, the x, y
and z coordinates of each of the nodes must be specified. The
mid-node coordinates are added automatically by the RMA1 package
interpolating linearly between the coordinates of the corner nodes.

A boundary roughness value must be specified for each of the
cells but to reduce the number of data that must be entered into
RMA1 the cells are classified into a number of groups, each of which
has the same boundary roughness. The number of boundary roughness
groups allowed is unlimited but usually no more than 5 are required.
If one-and two-dimension solutions are to be utilised, it is
important to note in the application of RMA-2V to two-stage channels
that the boundary roughness values in the one-dimensional data set
will be different from the two-dimensional data set. This is
because in the one-dimensional data set, the composite roughness of
both the main channel and floodplain flow segments must be included.

In addition to the boundary roughness values that must be
specified for each cell, an eddy viscosity coefficient must also be
specified. The eddy viscosity coefficient incorporates the effects
of momentum exchange generated by the velocity gradient across the
section. This momentum exchange is approximated by multiplying the
velocity in each direction by the eddy coefficient in that
direction. For the most accurate results, therefore, the eddy
coefficient should be entered for each side of the element and the
the direction of the element to the dominant direction of flow also
noted. The RMA2 code can then distinguish between eddy coefficient
values parallel to the main flow direction and perpendicular to the
main direction of flow.

It can be difficult to establish a value of the eddy
coefficient, which has dimensions of $lb\text{-}sec/ft^2$. for a particular
element side. It is important to remember that the value of the

Chapter 8

coefficient depends on the momentum of the fluid and the distance
over which the momentum acts, divided by the velocity of the flow
and the surface area of the element. This means that as an
element's size increases the eddy coefficient increases, or when the
velocity of the flow increases the coefficient increases.

Up to ten eddy exchange coefficient values may be specified in
the RMA1 data set, and the classification of each element side in
one of these ten groups should be specified. Element sides with
short lengths and parallel to the dominant flow direction should
have the lowest coefficient values, whilst long element sides
perpendicular to the dominant flow direction should have higher
coefficient values.

Vreugdenhil (1973) suggests the following relationship for the
approximation of the eddy coefficient value but notes that the
relationship only gives coefficient values to the nearesr order of
magnitude. Vreugdenhil's relationship is:

$$E = \frac{6h}{C}\, gV^2 \qquad\qquad 8.2$$

where   h - water depth
         C - Chezy coefficient
         V - velocity

If too small values of the eddy exchange coefficient are
selected by the operator, then the solution of RMA-2V may become
unstable. This is because small values of the coefficient allow the
direction of the velocity vectors to vary widely. It is often
necessary, therefore, to increase the values of the coefficient
during the initialisation of the scheme.

Chapter 8

The maximum of nodes allowed in the package is 2100, whilst the maximum number of cells is 900. These limits can be easily altered in the source code of RMA-2V, although this consequently increases t he size of the buffers required for the operation of the package.

At the upstream and downstream extremities of the reach, boundary conditions must be specified. Usually a stage and discharge condition are entered at the upstream boundary and a rating curve is specified at the downstream boundary. The rating curve takes the form of a single power function typically:

$$Q = A_1 + A_2(ELEV-EO)^C \qquad\qquad 8.3$$

where A_1, A_2 and C are coefficients.

8.2.2 Establishing the criteria for wetting and drying of elements

One of the main features of RMA-2V is that as the inundation stage rises and falls, elements of the mesh enter and leave the solution. This is known as the wet/dry capability. This is important not only in improving the efficiency of the solution, but also in increasing the physical representation of the modelling of the floodplain inundation. As the inundation levels fall, the cells with the highest elevation leave the solution, exposing knolls in the floodplain. The velocity vector plots show this distribution and show how the vectors converge around such knolls. This level of topographic resolution would not be possible with a hydrologic approach.

The wet/dry capability of RMA-2V has recently been upgraded in the latest version, version 4.1. In previous versions, cells left

Chapter 8

the solution when the highest node in a cell fell below the stage
elevation, plus a specified drying criterion. Cells then re-entered
the solution when the highest node was below the stage elevation,
plus a specified wetting criterion. These wetting and drying
criteria are specified by the operator but the wetting criterion
must always be of a greater depth than the drying criterion. This
introduces a hysteric effect, shown in Figure 8.2, where the stage
elevation must be lower to cause a cell to go dry than the elevation
required for a cell to be inundated. However, the error involved in
this inaccuracy, especially if the difference between the specified
wet and dry criteria was small, are not significant. The reason for
keeping as many cells as possible in the solution is that it
improves the continuity of the computation and hence improves the
stability of the solution.

In version 4.1 of RMA-2V, the hysteric wet/dry behaviour has
been replaced by a pseudo-porosity or marsh element routine, (King
and Roig, 1988). Developed to improve the predictive accuracy of
RMA-2V in marsh environments, the stability of the solution is
improved as flow through cells is gradually increased and decreased.
When cells drop out of the solution, the discharge flowing through
the cell is very small and, therefore, the impact on the overall
solution is small. The introduction of marsh elements into RMA-2V
has not previously been validated. It is one of the objectives of
this investigation, therefore, to compare the results from
simulations utilising the wet/dry criteria and the marsh elements.

The behaviour of these marsh elements has been likened to the
effects of macroporosity. An effective depth parameter, h_o, has
been introduced which is a function of the porosity of the cell.
The effective porosity is defined such that:

$$h_o = \int_0^h K.dh \qquad\qquad 8.4$$

where h_o - effective depth

      K   - porosity

      h   - depth
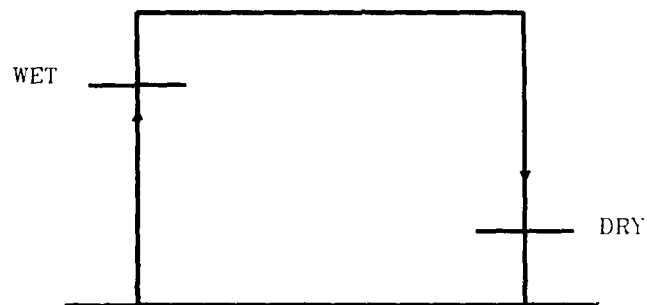
Figure 8.2
Hysteretic Effect of the Wet/Dry Capability
of RMA-2V, Version 3

Chapter 8

When an element is fully inundated all nodes are inundated at
a stage greater than the effective depth. As the stage falls, the
porosity weights the stage, generating the effective depth, thus
reducing the flow through the cell. The porosity varies at present
on a linear scale over the range of stage elevations, and this is
shown in Figure 8.3a. An S-shaped relationship would be physically
more realistic and such a relationship should be incorporated in the
next version of RMA-2V.

Figure 8.3 compares the wet/dry criteria with the marsh
element method of computation. The wet/dry criteria are illustrated
on the left-hand side of the diagram, whilst the marsh elements are
shown on the righthand side. The figure shows that as the
inundation depth falls, the cell is removed from the solution as
soon as one node falls below the drying criterion. The bottom
figure on the left-hand side shows the relationship this infers
between the conceptual porosity and stage elevation.

On the right-hand side of Figure 8.3, the diagram illustrates
how the porosity of the cell varies across the cell with the
variation of the depth of inundation. Segment 'a' has the lowest
depth of inundation and thus has the lowest porosity. This porosity
then weights the stage to give the effective depth which is
considerably lower than the actual depth; this reduces the
discharge prediction from segment 'a'. By contrast, in segment 'c',
the depth of inundation is greater, the consequent porosity is
larger and, therefore, the velocity prediction is reduced only
slightly.

When the depth of inundation is greater than 1m the porosity
of the cell is set at 1.0, so that the effective depth is the same
as the actual depth. The 1m rule has been set as an appropriate
value for floodplains, although it can be altered with reasonable
ease.
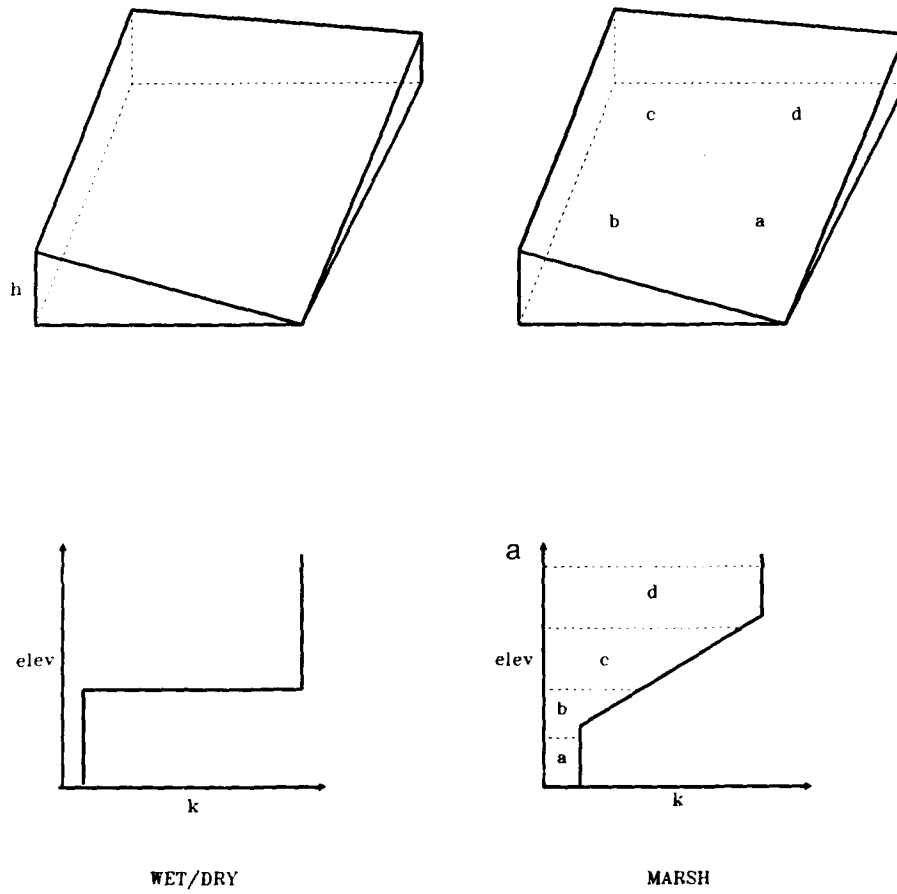
Figure 8.3
Comparison of the Wet/Dry Capability of Version 3 and Marsh
Element Capability of Version 4 of RMA-2V

Chapter 8

8.3　Application of RMA-2V

The objectives of undertaking an application of the RMA-2V model are to explore several areas.

1)　To establish whether a two-dimensional model of two-stage flow can be applied to large reach lengths, that is reach lengths of approximately 20km, and whether the simulation produces meaningful hydrograph solutions. Further, is the resolution of data available for the River Fulda catchment sufficiently great for such an application?

2)　To establish whether the predictive accuracy of RMA-2V is acceptable in comparison with the field data available, and to determine if the model can be used to extend the record of extreme events.

3)　To investigate the impact of the introduction of the marsh elements in RMA-2V by comparing the results from simulations utilising versions 3 and 4.

4)　To examine whether RMA-2V could be incorporated as a module in the composite modelling structure of MILHY3.

To undertake these objectives, a reach of the River Fulda between the gauging stations at Bad Hersfeld and Rotenburg was selected. This reach has been used in the analysis reported in Chapters 5 and 7, and was selected for this investigation as the inundation of the floodplain is extensive and defined on the available flood inundation maps.

The reach between Bad Hersfeld and Rotenburg is 24km (15 miles) in length, with a slope of 0.0008, that is a drop of 15m over the reach length. The floodplain is typically 1km wide and has a very shallow orthogonal slope to the main channel of around 0.0001.

Chapter 8

A typical scene along this reach is given in Figure 6.6, which shows
that the floodplains are bounded by steep hills which are often
forested.

Field estimates of the Manning's n coefficients of the
floodplain and channel along the reach length can be derived from
the photographs taken during visits to the River Fulda catchment,
using the tabulated values given in Chow (1959). Roughness values
were assessed as being 0.045 on the floodplain and 0.035 in the main
channel. However, in a few sections of the reach, the floodplain
roughness was considerably higher than 0.045, and for these sections
the Manning's n coefficient was estimated as being 0.07.

The cross-sectional geometry and rating curves are available
for the gauging stations at Bad Hersfeld and Rotenburg. At Bad
Hersfeld the channel is approximately is 4m deep and 30m wide,
whilst at Rotenburg the channel is 5.5m deep and 50m wide.

8.3.1 <u>System schematization</u>

RMA-2V utilises a finite element network composed of both
triangular and quadrilateral elements. Ground elevations are
defined at the corners of the elements and assumed to vary linearly
between corner nodes. In this investigation, the channel is
represented by a strip, two elements wide (Figure 8.4), producing a
triangular cross-section. Overbank areas were represented by much
larger elements. The triangular elements were most frequently used
in the description of the floodplain on the inner bank of the major
meanders in the main channel. The lateral extent of the network was
determined by a bluff line, beyond which none of the simulated flood
event would extend.

Two boundary roughness classes have been specified, one for
the channel cell elements and one for the floodplain elements. The
resulting finite element network is composed of 860 elements and

Figure 8.4
Elemental mesh for application of RMA-2V to the
River Fulda, West Germany

Chapter 8

2660 nodes. The ratio of the maximum element size to the smallest element size is approximately 200 to 1.

The rating curve relationship at the downstream station, Rotenburg, was developed using the single power relationship specified above. The exact form of the best-fit relationship is:

$$Q = 0.012H^{4.85}$$
<div style="text-align: right">8.5</div>

This relationship was developed using the flood frequency data for out-of-bank events. Figure 8.5 illustrates this single-power relationship and compares the curve with the data from the flood frequency analysis. The figure shows the inadequacy of the single power function to describe the rating relationship, even though only the out-of-bank events have been used. A trial using in-bank and out-of-bank events showed that the single power relationship could not satisfactorily describe the rating relationship.

8.3.2 Storm events

As this investigation is the first application of RMA-2V at this scale, two storm events were selected. These are the 1 in 10 year event (Storm 1), and the 1 in 100 year event (Storm 2), both used in the other parts of the evaluation program of MILHY3 reported in Chapters, 4,5 and 7.

The objectives of this investigation have been identified above. The primary objective is to investigate the utility of RMA-2V for extending the record of extreme events, and thus validating MILHY3 by investigating the stability and accuracy of the two model versions. The secondary objective is to investigate whether it would be feasible to incorporate RMA-2V as another module in the composite structure of MILHY3.

These two objectives require different simulations of Storm 1
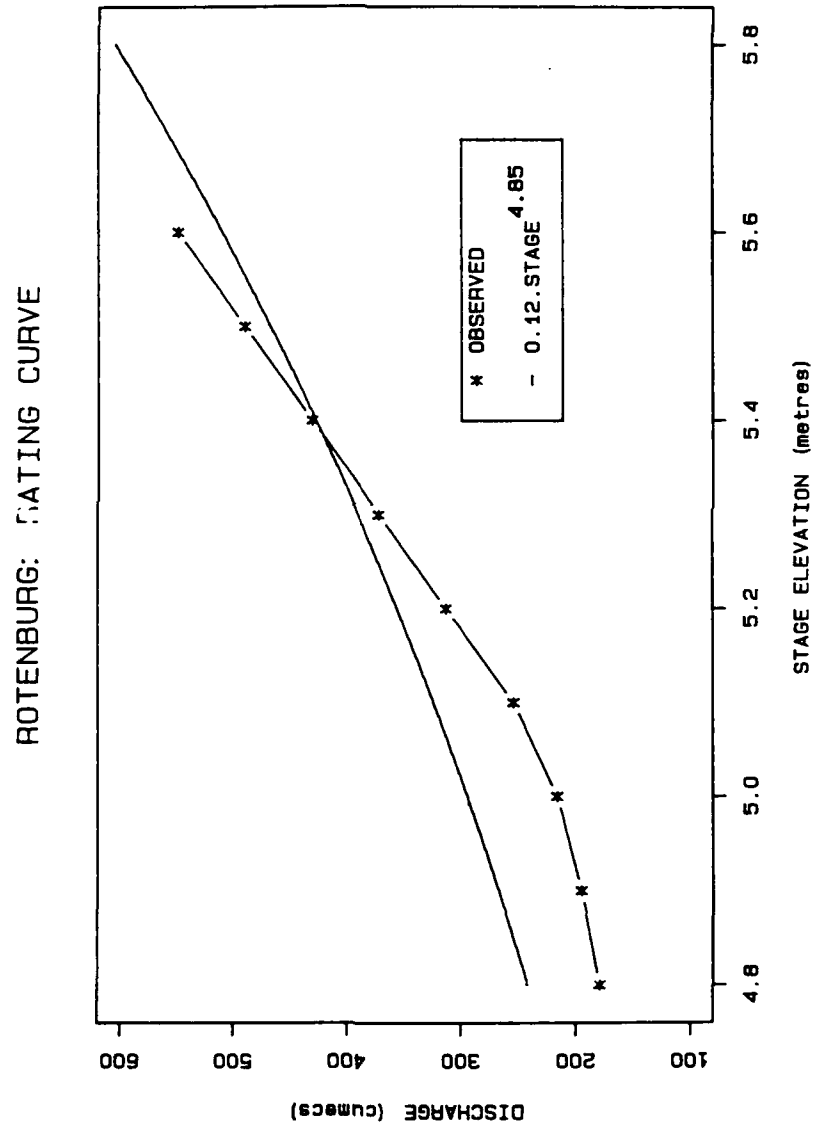
Figure 8.5
Comparison of observed and generated rating curve relationships
for Rotenburg

Chapter 8

using RMA-2V. In the first objective, the first aim is to show that
RMA-2V is capable of simulating storm events at this scale of reach,
and that the predictive accuracy in comparison with observed storm
events is acceptable. This requires, therefore, the comparison of a
simulated hydrograph with an observed hydrograph at the downstream
station, using the observed upstream hydrograph as the input.

The secondary objective (to investigate the incorporation of
RMA-2V as part of the MILHY3 scheme) requires a comparison of the
relative performances of the MILHY3 downstream conveyance models
with RMA-2V. This comparison can be partly achieved using the
simulation type identified in the primary objective, but also
requires the simulation of the storm events from Bad Hersfeld to
Rotenburg using RMA-2V, using the output from the MILHY3 simulation
to Bad Hersfeld as the input. This will enable the relative
advantage of RMA-2V in a catchment simulation to be judged.

These two investigations are reported in section 8.4 and 8.5.

8.3.3 <u>Initialisation of the River Fulda simulations</u>

As the application of RMA-2V to a reach on the River Fulda
was to be the first application of the model at this scale, a series
of trials were undertaken. The purpose of these trials was to
identify any conceptual or operational difficulties, and to
initialise the scheme ready for the simulation of the storm events.
The first task in the initiation of the simulations is to generate
the baseflow conditions in the reach. This is achieved by
undertaking a drawdown simulation where the reach is inundated with
water to such a depth that thehre is no water slope from the
upstream to downstream extremities of the reach, rather like a
reservoir. This water is then allowed to flow out of the reach
until steady conditions are reached.

In addition to the generation of the baseflow conditions,

Chapter 8

this initialisation allows the grid network to be checked for gaps
in the elements. With approximately 15,000 three and four digit
numbers to be entered into the computer to generate the River Fulda
mesh, the potential for missing a cell and creating a hole through
which the water could drain was great. With logical cell and node
numbering, such gaps are relatively easily found and the data set
corrected.

More of a problem was the generation of the baseflow
conditions by the lowering of the downstream elevation of the
'reservoir dam'. As the length of the reach is much larger than any
previous application, the consequent overall drop in the channel bed
elevation, (some 15m), is also large. To force the generation of
baseflow conditions, the incremental stage drop in the drawdown test
had to be reduced to 0.2m steps. The generation of baseflow
conditions, therefore, took much longer than anticipated. It is
also important to note that once the baseflow conditions have been
generated, then no alterations to the specifications of the grid
network must be made.

The initialisation also showed that the time increment of the
inflow hydrograph need only be 0.5 hours. Trials with a 0.25hr
increment did not improve the accuracy of the outflow hydrograph
and, therefore, it was not utilised. Throughout the analysis, to
reduce the computational requirements of the simulations, only the
rise of the hydrograph and the first part of the decline of the
hydrograph were simulated. This accounted for just over 20 hours of
the hydrograph and 40 computational steps. As the peak of the
hydrograph has been the primary area of interest in this report, and
because of the exploratory nature of these applications, the
limitations of simulating only the first 20 hours of the hydrograph
were accepted.

The computational requirements for simulating some 40 time
increments in the relatively large grid network for unsteady flow

Chapter 8

conditions were considerable. Each simulation took several hours on
the *Harris 100 super microcomputer*. It was important, therefore, to
select the simulations required with care.

8.4 RMA-2V Simulations Using Observed Inflow Hydrographs

The first aim of this investigation is to establish the
stability of the RMA-2V solutions for a variety of initial
conditions. Having established the grid network of the reach, which
is determined by the geometry of the reach, and having established
the baseflow conditions, three variables can be identified as
controlling the behaviour of the reach under different flow
conditions. These three variables are:

1)   boundary roughness - specified by Manning's n
      coefficients

2)   eddy coefficient - which incorporates the effects of
      turbulent exchange

3)   wet/dry criteria - version 3 only

The boundary roughness and wet/dry criteria are investigated
in this analysis. However, the sensitivity of the solution to
variation in the eddy exchange coefficient has not been
incorporated. A single eddy exchange coefficient of 50 which has
been utilised for all the element sides, has been used in all the
simulations. It is accepted that it is very important to
investigate the effects of variation in the eddy coefficient
exchange. However, the time available for this investigation was
limited. The value of 50 is the adjusted figure after the stability
of the solution has been ensured. The investigation of the effects
of variation in the eddy exchange coefficient has been identified,

Chapter 8

therefore, as a priority area for any further work on the utility of
RMA-2V in large-scale applications.

In the next two sub-sections, the effects of variation in the
two remaining variables, that is the boundary friction variable and
the handling of the wet/dry criteria, are investigated.

8.4.1 The effects of variability in boundary friction

As the turbulent exchange of momentum has been incorporated in
the two-dimensional solutions of RMA-2V, it is recommended in King
and Norton (1978)   at the Manning's n coefficients utilized to
incorporate the effects of boundary friction should be lower than
the n values recommended in texts such as Chow (1959).   To
investigate this recommendation in the context of a long reach
application, and to establish the sensitivity of the solutions to
the friction variables, the first set of simulations of RMA-2V used
a variety of the friction values.

Figure 8.6 illustrates the simulation of Storm 1, the 1 in 10
year event, using version 4 of RMA-2V that incorporates the marsh
elements.   The figure illustrates the effect of increasing the
Manning's n coefficient of the floodplain elements from 0.045 to
0.07, and compares these two simulated outflow stage hydrographs
with the observed hydrograph at the downstream station, Rotenburg.
All other variables are kept constant, the Manning's n coefficient
of the main channel being 0.035 and the eddy exchange coefficient
being 50.

Figure 8.6 shows that the adoption of the Manning's n
coefficient of 0.045 generates a downstream hydrograph that arrives
too soon in comparison with the observed hydrograph.   This suggests
that the reach is transmitting the hydrograph too efficiently.
Increasing the Manning's n coefficient to 0.07 reduced the
efficiency of the reach and the match between the observed and

Figure 8.6
Comparison of observed and RMA-2V, version 4, simulated hydrographs
with variations in the floodplain Manning's n, of the 1 in 10 year
event at Rotenburg

Chapter 8

simulated hydrographs is much improved.

The effects of increasing the floodplain Manning's n
coefficient in Storm 2, the 1 in 100 year event are shown in Figure
8.7. The 1 in 100 year event has been generated from the 1 in 10
year event using the flood frequency data available, and it is
interesting to note, therefore, the much more rapid travel time of
the peak stage in the 1 in 100 year event in comparison with the 1
in 10 year event. This faster travel time can be attributed to the
greater inundation depths on the floodplain and consequently the
diminished friction retarding effects of the boundary roughness.

This reduced effect of the boundary roughness in Storm 2 is
confirmed in the behaviour of the simulated hydrograph, when the
Manning's n coefficient is increased to 0.07. Although, as in Storm
1, the travel time of the peak is increased, in comparison with
Storm 1 the relative increase in the travel time attributable to the
increase in boundary roughness is small.

The effect of increasing both the main channel and floodplain
roughness coefficients in version 3 of RMA-2V can be seen in Figure
8.8. Version 3 incorporates the wet/dry criteria where elements
leave or enter the solution depending on the depth of inundation.
Figure 8.8 shows that as the Manning's n coefficient is increased,
the stability of the solution is reduced. As this behaviour was not
experienced in Version 4 of RMA-2V, this instability must be due to
the handling of the wet/dry criteria rather than directly
attributable to the boundary friction effects.

8.4.2 Variation in the handling of the wet/dry criteria

The previous sub-section illustrated that the stability of the
two versions of RMA-2V is different when the Manning's n roughness
coefficient is varied. Version 4, which incorporated the marsh
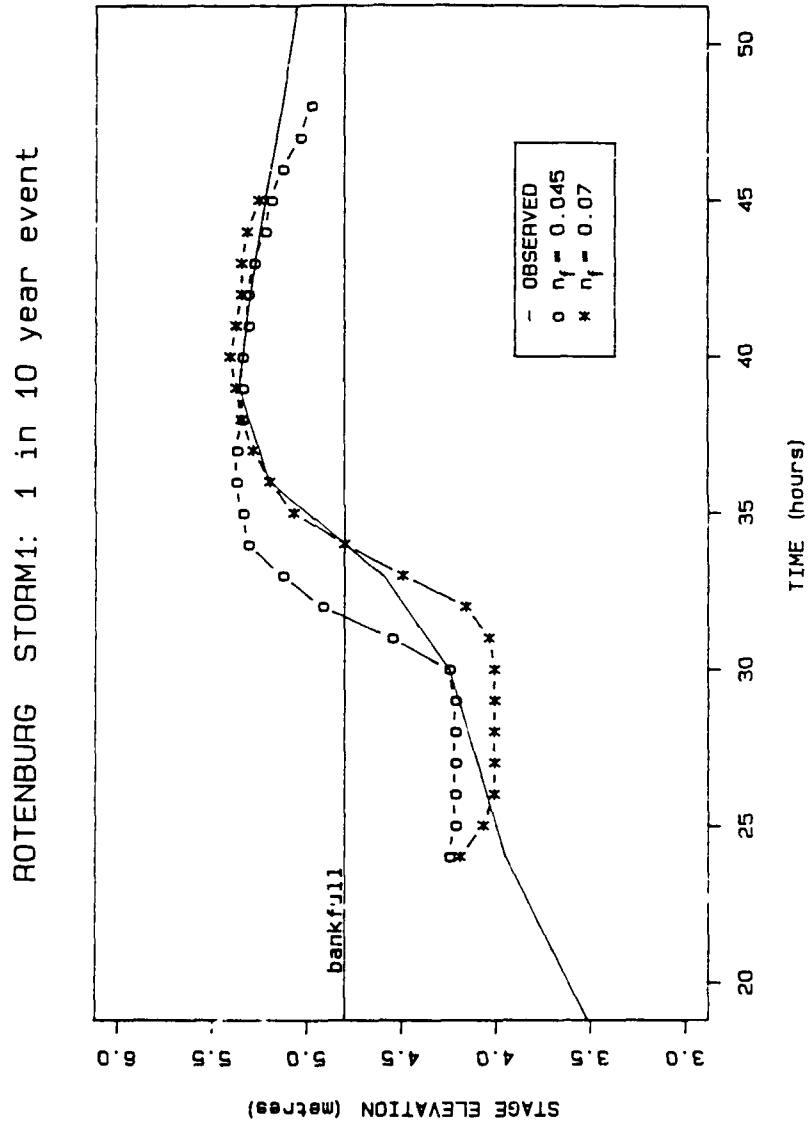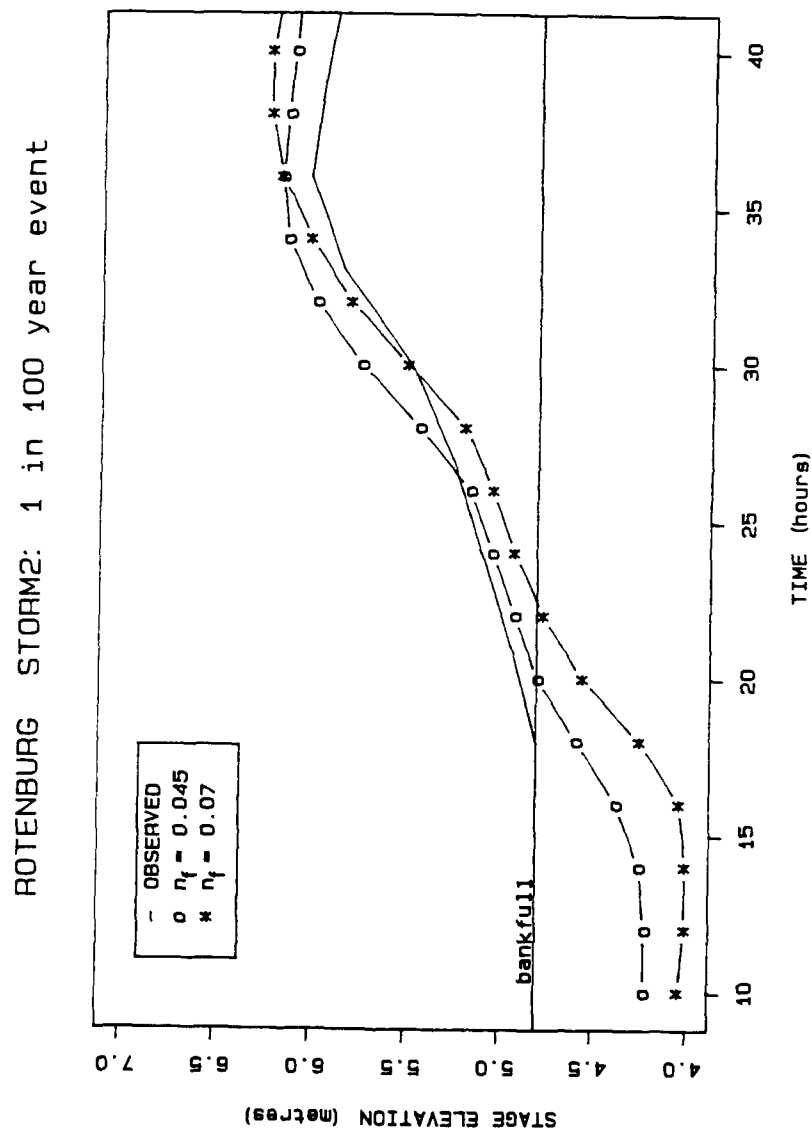elements, seems more stable than Version 3, which is based on the

Figure 8.7
Comparison of observed and RMA-2V, version 4, simulated hydrographs
with variations in the floodplain Manning's n, of the 1 in 100 year
event at Rotenburg
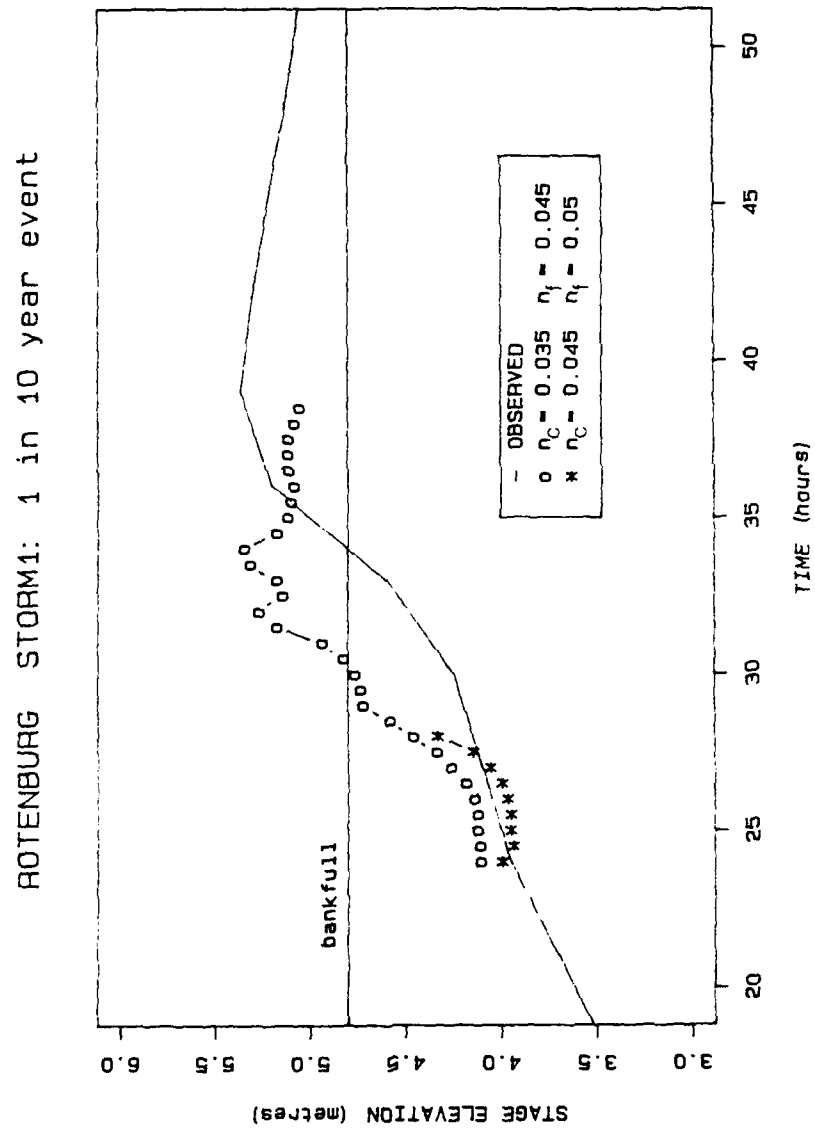
Figure 8.8
Comparison of observed and RMA-2V, version 3, simulated hydrographs
with variation in the floodplain and main channel Manning's n, of the
1 in 10 year event at Rotenburg

Chapter 8

wet/dry elements.

Analysis of the corresponding velocity vector plots for Figure
8.8 showed that most of the flow in the simulation of Storm 1 using
Version 3 is concentrated in the main channel, irrespective of the
Manning's coefficient values. It is probable, therefore, that the
failure of the simulations is due to a channel element falling out
of the solution as an element became dry.

One way of testing this hypothesis would be to investigate the
effects of varying the wet/dry criteria. Figure 8.9 shows the
effects of four different wet/dry combinations on the simulation of
Storm 1 using Version 3 of RMA-2V. The effect of decreasing the wet
and dry criteria is to extend the stage elevations for which an
element is included in a particular solution. This should ensure
that all the channel elements remain in the solution and, therefore,
that the length of the simulation is increased. In addition,
reducing the wet/dry criteria should increase the number of
floodplain elements that are in the solution, so that the spatial
extent of the floodplain inundation is increased. The data
available for the 1 in 10 year event indicate that the 1 in 10 year
event generates a large inundated area and that nearly all the
elemental areas, except the boundary elements, should be inundated.

Figure 8.9 shows that as the wet/dry criteria are decreased
from 1.0/0.5 to 0.6/0.1, the stability of the hydrograph solution is
increased and the length of the simulation is increased. Further
decreases to 0.4/0.05 and 0.2/0.05, however, reduce the stability
and hence length of the solution. This decrease in stability of the
solution as the wet/dry criteria are reduced further, is
theoretically unsound. However, the coding of Version 3 of RMA-2V
prevents the criteria tending to zero. This limitation has only
become apparent in this application because of the very low slope
across the elemental areas. In previous applications, the criteria
have been set to exceed the slope of the individual elements. These
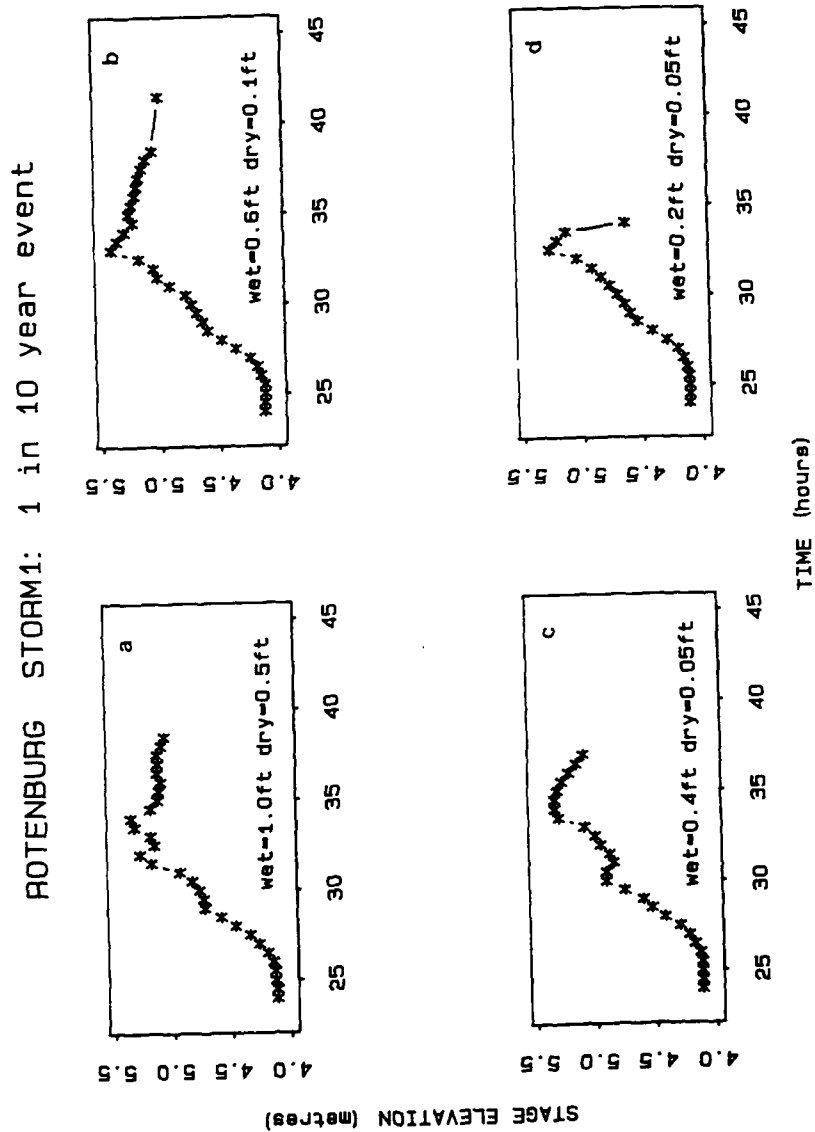
Figure 8.9
Comparison of the stability of solutions of RMA-2V, version 3, for four
wet/dry parameter combinations, of the 1 in 10 year event at Rotenburg

Chapter 8

slopes, however, are of a greater magnitude than the slopes of the
elements in this application, particularly in the direction
orthogonal to the main channel.

The stability of the solution is, though, improved by the
lowering of the wet/dry criteria before this limitation is reached.
The effects of lowering the criteria to 0.6/0.1 improves the
stability of the solution, and the extent of the floodplain
inundation should also be increased. Figures 8.10 and 8.11 are the
velocity vector plots for the peak discharge conditrions of the
initial wet/dry criteria, that is 1.0/0.5, and the improved
stability solution with wet/dry criteria of 0.6/0.1. Comparison of
these two vector plots, however, shows that the area of inundation
is more or less identical in the two solutions. In both vector
plots, the area of inundation is too small for the size of the 1 in
10 year event.

The failure of the manipulation of the wet/dry criteria to
have any impact on the area of inundation suggests that too much of
the flow is being carried in the main channel element rather than on
the floodplains. The main channel is represented by a triangular
cross-section consisting of two elements. This simple represent-
ation was made to reduce the number of elements used in the
schematization of the reach to improve the performancne of RMA-2V.
The premise of this simplification was that the main area of
interest in this investigation was the floodplain. These results
suggest, however, that the representation of the channel was
insufficient to ensure that the bankfull channel capacity was
accurately modelled. In further applications of this type,
therefore, it is recommended that the cross-sectional geometry be
more accurately given.

Comparison of the simulation utilising the two versions of
RMA-2V of Storm 1 with identical Manning's n coefficients is shown
in Figure 8.12. The comparison of the wet/dry solution (Version 3)

Figure 8.10
Velocity vector plot for the peak discharge condition simulated
utilising RMA-2V, version 3, with wet/dry criteria of 1.0/0.5

Figure 8.11
Velocity vector plot for the peak discharge condition simulated
utilising RMA-2V, version 3, with wet/dry criteria of 0.6/0.1
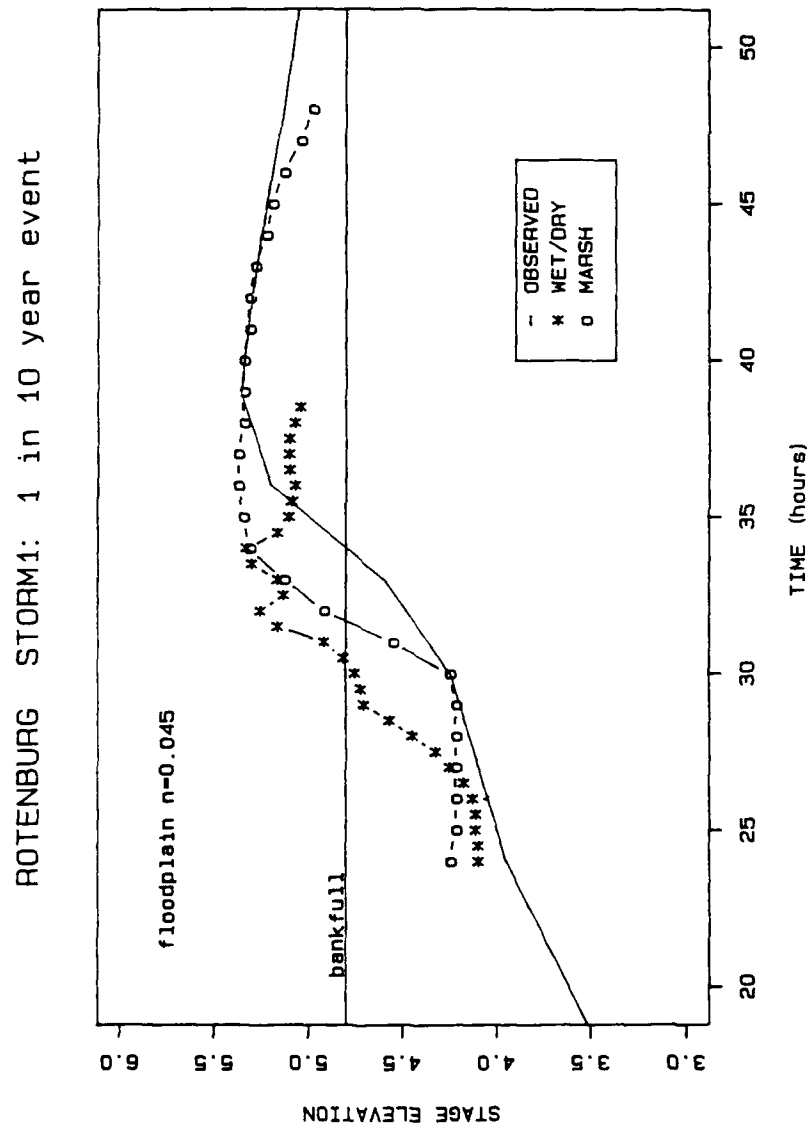
Figure 8,12
Comparison of observed and simulated hydrographs generated by
RMA-2V, versions 3 and 4, of the 1 in 10 year event

Chapter 8

and the marsh element solution (Version 4), shows that the wet/dry
solution is not as smooth as the solution of Version 4. This is
because in Version 3 elements are entering and leaving the solution,
which generates rapid increases and decreases in the flow area and
velocity distribution across the floodplain. The smoother solution
of Version 4, and the superior fit of Version 4 to the observed
hydrograph, show that the more gradual reduction or increase in flow
through the elements incorporated in Version 4, is more physically
realistic or, at least, the predictive accuracy of the version is
improved.

The stability of the marsh elements version when subjected to
variation in the Manning's n coefficients and the superior fit to
the observed hydrographs suggest that the development of the marsh
elements has made a significant improvement in the predictive
behaviour of RMA-V2. It is proposed, therefore, that Version 4 be
adopted for further validation.

8.4.3 Conclusions

The application of RMA-2V to the River Fulda reach using
observed inflow hydrographs and comparing the simulated outflow
hydrographs at Rotenburg, has shown that RMA-2V can be used on
reaches of this length. It has also shown that a topographic map
and upstream/downstream cross-sectional data provide adequate data
for the derivation of a stable solution.

Comparison of Versions 3 and 4 of RMA-2V have shown that
Version 4 is superior. The solutions are stable to variations in
the specifications of the boundary roughness specifications, and the
shape of the hydrograph using Version 4 fits the observed hydrograph
to a much greater degree.

However, neither version of RMA-2V produced reasonable
estimates of the inundated area of the floodplain. This has been

Chapter 8

attributed to the poor representation of the main channel. Overall, the results are promising for the utility of RMA-2V as a tool for testing simpler hydrologic models. Most important is the generation of a stable solution of RMA-2V for a relatively large reach with limited data.

8.5 Inclusion of RMA-2V as a Module of MILHY3

The results of the analysis reported above, show that it is feasible to incorporate RMA-2V as a module of MILHY3. The scale of the reach has not proved to be a problem, nor has the amount and quality of the data set. However, these initial results have shown that the time taken to initialise the network is extensive, and the level of expertise required is much higher than for the simpler MILHY3.

Before the inclusion of RMA-2V can be recommended, it is necessary that a set of circumstances be identified where the advantages of using RMA-2V would outweigh the disadvantages of using RMA-2V. It is important to compare the performance of MILHY3 and RMA-2V, and to identify the possible advantages of either scheme.

Figure 8.13 compares the performance of MILHY, MILHY3 and RMA-2V against the observed outflow hydrograph at Rotenburg. All schemes have only modelled the reach between Bad Hersfeld and Rotenburg, and all have used the observed hydrograph at Bad Hersfeld as the inflow hydrograph. The MILHY3 model has utilised both the momentum exchange and multiple routing routines and is the version that best-fits the observed hydrograph identified in Chapter 7. The RMA-2V model utilised is Version 4.

Figure 8.13 shows that the MILHY prediction is the least accurate of the three models, and that RMA-2V provides the closest fit to the observed hydrograph. Not surprisingly, the difference
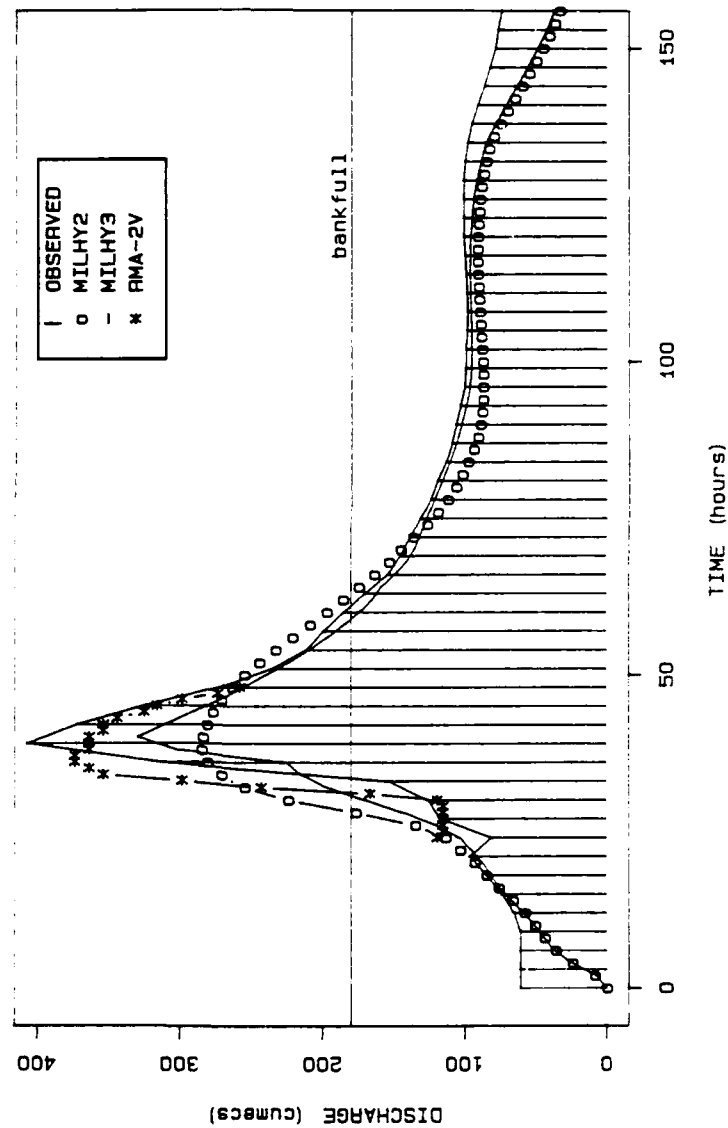
Figure 8.13
Comparison of observed and simulated hydrographs generated by
MILHY2, MILHY3 and RMA-2V, of the Bad-Hersfeld-Rotenburg reach
for the 1 in 10 year event

Chapter 8

between the MILHY, MILHY3 models is smaller than the difference
between the two MILHY models and RMA-2V. However, the difference
between the three models is less than the error between any of the
three simulations and the observed event. This figure suggests,
therefore, that for the resolution of data available, the improved
accuracy of the predicted hydrograph using RMA-2V does not
automatically outweigh the disadvantages of the initiation of
RMA-2V. If a highly accurate model of just the downstream
conveyance of a reach is required, then RMA-2V does provide a more
accurate hydrograph than MILHY3, and undoubtedly RMA-2V's accuracy
could be increased with a higher data resolution.

In the context of the ungauged catchment, however, where it is
unlikely that more data would be available, the use of RMA-2V as an
alternative to MILHY3 in the prediction of the hydrograph in a
single reach is not so attractive. However, where data are required
on the extent of the floodplain inundation, or the velocity of the
inundated flow, then RMA-2V undoubtedly is a superior model. The
accuracy of the prediction of the inundated area and the velocity of
the flow in inundated areas, has not been evaluated in this
analysis. It is suggested that a data set should be established to
enable this evaluation at this scale of application as a matter of
priority.

Figure 8.14 compares the performance of RMA-2V in the
prediction of the outflow hydrograph as a catchment model. RMA-2V
has been used to replace the MILHY3 scheme on the last section of
the reach between Bad Hersfeld and Rotenburg. The rest of the
catchment has been modelled using MILHY3; the inflow at Bad
Hersfeld for the RMA-2V scheme is generated using MILHY3. Figure
8.14 compares the performance of the replacement of this last reach
with RMA-2V, with the prediction using MILHY and MILHY3 for the
entire catchment.

Comparison of the MILHY models and the MILHY3+RMA-2V model
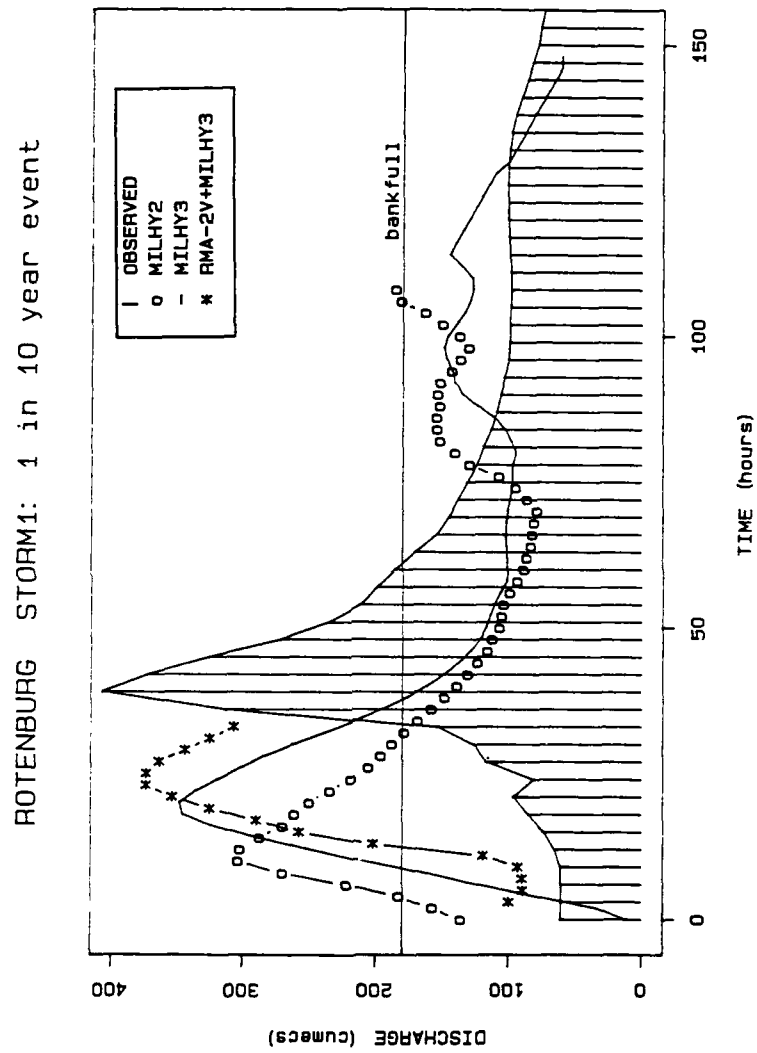
Figure 8.14
Comparison of observed and simulated hydrographs generated by MILHY,
MILHY3 and MILHY3 + RMA-2V, of the River Fulda catchment, for
the 1 in 10 year event

Chapter 8

shows that the difference between the MILHY models is much greater
than the difference generated by the introduction of RMA-2V in the
last section of the reach. In the prediction of the response of the
entire catchment, the introduction of the infiltration algorithm has
a greater effect than the more accurate modelling of the last reach.

These results suggest that the inclusion of RMA-2V as a
module into MILHY3 is not recommended if the operator intends to use
the model for the prediction of an outflow hydrograph. If the
operator requires information on the nature of the floodplain
inundation, then the inclusion of RMA-2V for the ar r prone to
inundation may prove worthwhile. It should be note again, however,
that whilst the accuracy of the predicted hydrograph produced by
RMA-2V has been evaluated in this analysis, and shown to be more
accurate than MILHY3, the predictive accuracy of the extent of
floodplain inundation and velocity vectors remains unevaluated.

8.6   Conclusions

The objective of this chapter was to investigate whether a
state-of-the-art model could be used to extend the record of extreme
event hydrographs, so that simpler models, such as MILHY3, can be
evaluated. Analysis of the sophisticated models available showed
that these models are still essentially research models and have not
been evaluated themselves. As a result of this, it was accepted
that the investigation should concentrate on the downstream
conveyance modules of MILHY3, and attempt to identify a
sophisticated model for conveyance.

A two-dimensional approach was identified as one which
incorporated the cross-sectional geometrical effects of two-stage
flow, and yet still offered a range of evaluated models. The
finite-element solution of the equations of flow in two-dimensions
was identified as being the method capable of incorporating the plan
geometry of the system.

Chapter 8

However, analysis of all the two-dimensional models available
showed that none had been applied to reach lengths of the scale
required for the evaluation of MILHY3. Most schemes were limited to
scales of around 2 km, whereas reach lengths on the River Fulda are
typically 20km. It was not known whether such hydraulic models
could be utilised at these larger scales, if their solutions would
be stable, or if the concepts on which they are based could be
scaled up.

The RMA-2V model was selected to investigate the suitability
of hydraulic models in general for application to these larger scale
reaches. If successful, they could not only be used to evaluate
simpler models but also to replace them.

The results of the application of RMA-2V to the River Fulda
are very promising. The latest version of the model that
incorporates marsh elements is stable for a variety of boundary
roughness conditions, and the predictive accuracy of the model seems
better than the predictive accuracy of MILHY3. In addition, the
application of RMA-2V provides the potential for more detailed
modelling of the floodplain, as the inundated extent and velocity
vectors are computed.

Before RMA-2V is ready for application to the larger scale
catchments, however, it is important that certain areas not
included in this analysis should be investigated and evaluated as a
matter of priority. These areas include:

1)   the sensitivity of the RMA-2V solution to variation in the
      eddy exchange coefficient.

2)   the evaluation of the predicted area of floodplain
      inundation against a field data set

3)   the evaluation of the accuracy of the predicted velocity
      vectors against a field data set

Chapter 8

Once these areas have been evaluated, then RMA-2V could be
used to generate hydrographs from the flood frequency data to
validate simpler hydrologic models for extreme events. The
investigation of the above areas should also enable the set of
circumstances where the inclusion of RMA-2V in a catchment model
such as MILHY3 would be profitable. The results reported above
suggest that including RMA-2V in a catchment model would be
profitable where a higher level of predictive accuracy is required
in the simulated hydrograph, or where details of the floodplain
inundation would be useful.

The success of the RMA-2V application to a large-scale
catchment shows that the separation of hydraulic and hydrologic
modelling on the grounds of scale alone is not a valid one. RMA-2V,
a hydraulic model, operates successfully on a scale usually reserved
for hydrologic approaches. In addition, the results suggest that
RMA-2V could be successfully incorporated into a composite modelling
strategy. The combining of hydrologic and hydraulic approaches in a
single modelling structure provides a powerful and flexible tool for
the prediction of floods in ungauged catchments.

Chapter 9

Chapter 9
Floodplain Inundation Modelling Utilising RMA-2V

The results shown in Chapter 8 of this report indicate a
promising future for the linking of the RMA-2V and MILHY3 schemes.
Initial results from the River Fulda show that large-scale
floodplain modelling using RMA-2V is possible, even with
parsimonious dats sets. The analysis carried in Chapter 8, however,
concentrated on the predictive accuracy of the outflow hydrograph at
the Rotenburg station on the River Fulda. The objective of this
chapter is to continue to explore the utility of RMA-2V but
specifically to investigate the two-dimensional components of the
model. The application of RMA-2V to shallow floodplain environments
is investigated from a more "operational" perspective, with
questions on resolution and topographic representation explored more
explicitly than in Chapter 8.

For this investigation a new study reach, the River Culm in
Devon, England, has been established. The River Culm offers a more
detailed inundation data set than available for the River Fulda and,
in addition, provides a very much more topographically complex
terrain to simulate (see section 9.1). The problems associated with
establishing the River Culm elemental mesh are discussed in section
9.2, and the results of simulations of the scheme are presented in
section 9.3. In section 9.4, the implications of these results for
ungauged flood forecasting are discussed and section 9.5 provides
guidelines and recommendations for future applications.

9.1   River Culm

The River Culm is a tributary of the River Exe, joining the

Chapter 9

Exe approximately 3km north of Exeter (see Figure 9.1). It has a catchment of 275 km^2 and in its lower reaches has a well-developed floodplain averaging 500m in width. The main channel is gravel-bedded and approximately 12m wide. The banks are 1m high and consist of fine alluvial material. Overbank flooding is relatively frequent during the winter months when usually ten overbank events a year occur. During these events, a substantial area (5.5 km^2) is inundated, with typical inundation depths being 40cm for the mean annual event and 70cm for a 50 year event. Land use on the floodplain is almost exclusively permanent pasture (see Figure 9.2) which is used for summer grazing, hay and silage production.

This study has focused on the 11km stretch of the River Culm between the flow gauging stations at Woodmill (upstream) and Rewe (downstream), see Figure 9.1. Between these gauging stations the tributary, the River Weaver, joins the River Culm but flows from the Weaver especially during flood events on the Culm are small enough to be ignored for the purposes of this investigation.

Along this stretch of the River Culm the channel is restricted in two places by paper mills at Hele and Silverton. Figure 9.3 shows the main channel constricted through the mill at Hele. Both Figures 9.2 and 9.3 were taken during a visit to the reach in October 1989. The overall slope between the Woodmill and Rewe gauging stations is 0.002, although this varies considerably within the reach.

In comparison with the River Fulda, Bad Hersfeld to Rotenburg reach, the identified stretch of the River Culm is a highly complex environment. Inundation is very spatially variable with areas of storage and areas of fast moving floodplain flows. Figure 9.4 illustrates this variability through a radiological investigation carried out by Walling et al. (1986).
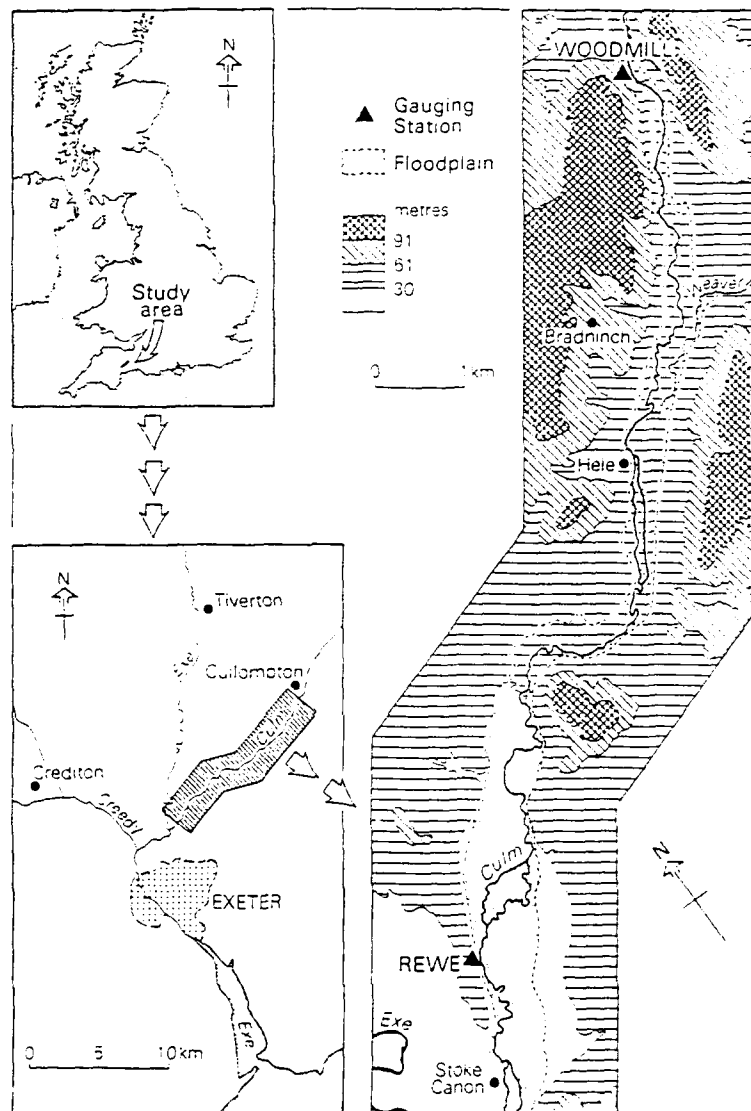
Figure 9.1
Location of River Culm reach, Devon, U.K.

Figure 9.2
Channel and Floodplain Cross-Section 2km Upstream
of Rewe

Figure 9.3
Hele Mill Race, River Culm

Chapter 9

Figure 9.4 shows the Caesium 137 activity of sediment cores
taken at various locations throughout the reach. The wide variation
in the C^{137} activity of these cores illustrates the spatial and
temporal variability of floodplain deposition since nuclear tests
carried out in the late 1950s. Caesium 137 released during these
nuclear tests which peaked in 1964, was rapidly absorbed in the
upper soil horizons. Subsequent movement of C^{137} within the
landscape is therefore associated with the erosion transport and
deposition of sediment particles (Walling et al., 1986). Enhanced
levels of C^{137} above a background level can, therefore, be
associated with deposition of sediment eroded from elsewhere in the
catchment.

The radiological investigation conducted by Professor Des
Walling and his team at the University of Exeter, UK, has generated
a large volume of inundation data. Access to this data set has
proved an invaluable part of this investigation, and the help
of Professor Walling is acknowledged.

9.2   River Culm Elemental Mesh

Figure 9.5 shows the completed mesh for the River Culm between
Woodmill and Rewe. This mesh has been generated from the 1:2500
series of topographic maps of the area, maximum flood extent maps
from the National River Authority, air photographs of flood events
and ground surveys, and drawings taken during visits to the
catchment. Generally, the data available enabled a more
topographically detailed mesh than the River Fulda mesh (see Figure
8.4), and this is highlighted in the smaller elemental areas
utilized. River Fulda elemental areas averaged 200m by 200m, whilst
River Culm elements are generally 100m by 100m.

Following the conclusions of the River Fulda applications,
section 8.4.2, the River Culm mesh incorporates a more accurate
channel cross-sectional geometry. Summarized in Figure 9.6, the
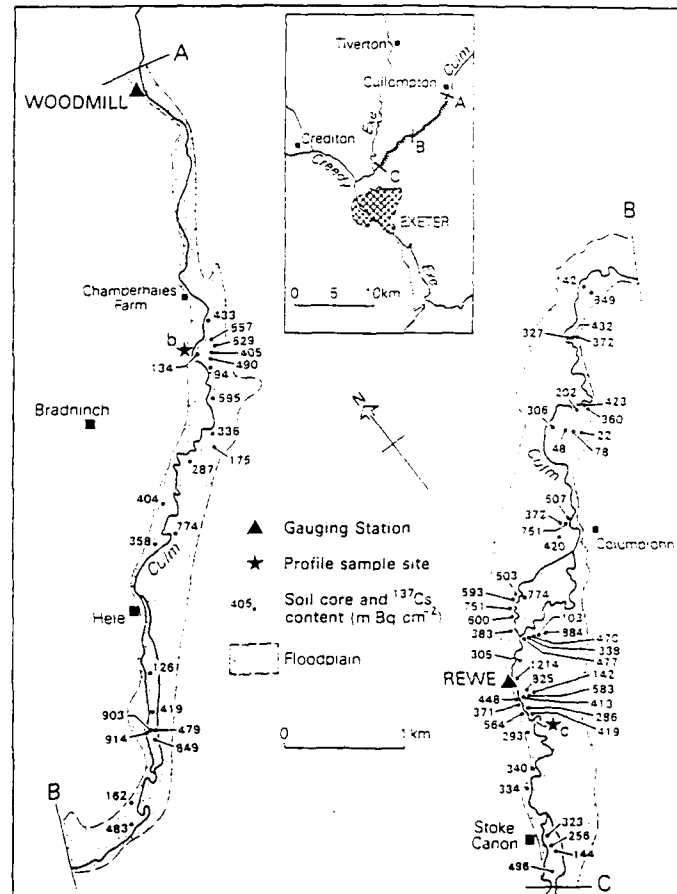
Figure 9.4
Caesium 137 distribution from experimental data by
Walling et al. (1986)
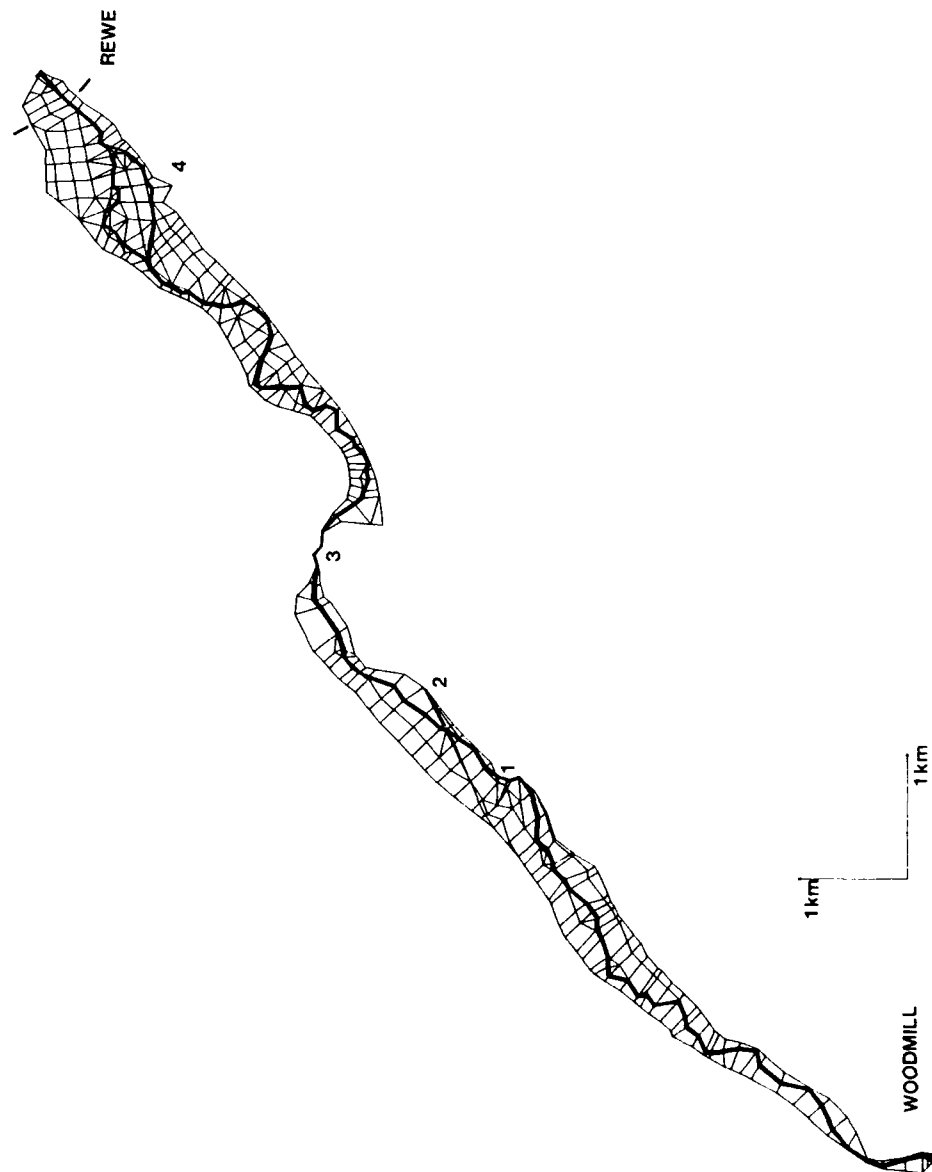
Figure 9.5
River Culm elemental mesh for application of RMA-2V

Chapter 9

River Fulda channel can be seen to be represented by a two element
strip generating a triangular cross-section. This proved to be too
efficient a shape. The River Culm mesh, therefore, utilizes a
trapezoidal cross-section with a three element strip representing
the channel. In addition, this three element strip is flanked by
another element either side of the channel to represent bankside
vegetation.

Ten boundary roughness and hence ten element groups have been
identified. These are:

		Number of elements
1	Channel bed	164
2	Channel bed, vegetated	6
3	Channel bank sides, grass	269
4	Channel bank sides, trees	1
5	Channel bank sides, scrub	3
6	Bankfull, trees	27
7	Bankfull, scrub	6
8	Bankfull, grass	227
9	Floodplain, grass	374
10	Floodplain, woodland/carr	12

Approximately 1090 elements have been utilized, the
distribution of which is indicated above.

Several specific features of the River Culm reach were also
incorporated, identified on Figure 9.5. These are:

1   Hele mill
2   Railway embankment
3   Silverton mill
4   Channel bifurcation

Chapter 9

The two paper mills at Hele and Silverton are accurately represented as channelized channels, with low boundary friction and high velocities. Silverton mid flows are contained entirely within the race and no floodplain elements are required. The railway embankment creates a barrier across the floodplain which, since raising of the line in 1989, has not been breached. This feature, therefore, creates a large pond of low velocity flow and the funnelling of flow through a bridge under the embankment. The bifurcation near the downstream gauge creates a large complex floodplain island, part of which may be seen in Figure 9.2. Flows are equally divided between the two parts of the channel, and the bifurcation is approximately 1.5km in length.

9.2.1 Mesh development

Figure 9.5 represents the final version of the elemental mesh developed for the River Culm; several intermediate versions have been discarded. Application of RMA-2V to the River Culm generated some new and novel problems, particularly in the resolution of topographic representation. Taking each of the developmental stages in turn, the first mesh version incorporated all the topographic details available from the data set. Having ensured there were no errors in the generated mesh, a test run was undertaken which proved to be very unstable. Interrogation of the results files enabled several problematic areas of the mesh to be identified. These were characterized in general by one or more of the following problems:

1) areas where large and small elemental areas are adjacent

2) areas of steep lateral or longitudinal slope

3) sharp changes in the direction of flow

4) all four of the specific features (mills, etc.) identified earlier

Chapter 9

Each of these problems created a numerical "shock" to the
solution, which either were overcome with poor continuity solution
or perturbated until finally the solution failed. To overcome
these problems, a degree of "smoothing" of the mesh was required.
This created some fundamental questioning of the application of
finite-element schemes to large scale reaches. In particular, can
enough topographic resolution be incorporated to provide a
meaningful solution and to meet the numerical stability of the
program?

It is important here to distinguish between topographic
resolution and mesh resolution. Mesh resolution may be increased
without gaining topographic resolution by interpolating inter-
mediate data. Decreasing topographic resolution requires smoothing
physical features of the system, although mesh resolution may
increase or decrease.

The first problem tackled war in areas where very large
elements were adjacent to very small elements. This situation
almost always occurs at the floodplain channel interface. This
required widening of the channel side elements (see Figure 9.6) and,
by necessity, to maintain channel volume narrowing of the channel
bed elements throughout the reach. This improved the stability of
the solution without reducing topographic resolution. Such
adjustments were, however, not enough to overcome the fatal
perturbations generated elsewhere in the mesh.

The second set of modifications undertaken were to the lateral
slopes of the floodplain and channel elements. Figure 9.6 shows the
conceptual cross-sectional structure adopted for the River Culm, and
shows that the bankside elements have been assumed to be horizontal.
This geometrical combination not only provides a lack of continuity
in the lateral slopes, but also means that a very small variation in
stage elevation will cause these elements to be either totally
inundated or totally dry. Given the success of the marsh element

296
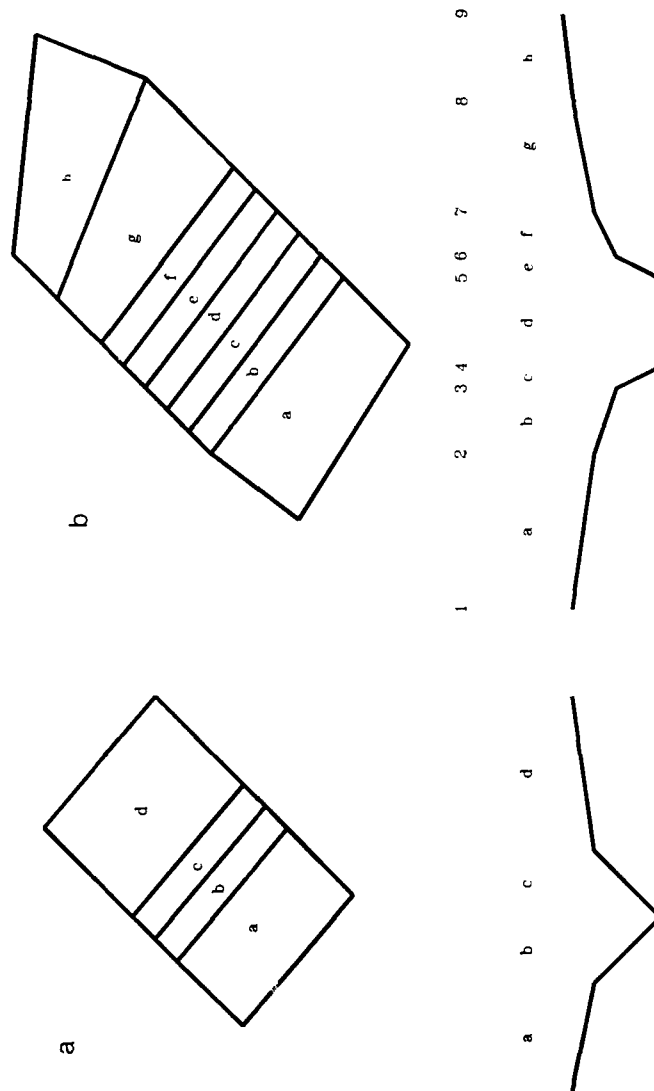
Figure 9.6
Conceptual Mesh Cross-Sections for
a) River Fulda
b) River Culm

Chapter 9

version of RMA-2V, discussed in section 8.2.2, in gradually phasing
elements in and out of the solution, it was decided to introduce a
slight slope to the bankside elements. In other areas of the mesh
the lateral slopes within elements were decreased such that no
element contained an elevation drop of greater than 3m (10ft.).
This change necessitated some loss of topographic resolution. Once
again the stability and continuity of the solution were improved,
but "shocks" to the system still occurred.

The third series of modifications undertaken are those seen
most clearly when comparing a segment of the two versions on Figure
9.7, and involving modifying the sharpness of angle in the direction
of flow. Most of these modifications were to reduce the sinuosity
of the main channel. Close examination of Figure 9.7 shows that
this straightening has been achieved through the removal of small
meander bends and the straightening of larger bends. No channel
meander is now more acute than 110°. These changes also meant
several smaller elements, situated within meander bends, were no
longer required. These changes made throughout the reach made a
noticeable improvement in the efficiency of the program. The front
width was reduced from 260 to 210 and stability was much improved.
Comparison of Figures 9.7a and 9.7b also shows that the downstream
extremity of reach in version 3 has been stretched. This was to
allow the positioning of the downstream gauge away from the effects
of the outflow control structure.

The final modifications to the mesh involved adjustment of the
longitudinal slope and coincided with the release of version 4.2c of
RMA-3V. The modifications involved distributing the relatively
steep longitudinal slope of a short section of the reach, close
to the upstream gauge, over a longer distance. The area concerned
had an elevation drop of approximately 0.75m every 150m; this was
followed by a section with 0.003m drop per 150m. These two slopes
were then averaged over the two reach segments. These changes,
together with the modifications to the wetting and drying

Figure 9.7
Evolution of mesh for the bifurcation on the River Culm
a)   field data
b)   smoothed

Chapter 9

sequence in the new release of RMA-2V, proved successful and a
stable initialisation solution was achieved.

This series of modifications indicates fairly clearly that
there is a limit to the topographic resolution for RMA-2V
applictions at this scale. Attempts to improve the stability of the
solution by increasing the mesh resolution of topographically
complex areas failed. Figure 9.8 shows an extreme example of this,
where a complex S bend just upstream of Silverton Mill was being
simulated. Figure 9.8a illustrates the first mesh established,
whilst figure 9.8b shows an increased resolution of mesh initialised
when the first mesh solution failed. Comparison of Figures 9.8a and
9.8b also illustrates the widening of the channel side elements and
narrowing of the channel bed elements. Figure 9.8c shows the final
solution where the bend has been totally removed. Although this is
the most extreme example on the River Culm application, it does
serve to show the problem of topographic and mesh resolution.

From the establishment and initialisation of the River Culm
mesh, it is possible to suggest several guidelines for future
applications of RMA-2V at this scale. These are:

1.   Channel platform - an upper limit of 110° has been found
      to apply to the representation of meanders. This criteria
      then sets constraints on the minimum length of channel
      element.

2.   Channel long profile - an upper limit for slopes appears to be
      0.3m drop per 150m.

3.   Lateral slopes - an upper limit here appears to be 3m in any
      one element.

4.   Floodplain topographic representation - resolution appears
      limited to features 10 - 100m in size, rather than 1-10m.

300

a

b

c
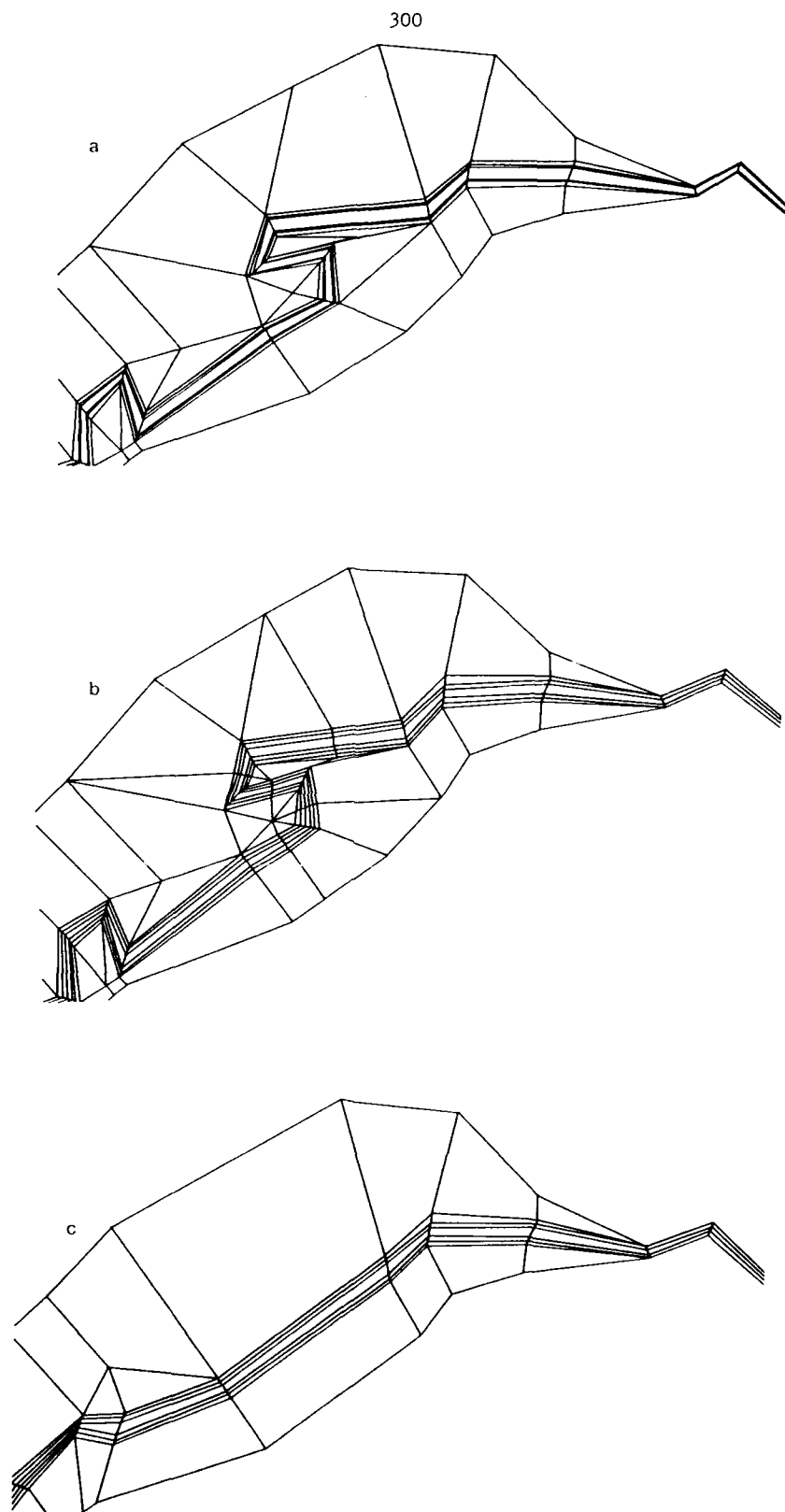
Figure 9.8
Evolution of mesh for a double bend on the River Culm
a) field data, b) increased mesh resolution, c) smoothed

Chapter 9

9.3   Application of the River Culm

The overall objective of applying RMA-2V to the River Culm
reach is to continue evaluating the performance of RMA-2V at this
scale. In particular, the River Culm has allowed the evaluation in
a more complex topographic terrain than previously undertaken, and
the more exhaustive data set will allow rigorous evaluation of the
simulated inundation distributions as well as predicted outflow
hydrographs. The establishment and initialisation of the mesh has
already proved useful in exploring topographic and mesh resolution
issues and these issues will be further discussed later in this
chapter. The remaining sections of the chapter explore the
sensitivity of RMA-2V and more practical issues of reach calibration
and the interpretation of results. To calibrate the reach some
indication of the sensitivity of the reach to parameter variability
is required, and it is to this objective that the rest of this
section is dedicated.

9.3.1 Sensitivity of the River Culm Application

The results from the River Fulda application suggested that
applications of RMA-2V are most sensitive to changes in the
Manning's 'n' coefficient. However, other parameters identified in
Chapter 8 must not be ignored, and include:-

-    turbulent eddy coefficients
-    marsh element parameters
-    rating curve relationship
-    mesh resolution
-    time step resolution

As the objective of this analysis is not to undertake an
exhaustive and full sensitivity analysis, but rather to explore
sensitivity for the purposes of calibration, each of the above
groups of parameters is explored somewhat more subjectively.

Chapter 9

Firstly, Manning's n having been identified by the River Fulda application. A series of steady-state applications were undertaken where individual or groups of Manning's n elements were varied, and the impact of this sensitivity assessed on the specific flow (depth x velocity) across a continuity line close to the downstream gauging station. The continuity line includes all nodes from the boundary of one floodplain across the channel and through the opposite floodplain, and the position of this line is shown on Figure 9.5. Figure 9.6b identifies the position of the nodes specified in the analysis.

Tables 9.1 and 9.2 collate the results of varying the Manning's n coefficients under two flow regimes. Table 9.1 shows the results for bankfull conditions (24m elevation, 30 m^3s^{-1} discharge), whilst Table 9.2 shows the results for the peak of the 1 in 10 year event, where floodplain inundation depths are 80cm and discharge is approximately 120 m^3s^{-1}. Both tables make comparisons with original Manning's 'n' values specified by Chow (1959) during visits to the reach. The original Manning's n values for each element type were specified as:

Element type		Manning's n
1	Channel clear of vegetation	0.03
2	Channel, vegetated	0.035
3	Channel bank sides, grass	0.04
4	Channel bank sides, trees	0.042
5	Channel bank sides, scrub	0.04
6	Bankfull, trees	0.05
7	Bankfull, scrub	0.05
8	Bankfull, grass	0.045
9	Floodplain, grass	0.045
10	Floodplain, woodland/carr	0.055

Table 9.1

Specific flow results with variations in Manning's n for bankfull conditions

Specific flow ($ft^2 s^{-1}$)

Node	Original	$n_9 = 0.1$	$n_8 = 0.1$	$n_3 = 0.1$	$n_1=n_2 = 0.1$	$n_3=n_4=n_5=0.1$	$n_6=n_7=n_8=0.1$	$n_9=n_{10} = 0.1$
1	0.30	0.278	0.360	0.342	0.361	0.382	0.360	0.277
2	1.215	1.051	1.188	1.395	1.346	1.395	1.188	1.049
3	4.033	4.824	3.089	3.425	3.787	3.425	3.089	4.824
4	17.252	19.735	14.403	13.173	13.589	13.174	14.403	19.735
5	18.202	21.086	15.591	13.382	14.139	13.382	15.590	21.086
6	4.248	5.190	3.406	3.289	3.961	3.289	3.406	5.190
7	1.156	0.955	1.210	1.333	1.289	1.333	1.210	0.955
8	0.179	0.174	0.226	0.239	0.227	0.239	0.226	0.173
9	0.097	0.103	0.126	0.133	0.125	0.133	0.126	0.103

Table 9.2

Specific flow results with variations in Manning's n for 1 in 10 year peak conditions

Specific flow ($ft^2 s^{-1}$)

Node	Original	$n_3 = 0.1$	$n_8 = 0.1$	$n_9 = 10$
1	2.551	2.708	2.700	2.478
2	4.940	4.931	4.419	4.702
3	9.122	7.389	6.877	11.429
4	24.336	18.451	20.019	29.759
5	24.888	18.314	20.942	30.778
6	9.104	7.022	7.157	11.450
7	4.735	4.807	4.526	4.245
8	1.856	2.003	2.012	1.875
9	1.304	1.421	1.431	1.414

Chapter 9

In each of the simulations documented in Tables 9.1 and 9.2, one or more of the element type Manning's n values were increased to 0.1. The simulations documented show not surprisingly that changing the n value in the most frequently occurring element groups has the most effect. Table 9.2, therefore, reports only the three most important element groups. Both Table 9.1 and 9.2 show that the solution behaves logically, with increasing n in a particular element type causing smaller specific flows in that group, and larger specific flows in other groups. Table 9.1 shows that variation in element type 3 (grassed channel sides) causes the greatest impact, both in the channel and on the floodplain. Channel element specific flow is decreased by an average 78%, whilst floodplain flows are increased by 123%. Comparison of Tables 9.1 and 9.2 show that the in 1 in 10 year specific flows are not as sensitive to Manning's n variations as the bankfull results. Nevertheless, raising the n value of element type 3 is still the most effective way of reducing channel flows. These results illustrate that fairly radical adjustments in the Manning's n coefficients can generate changes in the specific flow of up to 25%. Manning's 'n' is therefore a powerful tool in calibrating the reach and, in particular, is useful for apportioning the correct volumes of flow to the floodplain and main channel.

It is important to consider the physical realism of calibrating utilising the Manning's n coefficient. The variations shown in Tables 9.1 and 9.2 involved raising the coefficient to 0.1, a value corresponding to dense brush or a heavy stand of timber, according to Chow's (1959) tables. Such adjustments cannot, therefore, be justified physically. Instead the Manning's n values used in the RMA-2V scheme should be considered as belonging to a separate roughness scheme.

9.3.2 Hydrograph Simulation of the River Culm

The next stage in the calibration procedure was to attempt a

Chapter 9

dynamic simulation and compare predicted and observed hydrographs.
Figure 9.9 shows the observed inflow discharge hydrograph and
observed outflow stage hydrograph for an event commencing in January
1984. The figure shows, in a double peaked hydrograph, with the
first peak having a recurrence interval of approximately 1 year, and
the second peak 10 years. It is important to note the very
attenuated nature of both the peaks, and to consider that the
bankfull discharge at the downstream gauge is 30 $m^3 s^{-1}$.

Figure 9.10 illustrates a first pass at simulating this event,
using parameter values estimated in the field. Figure 9.10 shows
that a simulated stage hydrograph barely attenuates either of the
flood waves, and consequently predicted stage elevations are too
high. If this stage hydrograph is converted to a discharge
hydrograph, the discrepancy between the predicted and observed is
exacerbated due to the power function rating relation.

There are two important issues raised by this hydrograph. The
first and more significant for this scale of application is that the
"smoothing" or loss of topographic resolution in the mesh may have
created a system that is too efficient. Storage areas on the
floodplain and meander bends have both been lost to meet the
stability criteria of the model. The second issue is that of field
data accuracy, the error band associated with field data, and its
significance for RMA-2V simulation. RMA-2 requires a downstream
boundary condition, usually a rating relationship. The reliability
of out-of-bank rating relations, however, is relatively small. If
the observed outflow stage hydrograph is considered, for example, is
the attenuation of the inflow hydrograph a product of the topography
of the reach, or is there a problem with the catchment of floodplain
flows by the downstream stage recorder. A degree of attenuation can
be introduced into the RMA-2V prediction by increasing the Manning's
n roughness coefficients. Figure 9.10 shows the results of
increasing the floodplain roughness parameter and the impact of
increasing all the roughness value for all element types. Although
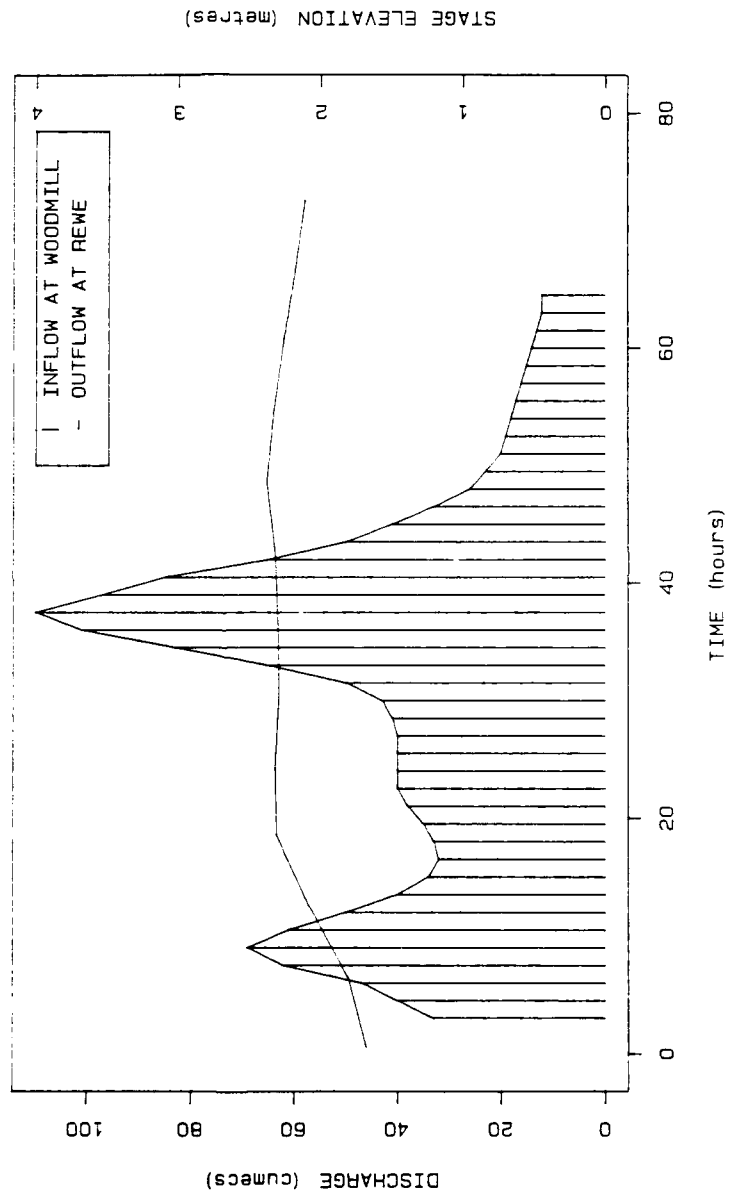
Figure 9.9
Comparison of observed inflow and outflow hydrographs
at Rewe for a 1 in 1 + 1 in 10 year event
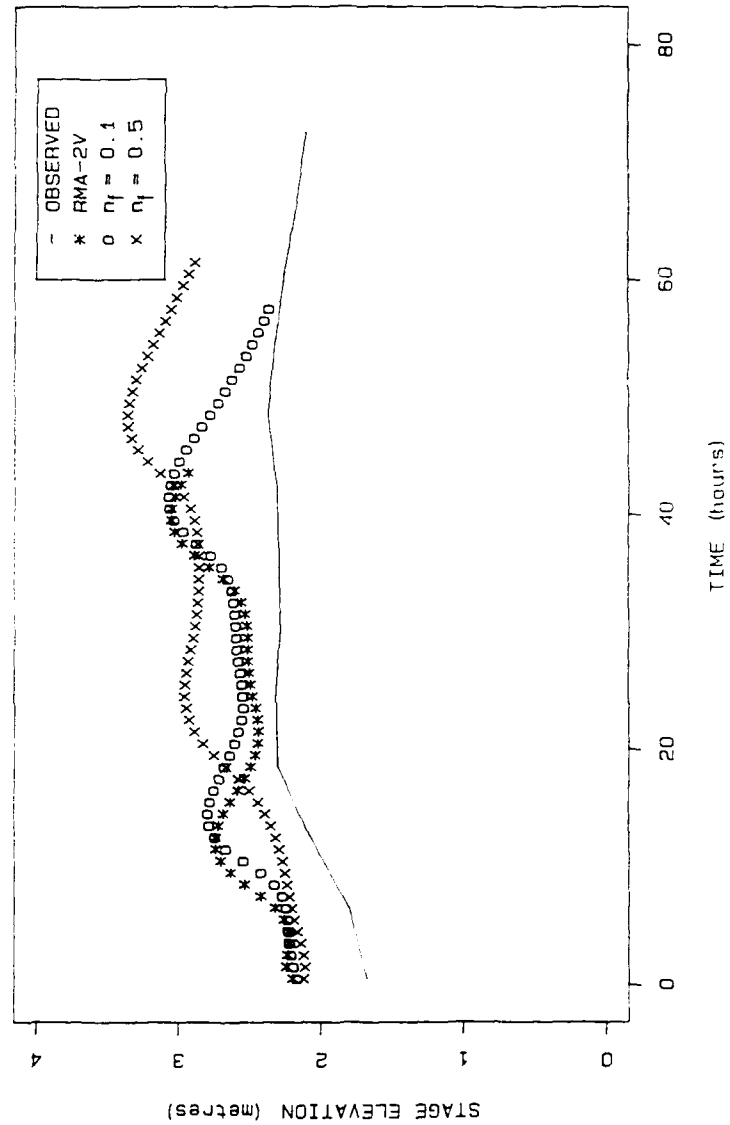
Figure 9.10
Comparison of RMA-2V predictions with varying floodplain roughnesses
at Rewe for a 1 in 1 + 1 in 10 year event

Chapter 9

the attenuation of the two flood waves is certainly increased, the
discrepancy in stage predictions is not improved. This suggests
that there may be a problem with both the topographic resolution and
field data accuracy.

9.4   Implications for Ungauged Flood Forecasting

The initial results from the application of RMA-2V to the
River Fulda reach highlight the issue of topographic representation.
Generation of stable initial conditions for the reach necessitated
a "smoothing" of the mesh and hence a loss of topographic
resolution. During dynamic simulation, however, a lack of field
data accuracy was identified with problems with the downstream
boundary conditions.

From tne ungauged perspective, the River Culm application has
shown that it is relatively easy to provide enough topographic
resolution to create stable initial conditions in a complex
floodplain environment at this large scale. The important issue is,
however, if the smoothing of the mesh generates a loss of
attenuation in the system, can this be overcome by parameter
calibration without contravening the objective of improved spatial
and temporal inundation prediction. This is an issue which requires
further investigation.

9.5   Conclusions

Application of RMA-2V to the River Culm has explored the issue
of topographic resolution and a series of guidelines for generation
at this scale have been generated. Although the initial objective
was to investigate the accuracy of the spatial and temporal
prediction of inundation, more fundamental issues have been raised.

Several important limitations of the topographic capabilities
of RMA-2V have been identified but, clearly, further work is
required.

Chapter 10

Conclusions

The aim of this report has been to investigate the issues
affecting flood forecasting in ungauged catchments. An ungauged
catchment has been defined as one for which the only available data
set consists of precipitation data, a topographic map, and a soil
classificatory map. In particular, no historical streamflow data
are assumed to be available.

The application of a model to an ungauged catchment is often
seen as the ultimate test of the ability of the model to accurately
predict the behaviour of that catchment. Despite this challenge,
flood forecasting in ungauged catchments has remained a relatively
uninvestigated part of hydrological modelling.

It is proposed in this report that the lack of interest in
ungauged flood forecasting is a side-effect of the general
philosophy that has been driving hydrological modelling for the past
twenty-five years. This philosophy is based upon the assumption
that the predictive performance of hydrological models will improve
when the physical representation of the processes in the catchment
are improved. Developments in models have therefore been conceptual
with increasing spatial or temporal resolution being incorporated in
the modelling of the processes. The SHE model (see, for example,
Bathurst, 1986), epitomises this philosophy as it incorporates the
most highly developed distributed physically-based routines
presently available.

The assumption that increasing the physical representation of
the processes in the catchment will increase the predictive
performance of the model, is not borne out in the studies comparing
different model types undertaken, for example, by Loague and Freeze

Chapter 10

(1985). These comparative studies have shown that even when the
state-of-the-art models are supplied with the extensive data sets
and the experienced operators they require, their predictive
accuracy is not significantly better than their simpler counter-
parts. Further, in the ungauged application these state-of-the-art
models are inappropriate.

It is accepted that this physically-based conceptual
philosophy must continue if our understanding of the catchment
processes is to improve, and that its role as a research tool is
vitally important. However, it is proposed that until the
predictive performance of state-of-the-art models can be improved,
perhaps with the incorporation of further physical representation of
the processes, then another approach to catchment modelling is
required.

This report shows there is a need to develop models specifically
from the perspective of the potential application and operator. The
application of hydrological models to ungauged catchments provides
an ideal opportunity to investigate modelling from this perspective.
In addition, the review of models suitable for application to
ungauged catchments has shown that many have been evaluated at a
late stage in the model devlopment programme and consequently are
conceptually unsuitable for ungauged applications. This report,
therefore, has developed a model specifically for ungauged catchment
applications and has attempted to consider the needs of the
potential operator of the model during its development.

This report has identified four issues that are considered to
be important to forecasting in ungauged catchments and may be of
relevance to hydrological modelling in other areas. These issues
are:

Chapter 10

1)   the impact of model complexity on model performance

2)   how composite modelling structures could develop model
      diversity whilst retaining model portability

3)   how techniques utilised in hydraulics could be applied to
      improve hydrologic modelling

4)   the development of validation strategies that are
      thorough and flexible

These four issues have been investigated through the
selection, development and validation of an ungauged flood
forecasting model, namely MILHY3. MILHY3 has been developed
specifically for application to ungauged catchments and in addition
it has been developed using relatively simple techniques, making it
easy to apply for the inexperienced operator. The objective of this
report has been to investigate the four issues identified above
through the development and validation of MILHY3.

The rest of this chapter is divided into two sections. The
first summarises the results of the development of MILHY3 and sets
out the specifications for the composite structure proposed. In the
second section, the potential for the further development of MILHY3
is identified and the implications of the results for the other
areas of hydrology are discussed.

10.1 Specifications of MILHY3

The objective of this report has been to identify and develop
and validate a model suitable for application to ungauged catchments
based on a composite modelling structure. A review of MILHY3 showed
that the model has a flexible structure and has been developed
specifically for application to ungauged catchments.

Chapter 10

10.1.1 Model Complexity versus Model Performance

This report concludes that there is a complex relationship
between model complexity and model performance.

The introduction of a composite modelling structure consisting
of process modules at varying levels of resolution and complexity
has allowed the exploration of this relationship. Results from the
comparison of the predictive performance of the infiltration
algorithm and the curve number routine in large catchments, a scale
previously unexplored, are reported in Chapter 7. The results of
the investigation showed that the predictive performance of the
infiltration algorithm was superior to the performance of the
simpler Curve Number routine. However, in the larger River Fulda
catchment, the analysis showed that this improvement was only
significant if the precipitation event had a complex temporal
distribution. In Storm 1, the 1 in 10 year event, the precipitation
pattern was simple with the majority of the rainfall falling at the
beginning of the event. The improvement in the predictive accuracy
of the infiltration algorithm over the Curve Number routine was
therefore small, and not considered to be significant. In contrast,
the precipitation pattern of Storm 3, the 1 in 1.5 year event, was
complex with rainfall falling in two peaks, with a period of very
low intensity rainfall between the two peaks. The improvement in
the predicted hydrograph achieved by the infiltration algorithm was
still evident and significant at the outflow of the reach at the Bad
Hersfeld station.

The time taken to initiate and simulate a storm event using
the infiltration algorithm for a catchment the size of the River
Fulda basin, which is approximately 2500 km^2, is significantly
greater than the time taken by the Curve Number. In the case of
Storm 1, for example, the infiltration algorithm version of MILHY3
took approximately nine hours of CPU, whilst the curve number
routine took only about one hour of CPU on the SUN workstation.

Chapter 10

*The results of the sensitivity analysis suggest that for large
catchments the infiltration algorithm need only be invoked for
complex storm events.*

These results show that there is not a simple relationship
between model complexity and model performance. The predictive
performance of the infiltration algorithm is better than the
performance of the simpler Curve Number routine but this difference
in performance is only significant in large catchments for storm
events with a complex rainfall distribution. Given the extra time
taken to set up the data set required by the infiltration algorithm
and the larger computational demands of the algorithm, the operator
of the model must consider the size of the subcatchments being
utilised, the complexity of the storm event and the accuracy
required in the outflow hydrograph.

10.1.2 The Role of a Composite Modelling Structure

*This report concludes that the utilization of a composite
modelling structure allows model diversity to be developed whilst
model portability is maintained.*

It is proposed that a composite modelling structure could
potentially close the split between model developers and operators
by providing a flexible model structure into which new components or
modules could be slotted. The perspective of the composite model
would be biased towards the model operators such that a series of
guidelines could be developed to help the operator select the most
appropriate module combination for a particular application. It is
envisaged that such a composite structure would incorporate modules
simulating the same processes at different levels of spatial or
temporal resolution or complexity.

The results of this report have shown that a composite
modelling structure is a viable option. The results summarised

Chapter 10

above of the relative performance of the two runoff generation
routines has shown that simpler modules have an important role and
should not be discarded when more complex techniques become
available. The results of the evaluation of the new momentum
exchange and multiple routing routines, reported in Chapter 7, also
illustrate that techniques drawn from hydraulics can be incorporated
in a hydrologic composite structure.

The flexibility of a composite structure has been illustrated
in the evaluation programme reported in Chapter 7. The model has
also been developed in such a way as to maintain the portability of
the scheme. The new modules required no additional data and the
extra computational requirements are minimal in comparison with the
computational requirements of the infiltration algorithm. The
potential for the further development of the composite structure and
the implications this would make on the portability of the scheme
are discussed in Section 10.2.

10.1.3 Hydraulic versus Hydrologic Modelling

This report concludes that the concepts and techniques
developed in hydraulics are appropriate for inclusion in hydrologic
catchment models, and that the traditional distinction between
hydraulics and hydrology, based on scale, is no longer valid.

The need to investigate methods of incorporating the cross-
sectional and plan geometrical effects of two-stage flows has been
identified. Review of current modelling capabilities has shown that
this is an area that has not previously been incorporated in
hydrological catchment models. Investigations into the behaviour of
two-stage flows have almost exclusively been carried out in a
hydraulic approach. This report has aimed to investigate these
hydraulic approaches and see if they are appropriate for
applications to hydrologic models.

Chapter 10

The behaviour of flow in two-stage flow was investigated and
the review of the literature highlighted the importance of the
effects of momentum exchange between the main channel and floodplain
flow segments. The momentum exchange was shown to have significant
effects on the velocity of flow in the two flow components and to
affect the conveyance capacity of the whole cross-section. The
implications of this exchange on the prediction of discharge from
the reach were, however, not clear. In addition, the relative
importance of momentum exchange in comparison with the effects of
boundary friction and the downstream effects of two-stage flow were
not assessed. The results of the sensitivity analysis of the Ervine
and Ellis scheme isolated the effects of boundary friction and the
importance of the difference between the length in the downstream
routing pathways of the floodplain and more sinuous main channel
flows.

The development of a momentum exchange module was investigated
in Chapter 4, by firstly exploring the process of momentum exchange.
Flume investigations showed that the most useful concept is to
consider the exchange of momentum to be taking place across an
interface between the main channel and floodplain. The extent of
the exchange can then be computed by calculating the apparent shear
stresses that would occur if the interface were a real boundary.
This concept of an interface and the use of apparent shear stresses
is widely used in hydraulic analysis to compare computed and
observed discharge and velocity values, but this approach has not
been incorporated into any hydrological models.

In hydraulic analyses a measured shear stress distribution is
used to estimate the position of the interface and the stresses on
the interface. In a hydrologic approach this is not possible and
some estimate must be made of both the position of the interface and
the stresses upon it. Analysis of these assumptions in comparison
with flume studies has been attempted by many authors, for example
Wormleaton et al. (1982), and Knight and Demetriou (1983), but no

Chapter 10

one clear technique has been identified. In addition, the flume
investigations have concentrated on river reaches where the
floodplain width is relatively small and the boundary roughnesses of
the floodplain are small (see Table 4.1).

In order to investigate a variety of floodplain widths and
boundary roughnesses, four interface position and stress
combinations were incorporated into the momentum exchange module.
These four techniques, tabulated in Table 4.2, include vertical and
diagonal interfaces with an apparent shear stress ratio of 1 and 0.
The analysis of the effects of the four techniques on the prediction
of the rating curve showed that the techniques which introduced the
most exchange reduced the capacity of the cross-section to the
greatest degree. The longer the interface or higher the apparent
shear stress ratio, the greater the amount of momentum exchange
incorporated and hence the more turbulent friction incorporated.

The development and incorporation of a multiple routing module
was investigated in Chapter 5. This module incorporated the effects
of the short-circuiting of floodplain flows around the sinuous main
channel flows. Analysis of the alternative methods utilised shows
that the only techniques that had been previously used were either
(1) the use of empirical adjustments, or (2) the replacement of the
scheme with a hydraulically-based St. Venant scheme developed by
Fread (1976).

The results of the inclusion of multiple routing reaches
showed that the impact of the routine was greatest when the depth of
water on the floodplain was small, that is when the depth ratio
(floodplain depth : main channel depth) was less than 0.4 but more
than 0.1. At this range of inundation depths, the multiple routing
routine significantly reduces the error in the prediction of the
peak discharge. In comparison with MILHY2, the error in the
prediction of peak discharge is halved. The results also showed
that reducing the length of the floodplain routing length to mimic

Chapter 10

the effects of the "short-circuiting", was only significant when the
floodplain length was approximately 30% shorter than the main
channel length. In these circumstances, the attenuation of the
floodwave is decreased and a higher peak discharge is predicted.

The momentum exchange and multiple routing routines have been
successful, therefore, in incorporating their respective effects of
turbulent exchange and the short-circuiting of flow. Both modules
have been shown to improve the predictive accuracy of the model and
in addition, by removing the effects of the two processes from the
selection of the Manning's n coefficient, have made the selection of
the most appropriate value a simpler task.

The success of these two modules in incorporating the effects
of two different processes has shown the portability of the concepts
of traditionally hydraulic approaches to hydrologic modelling. The
limitations posed by the ungauged nature of the catchment modelling
have been shown not to restrict this portability.

Application of hydraulic techniques to a hydrologic model are
considered in Chapters 8 and 9, where the inclusion of RMA-2V as a
module of MILHY3 is considered. RMA-2V has been shown to be capable
of application not only to the scale of reach required for a
hydrologic approach but also to meet the limitation of an ungauged
hydrologic approach. The operational guidelines for application of
RMA-2V to such large scale reaches are summarized in Table 9.3.

The analysis of the relative performance of RMA-2V as a module
in a catchment model is reported in section 8.5. This section
concludes that the impact on the accuracy of the outflow hydrograph
of the inclusion of RMA-2V in the lower reaches of the River Fulda
is less than the impact of the inclusion of the infiltration
algorithm. The inclusion of RMA-2V is therefore only recommended if
more detailed information is required on the extent or behaviour of
the floodplain inundation.

Chapter 10

10.1.4 Model Evaluation and Validation Strategies

This report proposes that optimization techniques provide a viable alternative to traditional factor perturbation analysis as part of a model validation strategy. It is also proposed that state-of-the-art process models could be used to provide "ground-truth" conditions for the evaluation of simpler models, and this evaluation technique is potentially most useful in the prediction of extreme events.

The introduction of a composite structure generates variability in the structure of the model in addition to the existing parameter variability within the process modules. A sensitivity analysis must assess, therefore, not only the impact of changes in the module's parameters but also the impact of different module combinations, and the interaction between these two sorts of variability. Given the large number of variables involved in the composite structure, alternative methods of undertaking a sensitivity analysis were examined. The potential for using optimization techniques as part of a sensitivity analysis was investigated. Optimization techniques have not been utilized in this way before and consequently the application of the technique was rather exploratory. The results from the investigation were promising, provided that the interpretive skills necessary to understand the results files can be established. The potential for the further development of the optimization technique is discussed in section 10.2.

The aim of the optimization technique, in addition to investigating the utility of the technique, was to investigate the sensitivity of the predicted hydrograph to variation in five key parameters: Manning's n coefficient for the floodplain and the main channel, the longitudinal slope for the floodplain and main channel, and the floodplain routing reach length. The results showed that when the longitudinal slopes are greater than 1×10^{-2}, then the

Chapter 10

slope is the dominant parameter controlling the shape of the
simulated hydrograph. When the slopes are less steep then the
Manning's n coefficient is the dominant paremeter.

The optimization results also showed that when both the
momentum exchange and multiple routing routines are utilised, then
the variation in the predicted peak discharge is as great as
variation generated by variation in the Manning's n coefficient.
This suggests that the incorporation of the momentum exchange and
multiple routing routines is significant in comparison with the
effect of boundary friction. This result, therefore, supports the
inclusion of the momentum exchange and multiple routing routines in
the MILHY3 model.

Analysis of the momentum exchange and multiple routing
routines showed that the relationship between them is an extremely
complex one which depends on the exact nature of the storm event.
Despite the effects of the momentum exchange routine on the
predicted rating curve, the results reported in Chapter 7 show that
the routine has no impact on the predicted hydrograph when applied
without the multiple routing routine. When the momentum exchange
and multiple routing routine were applied, they had an impact which
was visible on the predicted hydrograph and this impact was
different to the impact of the application of just the multiple
routing routine. The effect of the momentum exchange routine is to
make changes in the rating curve of a reach. These changes only
make significant differences to the hydrograph if the multiple
routing routine is also applied.

The impact of the multiple routing routing, as reported in
Chapter 5, is dependent on the proportion of the total flow that is
contained on the floodplain. If the floodplain inundation depth is
very small, then the travel time of the floodplain flow will be
large, for example a hundred hours. More significant in low
floodplain inundation depths is the travel time of the main channel

Chapter 10

which is reduced in comparison with the composite travel time where
the average time for the floodplain and main channel is used. This
means that in low floodplain inundation conditions the attenuation
of the floodwave is reduced in comparison to the composite approach.
Where floodplain inundation depths are larger and floodplain flows
contribute a significant proportion of the total discharge, a
proportion of around 15%, then the attenuation of the floodwave is
increased as there are effectively two floodwaves, one from the main
channel and one from the floodplain. When the proportion of flow in
the floodplain exceeds 15%, then the joint application of the
momentum exchange and multiple routing routines improves the
accuracy of the predicted hydrograph. It is suggested, therefore,
that the potential operator of the MILHY3 scheme uses both the
momentum exchange and multiple routing routines for out-of-bank
events.

A third part of the model validation and evaluation programme,
is reported in Chapter 8, and investigates the feasibility of using
RMA-2V to extend the record of "observed" extreme events, in order
to further validate the performance of MILHY3. The application of
RMA-2V to the River Fulda catchment is the first application of a
hydrodynamic finite-element model to this scale of problem.

Previous finite-element applications to two-stage river
reaches have been limited to scales of around 2km. This is also the
first application attempted with a limited data set. Information in
this instance is limited to a topographic map and upstream and
downstream cross-sections and rating curves; in particular, no
intermediate reach data or velocity vector data are available. This
is also one of the first applications of version 4 of RMA-2V, which
incorporates the new marsh elements with pseudo-porosity effect.
The marsh elements allow elements to enter and leave the computation
smoothly and improve the stability and accuracy of the predicted
extent of inundation.

Chapter 10

The results of the application of RMA-2V to the River Fulda showed that the model could be applied to river reaches of a scale around 20 km, and that there seemed to be no inherent conceptual problems in such an application.

In Chapter 9 this theme is pursued from a more practical viewpoint with application of RMA-2V to the River Culm. The more exhaustive data set available for the River Culm and the more complex terrain environment of the reach, enabled a series of guidelines and limitations to be established for applications of RMA-2V to this type and scale of problem. Importantly, the River Culm highlighted the issue of the effect of topographic resolution on computational stability.

The results from the River Fulda and River Culm applications were promising in that reasonable predictions of both the discharge hydrograph and inundation distributions can be made with very limited topographic data. The results showed that RMA-2V can be used to extend "observed" data sets, and that incorporation of RMA-2V into a hydrological catchment model suite is viable and worthy of further investigation.

The guidelines generated for the application of MILHY3 have been summarized in Table 10.1. These guidelines represent the results of work undertaken in this report and, therefore, are appropriate for applications to large catchments, that is 1000 - 2500 km^2 (385 - 1000 sq.mi.).

10.2 Further Development of MILHY3 and Future Research Needs

This section considers the further development of MILHY3 and the composite modelling structure. The implications of the specifications already achieved, and the potential implications of further developments on other areas of hydrological modelling, will

Chapter 10

Table 10.1

Guidelines for the Application of MILHY3

to Large Catchments

Catchment Subdivision

Subcatchments size $\leqslant$ 60 km^2

Rainfall

Frontal type storms - consider use of radar data for
subcatchment $\geqslant$ 145 km^2.

For convective storms - consider use of radar data.

Soils Classification

Concentrate on the accurate representation of soils groups
with low hydraulic conductivities.

Runoff Generation

For complex precipitation patterns use the infiltration algorithm,
for simpler rainfall distributions consider advantages of
curve number routine.

Channel Geometry

For out-of-bank events - use both the momentum exchange and
multiple routing routines.

Chapter 10

be briefly discussed.

Figure 10.2 shows the components of MILHY3 that have developed and validated in this paper. Throughout this report, alternatives have been discarded for a variety of reasons. Certain processes, such as the secondary current system, were not included in the final specifications of MILHY3 because other processes were considered to be of more significance. Alternative methods of modelling processes were excluded on the grounds that they were difficult to incorporate into the MILHY scheme. This was true for the modelling of multiple routing routines, where the simplest approach was incorporated so that the relative importance of the process could be considered.

If the out-of-bank flood forecasting of MILHY3 is to be improved, then the results of this report suggest several steps that could be taken to achieve this. These steps include:

1)   The upgrading of the handling of the multiple routing routine. The results of this report have shown that this routine has a significant effect on improving the predictive accuracy of the outflow hydrograph. Several alternatives have been suggested in Chapter 5.

2)   Linking of RMA-2V as a module in the MILHY3 model suite. The results of applications of RMA-2V reported in Chapters 8 and 9, suggest that RMA-2V can provide more accurate discharge and inundation predictions in ungauged environments. The operational guidelines developed suggest this may be achieved in a limited time frame.

If the performance of MILHY3 is to improve for all types of applications, both in-bank and out-of-bank, then this report has identified several other steps that could be taken. These include:

Chapter 10

1)   An investigation into the relationshipo between the resolution
      of subcatchment area required for the accurate prediction of
      the time to peak discharge. Potentially, th's may require the
      introduction of the modelling of the overla..' routing of the
      runoff to the channel.

2)   Investigation of the packages available to incorporate the
      relationship between the resolution of rainfall required for
      particular storm characteristics and subcatchment sizes.

3)   Assessment of the importance of a secondary current module for
      sinuous channels for in-bank events.

4)   More accurate representation of the effects of boundary
      friction, to include the stage/roughness relationships and an
      assessment of the spatial resolution of boundary roughness
      classification required.

      The validation strategy developed in this report has proposed
the utilization of optimization techniques and the application of
RMA-2V for the extension of the record of "observed" events. New
validation techniques need to be considered if the composite
modelling structure is to be thoroughly evaluated and the gap
between model development and operation to be bridged.

      The optimization techniques could be used by any model that
allows the comparison of a simulated and observed hydrograph or
similar output. The volume of output from the application of the
optimization technique in this report and the interpretive skills
required, however, suggest that the optimization technique would not
be appropriate if a larger number of parameters needed to be
assessed. Optimization techniques would not be suitable, therefore,
for assessing the sensitivity of physically-based distributed models
which have a very large number of parameters. The optimization
technique was used in this report to assess the sensitivity of the

Chapter 10

outflow hydrograph to variability in five parameters. Given the
volume of output from this analysis, an upper limit of the testing
of ten parameters sensitivities would seem an appropriate guideline.
For simple models, or as in this case as part of an analysis
incorporating many different approaches, then optimization is a
viable and promising alternative.

The application of RMA-2V to the River Fulda and River Culm
was also a new approach to the validation of MILHY3. The aim of the
approach was to utilise the RMA-2V to extend the record of storm
events, providing a ground-truth against which MILHY3 could be
validated. The need to extend the record of extreme events stems
from the inherent difficulties of collecting data for events which
are either impossible to measure or occur too infrequently.

The results of the application of RMA-2V are promising enough
for it to be suggested that this approach could be utilised in other
processes of hydrology where extreme events are simulated. The
approach relies on the availability of a state-of-the-art model that
has been validated and has a good predictivve performance. This
precludes, therefore, catchment models which are still basically
research tools. The approach is, therefore, most suitable for the
validation of certain process modules within catchment models for
which state-of-the-art models exist. This could include, for
example, the validation of catchment stability models against
engineering stability models, or the validation of catchment
throughflow modules on detailed hillslope models.

The potential of a composite modelling structure for the
bridging of the gap between model developers and operators has been
stressed for ungauged flood forecasting. The utility of
incorporating concepts and techniques from the field of hydraulics
has also been highlighted. The potential flexibility of the
composite modelling structure, however, does not stop with
hydraulics. Other engineering disciplines such as soil mechanics

Chapter 10

for the modelling of river bank stability could also be potentially
incorporated.

This report has shown that a composite modelling structure can
support a multi-disciplinary approach. In addition, the application
of concepts and techniques from the field of hydraulics has shown
that the incorporation of engineering techniques is feasible and
appropriate. With the application of an expert system, a composite
modelling structure encompassing the disciplines of hydrology and
engineering may help to bridge the gap between model developers and
model operators.

Literature Cited

Anderson, M.G. (1982). Assessment and implementation of drainage basin runoff models. U.S. Army European Research Office, Final Technical Report, DAJA37-82-C-0092, 74pp.

Anderson, M.G. and Howes, S. (1984). Streamflow modelling. U.S. Army European Research Office, Final Technical Report, DAJA37-81-C-0221, 130pp.

Anderson, M.G. and Howes, S. (1986). Hydrological modelling in ungauged watersheds. U.S. Army European Research Office, Final Technical Report, DAJA45-83-C-0029, 147pp.

Anderson, M.G. and Sambles, K.M. (1988). A review of the bases of geomorphological modelling. In Anderson, M.G. (ed.) Modelling Geomorphological Systems, John Wiley and Sons, 1-32.

Armstrong, A.C., Rycroft, D.W. and Welch, D.J. (1980). Modelling watertable responses to climatic inputs - its use in evaluating drainage designs in Britain. Journal of Agricultural Engineering Research, 25, 311-323.

Asano, J., Hashimoto, H. and Fujita, K. (1985). Characteristics of variation of Manning's roughness coefficient in a compound cross-section. Proceedings of the Twenty-First Congress of the International Association for Hydraulic Research, 6, 30-34.

Aston, A.R., Sandilands, D. and Dunin, F.X. (1980). WATSIM - a distributed hydrologic model. Commonwealth Scientific and Industrial Research Organisation, Australian Division Plant Industry Technical Paper, 35.

Banks, D.J. and Falconer, R.H. (1989). The White Cart Water alleviation study using hydrodynamic mathematical modelling techniques. Journal of the Institution of Water and Environmental Management, 3, 375-386.

Bathurst, J.C. (1986). Physically-based distributed modelling of an upland catchment using the Systeme Hydrologique Europeen. Journal of Hydrology, 87, 79-102.

Beckett, P.H.T. and Webster, R. (1971). Soil variability: a review. Soil and Fertilizers, 34, 1-15.

Beven, K.J. and Hornberger, G.M. (1981). The effects of spatial variability in precipitation on streamflow. State Water Survey Division Technical Report 6.

Bhomick, N.G. and Demissie, M. (1982). Carrying capacity of flood
        plains. Journal of the Hydraulic Division, Proceedings of
        the American Society Civil Engineers, 108(HY3), 443-452.

Brakensiek, D.L. and Rawls, W.J. (1983). Use of infiltration
        procedures estimating runoff. Paper presented to United
        States Department of Agriculture Soil Conservation Service,
        National Engineering Workshop, Tempe, Arizona, USA, 23pp.

Cauchy, A.L. (1847). Methode generale pour la resolution des
        systemes d'equations simultaneous. C.R. Read. Sci., 25,
        536-538.

Chang, H.H. (1983). Energy expenditure in curved open channels.
        Journal of Hydraulic Engineering, Proceedings of the
        American Society of Civil Engineers, 109, 1012-1022.

Chow, Ven Te. (1959). Open Channel Hydraulics, McGraw-Hill,
        New York, USA, 680pp.

Cluckie, I.D., Ede, P.F., Owens, M.D., Bailey, A.C. and Collier,
        C.G. (1982). Some hydrological aspects of weather radar
        research in the United Kingdom. Hydrological Sciences,
        32(3), 329-346.

Collinge, V.K. and Kirby, C. (eds.) (1987). Weather Radar and Flood
        Forecasting, John Wiley and Sons, 296pp.

Corrandni, C. and Singh, V.P. (1985). Effect of spatial variability
        of effective rainfall on direct runoff by a geomorphic
        approach. Journal of Hydrology, 81, 27-43.

Crory, P.M. and Elksawy, E.M. (1980). An experiment at
        investigation into the interaction between a river's deep
        section and its floodplain. Symposium on River Engineering
        and its Interaction with Hydrological and Hydraulics
        Research, International Association for Hydraulic Research.

Cunge, J.A., Holly, F.M. and Verwey, A. (1980). Practical aspects
        of computational hydraulics. Pitmans.

Dawdy, D.R. and Bergman, J.M. (1969). Effects of precipitation
        variability of streamflow simulation. Wateer Resources
        Research, 5, 958-966.

Deuller, J.W., Toebes, G.H. and Udeozo, B.C. (1967). Uniform flow
        in idealized channel geometries. Proceedings of the Twelfth
        International Congress of the International Association for
        Hydraulic Research, Fort Collins, USA.

Einstein, H.A. and Shen, H.W. (1964). A study of the meandering in
        straight alluvial channels. Journal of Geophysical
        Research, 69, 5239-5247.

Engdahl, T.L. and Collins, J.G. (1985). Sensing the spatial character of storms for hydrologic application. *Proceedings of the Nineteenth International Symposium of Remote Sensing of Environment*, Michigan, USA

Ervine, D.A. and Ellis, J. (1987). Experimental and computational aspects of overbank floodplain flow. *Transactions of the Royal Society of Edinburgh, Earth Sciences, 78,* 315-325.

Fread, D.L. (1976). Flood routing in meandering rivers with flood plains. *Symposium in Inland Waterways for Navigation Flood Control and Water Diversions, Proceedings of the American Society of Civil Engineers,* 16-35.

Fread, D.L. (1985). Flood routing. In Anderson, M.G. and Burt, T.P. (eds.), *Hydrological Forecasting*, John Wiley and Sons, 437-504.

Ghosh, S.N. and Jena, S.B. (1971). Boundary shear distribution in open channel compound. *Proceedings of the Institute of Civil Engineers, 49,* 417-430.

HEC-1 (1981). HEC-1, flood hydrograph package users manual. *U.S. Army Corps of Engineers, Hydrologic Engineering Center,* Davis, California, USA, 192pp.

Hermann, C.F. (1967). Validation problems in games and simulations with special reference to models of international politics. *Behavioural Science, 12,* 216-231.

Herrling, B. (1978). Computation of shallow water waves with hybrid finite elements. *Advances in Water Resources, 1,* 313-320.

Hey, R.D. and Thorne, C.R. (1975). Secondary flows in river channels. *Area, 7,* 191-195.

Holden, A.P. and James, C.S. (1989). Boundary shear distribution on flood plains. *Journal of Hydraulic Research, International Association for Hydraulic Research, 27,* 75-89.

Holtz, P. and Nitsche, G. (1980). Tidal wave analysis for estuaries with inter-tidal flats. *Proceedings of the Third International Conference on Finite Elements for Water Resources,* University of Mississippi, Mississippi, USA, 5113-5126.

Hornberger, G.M. and Spear, R.C. (1981). An approach to the preliminary analysis of environmental systems. *Journal of Environmental Management, 12,* 7-18.

Howes, S. (1986). *A mathematical hydrological model for the ungauged catchment.* PhD Thesis, University of Bristol, unpublished, 404pp.

Howes, S. and Anderson, M.G. (1988). Computer simulation in geomorphology. In Anderson, M.G. (ed.), Modelling Geomorphological Systems, John Wiley and Sons, 421-440.

Huff, F.A. (1967). Time distribution of rainfall in heavy storms. Water Resources Research, 3, 1007-1019.

Huff, F.A. (1968). Spatial distribution of heavy storm rainfalls in Illinois. Water Resources Research, 4, 47-54.

Ibbit, R.P. and O'Donnell, B. (1971). Fitting methods for conceptual catchment models. Journal of Hydraulic Engineering, Proceedings of the American Society of Civil Engineers, 97, 1331-1342.

James, W.P. and Stinson, D. (1981). Student workbook on streamflow forecasting: Military Hydrology Project. U.S. Army Engineer, Waterways Experiment Station, Mississippi, USA, 215pp.

Jones, D.A. (1982). Various approaches to the sensitivity analysis of SHE: a discussion. European Hydrologic System report 20, Institute of Hydrology, Wallingford, 10pp.

Keller, E.A. amd Melhorn, W. (1973). Bedforms and fluvial processes in alluvial stream channels: selected observations. In Morisawa, M. (ed.) Fluvial Geomorphology, SUNY Binghampton, Publications in Geomorphology, 253-83.

King, I.P. and Norton, W.R. (1978). Recent applications of RMA's finite element model for two-dimensional hydrodynamics and water quality. Proceedings of the Second International Conference on Finite Elements for Water Resources, Imperial College, London, 2, 81-99.

King, I.P. and Roig, L.C. (1988). Two-dimensional finite element models for flood plains and tidal flats. In Niki, K. and Kawahara, M. (eds.) Computation Methods in Flow Analysis, Proceedings of the International Conference on Computational Methods in Flow Analysis, Okayama, 711-718.

Klassen, G.J. and Zwaard, J.J. (1974). Roughness coefficients of vegetated flood plains. Journal of Hydraulic Research, International Association for Hydraulic Research, 12(1), 43-63.

Knight, D.W. (1989). Hydraulics of flood channels. In Beven, K. and Carling, P. (eds.). Floods: Hydrological, Sedimentological and Geomorphological Implications, John Wiley and Sons, 83-105.

Knight, D.W. and Demetriou, J.D. (1983). Flood plain and main channel flow interaction. Journal of the Hydraulic Division, Proceedings of the American Society of Civil Engineers, 108(HY8), 1073-1092.

Knight, D.W. Demetriou, J.D. amd Hamed, M.C. (1983). Hydraulic analysis of channels with floodplains. International Conference on the Hydraulic Aspects of Floods and Flood Control, British Hydromechanics Research Association, Paper E1, 129-144.

Knight, D.W., Demetriou, J.D. and Hamed, M.E. (1984). Stage discharge relationships for compound channels. In Smith, K.V.H. (ed.), Proceedings of the First International Conference on Hydraulic Design in Water Resources Engineering, Channels and Channel Control Structures, University of Southampton, Southampton.

Knight, D.W. and Hamed, M.E. (1984). Boundary shear in symmetrical compound channels. Journal of Hydraulic Engineering, Proceedings of the American Society of Civil Engineers, 110, 1412-1430.

Knight, D.W. and Lai, C.J. (1985). Turbulent flow in compound channels and ducts. International Symposium on Refined Flow Modelling and Turbulence Measurements, Iowa, USA.

Lesleighter, E.J. (1983). Flood plain flow using a two-dimensional numerical simulation. International Conferencec on the Hydraulic Aspects of Floods and Flood Control, British Hydromechanics Research Association, Paper H1, 207-215.

Loague, K.M. and Freeze, R.A. (1985). A comparison of rainfall-runoff modelling techniques on small upland catchments. Water Resources Research, 21, 229-248.

Lotter, G.K. (1933). Considerations of hydraulic design of channels with different roughness walls. Transactions of the Union of Scientific Research, Institute for Hydraulic Engineering, Leningrad, 9, 238-241.

McAnally, W.H. Jr., Letter, J.V., Stewart, J.P., Thomas, W.A. and Brogdon, N.J. (1984a). Columbia River Hybrid Modeling System. Journal of Hydraulic Engineering, Proceedings of the Amercian Society of Civil Engineers, 110, 300-311

McAnally, W.H. Jr., Letter, J.V., Stewart, J.P., Thomas, W.A. and Brogdon, N.J. (1984b). Application of Columbia Hybrid Modeling System. Journal of Hydraulic Engineering, Proceedings of theAmerican Society of Civil Engineers, 110, 627-642.

McCuen, R.H. (1973a). Role of sensitivity analysis in hydrologic modelling. Journal of Hydrology, 18, 37-53.

McCuen, R.H. (1973b). Component sensitivity: a tool for the analysis of complex water resource systems. Water Resources Research, 9, 243-246.

McCuen, R.H. (1976). The anatomy of the modeling process in mathematical models for environmental problems. In Brebbia, C.A., Proceedings of the International Conference, 401-412.

Militeev, A.N. and Sckolmikov, (1981). Numerical modelling of two-dimensional river flows in plan during flood. Proceedings of the International Conference on Numerical Modelling of River Channels and Overland Flow, International Association of Hydraulic Research.

Miller, D.R., Butler, G. and Bramall, L. (1976). Validation of ecological system model. Journal of Environmental Management, 4, 383-401.

Myers, W.R.C. (1978). Momentum transfer in a compound channel. Journal of Hydraulic Research, International Association for Hydraulic Research, 16, 139-150.

Myers, W.R.C. (1984). Frictional resistance in channels with floodplains. In Smith, K.V.H. (ed.), Proceedings of the First International Conference on Hydraulic Design in Water Resource Engineering: Channels and Channel Control Structures.

Myers, W.R.C. (1987). Velocity and discharge in compound channels. Journal of Hydraulic Engineering, Proceedings of the American Society of Civil Engineers, 113(6), 753-766.

Nguyen, V.L. and Berndsson, A. (1986). A simple and efficient conceptual catchment model allowing for spatial variation in rainfall. Journal of Hydrological Sciences, 31, 475-487.

Norton, W.R., King, I.P. and Orlob, G.T. (1973). A finite element model for Lower Granite reservoir, prepared for U.S. Army Engineer District, Walla Walla, Washington. Water Resources Engineers, Walnut Creek, California.

Noutsopoulos, G. and Hadjipanos, P. (1983). Discharge computations in compound channels. Proceedings of the Twentieth Congress of the International Association for Hydraulic Research, 173-180.

Pangburn, T. (1987). Documentation of cold regions modification to the MILHY model. US Army Cold Regions Research and Engineering Laboratory, N.H., USA.

Pasche, E. and Rouve, G. (1985). Overbank flow with vegetatively roughened flood plains. Journal of Hydraulic Engineering, Proceedings of the American Society of Civil Engineers, 111, 1262-1278.

Patel, V.C. (1965). Calibration of the Preston tube and limitations of its use in pressure gradients. Journal of Fluid Mechanics, 23(1), 185-207.

Perkins, F.E. (1970), Flood plain modelling. Water Resources Bulletin, 6(3), 375-383.

Petryk, S. and Bosmajian, G. (1975). Analysis of flow through vegetation. Journal of the Hydraulics Division, Proceedings of the American Society of Civil Engineers, 101(HY7), 871-884.

Pilgrim, D.H. and Doran, D.G. (1987). Choice of flood estimation method. In Pilgrim, D.H. (ed.), Australian Rainfall Runoff: A Guide to Flood Estimation, 1, 251-266.

Prinos, P., Townsend, R. and Tavoularis, S. (1985). Structure of turbulence in compound channel flows. Journal of Hydraulic Engineering, Proceedings of the American Society of Civil Engineers, 101(HY7), 871-884.

Radojkovic, V. (1976). Mathematical modelling of rivers with flood plains. Symposium on Inland Waterways for Navigation Flood Control and Water Diversions, Proceedings of the American Society of Civil Engineers, 1, 56-64.

Rajaratnam, N. and Ahmadi, R.M. (1979). Interaction between main channel and flood plain flows. Journal of the Hydraulics Division, Proceedings of the American Society of Civil Engineers, 105(HY5), 573-587.

Richards, K.S. (1982). Rivers: form and process in alluvial channels. Methuen, London, 358 pp.

Samuels, P.G. (1983a). Two dimensional modelling of flood flows using the finite element method. International Conference on the Hydraulic Aspects of Floods and Flood Control, British Hydromechanics Research Association, 229-240.

Samuels, P.G. (1983b). Computational modelling of flood flows in embanked rivers. International Conference on the Hydraulic Aspects of Floods and Flood Control, British Hydromechanics Research Association, 257-270.

Samuels, P.G. (1985). Modelling of river and floodplain flow using the finite element method. Hydraulics Research Laboratory Report Number SR61, 250pp.

Sargent, R.G. (1982). Verification and validation of simulation models. In Cellier, F.E. (ed.) Progress in Modelling and Simulation, Academic Press, London, 159-172.

Schmitz, G., Seus, G.J. and Czirwitzky, H.J. (1983). Simulating two dimensional flood flow. International Conference on the Hydraulic Aspects of Floods and Flood Control, British Hydromechanics Research Association, 195-206.

Sellin, R.H.J. (1964). A laboratory investigation into the interaction between flow in the channel of a river and that over its floodplain. La Houille Blanche, 7.

Smith, C.D. (1978). Effect of channel meanders of flood stage in valley. Journal of the Hydraulics Division, Proceedings of the American Society of Civil Engineers, 104(HY1), 49-58.

Smith, V.E. (1976). The application of HYMO to study areas in S.W. Wyoming for surface runoff and soil loss estimates. Water Research Series Number 60, Water Resources Institute, University of Wyoming, Laramie, USA, 38pp.

Su, T.Y., Wang, S.Y, and Alonso, C.V. (1980). Depth-averaging models of river flows. Proceedings of the Third International Conference on Finite Elements in Water Resources, University of Mississippi, Mississippi, USA.

Tabios, G.Q., Obeyserkera, J.T.B. and Shen, H.W. (1986). The influence of storm movement on streamflow hydrograph through space-time rainfall generation and hydraulic routing. EOS, Transactions of the American Geophysical Union, 67, paper H11A-04.

Thomas, W.A. and McAnally, W.H. Jr. (1985). User's manual for the generalized computer program system, open channel flow and sedimentation, TABS-2. U.S. Army Engineer, Waterways Experiment Station, Vicksburg, Mississippi, USA.

Tingsanchali, T. and Ackermann, N.L. (1976). Effects of overbank flow in flood computations. Journal of the Hydraulic Division, Proceedings of the American Society of Civil Engineers, 102(HY7), 1013-1025.

Toebes, G.H. and Sooky, A.A. (1967). Hydraulics of meandering rivers with flood plains. Journal of the Waterways and Harbours Division, Proceedings of the American Society of Civil Engineers, 93(WW2), 213-236.

Tominga, A., Nezu, I., Ezaki, K. and Nakagawa, H. (1989). Three-dimensional turbulent structure in straight open channel flows. Journal of Hydraulic Research, International Association for Hydraulic Research, 27(1), 149-173.

Tseng, M.T. (1975). Evaluation of flood risk factors in the design of highway stream crossing. Finite element model for bridge backwater computation. Offices of Research and Development, Federal Highway Administration, Washington, D.C. report FHWA-RD-75-73, vol. III.

Vreugdenhil, C.B. (1973). Computational methods for open-channel flows. Hydraulic Research for Water Management, Delft Hydraulics Laboratory, Report 100.

Vreugdenhil, C.B. and Wijbenga, J.H.A. (1982). Computation of flow patterns in rivers. Journal of the Hydraulics Division, Proceedings of the American Society of Civil Engineers, 108(HY11), 1296-1310.

Williams, J.R. (1975). HYMO flood routing. Journal of Hydrology, 26, 17-27.

Williams, J.R. and Hann, R.H. (1973). HYMO: a problem orientated computer language for hydrologic modelling - user's manual. Agricultural Research Service, Southern Region, Report ARS-S-9.

Wilson. C.B., Valdes, J.B. and Rodriguez-Iturbe, I. (1978). On the influence of the spatial distribution of rainfall on storm runoff. Water Resources Research, 15, 321-328.

Wormleaton, P.R., Allen, J. and Hadjipanos, P. (1980). Apparent shear stresses in compound channel flow. Symposium on River Engineering and its Interaction with Hydrological and Hydraulic Research, International Association for Hydraulic Research, Belgrade.

Wormleaton, P.R., Allen, J. and Hadjipanos, P. (1982). Discharge assessment in compound channel flow. Journal of Hydraulic Division, Proceedings of the American Society of Civil Engineers, 108(HY9), 975-994.

Wright, R.R. and Carstens, H.R. (1970). Linear momentum flux to overbank sections. Journal of the Hydraulics Division, Proceedings of the American Society of Civil Engineers, 96(HY9), 1781-1794.

Yen, B.C. (1967). Some aspects of flow in meandering channels. Proceedings of the Twelfth Congress of the International Association for Hydraulic Research, 465-471.

Yen, B.C. and Yen, C. (1984). Flood flow over meandering channels. In Elliott, C.M. (ed.), River Meandering: Proceedings of the Conference on Rivers, American Society of Civil Engineers, New York, 554-561.

Yen, C.L. and Overton, D.E. (1973). Shape effects on resistance in
    floodplain channels. Journal of the Hydraulics Division,
    Proceedings of the American Society of Civil Engineers,
    99(HY1), 219-238.

Zheleznyakov, G.V. (1965). Relative deficit of mean velocity of
    unstable river flow; kinematic effect in river bend with
    floodplains. Proceedings of the Eleventh Congress of the
    International Association for Hydraulic Research, Leningrad,
    USSR.

Zheleznyakov, G.V. (1971). Interaction of channel and flood plain
    streams. Proceedings of the Fourteenth Congress of the
    International Association for Hydraulic Research, Paris,
    France.

Zielke, W. and Urban, W. (1981). Two-dimensional modelling of
    rivers with flood plains. Proceedings of the Conference on
    Numerical Modelling of River Channel and Overland Flow,
    International Association for Hydraulic Research.